Androgens and the Ovary

Victoria Tyndall

BSc (Hons), University of Edinburgh

MRC Centre for Reproductive Biology
Queen's Medical Research Institute
47 Little France Crescent
Edinburgh, EH16 4TJ
United Kingdom

A thesis submitted to the University of Edinburgh for the Degree of Doctor of Philosophy in the Faculty of Medicine and Veterinary Medicine

31st May 2011

For mum and dad,

thanks for believing

“When we cast our bread upon the waters, we can presume that someone downstream whose face we will never know will benefit from our action, as we who are downstream from another will profit from that grantor's gift”

- Maya Angelou (b. 1928)

Declaration

I declare that all the experiments detailed in this thesis were the unaided work of the author except where acknowledgement is made by reference. No part of this work has previously been accepted for any other degree, nor is being concurrently submitted by the candidate for another degree.

Victoria Tyndall

Tuesday 31st May 2011

Acknowledgements

First and foremost I would like to thank my supervisor Prof. Alan McNeilly for all his support and for allowing me the privilege to complete PhD at the MRC Human Reproductive Sciences Unit. Also thanks for having a 'backup' project in the works! The rest of my thankyous may appear as a selection of lists, but so many people have supported me over the last 3+ years I don't want to leave anyone out...

Of course a huge amount of gratitude is due to the whole McNeilly lab group for all their support and excellent chat during the last three years; Yvonne Brown/White for showing me around on my first day, introducing me to people and generally making me feel right at home! Judy for the reams of immuno help and for teaching me so patiently how to do smears and cardiac puncture; Linda for teaching me how to design primers and order reagents on the portal (quite possibly the most stressful piece of software I've ever had to deal with!). Carlos, Julia and Sarah for the boozy nights out and excellent chat. I'd also like to say a big thank you to Dr Mandy Drake for teaching me how to dissect pretty much everything metabolic and for pointing us in the right direction when the rats got fat. I want to thank my biology teacher Mrs Ruth Fairburn for all her passion and dedication to the subject, and without whom I probably would not have developed a taste for the scientific. A special mention should be made to Carol Adam who passed away earlier in 2010; she was the one always there for a quick natter and who called to offer me this studentship back in 2007. Thanks Carol, I'll never forget you.

I want to thank the many technical staff of the HRSU without whom this thesis would not exist, so in some sort of chronological order thanks go to: Lee Smith and Prof. Phillipa Saunders (Second supervisor) for the GCARKO project-sorry it didn't work out! Mike Millar for always being there when the slide printer stuck; Mark Fisken (friendly hurricane!) at Little France and Linda at the Western for all their help and support with my *in vivo* work; Sheila for answering anything and everything I could ever have dreamed of asking about histology; Nancy Nelson for teaching me basic PCR and electrophoresis; Marion for teaching me how to work

(and resist the temptation to smash) the Stereologer; Nancy Evans and Ian Swanson for assay help and reagents; Rosie Bayne for all her help teaching me how to setup carry out SYBER green PCR; Pam for believing and exonerating me when I said the PCR machine was at fault and not me (booooo ABI); Pedro for teaching me the Bradford assay and Chris Harlow for teaching me primary cell culture technique.

Next up I want to say a BIG THANKS!! to my fellow PhD students – especially Laura 'Lulu' O'Hara and Sam Garside, it was so good to have people around me going through the exact same things so thanks for the tea, coffee and gin times (and Lulu thanks for the falafel times also). Hugs and thanks to my 'girlfriend' Kirsten 'Kiki' Hogg for keeping me down to earth, being the best wingman ever (Maverick to my Goose) and introducing me to Spain. Acknowledgments must go to The Rorge (Rowan and George) for keepin' it real and trying to balance out the estrogen-heavy band of students whilst you were here (maybe you overcompensated but it was a lot of fun). To Alison Wallace and Carol Fitz for the advice when I was a young 'un and their banter on nights out. To Sharon, Afshan and Pedro for always being good chat both in the lab and on a Friday night in Assembly (we're possibly collectively responsible for keeping that place running).

I want to thank my boyfriend Matthew for all his love and support, and for getting my geeky ways and keeping my hydrated with tea when I spend hours at a time on my laptop. Thanks for keeping me sane, reminding me to eat and giving me a sense of perspective. Thanks also to Yvonne Nelson for introducing us and always being up for a bottle of wine when the occasion calls for it!

A special mention also goes to my Nana Sheila for bragging about her granddaughter the scientist down at the day-clinic; you're the best. My final and biggest thanks go to my 'Mummy dearest' Noreen and my Dad Alan. I can't convey how much I appreciate having such supportive, loving parents. Thank you both for always letting me follow my heart and do what I've really wanted in life without pressure and always with reassurance and (often dark!) humour – I love you.

Abstract

Between 10-15% of women suffer from polycystic ovary syndrome (PCOS), making it the most common cause of female infertility. Clinical features of PCOS include high circulating levels of ovarian androgens (T and A4), anovulation and obesity. The aetiology of this reproductive endocrinopathy is likely to be multi-factorial, through the interplay of genetics, epigenetics and environmental factors. Primate research into sexual behaviour development noted that fetally androgenised monkeys developed symptoms like those of PCOS. There are now multiple animal models of PCOS using primates, sheep, rats and transgenic mice. The investigations described in this thesis use rodent models to examine the role of androgens in the pathogenesis of female infertility. An attempt to generate a granulosa cell specific androgen receptor knockout mouse model will first be described, followed by several studies into the developmental programming of female Wistar rat infertility and metabolism by steroid hormones.

Initial investigations showed that testosterone proprionate (TP) administered to female rats during different windows of fetal and neonatal life alters the reproductive and metabolic axes of the adult animals. Fetal plus neonatal TP exposure led to complete ovarian dysgenesis, while postnatal exposure produced a PCOS-like phenotype. Animals which received TP postnatally were heavier and had an increased proportion of primordial follicles in their ovaries by postnatal day (pnd) 90 of life.

Evaluation of this PCOS model showed that neonatally androgenised rats had ovarian follicles with larger antra and a greater ovarian stromal compartment. In addition, these animals were heavier when compared to controls. However, unlike human studies, neonatally androgenised rats showed no differences in circulating gonadotrophin or ovarian androgen levels. Nor did they show any programming effect of neonatal TP upon the theca interna by pnd 90. Further investigations to narrow the windows and dose of TP required to produce a PCOS phenotype showed that TP administered in an early window of neonatal life, between postnatal days

(pnd) 1-6 not only led to anovulation, but potentially reprogrammed the hypothalamic-pituitary axis, as there was minimal gonadotrophin response to reduced ovarian negative feedback (inhibin B and estradiol) in these rats.

Neonatal TP also affected the rat metabolic axis with adult animals becoming heavier after weaning without any change in food intake. Animals developed mesenteric and retroperitoneal obesity along with insulin resistance (IR). Increased hepatic glucocorticoid turnover and altered adipokine expression were also noted in neonatally androgenised females, possibly contributing to the pathogenesis of obesity. No effect of TP dose upon the severity of infertility or metabolic abnormalities in adult animals was observed.

To delineate which features of the rat PCOS model resulted from androgenic, estrogenic or corticosteroid action, a final study used administration of different steroids during the early window of postnatal life: TP, estradiol valerate (EV), dihydrotestosterone (DHT), dehydroepiandrosterone (DHEA) and dexamethasone (DEX). The anovulatory PCO-like phenotype observed with TP was also seen in animals which received EV, but not those which received DHT, DHEA or DEX. TP and EV treatment also resulted in a reduction of ovarian follicle numbers and activated follicle proportions, with an increase in primordial follicle proportions. Although glucose tolerant, animals treated with TP and EV were highly IR. Unlike dexamethasone, DHT and DHEA also produced IR in adult animals, to a lesser extent than TP and EV.

Taken collectively, the results described in this thesis demonstrate that the PCOS-like phenotype observed in the neonatally androgenised female rat is likely to be due to the estrogenic actions of testosterone, potentially through as yet unknown epigenetic mechanisms. The programming of the metabolic components described may additionally be due to the actions of androgens. Furthermore, these studies demonstrate a novel estrogenic effect of neonatal steroids upon primordial follicle populations and show that the neonatally androgenised rat may be a rational PCOS model in a poly-ovulatory species.

Table of Contents

Chapter 2. Materials and Methods 61

List of Figures

List of Tables

List of Equations

List of Abbreviated Terms

Abbreviation	Long Form
α	Greek: *Alpha*; First
A4	Androstenedione
ACTH	Adrenocorticotropic Hormone
AGD	Ano-Genital Distance
αGSU	Common alpha gonadotrophin protein subunit
AHA	Anterio-Hypothalamic Area
AMH	Anti-Mullerian Hormone
AP-1	Activating Protein-1
AR	Androgen receptor
ARC	Arcuate Nucleus
ARE	Androgen Response Element
ARKO	Androgen Receptor Knockout
ATD	Amino-Terminal protein Domain
AVPV	Antero-ventral Peri-ventricular nucleus
β	Greek: *Beta*; Second
bFGF	Basic Fibroblast Growth Factor
BMI	Body Mass Index
BMP	Bone Morphogenetic Protein
BrdU	5-bromo-2-deoxyuridine
BpA	Bisphenol-A
Camp	Cyclic Amino-Monophosphate
C/EBP	CCAAT/enhancer binding protein
cGC	Cumulus Granulosa Cell
Cg	Chromogranin
CL	Corpus Luteum
COC	Cumulus-Oocyte Complex
COX-1	Cyclo-oxygenase 1
CRH	Corticotrophin Releasing HOmrone
CTD	C-Terminal protein Domain
CVD	Cardiovascular Disease
Δ	Greek: *Delta*; Difference in
DAB	Diaminobenzidine
DBD	DNA Binding protein Domain
DHT	Dihydrotestosterone
DHEA(S)	Dehydroepiandrosterone (sulphate)
DEX	Dexamethasone
D/VMN	Dorso/Ventro-Medial Nucleus
DNA	Deoxyribonucleic acid
dH_2O	Distilled MilliQ Water
dpc	Days post coitum

E	Estrogen(s)
E1 / E2 / E3	Estrone / Estradiol / Estriol
ERα / β	Estrogen receptor alpha / beta
EV	Estradiol valerate
e	Embryonic day *example:* e17.5
ESC	Embryonic Stem Cell(s)
EYFP	Enhanced Yellow Fluorescent Protein
FAS	Fatty Acid Synthase
FFA	Free Fatty Acid
Fgf9	Fibroblast growth-factor 9
FOX	Human Forkhead-box
FSH	Follicle stimulating hormone
GALT	Galactose-1-phosphate uridyltransferase
GC	Granulosa Cell(s)
GCARKO	Granulosa Cell Androgen Receptor Knockout
GDF-9	Growth Differentiation Factor 9
GnRH	Gonadotrophin Releasing Hormone
GPCR	G-Protein Coupled Receptor
GR	Glucocorticoid receptor
GTT	Glucose Tolerance Test(ing)
Hcg	Human Chorionic Gonadotrophin
HFD	High Fat Diet
HPA(A)	Hypothalamic-pituitary adrenal (axis)
HPG(A)	Hypothalamic-pituitary gonadal (axis)
HRP	Horseradish peroxidase
HRT	Hormone Replacement Therapy
HS	Heptatic Steatosis
HSL	Hormone Sensitive Lipase
IGF	Insulin-like Growth Factor
IHC	Immunohistochemistry
IHF	Immunofluorescence
IR	Insulin Resistance
Kiss	Kisspeptin
KL	Kit Ligand
λ	Greek: *Lamda*; Wavelength
LBD	Ligand Binding protein Domain
LDL	Low Density Lipoprotein
LH	Luteinizing Hormone
LPL	Lipoprotein Lipase

µ	Greek: *Mu*; Micro
MBH	Medio-Basal Hypothalamus
ME	Median Eminance
MFO	Multi-Follicular Ovaries
mGC	Mural Granulosa Cell
MIX	Methylisobutylxanthine
MMP	Matrix Metalloproteinase
MR	Mineralocorticoid Receptor
NAD(H)	Nicotinamide adenine dinucleotide (hydride)
(N)AFLD	(Non)-Alcoholic Fatty Liver Disease
NGS/NRS	Normal Goat/Rabbit Serum
NR	Nuclear Receptor
OC	Optic Chiasm
OT	Oxytocin
P4	Progesterone
PAR	Predictive-Adaptive Response
PCNA	Proliferating Cell Nuclear Antigen
PCO(S)	Polycystic Ovary (Syndrome)
PEPCK	Phosphoenolpyruvate Carboxykinase
PGCs	Primordial Germ Cells
PGF2α	Prostaglandin F-2α
PitIRKO	Pituitary Insulin Receptor Knockout
PK-A/B/C	Protein Kinase A/B/C
Pnd	Postnatal day
POA	Pre-Optic Area
POF	Premature Ovarian Failure (aka POI)
POI	Primary Ovarian Insufficiency (aka POF)
POMC	Proopiomelanocortin
PPARα/γ	Peroxisome Proliferator-Activated Receptor-α/γ
PR	Progesterone Receptor
Ptgds	Prostaglandin-D synthase
RNA	Ribonucleic acid
rpm	Revolutions per minute
Rspo-1	R-Spondin homologue 1
scc	Side chain cleavage enzyme
SCARKO	Sertoli Cell Androgen Receptor Knockout
SCF	Stem Cell Factor
SCN	Suprachiasmatic Nucleus
SERM	Selective Estrogen Receptor Modulator
Sg	Secretagranin
SHBG	Sex-Hormone Binding Globulin
Sox-9	SRY-box containing gene 9
Sry	Sex determining region of the Y chromosome

T	Testosterone
T2DM	Type-2 Diabetes Mellitus
TP	Testosterone Proprionate
TDF	Testis Determining Factor
TGF-β	Transforming Growth Factor β
TMB	Tetramethylbenzidine
TNF	Tumour Necrosis Factor
W:H	Waist-to-hip circumference ratio
Wnt-4	Wilms tumour 1 homologue
XX	Diploid female chromosomal content
XY	Diploid male chromosomal content
X-CI	X-Chromosome Inactivation
ZP	Zona Pellucida
5αR	5 alpha Reductase
17αOH	17 alpha Hydroxylase
3β-HSD	3 beta Hydroxysteroid Dehydogenase
5βR	5 beta Reductase
11βHSD	11 beta Hydroxysteroid Dehydrogenase

Chapter 1. Introduction: Literature Review

1.1. Introduction

Female reproductive dysfunction accounts for approximately 50% of all infertility, around one third of which is due to problems with ovulation (Templeton 2000; Case 2003). This literature review will cover sexual development and function of the ovary and hypothalamic-pituitary gonadal (HPG) axes, before discussing the role of androgens and steroid hormones in female reproduction. Finally, female infertility disorders and animal models of reproductive dysfunction will be introduced.

A strictly orchestrated reproductive cycle preserves several key functionalities important for a successful pregnancy; a healthy egg, properly timed ovulation, implantation in the correct place, and a receptive uterine environment for both spermatozoa and blastocyst. When these aspects of reproduction are out of synchronisation, or do not function correctly, female sub-fertility and infertility result. Infertility can be defined clinically as "*Failure to conceive after one year of unprotected intercourse*" (Case 2003). It is known that exposure to steroid hormones or their analogues can alter mammalian reproductive system *in utero* or in early life so that it functions incorrectly within the adult animal (Sharpe, Rivas et al. 2003; Ortega, Rey et al. 2010). The investigations of this thesis examine the role which steroid hormones, specifically androgens and their cognate receptor, play in female infertility using the rodent as a model system.

1.2. Sex determination

The physical traits of offspring are largely determined by genetic inheritance from the parental generation, and the characteristic of sex is no exception. At the point of fertilization a mammalian zygote will inherit an X chromosome from the female gamete and can receive either an X or Y from the male gamete depending which sex chromosome the sperm is conveying (Bridges 1916). The presence or

absence of the Y chromosome predestines offspring to develop as XY males or XX females (Ford, Jones et al. 1959; Jacobs and Strong 1959).

When elucidating exactly how the Y chromosome instructs sexual development down a male pathway, human instances of sex reversal were informative, allowing researchers to pinpoint this 'testis determining factor' (TDF) (Buckle, Boyd et al. 1987). The TDF specific to the Y chromosome was identified as a conserved 35 kilobase area, known as *Sry* –'sex determining region-Y' (Berta, Hawkins et al. 1990; Sinclair, Berta et al. 1990). *Sry* encodes a 79 amino acid protein product, transiently expressed in the pre-Sertoli cells of the testis, that up-regulates expression of *Sox9*, driving the establishment of Sertoli cells, testosterone (T) release and testis formation (Sekido, Bar et al. 2004).

This process of sex determination in the male occurs at around 42 days post coitum (dpc) in humans and 11.5 dpc in mice. In females, sex determination occurs slightly later in both species; around 49 and 13.5 dpc respectively (Soder 2007). Initially, the process of sex determination in females was thought to occur via a default pathway of sexual development, being driven by the absence of *Sry*. However, recent research indicates that an antagonistic set of signalling molecules in XX females repress male pathway gene expression, in addition to driving ovarian differentiation. Although the exact mechanisms of female gonad differentiation are still unclear, *Rspo1*, a member of the R-Spondin family, is thought to be the gene responsible for tipping the bipotential gonad towards ovarian development. It is postulated that *Rspo1* activates and synergises with *Wnt4* expression in the XX gonad, stabilising β-catenin expression, and activating target genes associated with ovarian differentiation (Yao, Matzuk et al. 2004; Lau and Li 2009). Indeed, *Wnt4* is present in the bipotential gonad of both mammalian sexes, but is strongly up regulated in XX gonads as they begin to differentiate (Chassot, Gregoire et al. 2008). Additional studies have also demonstrated that male pathway genes SRY and *Sox9* act to repress Wnt4/βcatenin signalling, and the interactions of the main sex determining factors are summarised in Figure 1.1.

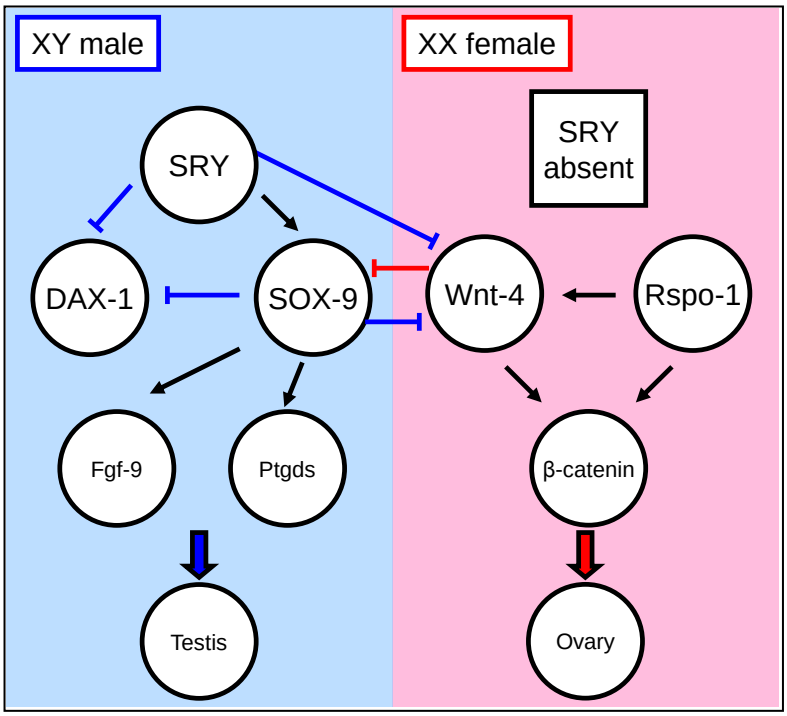

Figure 1.1: Sex determining factors in XY males and XX females: In the absence of SRY, ovary determining factors suppress testis-determining factors (Adapted from Vainio, Heikkila et al. 1999; Yao, Matzuk et al. 2004; Chassot, Ranc et al. 2008).

The expression of SRY in the male leads to testosterone production which functions to masculinise the male reproductive tract and neuroendocrine axis, the latter via the aromatisation of testosterone to estrogen in the brain (Morris, Jordan et al. 2004).

1.2.1. Sexual dimorphism of the neuroendocrine system

Many aspects of the mammalian neuroendocrine system are sexually dimorphic due to differing hormonal milieus during fetal and neonatal development, key examples of which are shown in Table 1.1 (Ward, Wexler et al. 1996; Morris, Jordan et al. 2004). We now know that masculinisation of certain reproductive features in the male brain occurs through the aromatisation of testicular T (released both before and after birth) to estrogen (Lephart, Call et al. 2001). In addition estrogen is required for normal reproductive endocrine development in the female

(Dohler, Srivastava et al. 1984; Dohler, Coquelin et al. 1986). Furthermore, structural changes in the neuroendocrine system occur in both sexes at puberty, when again circulating steroidal milieu becomes particularly important (Ahmed, Zehr et al. 2008; Evuarherhe, Leggett et al. 2009; Schulz, Molenda-Figueira et al. 2009).

Table 1.1: Summary of the sexually dimorphic areas of the mammalian nervous system: These areas are affected by changes hormonal milieu during neonatal development in the rat (Adapted from Morris, Jordan et al. 2004).

Brain region	Main function(s)	Males	Females
Sexually dimorphic nucleus of the preoptic area (SDN-POA)	Copulation behaviour	Larger, more numerous neurons	Smaller, fewer neurons due to ↑ apoptosis between pnd 0 - 9
Anteroventral paraventricular nucleus (AVPv)	Gonadotrophin secretion (LH surge in females)	Smaller, lower density of neurons due to ↑ apoptosis between pnd 0 - 4	Larger, ↑ density of neurons with more dopaminergic and kisspeptin neurons
Ventromedial hypothalamus (VMH)	Marking and lordosis behaviour	Larger in males, same neuronal density but an ↑ neuronal synapses	Smaller in females, same neuronal density
Spinal nucleus of the bulbocavernosus (SNB)	Motor neurons which attach to penile muscles	Larger more numerous neurons	Smaller, fewer neurons

LH=luteinising hormones; pnd=postnatal day; ↑=increase in.

1.3. The Ovary

Unlike the testes where spermatozoa are perpetually produced from a germ cell population under the influence of testosterone, the ovary contains all the gametes a female mammal will possess during the course of her reproductive lifespan (Bukovsky, Caudle et al. 2005). Each oocyte is meiotically arrested within the follicle and resumes meiosis to achieve a fertilizable capacity after ovulation (Reviewed in Marteil, Richard-Parpaillon et al. 2009). Before ovulation, the somatic cells of the follicle proliferate and differentiate around the somewhat quiescent oocyte (Eppig 2001; Edson, Nagaraja et al. 2009). Timing is crucial in the human menstrual cycle and the rodent estrus cycle, the physiological purpose being a successful pregnancy through specifically scheduled events which are regulated by hormonal signals between the ovary and the brain. The following section will cover an overview of fembale reproduction in humans followed by a more detailed description of rodent follicle development and reproduction that has particular relevance to the findings presented in this thesis.

1.4. Overview of human female reproduction

The human ovary is formed by around 75 dpc and contains between six and seven million germ cells with the potential to become oocytes (Matzuk, Burns et al. 2002; Bukovsky, Caudle et al. 2005). Most of these germ cells subsequently undergo programmed cell death during prenatal development. A proportion which do not develop into primordial and primary follicles by gestational day 170 (Forabosco, Sforza et al. 1991). At birth the human ovary contains around 4-700,000 oocytes, which are further depleted through natural atretic mechanisms to around just 4000 oocytes by puberty, up to half of which may be pre-antral follicles (Bukovsky, Caudle et al. 2004).

Each oocyte is enclosed by a follicle of supporting somatic cells. Most follicles are quiescent primordial follicles and develop later in life, but a sub-population of follicles is recruited to grow with each reproductive cycle, most of

which undergo atresia (Quirk, Cowan et al. 2004). The process of follicle development comprises several stages in humans and takes around three months from the primordial stage through to ovulation of a single oocyte (Figure 1.2).

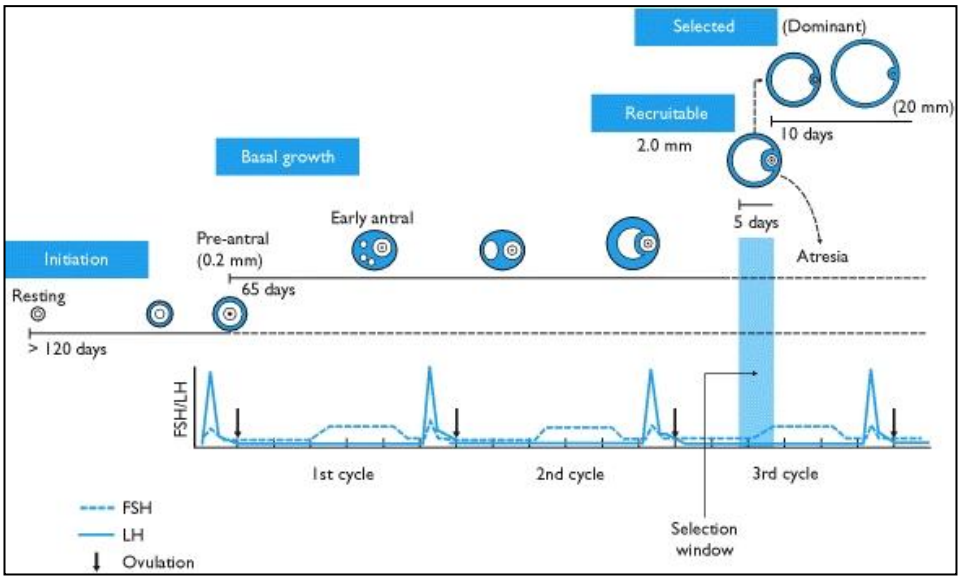

Figure 1.2: Follicle recruitment and development across three human menstrual cycles. An LH surge mid-cycle induces ovulation (Taken from S.S. Nussey 2001).

The gonadotrophins, follicle stimulating hormone (FSH) and luteinizing hormone (LH), are two glycoprotein hormones released by the pituitary gland in response to signals from the hypothalamus (discussed in Section 6 of this Chapter). Under the stimulation of pituitary FSH released during the follicular phase of the cycle, selected follicles develop and produce increasing amounts of the steroid-hormone estrogen (Figure 1.3). Ovarian estrogen secretion rises as a dominant follicle becomes ready for ovulation (Baird and Fraser 1974). Estrogen also stimulates mucosal secretion and vascularisation of the endometrial lining, which helps to facilitate entry of spermatozoa into the mucosa (Reviewed in Kelly and Critchley 1997; Critchley, Kelly et al. 2006; Jabbour, Kelly et al. 2006). Once a threshold of estrogen production is reached, a gonadotrophin releasing hormone (GnRH) surge from the hypothalamus, stimulates a further surge of pituitary LH into the circulation which induces ovulation (Midgley and Jaffe 1968; Midgley and Jaffe 1971; Knobil 1974).

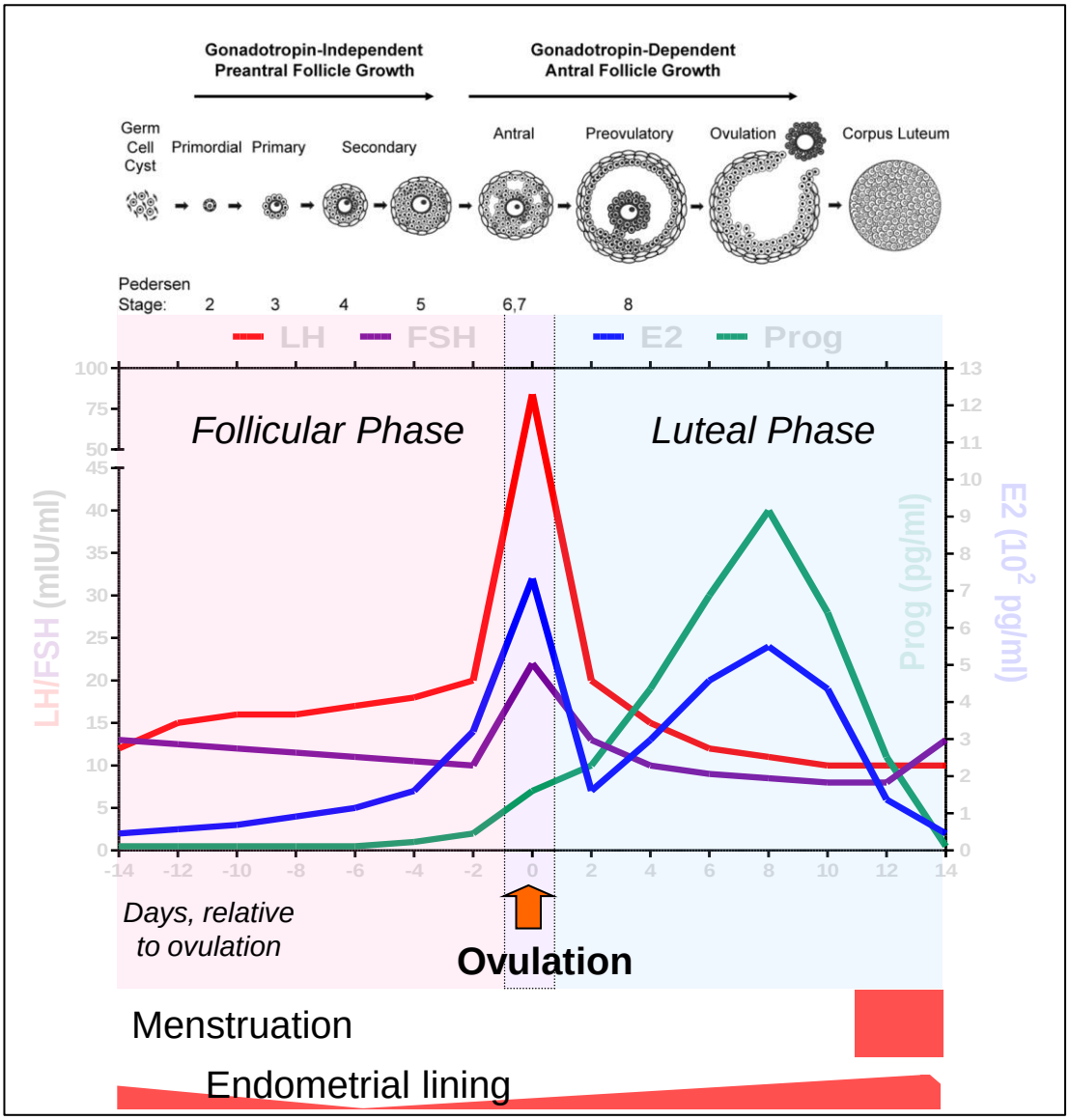

Figure 1.3: Timing is everything: gonadotrophin, progesterone and estradiol changes across the human female menstrual cycle. Development of one oocyte from a primordial follicle through to ovulation occurs over the course of several menses (Adapted from Speroff and Vande Wiele 1971; Edson, Nagaraja et al. 2009)

Ovulation is inflammatory; the follicle luteinizes and ruptures, releasing the egg and leaving behind the supporting cells which regress to form the corpus luteum (CL). During the subsequent luteal phase of the cycle, the CL releases E2 and progesterone (P4), another steroid hormone that causes the endometrial lining to become more viscous and less alkaline in preparation for embryo implantation (Short 1964; Baird and Fraser 1975; Jabbour, Kelly et al. 2006). Activin A produced by the

CL acts in a paracrine manner and stimulates CL regression during the luteal phase (Myers, Gay et al. 2007; Myers, van den Driesche et al. 2008). After ovulation, the egg moves into the oviduct and through the fallopian tubes, at which point if sperm are present fertilization can occur as haploid male and female gametes fuse to form a zygote. Once the initial stages of implantation are complete, the blastocyst releases a further endocrine regulator, human chorionic gonadotrophin (hCG), which maintains CL function and P4 release during early pregnancy (Reviewed in Sonderegger, Pollheimer et al.). Without hCG, CL function is not maintained and P4 withdrawal occurs as the CL regresses and the superficial layer of the endometrium is shed (Baird, Brown et al. 2003). This process is known as menstruation, and in women a menstrual period usually lasts between four and six days.

1.5. Rodent follicle development and ovulation

Female rodent endocrinology is different to that of humans in that rodents are poly-ovulatory and have an estrus cycle of around four days instead of a 28 day menstrual cycle. The stages of the rodent estrus cycle can be identified by the cell types present in the vagina when examining smear samples under a light microscope (Table 1.2).

Table 1.2: Length and cell types present in the vaginal epithelium across each stage of the rodent estrus cycle (Adapted from Larsen, Markovetz et al. 1977).

Estrus cycle stage	Length (hours)	Vaginal smear pattern (cell types present)
Proestrus	12 – 14	Clusters of round nucleated epithelial cells
Estrus	25 – 27	Mainly cornified squamous epithelial cells
Metestrus (Diestrus 1)	6 – 8	Granular leukocytes
Diestrus-2	55 – 57	Leukocytes, some nucleated epithelial cells

This section will describe rodent ovarian physiology and follicle development; a four day estrus cycle allows rodents to breed frequently (Figure 1.4).

Figure 1.4: Hormone levels across the rodent estrus cycle: From top to bottom – progesterone, prolactin, estradiol, LH and FSH levels at the estrus, diestrus(1), metestrus (also known as diestrus 2) and proestreus phases of the four day cycle. Samples were taken at 2 hour intervals and black bars represent hours of darkness. X-axis numbers represent the time of day by 24 hour clock (Taken from Smith, Freeman et al. 1975).

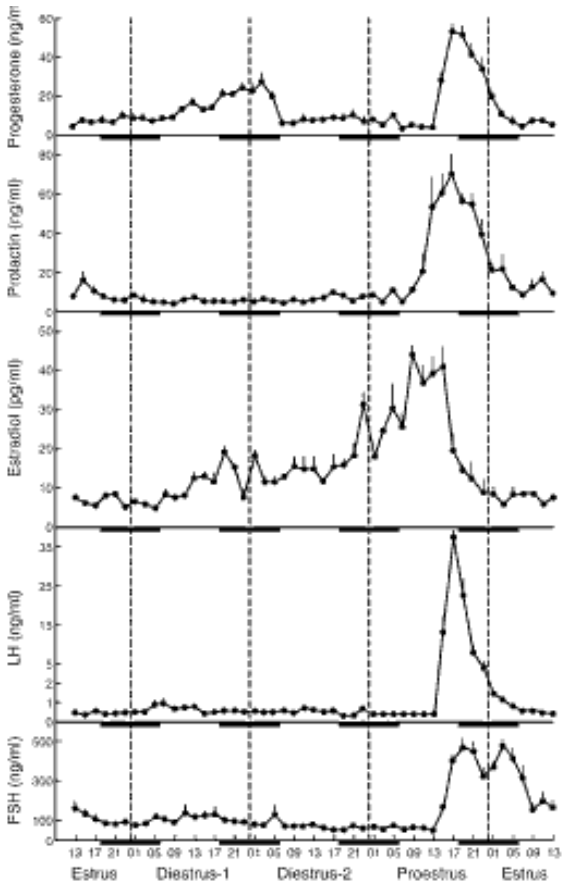

1.5.1. Germ cell nest breakdown and primordial follicle assembly

During rodent embryonic gestation a founder population of about 45 primordial germ cells (PGCs) migrate through the hindgut and by embryonic day (e) 11.5 have colonised the developing gonad (Greenfeld, Pepling et al. 2007). These PGCs, now termed oogonia, proliferate by mitosis to a point of incomplete cytokinesis until embryonic day e13.5, at which point these clusters (or nests) of oogonia are connected by intercellular bridges (Pepling 2006). Oogonia are then able to enter meiosis, arresting at the diplotene stage of meiotic prophase I and forming a finite founder population of germ cells now termed oocytes (Spradling, de Cuevas et al. 1997; Steckler, Wang et al. 2005).

At birth (corresponding to e75 in humans) around 70% of germ cells are lost, mostly via programmed atresia (McNatty 2000). Accordingly, the germ cell nests breakdown and the remaining oocytes become surrounded by a flattened layer of squamous pre-granulosa somatic cells, to form primordial follicles (Matzuk 2000). Pooled recruitment of primordial follicles can subsequently occur, but folliculogenesis before puberty is restricted up to the small antral stage due to low-activity of the gonadotrophin releasing hormone (GnRH) 'pulse generator' to the pituitary and correspondingly low levels of LH and FSH (Section 6).

Studies into rodent germ cell nest breakdown and subsequent primordial follicle assembly conducted in mice used the bioavailable phytoestrogen genistein, which disrupts nest breakdown, but doesn't affect granulosa cell (GC) association with the developing oocyte. *In vivo* mouse follicle assembly and *ex-vivo* rat primordial follicle assembly are also inhibited by P4 as well as estrogens (Kezele and Skinner 2003). It is now believed that these hormones are essential during rodent fetal life to prevent breakdown of clusters and maintain germ cells as arrested oogonia. At birth, and outside the endocrine environment of the mother, levels of estrogens and P4 in the neonate fall and nest breakdown and programmed germ cell loss initiates (Figure 1.5), possibly driven by local tumour-necrosis factor (TNF) expression and Notch signalling (Pepling and Spradling 2001). Recent research also indicates a role for activin in the breakdown of germ cell nests; in the mouse local inhibin levels decline at birth and injection of mice with activin at this point leads to an increase in the number of primordial follicles formed in the neonate (Trombly, Woodruff et al. 2009). Proteins with nuclear binding properties such as factor in the germline α (Figla), octamer-binding transcription factor 4 (Oct-4) and members of the leucine-rich repeat and pyrin domain containing (Nlrp) gene family are also thought to initially drive primordial follicle formation (Edson, Nagaraja et al. 2009).

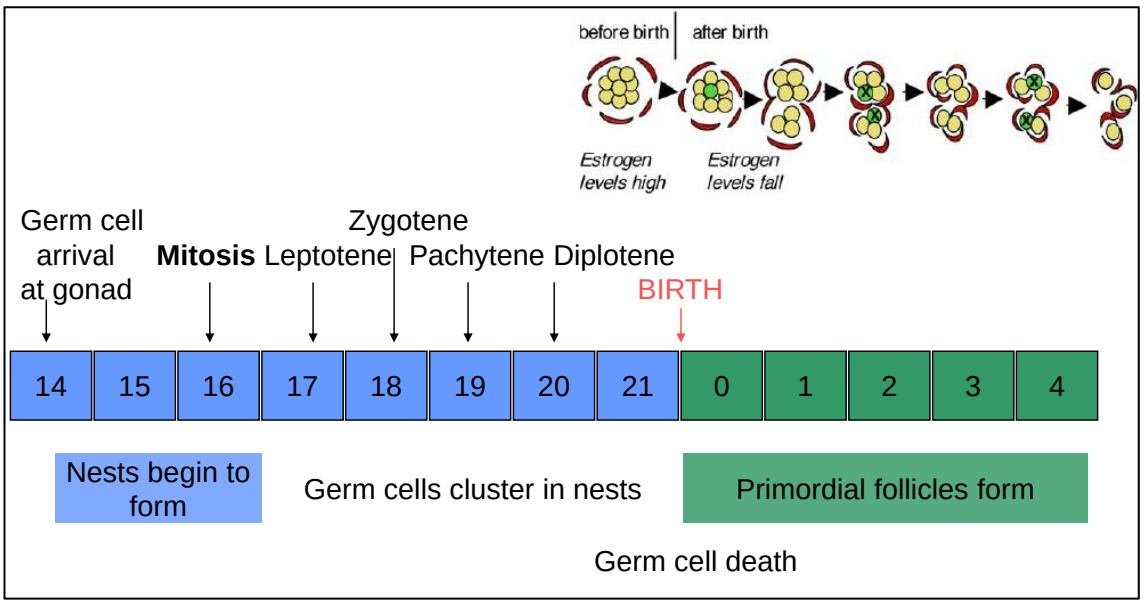

Figure 1.5: Timeline of germ cell nest breakdown after birth in the rodent and primordial follicle formation: After arriving at the gonad, germ cells cluster in nests and progress through the various mitotic stages and arresting at the diplotene stage. After birth germ cells undergo programmed cell death, with the remaining germ cell population continuing into postnatal life. Each germ cell becomes surrounded by squamous granulosa cells as a primordial follicle (Adapted from Jefferson, Newbold et al. 2006).

1.5.2. Primordial follicle recruitment

Transition of a quiescent primordial follicle into a developing primary follicle is thought to involve a number of oocyte derived and squamous GC derived factors, many belonging to the transforming growth factor-β (TGFβ) superfamily of proteins (Figure 1.6). For instance, growth differentiation factor-9 (GDF-9) secreted by the oocyte is required for follicle development (Nicol, Bishop et al. 2009; Sugiura, Su et al. 2010). GDF-9 deficient female mice are infertile and unable to develop follicles which have more than a single layer of cuboidal granulosa cells (Dong, Albertini et al. 1996). Further knockout studies have shown that GDF-9 is not only essential in mediating somatic cell growth in early follicle development, but is required for proper granulosa cell steroidogenic gene expression and oocyte growth (Carabatsos, Elvin et al. 1998; Elvin, Clark et al. 1999; Elvin, Yan et al. 1999).

Conservation of the primordial follicle pool is also important in maintaining female fertility. Mice with phosphatase and tensin homologue (Pten) deficient

oocytes show depletion of primordial follicles and eventually complete follicle loss much earlier than occurs in normal ovarian ageing (Reddy, Liu et al. 2008). Oocytes from these mutant animals have high levels of Akt, which phosphorylates and thus inactivates Foxo3a (Reddy, Shen et al. 2005). Foxo3a is expressed in the nuclei of primordial and early primary follicles and expression levels decrease in more developed follicles (Castrillon, Miao et al. 2003). Foxo3a knockout female mice have complete follicle loss by week 15 of life leading to the conclusion that Foxo3a is another inhibitory regulator of primordial follicle recruitment shown in Figure 1.6 (Castrillon, Miao et al. 2003; Liu, Rajareddy et al. 2007).

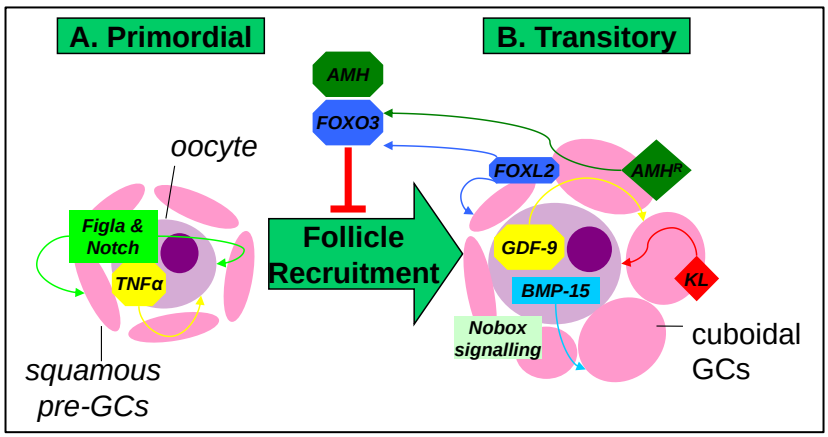

Figure 1.6: Summary of induction and inhibition of primordial follicle transition into the transitory primary follicle: (A) Oocyte transcription factors in the primordial follicle instigate follicle recruitment leading to production of further transcription factors and TGFβ family proteins: These factors initiate oocyte enlargement and establish the formation of cuboidal GCs; **(B)** NOBOX signalling leads to the expression of GDF-9 in addition to bone morphogenetic protein-15 (BMP15). Expression of zona pellucida proteins ZP1 and ZP3 begins after the activation of spermatogenesis and oogenesis helix-loop-helix 1 (SOHLH) proteins (not shown). In addition, kit ligand (KL) signalling is essential for healthy primordial to primary transition. In terms of GCs, the transcription factor forkheadbox ligand-2 (FOXL2) is also required the transition from a squamous to a cuboidal phenotype. Nuclear forkheadbox O3 (FOXO3) signalling in addition to anti-Müllerian hormone (AMH) produced by cuboidal GCs are known to prevent primordial to primary follicle activation, but the precise mechanisms involved remain to be elucidated (Adapted from Eppig 2001; Su, Sugiura et al. 2008; Edson, Nagaraja et al. 2009).

TGFβ proteins are a superfamily of secreted molecules which hetero- or homodimerize to activate serine/threonine kinase Alk receptors at the cell membrane. Binding and autophosphorylation of a type II Alk receptor initiates type I receptor

phosphorylation and signal transduction via receptor smad proteins (Reviewed in Knight and Glister 2003). Sub-group proteins of the TGFβ superfamily include the bone morphogenetic proteins (BMPs) in addition to activin and inhibin dimers which play major roles in the auto- and paracrine regulation of follicle development (Trombly, Woodruff et al. 2009).

Recent computational analysis of follicle spatial patterns points towards a potential inhibitor of primordial follicle recruitment, since closer proximity to a primordial follicle reduces the likelihood of recruitment (Da Silva-Buttkus, Marcelli et al. 2009). Conversely proximity to already growing follicles denotes an increased likelihood of recruitment. However, the paracrine signal which in theory emanates from primordial follicles has yet to be found (Da Silva-Buttkus, Marcelli et al. 2009).

At this point in follicle development, the oocyte-derived *GDF-9* and *BMP-15*, together with granulosa-derived *KL*, form a regulatory loop leading to cuboidal GC (cGC) formation and oocyte enlargement, thus establishing a primary follicle (Eppig 2001). In mammals grouped recruitment of follicles from the primordial pool into the growing pool occurs once per cycle (every four days in rodents and roughly every 28 days in humans). This recruitment from the pool of primordial follicles is thought to be mainly regulated by the intra-ovarian AMH level. AMH is secreted by proliferating cuboidal GCs and inhibits further follicle recruitment until a cohort of follicles die/are ovulated; thus intra-ovarian AMH levels decline and a second cycle of recruitment initiates (Rey, Lukas-Croisier et al. 2003). Next, outward proliferation of cGCs surrounding the oocyte leads to the formation of multilayered secondary preantral follicles, which are subsequently enclosed in a basal lamina that structurally maintains follicle configuration during follicle growth and prevents blood vessel invasion from the newly forming theca cell layer (Da Silva-Buttkus, Jayasooriya et al. 2008; Young and McNeilly 2010).

1.5.3. Follicle growth and atresia

One of two possible fates will befall an ovarian follicle, either it will proceed to ovulation, or it will become atretic and die. Follicle development is influenced by paracrine, autocrine and endocrine factors from the primary right through to the ovulatory stage (Edson, Nagaraja et al. 2009). Before puberty the gonadotrophins have a permissive role in directing follicle development, with growth factors dictating the earlier stages as previously described. However, these growth factors may still be indirectly influenced by the gonadotrophins (Figure 1.7).

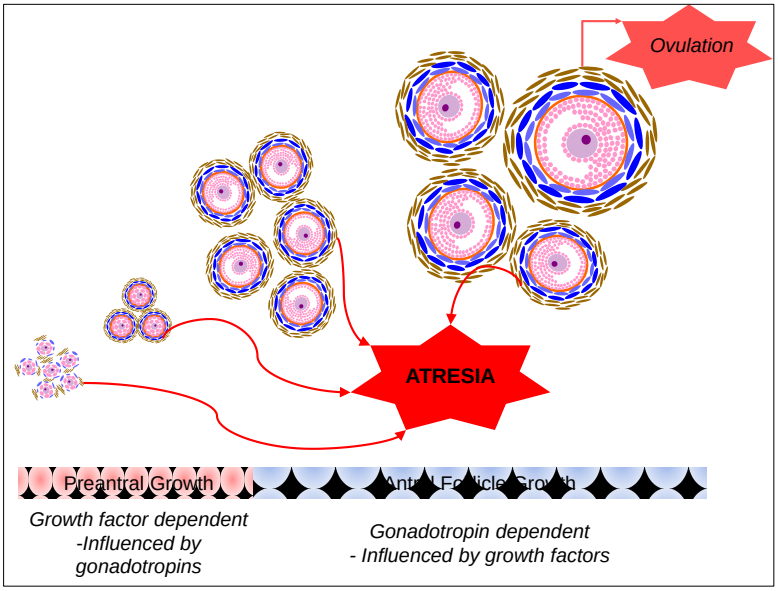

Figure 1.7: Follicle development in the mammal is initially growth factor dependent and after antrum formation becomes gonadotrophin dependent: Throughout follicle development follicles die via programmed atresia (Adapted from Irving-Rodgers, Krupa et al. 2003; Matsuda-Minehata, Inoue et al. 2006).

Early preantral folliculogenesis is influenced by local GC estrogen production, in addition to insulin-like growth factor (IGF) interactions (Demeestere, Gervy et al. 2004; Quirk, Cowan et al. 2004). Preantral GCs have been shown to express IGF binding protein 2 (IGFBP-2) and the IGF-1 receptor; IGFBP2 is able to regulate the bioavailability of both IGF1 and IGF2 proteins released by adjacent antral follicles (Webb et al 2004). Since IGF1 and EGF are known *in vitro* stimulants of preantral follicle growth, it may be that early antral follicles influence neighbouring preantral folliculogenesis in a paracrine fashion (Spicer, Voge et al. 2004). Furthermore, high levels of IGF1 may inhibit oocyte growth thus contributing to atresia (Webb et al 2004). However, it should be noted that such *in vitro*

investigations studies have not been performed across all model species or in humans.

Apoptosis of GCs occurs via caspase pathways; members of the TNF protein superfamily activate cell surface death receptors which trimerize and induce caspase cleavage and subsequent cell death (Matsuda-Minehata, Inoue et al. 2006). Work by Irving-Rodgers and colleagues in the last decade documented two specific types of follicular atresia in rodents. Firstly antral atresia, whereby GCs lining the antrum become apoptotic and cell death spreads outwards towards the basal lamina. Secondly, in basal atresia the reverse occurs whereby mGCs become apoptotic and the basal lamina develops convolutions, with cell death spreading inwards towards the oocyte. In both types of atresia macrophages and other immune cells are recruited by the apoptotic elements to endocytose any cellular remnants (Irving-Rodgers, Krupa et al. 2003). In the rodent, atretic events are marked by GC pyknotic nuclei, oocyte degeneration and the infiltration of immune cells. Although GC apoptosis is one known cause of follicle death across species, other mechanisms of cell death may exist within the mammalian follicle. Autophagy is one such process and has been shown to occur alongside apoptosis in Chinese hamster ovary cultures, where in nutrient deficient cultures, cells develop autophagosomes and self-degrade (Hwang and Lee 2008; Han, Kim et al. 2010). However, the precise mechanisms which earmark one follicle for atresia and another for ovulation remain poorly understood (Quirk, Cowan et al. 2004).

Earlier research into follicular hormone concentrations suggests that an increased androgen to estrogen ratio may also contribute towards atresia (Diaz, Sugiura et al. 2008). Furthermore, other studies indicate that an imbalance between follicular concentrations of P4 and estrogens may also influence follicle death. IGF-1 levels are lower in ruminant follicles undergoing atresia. However, it should be noted that significant differences in IGF expression patterns exist across species which remain to be fully characterised (Yu, Sui et al. 2004; Luo and Wiltbank 2006). As GCs become multi-layered and are surrounded by a basal lamina, follicles recruit a

steroidogenically inactive thecal cell layer from the contiguous cortical stroma known as the theca externa (Figure 1.8).

These cells proliferate adjacent to the basal lamina to form the theca interna, a highly vascularised layer of endocrine cells providing increased structural support; this differentiation of thecal cells is induced by paracrine signalling from GCs (Reviewed in Young and McNeilly 2010). Although the specific molecules involved have yet to be identified, candidates include follistatin, members of the IGF signalling family, stem cell factor (SCF) and GDF-9 (Magoffin 2005). The theca interna is steroidogenically active, producing the androgens androstenedione (A4) and T in response to LH, which in preantral follicles serve to augment GC proliferation as the follicle develops (Murray, Swales et al. 2008).

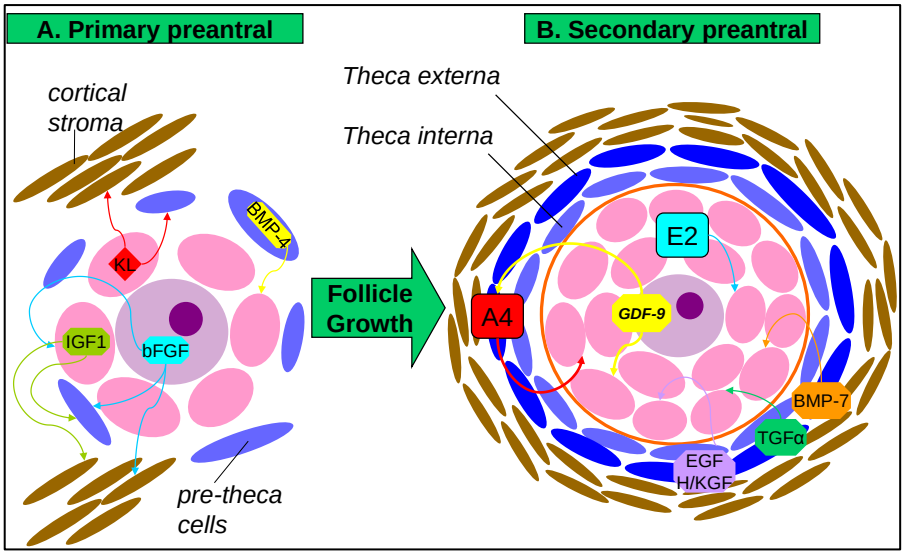

Figure 1.8: Summary of known bi directional paracrine communication in the induction and proliferation of the theca (A) basic fibroblast growth factor (bFGF) from the oocyte together with Kit ligand (KL) and insulin like growth factpr-1 (IGF-1) from granulosa cells (GCs), signal to the cortical stroma and induce theca externa formation. BMP-4 from pre-theca cells signals back to GCs indicating the presence of stroma. **(B)** Theca externa proliferates into steroidogenically active theca interna, forming a larger secondary preantral follicle within which GDF-9 produced by the oocyte acts to induce GC and theca cell proliferation, the resulting androgen produced by the theca acts on GCs to increase their proliferative capacity (Adapted from Orisaka, Tajima et al. 2009)

At the antral follicle stage, follicle expansion is rapid and GCs differentiate into two sub-populations, the first few layers in contact with the basal lamina known as mural GCs (mGCs) and those in contact with and surrounding the oocyte are known as cumulus GCs (cGCs). Exposure to FSH primes the cGCs which, in concert with EGF released from the oocyte, induces rapid cGC expansion forming a cumulus-oocyte-complex (COC) (Diaz, Wigglesworth et al. 2007). Concurrently the fluid-filled spaces between cGCs coalesce around the COC forming an antrum. However, the absence of tight junctions at the mGCs surrounding the basal lamina suggests that fluid accumulation cannot occur through an ionic osmotic gradient, i.e. through a high antral ion concentration. Fluid accumulation into the antrum is in fact determined by the presence of macromolecues such as glycosaminoglycans, hyluronan, chondiotin-sulphate and DNA, which interact and accordingly create an

osmotic gradient. It is also interesting to note that healthy antral follicles have twice the osmolality of atretic follicles (Clarke, Hope et al. 2006).

Antrum formation is FSH dependent and GCs serve as a blood-follicle barrier, with fluid transport occurring largely via a passive aquaporin protein mechanism through the GCs themselves (McConnell, Yunus et al. 2002). Subsequent to antrum formation FSH, augmented by androgens and estrogens, induces p450 aromatase expression in mGCs allowing A4 and T produced by the theca interna to be converted to estrogens (Figure 1.9). Although follicle survival is now gonadotrophin dependent, growth factors still play a role in follicular growth; GDF-9 is involved in GC proliferation and cGC expansion as well as in the induction of FSH receptor expression (Young and McNeilly 2010). Furthermore, expression of p450 aromatase in mGCs is FSH and steroid hormone dependent, but may be affected by a wide range of growth factors and protein molecules (Stocco 2008). Induction of aromatase and estrogen production is essential for follicle survival, the dominant follicles feeds back to the pituitary through the production of estradiol and inhibin, which induces the LH surge required for ovulation (Stocco 2008).

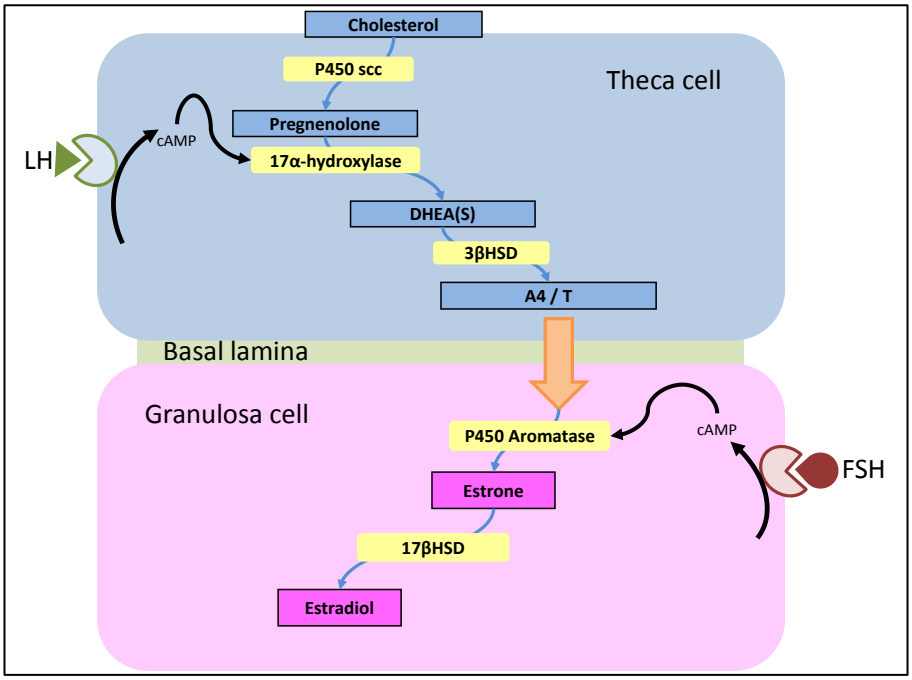

Figure 1.9: The two-cell two-gonadotrophin model: LH stimulates induction of steroidogenic enzymes within the theca interna via the LH GPCR while FSH activates a second cognate GPCR on mural GCs to induce P450 aromatase expression. Androstenedione and testosterone (A4/T) produced in the theca diffuses across the basal lamina and is converted to estrogens by P450 Aromatase which feeds-back to the pituitary (Adapted from Magoffin 2005; Young and McNeilly 2010).

1.5.4. Ovulation and CL function in the rodent

At the point of LH surge, follicles which do not express LH receptor (LHr) in mGCs undergo atresia (Pakarainen, Zhang et al. 2005). In follicles with functional mGC LHr expression, the LH surge induces ovulation and mGC steroid production switches from E2 to P4 as the supporting follicle cells luteinise (Hillier, Knazek et al. 1977; Daniel and Armstrong 1980; Hillier, Zeleznik et al. 1980; Jia, Kessel et al. 1985). Activation of mGC LHr at ovulation terminates GC proliferation at the G_0/G_1 phase of the cell cycle, inducing luteinisation of GCs and theca cells. In humans and non-human primates, the specific differentiation GCs into large hypertrophic granulosa-lutein cells, and luteinisation of the theca cells into smaller steroidogenic theca-lutein cells is well documented, although no such differentiation pattern is observed in the rodent (Stocco, Telleria et al. 2007).

A surge of prolactin (PRL) occurs in the evening of the LH proestrus surge (Figure 1.4) and after of P4 production ceases, caspase-3 mediated apoptosis of rodent CL tissue occurs; either in the current CL or those CL which are still present from previous estrus cycles (Gaytan, Morales et al. 1998; Gaytan, Morales et al. 1998). PRL induces tissue remodelling of the CL, with cleavage of the basement membrane by matrix metalloproteinases (MMP) into component collagens, fibronectins and laminins which help instigate GC luteinisation (Gaytan, Bellido et al. 1998; Rodgers, Irving-Rodgers et al. 2003). Concomitantly, pericytes invade from the theca cell layer and angiogenesis factors derived from the developing CL, such as vascular endothelial growth factor (VEGF), angiogenesis factor-2 (Ang2) and prokineticin-1 (Prok1), stimulate the formation of capillary blood vessels (Smith, McIntush et al. 1994).

Vascularisation of the CL provides the luteal cells with hormones, proteins and cholesterol required for steroid hormone (P4) production. Vascularised areas of the CL are recycled by fibroblasts and macrophages into collagen bundles, leaving behind an involuted ‘scar’ within the ovary known as the corpus albicans (Stocco, Telleria et al. 2007).

Inhibin B and P4 secreted by the rodent CL act at hypothalamo-pituitary sites to negatively regulate FSH synthesis and secretion immediately after ovulation during the evening of proestrus. Regression of the rodent CL takes place over several subsequent estrus cycles (Gaytan, Bellido et al. 1998). As the rodent CL produces no E2, negative feedback inhibiting pituitary gonadotrophin release is removed after CL formation. This allows the immediate recruitment and development of a further cohort of follicles for subsequent estrus cycles.

1.6. The Hypothalamic-Pituitary Gonadal axis

The hypothalamus is located at the middle of the base of the brain, directly beneath which the pituitary rests in sella turcica cleft of the skull (Amar and Weiss 2003). The pituitary is divided into the anterior and posterior lobes, controlled by the hypothalamus. Hypothalamic neurons contact the hypophyseal portal system, a network of isolated blood capillaries with the pituitary gland allowing hormones and neurotransmitters released by the hypothalamus to be transported directly to the anterior pituitary where they act on receptors at the cell membrane of the various trophic cell types within the anterior pituitary gland (Amar and Weiss 2003).

In males, LH released from the pituitary into the circulation stimulates testicular Leydig cells to secrete T, production of which is further augmented by prolactin (also released by the pituitary) and inhibin. FSH and testosterone act in concert upon testicular Sertoli cells, facilitating spermatogenesis within the seminiferous tubules. Spermatozoa are produced from a pluripotent self-replenishing 'stock' of spermatogonial stem cells (Reviewed in Huhtaniemi and Bartke 2001). Inhibin and testosterone produced by the testis negatively feedback to the pituitary and hypothalamus to regulate spermatogenesis (Meachem, Nieschlag et al. 2001).

In the female reproductive system, feedback regulation by the hypothalamus and pituitary is more complicated since unlike the testis, the pattern of gamete development and release is not continuous. The ovary contains no gamete-replenishing stem cells, and so release of an ovum is tightly regulated by the brain and pituitary to occur at a specific point during the menstrual and estrus cycles as previously described. The gonadotrophins act in concert to facilitate follicular development prior to ovulation. Estradiol and inhibin produced by the ovary in response to FSH and LH, feed back to the pituitary and hypothalamus. Before ovulation, estradiol production is highest (Figure 1.3 and Figure 1.4) and feeds forward to the hypothalamus which produces a GnRH surge, inducing a pituitary LH surge and causing ovulation (Sections 3-5 of this Chapter).

Differences exist across species between the feedback systems which regulate ovulation, CL formation and hence the length of the menstrual and estrus cycles. In ruminants, no E2 is produced by the CL and thus some negative regulation is removed from the pituitary allowing FSH secretion to rise again. Thus follicle development recommences earlier and the ruminant estrus cycle is shorter than the human menstrual cycle; between 17 to 21 days in length (Baird, Baker et al. 1975). Rodents have a four day estrus cycle, as the rodent CL continues to secrete P4 for just one to two days after ovulation (Sanchez-Criado, Ruiz et al. 1996).

1.6.1. Pituitary development and ontogeny of the gonadotrophs

During development, the hypophyseal placode of the oral ectoderm envaginates into Rathke's pouch while at the same time a second envagination of neural ectoderm occurs in the opposite direction allowing the two cell lineages to unite and develop into the distinct lobes of the adult pituitary, the secretory anterior lobe and the neural posterior lobe (Rizzoti and Lovell-Badge 2005; Kelberman, Rizzoti et al. 2009). The posterior pituitary is an extension of hypothalamic neurons in which hormonal proteins are synthesized at the hypothalamic apex (Rizzoti and Lovell-Badge 2005). These neuronal fibers traverse the hypophyseal space as the pituitary stalk where the hormones oxytocin and vasopressin, are stored in granules within neuronal terminals for release into the hypophyseal vein (Clarke and Cummins 1982; Clarke, Cummins et al. 1987). Conversely, the anterior pituitary receives hormonal signals from the hypothalamus via the hypophyseal portal sinusoid vessels, regulating in situ pituitary hormone synthesis and secretion (Rizzoti and Lovell-Badge 2005). The anterior pituitary contains various trophic cell types which synthesize and secrete trophic hormones that act on target endocrine organs to elicit a physiological response detailed in Table 1.3 (Besser 1974a; Besser 1974b; Besser and Mortimer 1974; Amar and Weiss 2003).

Table 1.3: Hormones released by the pituitary in response to hypothalamic paracrine signalling, their respective target organs and the main regulators of pituitary hormone release (Adapted using Amar and Weiss 2003).

Cell type / area	Hormone(s)	Releasing hormone	Target organ(s)	Main regulators
Anterior pituitary				
Corticotrophs	ACTH	CRH	Adrenal gland	Stress, glucocorticoids
Gonadotrophs	LH, FSH	GnRH	Ovary	Estrogens, progesterone inhibin
Lactotrophs	Prolactin	PRH	Breast, uterus	Light, stress, estrogens, glucocorticoids, suckling
Somatotrophs	GH	GHRH	Liver	Estrogens, insulin
Thyrotrophs	TSH	TRH	Thyroid gland	Thyroxine, Somatostatin,
Pars intermedia (rodents)	MSH	-	Skin melanocytes	UV light
Posterior pituitary				
PVN	Oxytocin		Brain, breast, uterus, cervix	Suckling, cervical contractions
SoN	Vasopressin (also known as Anti-Diuretic hormone)		Kidney, CNS, cardiovascular system	Blood volume, pressure and osmolality

ACTH=adrenocorticotrophioc hormone; CNS=central nervous system; CRH=cortocotrophic releasing hormone; GH=growth hormone; FSH=follicle stimulating hormone; GHRH=growth hormone releasing hormone; GnRH=gonadotrophin releasing hormone; LH=luteinising hormone; TSH=thyroid stimulating hormone; TSH=thyrotrophin releasing hormone; MSH=melanocyte stimulating hormone; PVN=paraventricular nucleus; SoN=supraoptic nucleus; UV=ultraviolet

One important feature of the hypophyseal portal system is a vascular arrangement allowing the precise conduction of undiluted hormonal signals from the hypothalamus directly to the cells of the anterior lobe, stimulating trophic cells to secrete hormone directly into the venous circulation (Amar and Weiss 2003). The hypophyseal artery divides into a selection of highly permeable sinusoid capillaries which contact the anterior pituitary allowing small macromolecules (such as GnRH) access to the trophic cell types (Amar and Weiss 2003). Both the anterior and posterior lobes contact venous sinusoid capillaries which empty into the hypophyseal vein (Besser 1974a; Besser 1974b).

In pre-gonadotroph cells, the common α gonadotrophin subunit (αGSU) is the first gonadotrophin subunit to be expressed as Rathke's pouch forms during mouse

pituitary development at e10.5, six days later LHβ subunit expression follows at e16.5 and the FSHβ subunit is expressed seven days later at e17.5 (Rizzoti and Lovell-Badge 2005; Kelberman, Rizzoti et al. 2009). Across mammalian species there is consistent basal activation of the gonadotrophin subunit genes affected by various transcription factors present within the gonadotrophs. When GnRH binds to its cognate receptor at the gonadotroph cell surface PKC, MAPK and calcium signalling can each affect subunit expression at the promoter level (Brown and McNeilly 1999).

At the endocrine level, steroid hormones also alter gonadotrophin subunit expression. E2 is known to decrease αGSU mRNA as well as LHβ mRNA via down-regulation of the transcription factor SF-1 and in addition, E2 and P4 both negatively regulate FSHβ expression via activating protein-1 (AP-1) (Wang, Fortin et al. 2008; Fortin, Lamba et al. 2009). Additionally, GnRH pulse frequency affects gonadotrophin transcription. A higher frequency favours αGSU and LHβ synthesis while a lower pulse frequency favours synthesis of FSHβ mRNA (Haisenleder, Dalkin et al. 1991; Haisenleder, Yasin et al. 1997).

1.6.2. The GnRH pulse generator

Gonadotrophin releasing hormone (GnRH) is a decapeptide, Glu-His-Trp-Ser-Tyr-Gly-Leu-Arg-Pro-Gly-NH_2, synthesized by the hypothalamus and released into the hypophyseal portal system in a pulsatile manner (Baba, Matsuo et al. 1971; Schally, Arimura et al. 1971). During development, GnRH neurons migrate from the medial olfactory placode into the brain and are distributed throughout the basal forebrain, medial septum and the medio-basal hypothalamus (MBH). In the adult, GnRH neurons can be found in the hypothalamus, the medial pre-optic area (POA), the retrochiasmatic area and the arcuate nucleus (ARC) (Ebling 2005). Such extensive distribution of GnRH neurons allows signal reception from a wide variety of steroid hormones, growth factors, neurotransmitters and other signaling peptides. There exists a clear link between pulsatile GnRH release and LH release (Figure 1.10), demonstrating that GnRH controls the female menstrual and estrus cycles in

two distinct fashions: (1) as a regulator of pulsatile LH secretion and (2) as an initiator of the pre-ovulatory LH surge (Clarke and Cummins 1982; Clarke and Cummins 1985; Clarke and Cummins 1987; Clarke, Thomas et al. 1987; Clarke, Cummins et al. 1989; Maeda, Tsukamura et al. 1995). However, GnRH neurons lack the necessary nuclear estrogen receptors (ER) which would mediate steroid hormone signals from the ovary back to the hypothalamus.

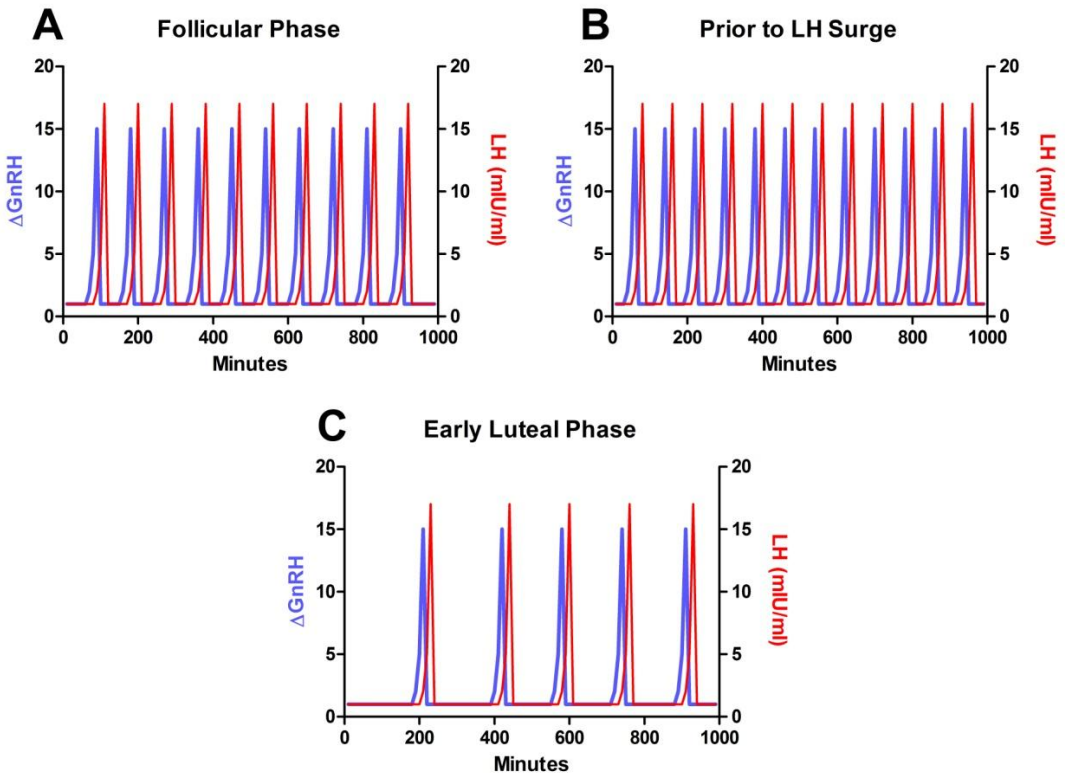

Figure 1.10: The GnRH pulse generator during the female menstrual cycle: (A) In the follicular phase, GnRH pulses operate at a frequency of 1 pulse every 90 minutes; **(B)** Just before the LH surge, GnRH pulse frequency operates at one pulse per hour, priming GnRH neurons for continued GnRH release; **(C)** After ovulation during the luteal phase, negative feedback from E2 reduces GnRH pulse frequency to one pulse approximately every 3 to 4 hours (Adapted from Clarke and Cummins 1982; Clarke and Cummins 1985; Clarke and Cummins 1987; Clarke, Thomas et al. 1987; Clarke, Cummins et al. 1989; Marshall and Griffin 1993).

The arcuate nucleus (ARC) and anteroventral periventricular nucleus (AVPV) are both discrete neuronal regions, but both use kisspeptin (kiss) signaling via orphan G-protein coupled receptor 54 (GPCR54), to regulate the GnRH release from GnRH neurons (Lee, Miele et al. 1996; Muir, Chamberlain et al. 2001). Kiss neurons of the ARC are responsible for GnRH pusatility and those at the AVPV for

the GnRH surge (Maeda, Adachi et al. 2007). Within the AVPV, plasma E2 activates ERα and ERβ on kiss neurons, which at a certain threshold positively feeds forward the signal required for the LH surge (Haisenleder, Yasin et al. 1997). In contrast, E2 feedback at the ARC is negative, modulating GnRH pulse frequency via ERα, with synchronized Kiss release by ARC neurons (Figure 1.11). This allows an episodic release of GnRH from the median eminence (Smith, Clifton et al. 2006). The precise mechanisms which govern E2 positive and negative feedback remain unclear. However experiments in female rats have shown that prior to the LH surge, both the number of Kiss expressing cells and amount of *Kiss1* transcription increase within the AVPV and concomitantly decrease within the ARC (Lin, Li et al.).

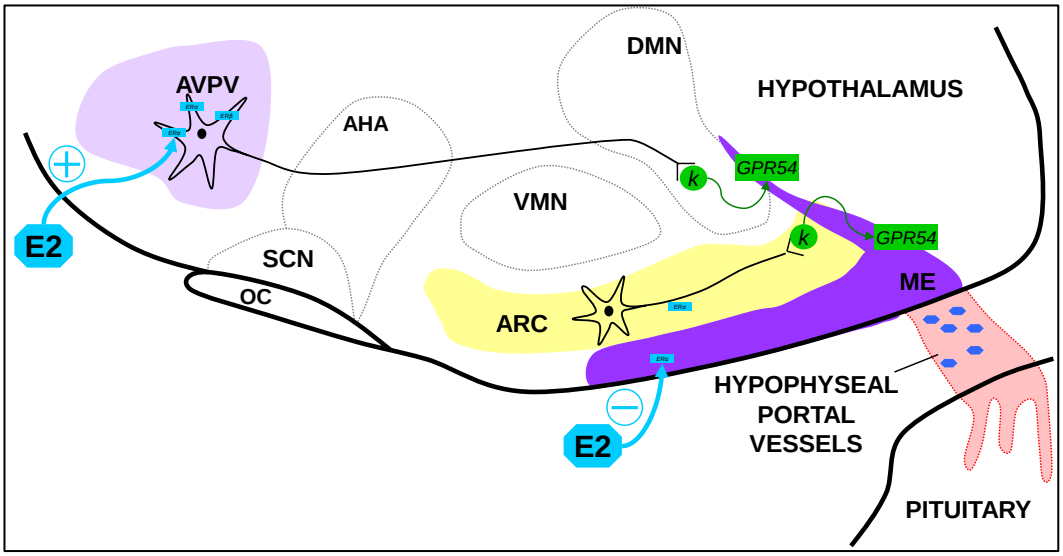

Figure 1.11: Estradiol (E2) feedback to kiss neurons in the anteroventral periventricular (AVPV) and arcuate nucleus (ARC) which synapse in the median eminence (ME) of the hypothalamus. Kisspeptin signals (k) are transmitted via GPCR54 to gonadotrophin releasing hormone (GnRH - blue hexagons) cells which release GnRH into the hypophyseal portal vessels: AHA=anterior hypothalamic area; SCN=suprachiasmatic nucleus; OC=optic chiasm; D/VMN=dorso/ventro-medial nucleus (Adapted from Smith, Clifton et al. 2006).

Androgen receptor has been located to the female pituitary, hypothalamus and POA and may be involved in the regulation of hypothalamic sensitivity to catecholamines and other adrenal hormones (Barley, Ginsburg et al. 1975; Handa and Resko 1989; Miyamoto, Matsumoto et al. 2007). However, the role for this receptor in relation to female reproduction, if such a role exists, remains unknown.

1.6.3. Regulation of gonadotrophin secretion

Gonadotrophin secretion varies over the course of the menstrual and estrus cycles as follicle development progresses towards ovulation (Chapter 1, Sections 3-5) LH release is predominantly regulated by GnRH pulsatility, and FSH release is constitutive, being directly related to the rate of FSHβ mRNA synthesis (McNeilly, Crawford et al. 2003). During the follicular phase of the menstrual cycle in humans, and during diestrus in rats, GnRH pulse frequency is increased favouring regulated LH synthesis and storage before the pre-ovulatory LH surge. During the luteal phase of the menstrual cycle and proestrus/estrus in rodents, GnRH pulse frequency is slightly slower, favouring constitutive FSH synthesis and secretion (Haisenleder, Ortolano et al. 1993; Marshall, Dalkin et al. 1993; Adams, Taylor et al. 1994; Sisk, Richardson et al. 2001). Both gonadotrophins are secreted by the same bi-hormonal gonadotroph cells (Figure 1.12), although distinct populations of smaller 'mono-hormonal' gonadotroph cells have been identified in primates, ruminants and rodents (Childs, Hyde et al. 1983; Childs 1985). The proportions of these distinct mono- and bi-hormonal cell populations change over the course of the cycle in rodents in response to negative and positive feedback mechanisms, although ovine studies have proved conflicting and the cyclical changes observed have yet to be investigated thoroughly in primates (Thomas and Waring 1997; Thomas and Clarke 1997).

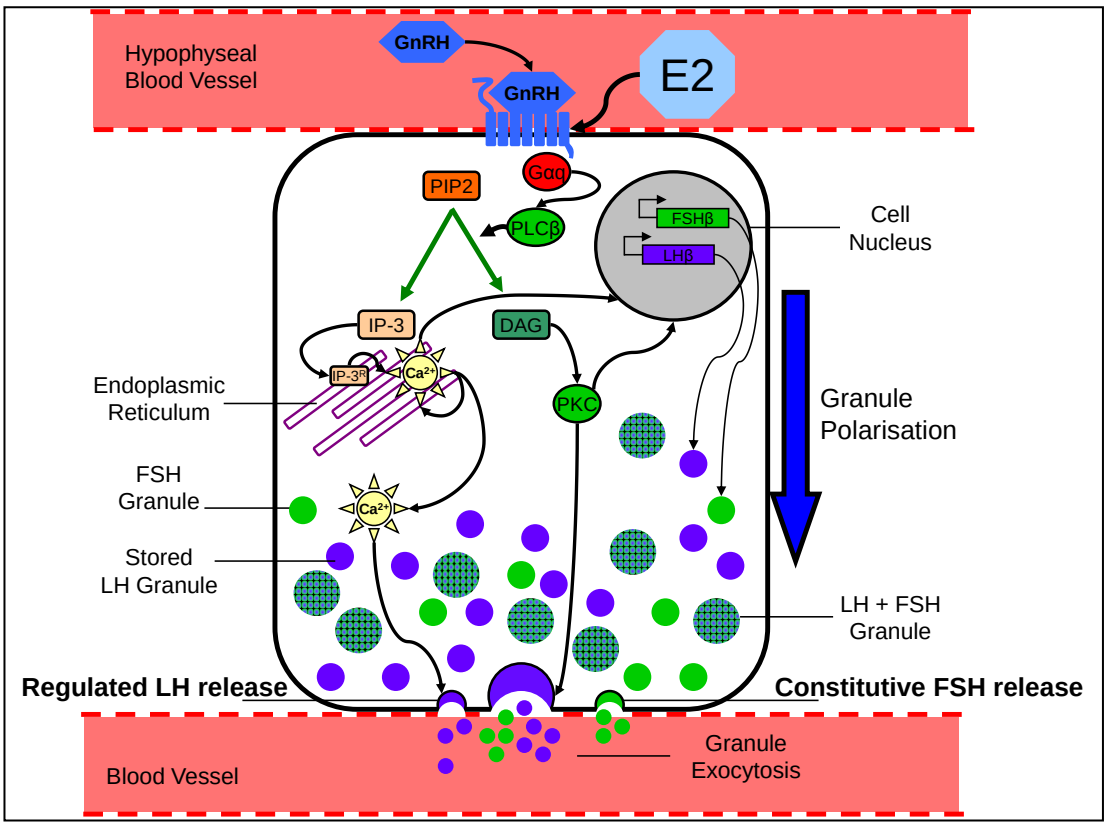

Figure 1.12: Mechanisms of regulated LH and constitutive FSH gonadotrophin storage and secretion (Adapted from McNeilly, Crawford et al. 2003; Naor 2009)

LHβ is constitutively synthesized and just 5% is secreted in a pulsatile manner during the luteal and follicular phases. LH pulsatility directly mimics that of GnRH, and studies in ruminants have demonstrated that 95% of LH synthesized is stored in granules within gonadotrophs (McNeilly, Crawford et al. 2003). During the follicular phase of the cycle, and through the influence of E2 and GnRH upon actin cytoskeletal components, LH granules move from the cytoplasm towards the hypophyseal sinusoids, the optimal site for gonadotrophin exocytosis into the circulation. Indeed more than 90% of LH granules are located at the cellular periphery during the LH surge, and this number drops to less than 20% in the luteal phase of the cycle (Crawford, Currie et al. 2000; Crawford and McNeilly 2002). LH granular storage is exhausted after ovulation and is replenished in the subsequent days of the luteal phase; basal pulsatile LH secretion (again, in line with that of GnRH) however resumes after 48 hours (Crawford, Currie et al. 2000).

FSHβ secretion, although constitutive and in line with FSHβ mRNA synthesis, is also related to GnRH pulsatility (McNeilly, Crawford et al. 2003). Up to two thirds of constitutive FSH release occurs in line with GnRH release. These studies noted that although distinguishing FSH protein isoforms together with the long half life of FSH mRNA, poses a significant problem when deducing the mechanism whereby FSH release occurs independently of GnRH (Padmanabhan and Sharma 2001). A specific FSH-releasing signal may yet exist since in the presence of GnRH antagonists a pulsatile element of FSH secretion remains. However, no protein or gene has been isolated to confer this function (Padmanabhan and McNeilly 2001). The disparate packaging of FSH and LH into distinct granules may explain how differential secretion is achieved (Nicol, McNeilly et al. 2002).

Investigations into protein packaging molecules, specifically secretagranins (Sg) and chromogranins (Cg) indicate that discrete gonadotrophin packaging mechanisms exist, even within the same cell, allowing the distinct secretory patterns of the gonadotrophins. SgII is one such granin associated with storage and secretion of hormones by endocrine cells (Courel, Soler-Jover et al. 2010). SgII is an electron dense secretagranin that binds calcium ions and has been localised to LH positive granules in pituitary gonadotrophs. Conversely CgA is an electron light chromogranin, localised to FSH positive granules. Such differential storage allows differential secretion, but does not account for the presence of basal LH secretion in the absence of GnRH receptor signalling (McNeilly, Crawford et al. 2003). Studies in sheep have demonstrated that SgII-negative granules containing LH exist, surrounded by FSH within the same granule, which may indicate one pathway of basal LH secretion (Crawford, Currie et al. 2000; Crawford and McNeilly 2002; Crawford, McNeilly et al. 2002; Crawford, McNeilly et al. 2004).

Gonadotrophin secretion is regulated at the endocrine level through feedback of growth factors and steroid hormones. FSH secretion is negatively regulated by estradiol as well as inhibin B, both of which increase GnRH pulse generator frequency, leading to increased GnRH signalling to gonadotrophs causing exocytosis

of LH into the general circulation, thus inducing ovulation (Padmanabhan and McNeilly 2001).

Furthermore, the actions of activin and inhibin feedback in the pituitary are antagonistic. Activin augments FSH synthesis and secretion while inhibin, follistatin and betaglycan bind available activin and type II activin receptors, lowering FSH synthesis. (Bilezikjian, Blount et al. 2006). Moreover, FSH synthesis and secretion may be further controlled by an activin/inhibin regulatory loop; recent *in vitro* studies have shown that activin-A also promotes synthesis of activin B, and to a lesser extent inhibin-B within pituitary LTβ2 gonadotroph cells. Activin-B then signals via smad2/3 phosphorylation to induce furin, a pro-convertase enzyme, which thus also promotes inhibin-B synthesis, and finally inhibin-B negatively regulates both furin production and FSH synthesis and secretion (Antenos, Zhu et al. 2008). Through these complex protein-protein interactions and phosphorylation signalling cascades, gonadotrophin synthesis and secretion is modulated throughout the female reproductive cycle.

1.7. Steroids in reproduction and metabolism

Steroid hormones are vital for proper maintenance of mammalian endocrinology; synthesis and release of steroids is appropriately timed and regulated in order for reproduction, metabolism and growth to function correctly. Steroid hormones are large hydrophobic compounds synthesised from a parent molecule of cholesterol derived from acetyl-coA (Rang, Dale et al. 2003). Steroid hormones can therefore be categorised into five major steroidogenic groups according to how many carbon molecules they comprise and their modes of action within the mammalian system (Rang, Dale et al. 2003). Exposure or lack of proper exposure to various steroids during development and in adulthood can potentially lead to certain pathophysiologies; hypospadias, cryptorchidism (males), premature ovarian failure, polycystic ovarian syndrome (females), congenital adrenal hyperplasia (CAH), and hypothyroidism to name a few (Kopelman 1994; Barnes 1997; Welsh, Saunders et al. 2008).

The synthesis of steroid hormones is dependent on the activity of tissue specific enzymes which catalyse the addition or removal of various chemical groups, for example a 17α hydroxylase enzyme will catalyse the addition of a hydroxyl OH group connected to the 17^{th} carbon in the molecule. The nomenclature and classes of steroid hormones synthesized by various steroidogenic enzymes within endocrine tissues are detailed in Figure 1.13. The genes encoding these steroidogenic enzymes along with tissue specificity are shown in Figure 1.14.

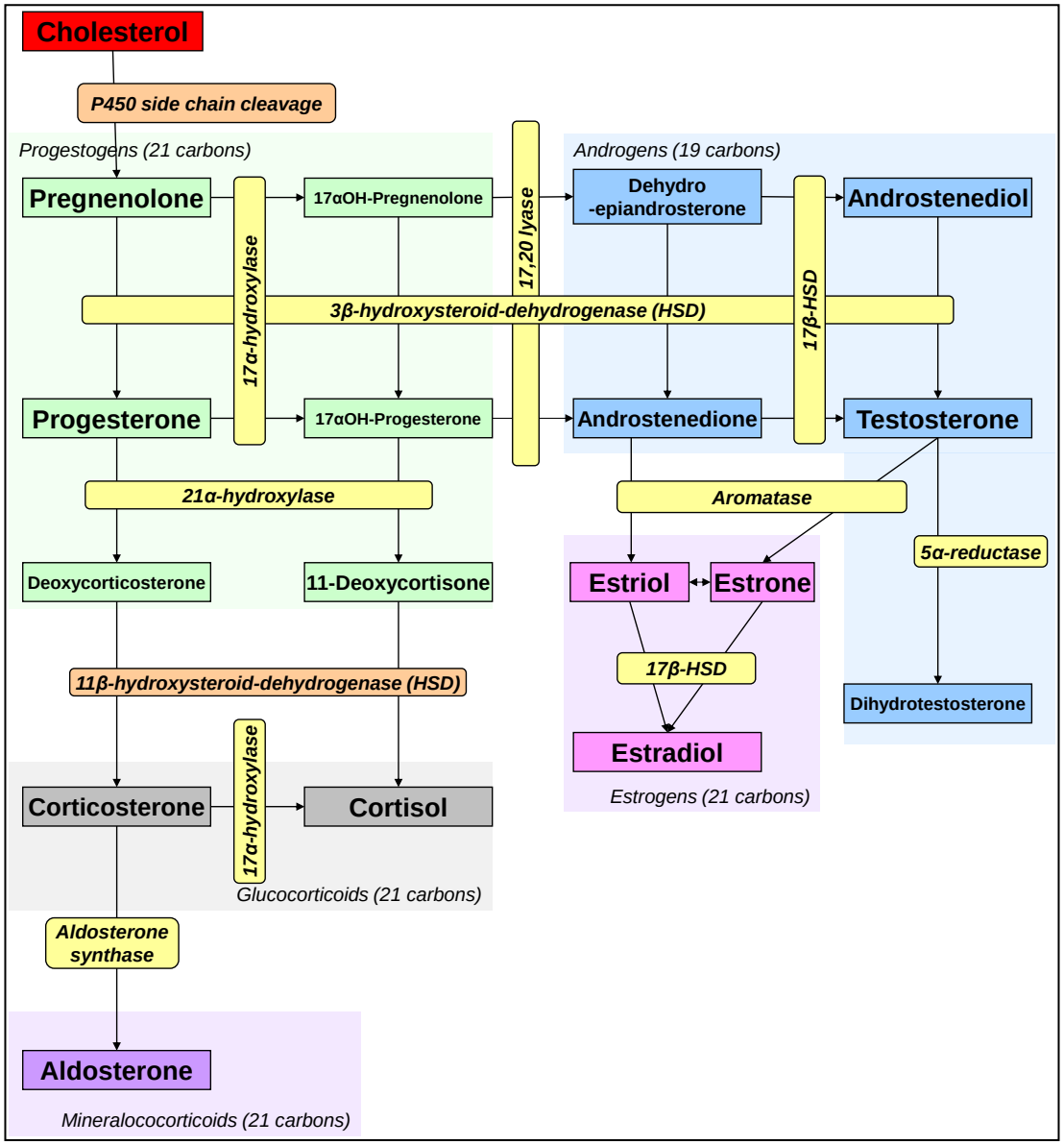

Figure 1.13: Ovarian and adrenal steroidogenesis by steroid type: Synthesis of progestagens (green boxes), androgens (blue boxes), estrogens (pink boxes) glucocorticoids (grey boxes), and aldosterone (purple box) by various steroidogenic enzymes located in the endoplasmic reticulum (yellow boxes) and cytoplasm (orange boxes) Steroids can be classified by their carbon chain number (Payne and Hales 2004).

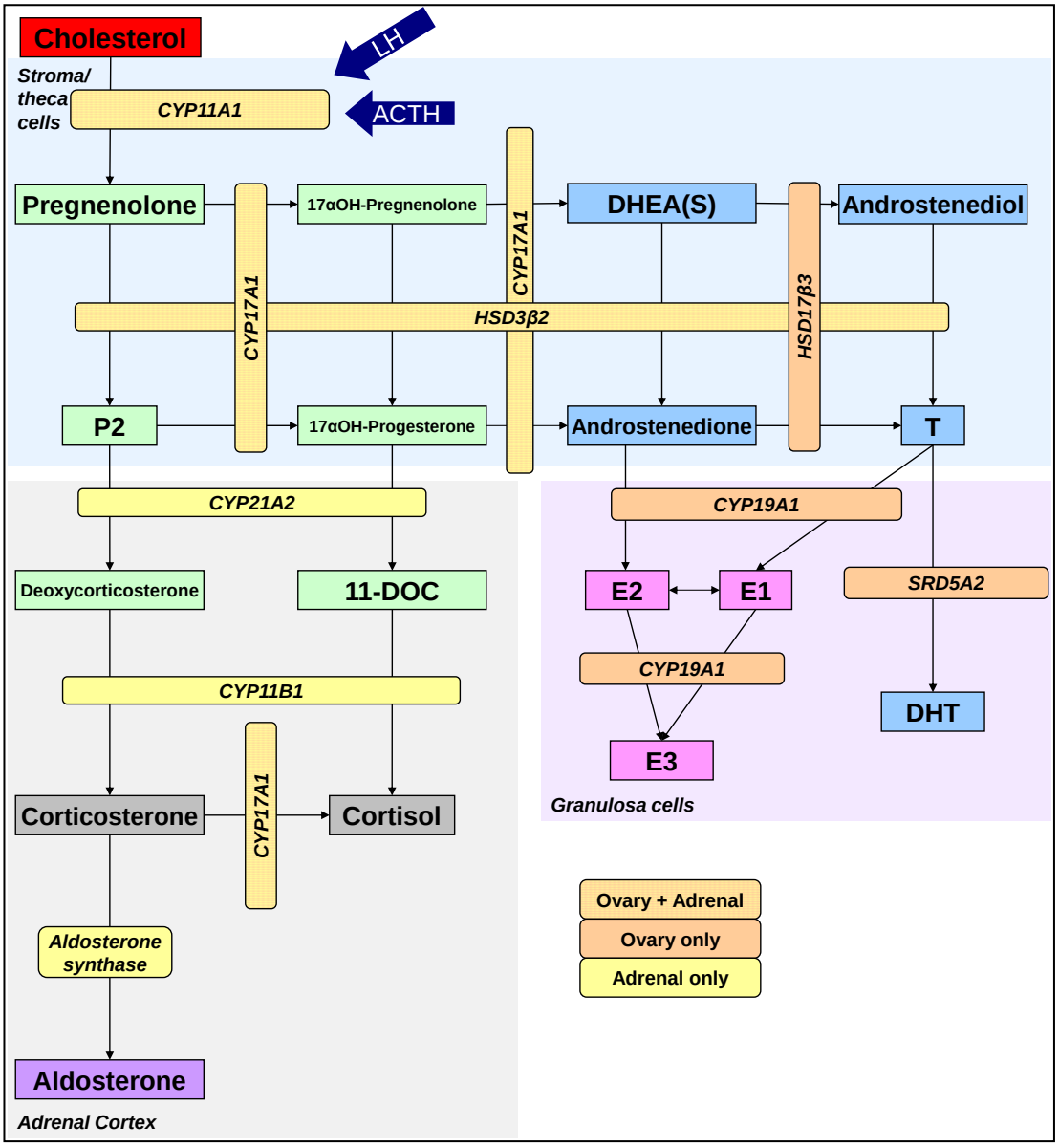

Figure 1.14: Ovarian and adrenal steroidogenesis by steroidogenic enzyme gene nomenclature: Progestagen, androgen, estrogen, glucocorticoid and aldosterone synthesis in various steroidogenic tissues including theca cells (blue box), granulosa cells (pink box) and adrenal cortex (grey box). Steroidogenic enzymes are shown by their gene names and correspond to the same enzymes detailed in Figure 1.13, these enzymes are expressed either in the ovary (orange boxes), the adrenal (yellow boxes) or both (orange and yellow boxes) (Payne and Hales 2004).

1.8. The role of androgens in reproduction

Androgens are often referred to as male hormones since production of T in the testes is required for spermatogenesis and therefore fertility in males. As shown in Figure 1.13 and Figure 1.14, androgens are also produced by the adrenal and ovary in response to endocrine signals from the brain. Within the ovary the main function of A4 and T is that they are precursors to the estrogenic hormones which feedback to the pituitary. However the androgen receptor (AR) is nevertheless present throughout the ovary, particularly in stromal, thecal and granulosa cell types. Moreover, AR knockout (ARKO) female mice are infertile and therefore androgens must have their own functions with regards to the developing follicle (Yeh, Tsai et al. 2002).

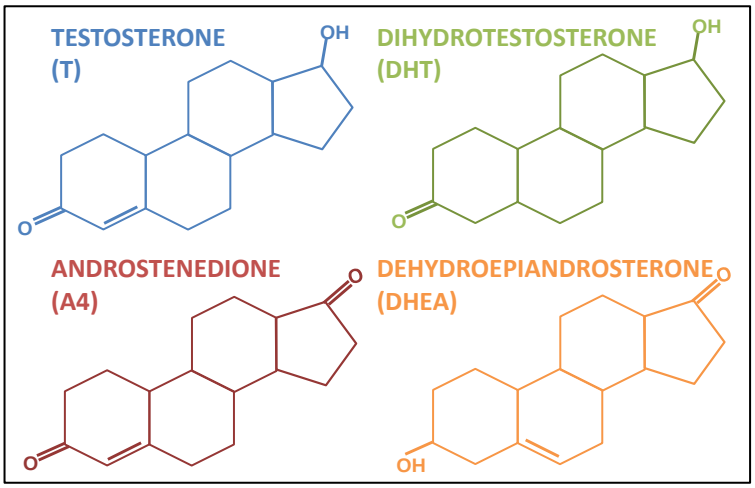

Figure 1.15: Molecular structures of endogenous androgens: DHT is the most potent androgen (against the androgen receptor) and is non-aromatisable, T and A4 are the second and third most potent androgens and are both aromatisable, while DHEA has the weakest potency and is also not aromatisable (Rang, Dale et al. 2003).

Although androgens have many physiological roles, particularly in reproduction and metabolism, other compounds which mimic the actions of androgens (and estrogens) and could potentially disrupt mammalian endocrinology, have been studied extensively. Humans are exposed to many organic and inorganic compounds during their daily lives and the physiological consequences of transmission of environmental toxins, either through the food chain or environmental exposure remain to be fully documented (Sharpe ; Bucher 2009).

1.8.1. The Androgen Receptor

The androgen receptor (AR), a member of the nuclear receptor (NR) superfamily, is present as two isoforms within humans, the second lacking a portion of the amino-terminal domain (ATD) that is involved in receptor transactivation (Wong, Burghoorn et al. 2004). In ruminants and rodents however, only one isoform of the AR is known. Across species, the AR gene, like that of other NRs, displays a high degree of homology and is located at chromosome position Xq11-q12 (Reviewed in Zheng, Yang et al. 2010). Indeed, many X-linked fertility disorders in males are the result of defective AR signaling, passed down maternally as X chromosome mutations (Stouffs, Tournaye et al. 2009; Stouffs, Vandermaelen et al. 2009; Zhang, Yang et al. 2010).

The AR protein has a similar conformation to other NRs most importantly a carboxyl terminal ligand binding domain (LBD), which can bind an androgen molecule. All NR LBDs contain twelve α-helices which co-ordinate into a hydrophobic 'pocket' and upon ligand binding helix 12 repositions to 'lock in' the steroid molecule. Another key element to NRs is the presence of a DNA binding domain (DBD), containing two Zinc molecules which co-ordinate the cysteine residues involved in DNA binding as the NR effects transcription events (Ribeiro, Kushner et al. 1995). Activation function (AF) segments (which, in other NRs have their own distinct protein regions) exist within the DBD and LBD and are responsible for activating the receptor complex, leading to dimerization, translocation and/or degradation (Dennis, Haq et al. 2001; Whittle, Powell et al. 2007). A more detailed exploration of AR gene and protein structure can be viewed in Figure 1.16.

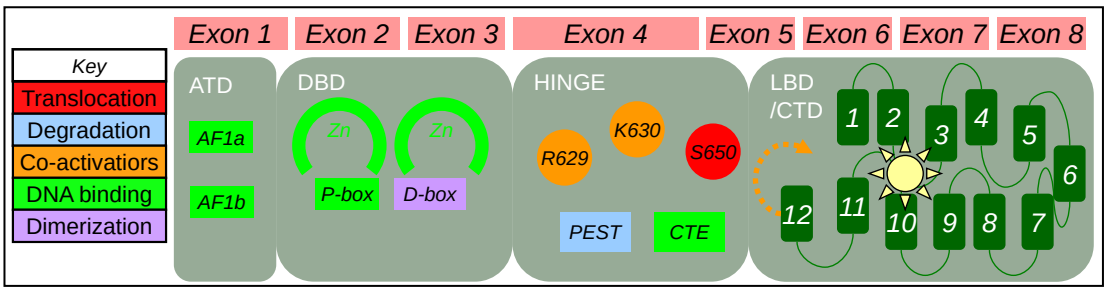

Figure 1.16: Structure of the AR coding sequences and protein: Key amino acid (aa) sequences are shown in boxes and single conserved aa in circles with colour coded functions. In the amino terminal domain (ATD) activation functions (AF) 1a and b serve to potentiate receptor activation of the ligand binding domain (LBD) in the presence of androgen ligand. Other nuclear receptors (NRs) however, possess specific AF domains. All NRs do contain a DNA binding domain (DBD), characterised by two conserved Zinc (Zn) fingers, the first of which includes a 'P-box' sequence containing conserved aa which recognise androgen response elements. The second Zn finger contains a 'D-box', necessary for DNA binding and dimerization. The hinge region may function as phosphate-acceptor to co-activators, in addition to playing a role in AR degradation. Finally, the ligand binding (LBD) or C-terminal domain (CTD) is similar to that of other NRs; 12 α-helices surround a ligand-binding cavity. Helix 12 acts as a second AF domain, repositioning upon ligand binding, closing the ligand cavity and allowing co activators to dock at the CTD before dimerization occurs (Adapted from Claessens, Denayer et al. 2008).

Upon ligand binding, the AR acts as a transcription factor; two AR dimerize and translocate to the cell nucleus, where they bind various co-activators/repressors, subsequently affecting gene transcription events through the recognition of hexameric AR response elements (ARE) (Centenera, Harris et al. 2008). All steroid receptors, not just the AR, bind specific inverted hexameric repeat sequences. Indeed the glucocorticoid (GR), mineralocorticoid (MR) and progestagen receptors (PR), in addition to the AR bind the consensus sequence 5`-TGTTCT-3`; conversely estrogen receptors ERα and ERβ bind the hexameric repeat 5`TGACCT-3`. More selective AREs exist that are not recognised by other NRs, and this together with tissue specific expression of steroid receptors, can alter disparate gene expression events across cell types (Claessens, Denayer et al. 2008).

Nuclear receptor actions were initially documented as alterations in gene transcription events over the course of hours and days. However, research into the effects of NRs lacking DBDs demonstrated short-term alterations in cellular function over the course of minutes and even seconds (Claessens, Denayer et al. 2008). This

led scientists to postulate that NR actions could also be non-genomic in nature, effecting calcium release and even ion channel function(s) and over the last decade, such non-classical actions of the AR and other steroid receptors have now been documented (Clarke and Khosla 2009).

Within the ovary, androgens act via the AR to promote GC proliferation as the follicle progresses from the primary to the early antral stage of follicular development. Furthermore androgens are precursors for mGC E2 biosynthesis (Hillier, Zeleznik et al. 1980; Hillier and De Zwart 1981; Hillier and Tetsuka 1997). In primary GC cultures DHT has been shown to inhibit aromatase activity and lead to follicular atresia, and so conversion of T by 5α-reductase to 5αDHT within the ovary may prevent follicles progressing to the pre-ovulatory stage (Hillier and De Zwart 1981). Thus modulation of androgen action via the activity and expression of androgen-converting enzymes is just as important as AR expression itself.

1.9. Developmental programming

The concept of developmental programming relates to how changes in the *in utero* or early life environment during key windows of development can detrimentally affect adult animal physiology. This link between development and adult disease was identified using epidemiological studies, such as investigations into the 1940s Dutch famine and it's affects upon adults born during this period - these people developed features of the metabolic syndrome including obesity, type-2 diabetes Mellitus (T2DM) and cardiovascular disease (CVD) (Roseboom, van der Meulen et al. 2001; Roseboom, van der Meulen et al. 2001; Painter, de Rooij et al. 2007). In 1997, Dr David Barker published his hypothesis on the fetal origins of adult disease, observing in animal models that lack of proper nourishment during development *in utero* was not directly the cause of the coronary heart disease phenotype observed in adult animals (Barker 1997). Instead, Barker hypothesized that alterations to the *in utero* environment somehow affected fetal growth in a disproportionate manner, particularly during mid/late gestation in humans, predisposing the adult offspring to various metabolic pathophysiologies (Barker 1997; Barker 1997). He also noted that different tissues have their critical periods of growth at different times of development (Barker 1997). Current research suggests a predictive adaptive response (PAR) of the fetus to the developing environment exists, whereby if nutrient restriction during development occurs offspring physiology compensates to account for nutrient restriction once outside of the womb (Reviewed in McMillen and Robinson 2005).

The mechanism(s) through which such developmental programming of adult disease occurs are thought to be epigenetic in nature i.e. alterations to gene expression without changes to the DNA sequence itself. Potential epigenetic alterations include changes to the methylation, phosphorylation or acetylation of histones in order to increase or decrease (silence) gene/promoter expression, in addition to changes in the expression of cofactors or enzymes involved in the transcription and modification of DNA coiling, RNA splicing and stability (Fowden and Forhead 2009). However, it should be noted that despite some research into the

mechanistic aspects of epigenetics, relatively little is known about epigenetic programming or the epigenome.

Mammalian development is mediated by the controlled expression of factors and hormones within the mother, placenta and fetus. Hormones expressed by the mother, placenta and fetus during development may respond to alterations in oxygen availability, temperature, photoperiod, nutrition and even maternal stress (Seckl, Cleasby et al. 2000; Fowden and Forhead 2004; Fowden, Giussani et al. 2005; Fowden, Forhead et al. 2008). Therefore, changes in the timing, duration and level of hormones or other signaling molecules secreted by the fetus, derived from the placenta or which cross from the mother through the placenta-fetal barrier, may alter the transcription or in/activation of other factors during development via epigenetic mechanisms (Figure 1.17).

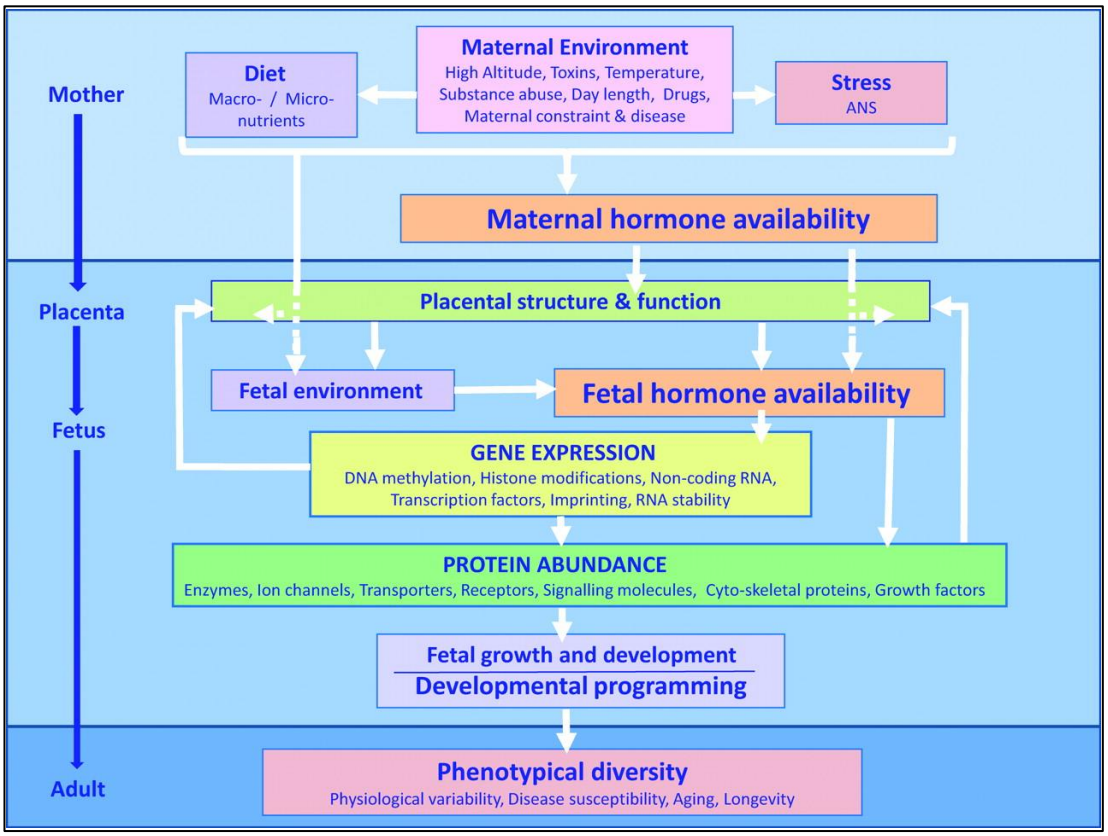

Figure 1.17: Hormones as epigenetic programmers of adult disease (Taken from Fowden, Giussani et al. 2005).

In terms of steroid hormones and their effects upon the developmental programming of mammalian development, estrogen is required in female mammals for the maintenance of primordial germ cell nests during development and testosterone is important for the proper progression of male sexual and behavioural development (Chapter 1, Sections 2 and 5). However, relatively little is known about the effects of these sex hormones when administered outside the critical windows of development. Some studies in male rodents have shown that exogenous testosterone exposure during periods of fetal and neonatal life leads to male reproductive dysfunction (Welsh, Saunders et al. 2008). Furthermore, exogenous androgens given during fetal life in primates and sheep has also been shown to produce a reproductive phenotype in the adult female animal (discussed in Section 11).

The majority of research into the fetal programming of adult disease has focused upon the effects of corticosteroids and other synthetic glucocorticoids, for example dexamethasone (DEX), upon metabolic development Exposure of a pregnant rats to corticosteroids leads to a reduced pup birth weight and development of metabolic syndrome in the adult offspring demonstrating insulin resistance, glucose intolerance and hypertension (Cleasby, Kelly et al. 2003; Buhl, Neschen et al. 2007). The consequences of synthetic corticosteroid administration to the rat vary as they depend on which stage of development the animals have reached and what doses are used. It should also be noted that DEX is almost sixty times more potent than it's physiological rodent analogue, corticosterone (Baldwin and Sawyer 1974). Disturbed menstrual cycles are a common feature in women with Cushing's Syndrome, and so researchers sought to investigate the effects of DEX upon adult reproductive function. Daily exposure of 0.25-0.4μg DEX to mature female rats resulted in dose dependent pseudopregnancy, indicating that corticosteroids can modulate prolactin secretion, elevating it for prolonged periods of time (de Greef and van der Schoot 1987). The same studies also noted that in adult females treated with DEX, the ovulation rate was significantly increased. This was later confirmed to result from an initial early phase obstruction of ovarian inhibin secretion by DEX, leading to reduced anterior pituitary feedback, subsequently followed by a later

phase of increased FSH release and the ovulation of more follicles (Tohei, Sakamoto et al. 2000; Tohei, Sakamoto et al. 2001). Such observations support the notion that corticosteroid treatment in human anovulatory disorders might be beneficial in restoring ovulation. In contrast, a higher 1mg/kg bolus dose of DEX given in adulthood, has been found to completely disrupt ovulation in the rat, lowering ovarian volume and causing aberrant nuclear receptor expression in granulosa and thecal cell compartments (Illera, Silvan et al. 2005). This may be because glucocorticoids are known steroidal anti-inflammatory compounds, and since ovulation is largely an inflammatory process, large doses of glucocorticoid would be expected to inhibit ovulation.

1.9.1. Endocrine tissues and development

Given that much of this thesis will focus upon the effect of steroid administration during fetal and neonatal development of the rat (Chapters 4-7), this section will cover the relevant endocrine systems discussed. Although parallels between rodent and human metabolic development exist, research into mid and late gestational development of human endocrinology and metabolism is difficult given the sensitive nature of such research and paucity of tissue samples during later gestation.

i. Adipose tissue

Fibroblasts originating from blastocyst mesoderm form preadipocyte cells which differentiate into adipocytes during late embryonic development and shortly after birth in humans. In rodents preadipocytes differentiation occurs after birth only (Ailhaud, Grimaldi et al. 1992; MacDougald and Lane 1995). Differentiation of preadipocytes is stimulated by a variety of metabolic factors, including insulin, glucocorticoids, and cAMP elevating agents. During the course of around one week, preadipocyte differentiation follows a cycle of mitosis and growth arrest before they differentiate into adipocytes (Ntambi and Young-Cheul 2000). Initially growth factors and hormonal signals influence the expression of transcription factors, which

in turn effects the transcription of adipocyte specific genes (Rodriguez-Acebes, Palacios et al. 2010), e.g. peroxisome proliferator activating receptor-γ (PPARγ). Together CCAAT/enhancer binding protein (C/EBP) and PPARγ cross talk within the preadipocyte cell to direct the expression of genes characteristic of adipocyte function for example leptin, resistin and the insulin receptor (Gregoire, Smas et al. 1998). As adipocyte-specific gene expression increases, fat droplet formation begins, marking the end of preadipocyte differentiation from a flat fibroblast-like cell into a spherical adipocyte. Most white adipose tissue (WAT) consists of differentiated adipocytes, although preadipocytes are also present (Ntambi and Young-Cheul 2000).

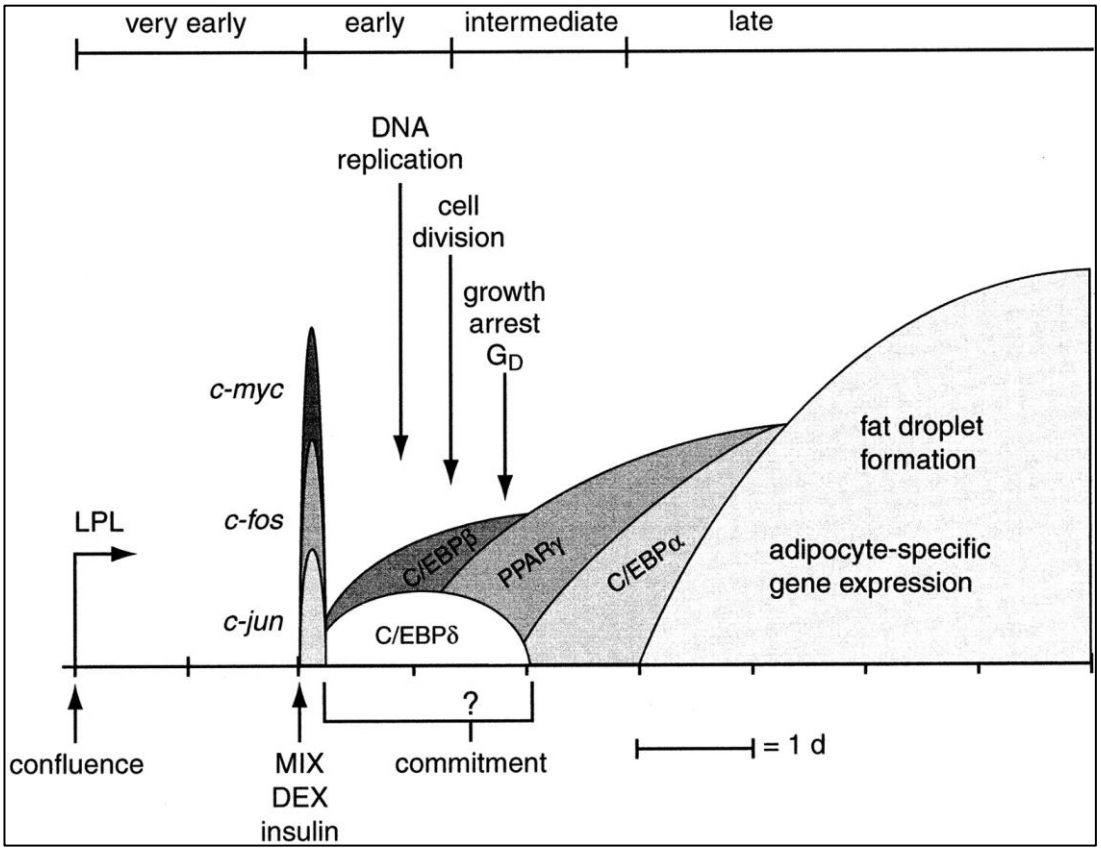

Figure 1.18: Preadipocyte differentiation *in vitro* presented chronologically with gene expression as designated (Taken from Ntambi and Young-Cheul 2000): LPL, lipoprotein lipase; C/EBP, CCAAT/enhancer binding protein, PPAR, peroxisome proliferator-activated receptor; MIX, methylisobutylxanthine; DEX, dexamethasone.

Through regulation by adipogenic factors, adipocytes are able to safely store free fatty acids (FFA) in the form of triglycerides through a process termed lipogenesis. Triglycerides may be broken down and released as FFA and glycerol from the adipocyte, in a process termed lipolysis (Fonseca-Alaniz, Takada et al. 2007). These processes protect the liver, pancreas and muscle organs from the lipotoxic effects associated with high circulating levels of FFA, as seen in clinical cases of lipodystrophy (Crandall, Quinet et al. 2006). Where lipogenesis is favoured over lipolysis, adipocytes become hypertrophied and obesity results (Buckle, Rubinstein et al. 1961; Caserta, Tchkonia et al. 2001). Obesity has far reaching systemic effects as adipocytes secrete hormones involved in the endocrine modulation of metabolism, called adipokines (Ahima 2008; Ahima and Antwi 2008). The adipokines include leptin, a hormone involved in the endocrine regulation of appetite and metabolism (Ahima 2008; Ahima and Antwi 2008), adiponectin, a hormone involved in the autocrine and paracrine regulation of FFA catabolism and glucose homeostasis (Ribot, Rodriguez et al. 2008) and resistin, a hormone involved in the inflammatory pathogenesis of obesity (McTernan, McTernan et al. 2002).

ii. Liver

Hepatocytes and biliary epithelial cells both originate from the endoderm, while the stromal cells, stellate cells, kuppfer cells and blood vessels, originate through the mesoderm (Zorn 2008). Although the liver is formed by embryonic day (e.) 8, hepatic maturation continues until birth in the rodent. During late gestation and early postnatal life, pre and postnatal androgen surges in male rats function to program liver enzyme activities to be low in presence of a highly androgenic environment (Gustafsson and Stenberg 1974; Gustafsson and Stenberg 1974). The adult testes release androgens and consequently inhibit the activity of 5α-reductases, allowing an androgenic hormonal milieu to be maintained. In female animals due to the absence of a postnatal androgen surge, 5α-reductase activity is between four and ten-fold higher than in males in the adult animal (Pak, Tsim et al. 1985). The hormonal milieu in the adult animal is thus programmed to remain in line with the requirements of the animal's physiology; high testosterone (a low level of hepatic

5α-reducion) in males, and low testosterone (a higher level of hepatic 5α-reducion) in females.

In the adult female mammal, the liver has both anabolic and catabolic functions. Of particular relevance to this thesis, is the role of phosphoenolpyruvate carboxykinase (PEPCK). This protein is not only expressed in periportal hepatocytes, but is also found in adipose tissue, kidney proximal tubule epithelium and ileum villar epithelium. Gene expression within these organs is driven by tissue-specific *cis* acting elements, which allows PEPCK to function in different metabolic roles; in the liver, PEPCK is gluconeogenic, whereas in adipose it is glyceroneogenic in function (Beale, Clouthier et al. 1992). Regulation of blood glucose is mediated through the balance of insulin and glucagon release. PEPCK, is the rate-limiting enzyme in hepatic gluconeogenesis and is quickly and dominantly inhibited by insulin release, but it's expression is induced during periods of stress and/or fasting by glucagon (Quinn and Yeagley 2005).

In type 2 diabetes mellitus, increased hepatic glucose production can lead to hyperglycaemia during fasting stages, thus insulin resistance can be reflected by increased hepatic PEPCK expression (Buhl, Neschen et al. 2007). Glucocorticoids also induce the expression of hepatic PEPCK, and so increased stress hormone output by the adrenal can contribute increase hepatic glucose production (Buhl, Neschen et al. 2007). Prenatal programming of PEPCK by steroid hormones has also been documented in the rat. In one study, administration of prenatal corticosteroid led to an increase in adult animals of hepatic PEPCK expression and activity, potentially contributing towards hyperglycaemia (Nyirenda and Seckl 1998).

Hepatic glucocorticoid metabolism occurs through the balance of 11βHSD and 5α-/5β-reductase enzyme activities (Cleasby, Kelly et al. 2003; Buhl, Neschen et al. 2007). In human obesity and in rodent models of obesity, increased glucocorticoid activation by 11β-HSD type 1 and increased glucocorticoid clearance by 5β-

reductase has been documented (Chin, Shackleton et al. 2000; Roelfsema, Kok et al. 2010). In high fat diet (HFD) fed male Wistar rats, this increase in GC turnover has been postulated to occur as a consequence of acute changes in diet and nutrition, whilst animals on a long term HFD, although obese and insulin resistant, show no such changes in corticosteroid metabolism (Drake, Livingstone et al. 2005; Drake, Walker et al. 2005; Stimson, Lobley et al. 2010). In young lean women diagnosed with infertility due to PCOS, two studies have documented glucocorticoid clearance through urinary metabolite analysis, with results inferring an increase in 5α-reduction of glucocorticoids, with no effect on 11βHSD-1 (Chin, Shackleton et al. 2000; Tsilchorozidou, Honour et al. 2003). These molecules of glucocorticoid clearance are therefore of importance when investigating the development of obesity (Chapter 5).

iii. Pancreas

Progenitor pancreatic cells develop from two envaginations of the posterior foregut at e.8.5 in the rodent (Figure 1.19), from which the mature pancreatic ducts, acini and islets all arise by e.13.5 (Kopinke 2008). Maturation of pancreatic islet function occurs shortly after birth in the neonatal rodent, and may be modulated by the nutritional and hormonal status of the postnatal environment (Martens GA, Pipeleers D.)

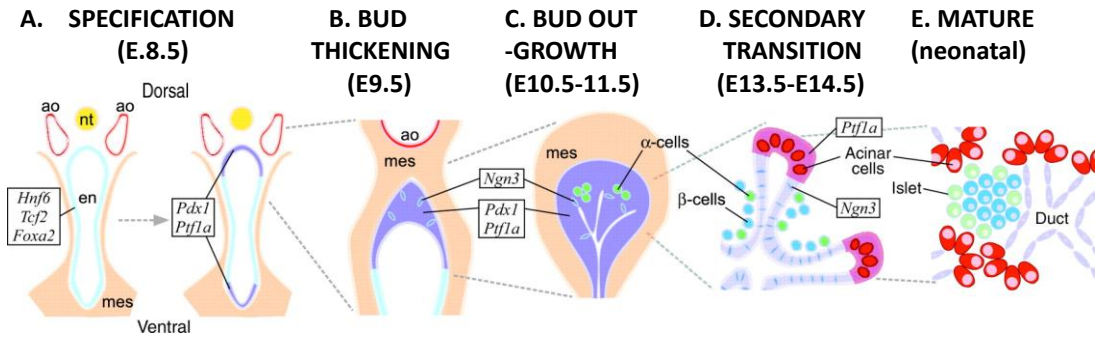

Figure 1.19: Stages of pancreatic development in the rodent during late fetal and early neonatal life (Taken from Kopinke 2008).

Pancreatic function may be assessed by measuring blood insulin and glucose before and after glucose challenge. This allows for observation of any increases in fasting insulin and glucose, in addition to insulin resistance.

iv. The hypothalamic-pituitary adrenal axis

The adrenal is an endocrine organ responsible for the homeostatic regulation of blood volume, steroid hormone secretion and the release of adrenalines in response to external stressors; the 'fight or flight' response (Lin and Achermann 2004). Two adrenals are located on top of each kidney in mammals and release of their secretagogues is directed via a negative feedback loop to the hypothalamic-pituitary axis in the brain (Figure 1.20).

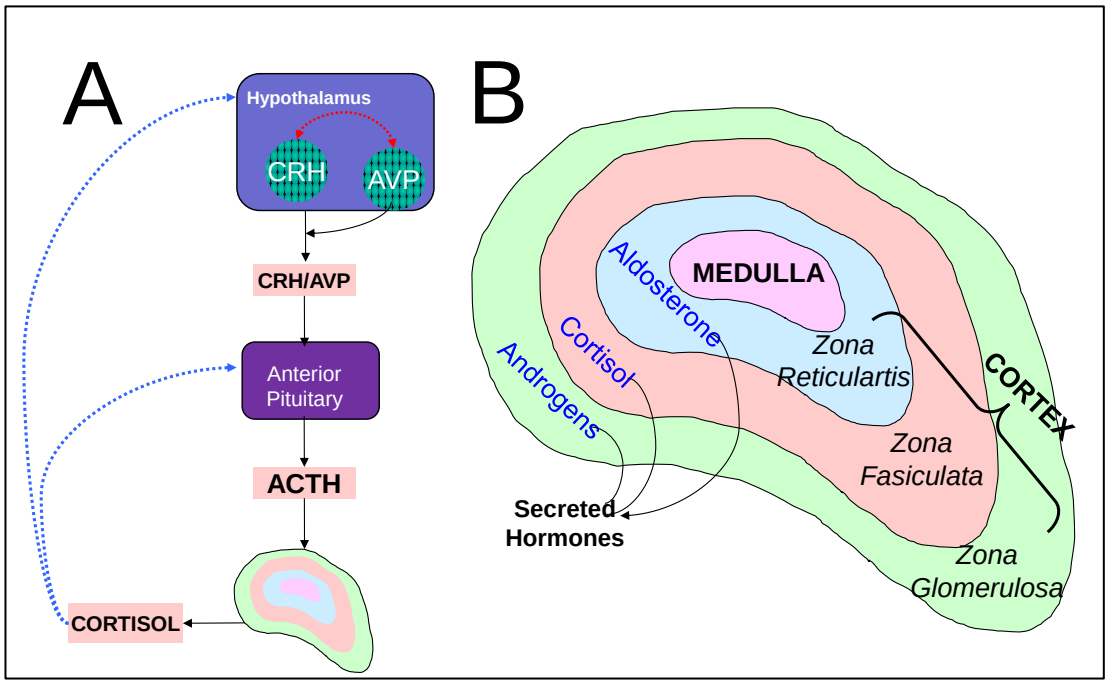

Figure 1.20: The hypothalamic-pituitary adrenal axis (HPAA); (A) The hypothalamus coordinates release of corticotrophin releasing hormone (CRH), which induces release of adrenocorticotrophioc hormone (ACTH). ACTH stimulates cortisol release from the adrenal zona glomerulosa which negatively feeds back to the brain (blue lines). (B) zonation of, and main hormones secreted by the adrenal gland (Adapted from Lin and Achermann 2004).

At the level of the hypothalamus, paraventricular nuclei coordinate with noradrenergic neurons of the central sympathetic nervous system. It is changes in the signals between these neurons, along with any external stressor stimulus (emotional or physical), which lead to the release of neuroendocrine hormones into the hypophyseal portal vessels that connect to the pituitary (Seckl, Dow et al. 1993; Papadimitriou and Priftis 2009). Thus, corticotrophic releasing hormone (CRH) acts in synergy with arginine vasopressin (AVP) to promote the posttranslational processing of proopiomelanocortin (POMC) into adrenocorticotrophic hormone (ACTH) and other molecules at the level of the pituitary (Papadimitriou and Priftis 2009). ACTH is the key regulatory hormone concerning the release of adrenal steroids and adrenalines and is secreted in a circadian pattern also adhered to by adrenal steroids. At the adrenal, ACTH stimulates the secretion of adrenal androgens, glucocorticoid (cortisol in humans, corticosterone in rodents) and aldosterone (Figure 1.20).

1.10. Premature ovarian failure

Premature ovarian failure (POF) (also known as primary ovarian insufficiency) is known to affect 0.1% of women under 30 and 1% of women under 40 with symptoms including amenorrhea and infertility. Women suffering from POF present with hypergonadotrophic hypogonadism, i.e. they exhibit high levels of gonadotrophins and low levels of steroid sex-hormones due to a deficit in ovarian inhibitory feedback at the level of the hypothalamus and pituitary. It is worth noting that although the symptoms of POF are menopausal in nature, POF itself is not considered an early menopause because in over half the women diagnosed, ovarian function remains unpredictable (Nelson 2009). Indeed, women with POF can still exhibit irregular patterns of estrogen secretion and thus may be able to ovulate and carry pregnancies to term after diagnosis, which currently occurs in roughly 10-15% of POI cases (Nelson 2009). Furthermore POF may be transient since treatment of any underlying causes can return the female endocrinology to its' normal state (Kalantaridou and Nelson 2000).

1.10.1. Clinical observations and treatments of POF

POF is defined clinically as a woman under 40 years of age with 4 or more months of disordered menses during which time two blood samples of FSH (1 month apart) yield a value similar to those found post-menopause (greater than 40mIU/mL) (Nelson 2009). Patients are differentially diagnosed by physical examination, signs and symptoms of estrogen deficiency, investigation of karyotype and blood testing for the autoimmune disorders, such as myasthenia gravis. POF patients, like menopausal women, will often be treated with hormone replacement therapy (HRT) via trans-dermal E2 device alongside methoxyprogesterone therapy 12 days on followed by 12 days off, in order to mimic normal hormonal changes seen in women. HRT aims to counteract the detrimental health effects of sex hormone loss which include ischemic heart disease, as well as increased risk of thrombo-embolism and fractures.

1.10.2. Idiopathic and acquired causes of POF

The aetiology of POF is complex given that various endocrine syndromes may underlie the disease, such as autoimmune diseases and mutations in genes involved in follicular development and steroid hormone synthesis. Each such disorder encompasses a distinct plethora of symptoms. To take two examples; myasthenia gravis is associated with chronic fatigue-like symptoms, while the galactose-1-phosphate uridyltransferase (GALT) mutation is associated with kidney failure, mental retardation and cateracts. In relation to immune function one common feature of POF regardless of aetiology is the infiltration of the theca interna with lymphatic cells which possibly contributes to increased atresia of developing follicles, sparing the remaining quiescent primordial follicles which have yet to activate. However, it should be noted that in more than 90% of POF cases, no cause can be identified (Nelson 2009).

A considerable proportion of POF cases are non-syndromic, exhibiting a genetic familial heritability. This has led researchers to focus upon the inheritance of specific gene mutations involved in follicular development. To date, rare mutations in genes involved in early follicular development have been found in patients with POF. Examples include *BMP-15*, *NOBOX* (Qin, Choi et al. 2007), steroidogenic factor 1 (*SF-1*) (Lourenco, Brauner et al. 2009; Martinerie, Bouvattier et al. 2009) POF gene (Lacombe, Lee et al. 2006), in addition to genes involved the gonadotrophic regulation of follicle development, such as LHr and FSHr and LH/FSHβ subunits (Simpson 2008). Furthermore, transgenic studies have documented that GC specific loss of retinoblastoma gene results in POF through increased follicular atresia, possibly via the dysregulation of pRb target genes essential for normal follicular growth and differentiation (Andreu-Vieyra, Chen et al. 2008).

1.11. Polycystic Ovarian Syndrome

Polycystic ovarian syndrome (PCOS) is the most widespread heterogeneous endocrinopathy of women and presents at reproductive age across a range of ethnic backgrounds.

1.11.1. Features of PCOS

Up to 22% of women may have polycystic ovaries (PCO) (Farquhar, Birdsall et al. 1994), but only around 5-10% of women develop the syndrome PCOS, associated with increased androgenisation, weight gain and infertility (Franks, McCarthy et al. 2006). Due to the heterogeneous nature of PCOS uniform diagnostic criteria were not firmly set out until 2004. PCOS is now clinically defined by the appearance of any two out of three diagnostic criteria, as set out by the Rotterdam consensus (Rotterdam Workshop, 2004); (1) the appearance of PCO on an ultrasound scan (2) biochemical or clinical evidence of hyperandrogenaemia (i.e. high levels of androgen hormones) which is not adrenal in origin, and (3) oligo- or anovulation. Studies in sheep (Steckler, Manikkam et al. 2007) and rhesus monkeys (Abbott, Dumesic et al. 1998) support the concept that PCOS develops as a consequence of overexposure during fetal life to androgens or potentially, estrogens (Abbott, Dumesic et al. 2002).

Ovaries from women with PCOS show a characteristic pattern of up to 12 follicles which are between two and nine millimetres in diameter, whereas a normal ovary would have between two and four follicles of this size (Balen, Laven et al. 2003; Dewailly, Catteau-Jonard et al. 2007). In the diagnosis of PCO, transvaginal ultrasound examination is informative. FIGURE 1.21 REMOVED. PCO demonstrate an increased ovarian volume in addition to an increased stromal area when compared to normal ovaries or multi-follicular ovaries (MFO). This stromal area also correlates to the biochemical parameters indicative of PCOS; high LH, T and A4 (Fulghesu, Angioni et al. 2007). Indeed, by analysing a planar ovarian for the stromal/total area ratio in PCOS patients, clinicians can both diagnose and differentiate between women with PCO and those with MFO (Fulghesu, Ciampelli et al. 2001).

The high levels of androgen associated with PCOS are thought to originate from the stroma and theca cell compartments of the ovary. Stimulation of these steroidogenically active tissues by LH leads to an increased production of ovarian androgens (T and A4). This disruption of hormonal milieu is thought to be responsible for the anovulatory phenotype observed in women with PCOS, and appears to be augmented in women who also exhibit obesity. A diagnosis of PCOS does not require features of obesity to be present (Norman, Noakes et al. 2004).

Due to the broad definition of PCOS, the affected female population is naturally heterogenic, and various types of the disorder exist under the umbrella term 'PCOS' shown in Table 1.4. However, it is important to note that women with PCOS have an increased likelihood of type 2 diabetes Mellitus (T2DM) and cardiovascular problems later in life, and such health risks are likely caused by the association of PCOS with obesity (Svendsen, Nilas et al. 2008). Metformin, a known insulin-sensitising agent, has shown some efficacy at improving menstrual frequency along with insulin resistance in PCOS subjects (Setji and Brown 2007). The full aetiology of PCOS remains unknown, however current hypotheses concur that the endocrinopathy likely results from a complex interplay between epigenetic programming by improper steroid exposure during development, genetic risk factors and environmental choices detailed in Figure 1.21 (Holte 1998; Abbott, Dumesic et al. 2002; Franks, McCarthy et al. 2006).

Table 1.4: The various types of PCOS found in women, their prevalence and features (Adapted from Abbott, Dumesic et al. 2002; Norman, Davies et al. 2002; Abbott 2010; Franks 2010; Wild, Carmina et al. 2010).

Human PCOS	Type 1 Classic	Type 2 Classic	Ovulatory	Normo - androgenic
Menstrual cycles	Irregular	Irregular	Normal	Irregular
Ovary	Polycystic	Normal	Polycystic	Polycystic
Androgens	High	High	High	Normal
Percentage of women obese	36%	47%	19%	18%
Percentage of all PCOS diagnoses	59%	10%	21%	10%

1.11.2. PCOS origins

The initial cause of PCOS likely lies at some point along the hypothalamic-pituitary-ovarian axis, and current evidence gathered from various animal models and cell cultures supports either an inherent ovarian or hypothalamic-pituitary defect, and are discussed in the next section. Developmentally timed exposure to androgens, may act as transcription factors directly via their cognate AR or indirectly via ER, and thus developmentally program various endocrine organs, including the ovary, pituitary, adrenal, hypothalamus, pancreas, fat and liver (Dumesic, Abbott et al. 1997; Abbott, Dumesic et al. 1998; Dumesic, Schramm et al. 2005; Franks, McCarthy et al. 2006; Franks 2010). In addition to both genetic and environmental factors, the dose and the length of *in utero* androgen exposure may affect the resultant PCOS phenotype in the immature, adolescent and adult animal (Gorski and Barraclough 1963; Goy and Phoenix 1972; Hickey, Marrocco et al. 2005; Padmanabhan, Sarma et al. 2010). The potential causes of PCOS are laid out in Figure 1.21, which also depicts the clinical indicators in addition to the various outcomes and risk factors associated with this endocrinopathy.

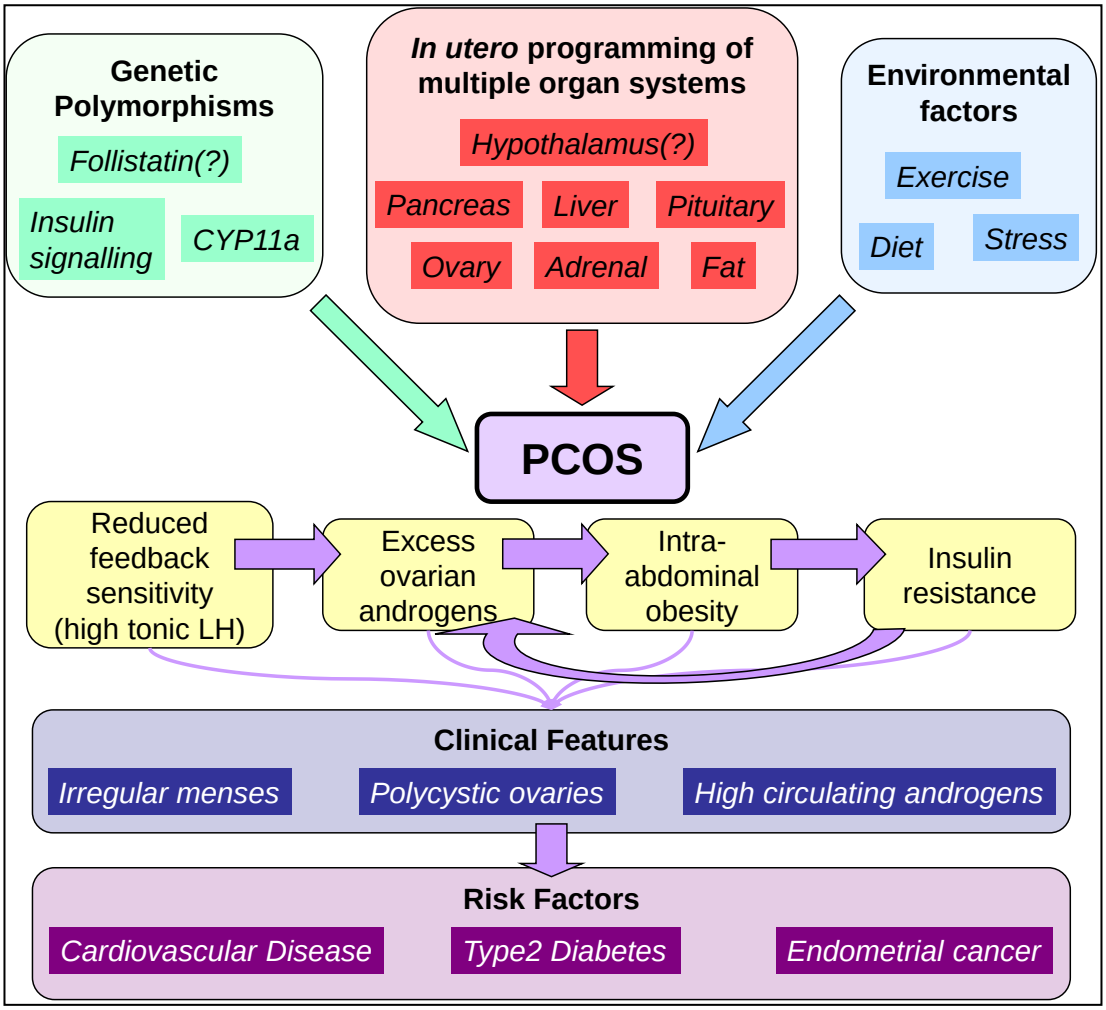

Figure 1.21: Scheme summarising the origins of PCOS: Programming of organ systems by fetal adrenal or ovarian androgens during a sensitive period in development is augmented by both genetic and environmental risk factors. PCOS is characterised by high LH, excess androgens and the metabolic syndrome, insulin resistance of which further augments reproductive dysfunction (Adapted from Abbott, Dumesic et al. 2002).

The source of the androgens able to program a female fetus during development without causing virilization have been debated for some time and are unlikely to be maternal in origin, largely due to the presence of sex-hormone binding globulin (SHBG) in the mother and the steroid metabolizing enzymes of the placenta. Together, these molecules act as a guard against transfer of steroidal compounds to the fetus. One potential source of androgens is the developing fetus itself - androgens which may be ovarian or adrenal in origin (Abbott, Dumesic et al. 2002).

To compensate for the differences in gene product dosage between XX females and XY males, X chromosome inactivation (XCI) takes place during early female development. Either the maternal or paternal X chromosome may be inactivated in different cell lineages, resulting in a mosaic pattern of XCI in the adult (Heard, Chaumeil et al. 2004; Panning 2008). XCI initiates at a locus on the X-chromosome, known as the X-inactivation center (Xic) (Borsani, Tonlorenzi et al. 1991; Tsai, Rowntree et al. 2008). At the Xic locus is the *Xist* gene, which produces a non-coding RNA involved in initiation of XCI (Cantrell, Carstens et al. 2009; Senner and Brockdorff 2009; Chaumeil, Waters et al. 2011). The Xist RNA attaches to the chromosome designated for inactivation extending the length of the chromosome itself through an as yet unknown process (Kalantry 2011). Subsequently, processes of histone methylation, acetylation and further aspects of chromatin remodelling begin (Murakami, Ohhira et al. 2009). XCI is then maintained in the cell and all subsequent daughter cells (Morey and Avner 2010). Theoretically the pattern of XCI is random and highly regulated (Reviewed in Morey and Avner 2010). However, X-inactivation skewing may occur in order to selectively remove cells which may go on to express harmful mutations or display deregulated gene expression (Belmont 1996).

PCOS displays familial clustering characteristic of a dominant gene with partial penetrance, yet standard genetic linkage analyses have struggled to find any causative genetic links, and few candidate genes or promoter repeat sequences have shown a correlation with PCOS. In one relatively recent study, epigenetic patterns of XCI and methylation around X-linked genes have been compared between sisters with varying degrees of PCOS across 40 families, the results of which suggest that XCI patterns, not just genetic sequences, dictate the reproductive phenotype, providing one explanation as to why studies on candidate susceptibility genes often yield negative results and leading to further research on the epigenetic status of X-linked genes, such as the AR (Hickey, Legro et al. 2006).

Sequencing of repeat polymorphisms within genes involved in steroidogenesis and folliculogenesis is the basis of many genetic association studies. Several studies have reported conflicting results when determining whether the number of CAG repeat polymorphisms within the AR gene is associated with factors of PCOS (Franks, Gharani et al. 1998; Hickey, Chandy et al. 2002; Jaaskelainen, Korhonen et al. 2005; Mohlig, Jurgens et al. 2006). The difficulty with such genetic association studies, and indeed with many of the theories surrounding the origin of PCOS, is that even if a correlation between gene expression/polymorphisms and PCOS exists, this does not necessarily imply causality. One problem with familial association PCOS studies is the lack of a corresponding male phenotype in brothers of women with PCOS. However, research into the metabolic phenotypes of the brothers and sons of women with PCOS has shown that these men are more likely to develop IR and central obesity, like many women with PCOS (Baillargeon and Carpentier 2007; Recabarren, Smith et al. 2008; Sam, Sung et al. 2008).

1.11.3. Animal models of PCOS

Several studies in rats have demonstrated that continuous exposure of post-pubertal animals to steroid hormones, either via regular subcutaneous dosing or continuous release pellet implant, produce a PCOS phenotype in these animals. The most recent and relevant studies are summarised in Table 1.5. The models described in this table recapitulate various features of PCOS and thus become useful when testing potential treatments for the syndrome, as several studies have gone on to do using insulin sensitizing agents (Misugi, Ozaki et al. 2006), electroacupuncture, and exercise (Manneras, Jonsdottir et al. 2008). Models of PCOS using higher mammals, specifically sheep (Steckler, Herkimer et al. 2009) and non human primates (Faiman, Reyes et al. 1988; Abbott, Tarantal et al. 2009), focus upon the adult consequences of fetal programming by administering androgen (usually T) during fetal life at a time when germ cells first begin to form primordial follicles. In rodents this period of exposure corresponds to early postnatal life (Section 5).

Table 1.5: Recent rat investigations which involve fetal, neonatal and adult administration of steroidal hormones:

Dose(s)	Window	Cull age	Ovary	Weight / IR	Hormones	Key Features of Study	Reference
TP daily 1mg	e14 – 19	d 90 – 94	-	↓ weight	n/a	Fetal TP can induce dystocia, weight loss & infertility in females	(Wolf CJ 2002)
TP daily 1mg/100g	d 21 – 56	d 56	Cystic; ↑ small antral	IR	↑ T	Ovarian homogenate showed ↑Bcl-2; Glucose levels normal/low	(Beloosesky, Gold et al. 2004)
TP 3mg	e16 – 19 Daily	d 60 – 70	↓ CL; Growing follicles ↑	Normal Insulin	↑ T, E2, P4 and LH	Response to E2 after OVX at day 60	(Wu, Li et al. 2010)
DHT 3mg							
DHT pellet 83µg/day	d 21 – 101	d 100	Smaller – PCO-like	Obesity and IR	Normal T and E2, ↑ P4	↑ adipocyte size and ↑ leptin ↑ mesenteric fat	(Manneras, Cajander et al. 2007)
Letrozole pellet 300µg			Heavier – large cysts	Obesity	Normal E2 ↑ T and P4	Normal adipocytes and leptin	
DHEA daily 6mg/100g	d 22 – 32	d 32	Cystic	-	↑ T, DHEA, A4, DHT Normal E1/E2, P4 FSH	Initial ↑ in prolactin which fell again after day 10↓ LH	(Anderson and Lee 1997)
DHEA daily 6mg/100g	d 22 – 29/37	d 30/38	GC atresia	-	-	Follicle atresia contributed to by matrix remodelling	(Honnma, Endo et al. 2006)
EV *2*mg	d 14	d 71	PCO-like	Normal	↑ E2	↑ Norepinephrine	(Rosa, Guimaraes et al. 2003)
EV *2*mg	d 45 - 55	d 60 – 105	PCO-like ↑ foll. diameter	-	↓ T, cort. & LH Diestrus FSH	↓ GC and thecal thickness	(Baravalle, Salvetti et al. 2007)
24h Light				-		↓ cort.	
Insulin pump 0.04iU/day	d 28	d 56	Erratic, long estrus cycles	IR	↑ T and DHEA(S), ↓P4	↓GDF-9 and activin receptor expression in ovaries (by IHC)	(Chakrabarty, Miller et al. 2006)

e=embryonic day; d=postnatal day; CL=corpora lutea; IR=Insulin resistance; T=Testosterone; E2=estradiol; EV=estradiol valerate; P4=progesterone; PCO=Polycystic ovary; foll=follicle; cort=Corticosterone; PCO=polycystic ovary; GC=granulosa cell; ↓=decreased; ↑=increased.

1.11.4. PCOS and metabolism

Since PCOS is associated with the development of obesity, patients frequently exhibit hyperinsulinaemia. Insulin and members of the IGF family are known to augment ovarian androgen production as well as promote weight gain; increased adiposity will not only increase insulin resistance (IR), but will reduce the amount of available SHBG, and hence may also increase the bioavailiblity of ovarian androgens, escalating PCOS severity (Botwood, Hamilton-Fairley et al. 1995; Panzer, Wise et al. 2006).

At the ovarian level, insulin and IGFs can impact ovarian functionality. Indeed in a mouse model of diabetes, gap junction communication in follicle COC was reduced in comparison with COC communication in non-diabetic mice. This implies a role for insulin in affecting oocyte quality and follicular dominance since bidirectional communication, as well as precisely timed gap junction disruption at the LH surge are both essential for ovulation (Ratchford, Esguerra et al. 2008). Ovarian theca and GCs are additionally responsive to insulin and IGFs, with both compounds shown to augment GC aromatase production in primary cell cultures (Hillier, Yong et al. 1991; Yong, Baird et al. 1992; Nahum, Thong et al. 1995). Insulin levels significantly increase during the pre-ovulatory period of cattle estrous cycles and may be stimulated by estrogen and insulin is also important in mediating nutrient uptake in cattle follicles (Webb, Garnsworthy et al. 2004). Other metabolic hormones have shown an association with female infertility and PCOS, for example, adiponectin impairs theca cell steroidogenesis and GC P4 production (Lagaly, Aad et al. 2008).

Obesity and hepatic function are important components in the pathogenesis of PCOS with one to two-fifths of the lean PCOS cohort demonstrating the same level insulin resistance as two thirds of obese PCOS women (Ciampelli, Fulghesu et al. 1997). In addition to these features, PCOS patients exhibit dyslipidemia, low grade chronic inflammation and an increased level of oxidative stress (Economou, Xyrafis et al. 2009). However, few studies have explored the role of the liver in the

pathogenesis of this syndrome. In one clinical study, all women with PCOS demonstrated reduced hepatic metabolism of insulin (inferred using plasma insulin:c-peptide ratio at fasting) independent of their body-mass index (BMI), leading to the proposal that hyperinsulinemia is a primary feature of PCOS, with insulin resistance forming as a result of obesity (Ciampelli, Fulghesu et al. 1997). Obesity and IR are both associated with development of non-alcoholic fatty liver disease (NAFLD) and hepatic steatosis (HS), characterised by elevated liver enzymes (Setji, Holland et al. 2006).

Two investigations have so far established convincing evidence that a subset (around 30%) of women with PCOS have elevated aminotransferases, at an average age of 29 years, much earlier than many humans would develop NAFLD/HS (Schwimmer, Khorram et al. 2005; Setji, Holland et al. 2006). In addition, type 2 diabetes and cardiovascular risk are both predicted by increased liver alanine transaminase (ALT) and γ-glutamyl transpeptidase (γGT) activities, which have recently been shown as elevated in highly obese PCOS women; but not in the lean PCOS cohort (Economou, Xyrafis et al. 2009). The clinical hope is that earlier liver screening may be used in conjunction with IR levels to asses PCOS patients who are at high risk of NAFLD. However, the aetiology of such liver dysfunction remains to be identified.

1.11.5. Treatment of PCOS

PCOS is a difficult endocrinopathy to treat clinically due to the heterogenic nature of this syndrome. Treatment usually relates to to one of two things; 1. The desire by the patient to become pregnant; 2. The impact of hirsutism or weight gain on the patient's quality of life. More often than not, these two aspects of PCOS treatment will go hand in hand, as physicians seek to improve a patient's weight in order to restore their fertility (ESHRE 2008). The easiest and primary treatment for women suffering from PCOS, especially those who are overweight or obese (BMI $\geq$ 26kg/m^2 and $\geq$30kg/m^2 respectively) is weight loss through exercise and dietary caloric restriction (Moran, Brinkworth et al. 2006; Norman, Homan et al. 2006).

Frontline drug treatment for women with PCOS remains the anti-estrogen clomiphene citrate (CC) and insulin sensitizers such as metformin may also be used for PCOS patients with glucose intolerance (Moran and Norman 2004). For the 25-27% of women who do not respond to ovulation induction with CC, gonadotrophin therapy may later be pursued (ESHRE 2008). In-vitro fertilization is usually only considered if a PCOS patient (or their partner) has associated reproductive pathologies (ESHRE 2008).

In the clinic, vaginal ultrasonography is used to quantify the size of the largest ovarian follicle in each ovary and document endometrial and ovarian responses to therapy (Parsanezhad, Bagheri et al. 2003; Ozcimen, Uckuyu et al. 2009). Furthermore, Doppler indices of blood flow within the stroma and follicle may be documented using this technique, particularly after laparoscopic ovarian drilling, a treatment known to successfully lessen PCOS symptoms, specifically ovarian blood flow velocity, along with vascular endothelial growth factor (VEGF), LH, and T levels (Amin, Abd el-Aal et al. 2003). Insulin-sensitising treatment of PCOS women who have developed glucose intolerance has also been shown to be effective

1.12. Main objectives of this thesis

The investigations described in this thesis use rodent models to examine the role of androgens in the pathogenesis of female infertility. An attempt to generate a granulosa cell specific androgen receptor knockout mouse model will first be described, followed by several studies into the developmental programming of female Wistar rat infertility and metabolism by steroid hormones.

These later investigations focus in particular upon the effects of neonatal testosterone proprionate (TP) treatment during different time windows and at varying doses upon rat fertility and metabolism. The neonatally androgenised rat will be evaluated as a rodent model for PCOS. Furthermore these studies investigate whether neonatally TP treated animals become anovulatory, obese, insulin resistant, or glucose intolerant. Finally, to elucidate whether the effects of TP observed occur through androgenic pathways or through the aromatisation of TP into estrogens, animals will be treated with TP in addition to other steroid hormones.

Chapter 2. Materials and Methods

2.1. General information

Unless otherwise stated, all solutions were prepared with distilled MilliQ water (dH_2O) and stored at room temperature. All liquid chemicals used were of analytical grade and were obtained from Fischer Scientific, while all solid chemicals were obtained from Sigma, unless otherwise stated.

2.2. Animal experimentation

All animal studies were carried out in accordance with the Animal (Scientific Procedures) act 1986 and were approved by the Home Office. Experimentation operated through personal licence number PIL 60/10682. Rodents were housed in clear solid-bottomed cages, containing bedding of wood shavings and corn cob.

2.2.1. Welfare Conditions

2.2.1.1. Transgenic mice

Mice were housed and bred in an animal facility provided by the University of Edinburgh. Rooms were temperature (20-25°C) and light controlled (14 hour light, 10 hour dark photoperiod) with food (standard laboratory chow) and water provided *ad libitum.* Mice also had a cardboard tunnel for environmental enrichment (BS&S, Scotland). Experimentation was carried out under licence PPL 60/3544 held by Professor Philippa Saunders. Culls were carried out by the author on site.

2.2.1.2. Rats

Wistar rats were bred and maintained in the Little France animal facility. Here, daily animal husbandry was carried out by MRC technician Mr Mark Fisken. Mr Fisken supervised handling of animals, and assisted during certain licensed procedures, for example glucose tolerance testing. All rats were housed and bred in a temperature (20-25°C) and light controlled room (14-h light, 10-h dark photoperiod), with *ad libitum* access to fresh tap water and a soy-free breeding diet (Type 3, soy

free, rat; SDS diets; Dundee, UK). Up to six females were housed together after mating and stud male rats were housed individually before and after mating. Pregnant dams were housed individually just prior to parturition and kept with the pups until weaning at postnatal day (pnd) 21. Experimentation was carried out jointly under two project licences, PPL 60/3232 and PPL 60/3914 held by Professors Alan McNeilly and Richard Sharpe respectively.

2.2.2. Injections

Immature rats were given subcutaneous (s.c.) injections of control oil or steroid hormone dissolved in oil (Table 2.1). For testosterone proprionate (TP) administration to pregnant dams during fetal life and dosing with 100mg/kg bromodeoxyuridine (BrdU), injections were administered intra-peritonealy (i.p.). Animals were treated and kept in the same experimental dose group. Pups were not mixed between litters since after injection, dams often groom pups around their injection sites and may ingest steroid hormone which has the potential to be absorbed and transmitted to other pups via suckling.

Table 2.1 Summary of steroid hormone injection protocols and doses administered:

Steroid	Dose(s)	How steroid was made up		
	(mg/kg)	Dry steroid (mg)	Ethanol (ml)	Oil (ml)
Testosterone proprionate (TP)	20mg/kg 5mg/kg 1mg/kg	100 20 5	0.5	9.5
Estradiol Valerate (EV)	1mg/kg	5	0.5	9.5
Dihydrotestosterone (DHT)	1mg/kg	5	0.5	9.5
Dehydroepiandrosterone (DHEA)	1mg/kg	5	0.5	9.5
Dexamethasone (DEX)	0.8mg/kg	4	0.5	9.5 (saline)

2.2.3. Smears

At maturity, rats were checked for the presence of vaginal openings and smeared gently to avoid triggering pseudopregnancy. Pseudopregnancy is caused by mechanical stimulation of the cervix, altering pituitary prolactin release. When taking a smear, water was dropped onto a slide, a wetted smear stick used to gently

scrub surface cells from the vagina, which were then scribbled onto the labelled slide. Smears were air dried briefly, fixed in methanol for 4 minutes, stained with giemsa diluted 1 in 20 with distilled water, for 15 minutes, washed gently with water and cover-slipped. Smears were viewed under a light microscope to check for regular estrus cycling and to time animal sacrifice at proestrus.

2.2.4. Tail nick blood sampling

Rats were wrapped in towels and handled by the author daily for at least two weeks to accustom them to the sampling environment. When taking tail bloods, each individual rat was wrapped in a towel on the author's knee, the tail extended and the end vein nicked with a size 10 scalpel. Blood was encouraged from the tail by massage; up to 200-250µl blood was sucked into pre-labelled capillary tubes (Sarstedt Microvette CB 300 with EDTA), which were cooled on ice until the end of the experiment. Samples were spun down at 6000 rpm for 10 minutes and the top plasma layer stored at -20°C. For glucose tolerance tests (GTTs), rats were fasted from 5.00pm the night before, and sampling began at 8.30am the next day. Tail nicks were taken from between 10 and 20 animals at a time, in the same order, over three time (*t*) points – *t*=0, *t*=30 and *t*=120 minutes. After the *t*=0 tail nick, animals were immediately gavaged with a 50% glucose solution (2g/kg) and returned to their cage. These samples were used for both glucose and insulin assays.

2.3. Necropsy

In all studies, female rodents were killed by cervical dislocation and a heparinised 25mm gauge needle attached to a 2ml syringe used to remove blood by cardiac puncture. The organs required were then located, removed, cleaned of surrounding fat, weighed and then fixed and/or frozen. Blood samples were kept on ice during necropsy and later spun down in a centrifuge for ten minutes at 10,000 rotations per minute (rpm) to remove cellular debris. Supernatant plasma was removed stored at -20ºC for subsequent steroid and protein hormone analysis.

2.3.1. Reproductive organs

An initial longitudinal incision opened the abdominal cavity exposing the internal organs. The uterus was located and disconnected from the base of the vagina, any attached fat or blood vessels were then disconnected from the uterus and the ovaries located and removed from the end of each uterine horn.

2.3.2. Hypothalamus and pituitary

The pituitary was located by removing the skin surrounding the skull and making an upward incision into the base of the skull. Flat scissor edges were then used to separate the skull bone into two pieces, allowing the brain to be lifted from the base of the cerebellum to expose the pituitary, subsequently removed by gently lifting it from the base of the skull with curved forceps. The hypothalamus was located by cutting the optic nerves and removing the triangular grey area located above the pituitary.

2.3.3. Endocrine organs

The ribcage was raised using forceps and a 45° cut made next to the attached liver tissue. Mesenteric fat was removed by a snip incision at the pancreatic-stomach join, allowing the fat pad to be pulled away from the intestine and cut off at the colon. Retroperitoneal fat was removed by successive blunt snipping away from the animal's right side at the base of the knee joint up to the base of the rib cage; at this point the right adrenal could easily be located above the kidney and also removed. Muscle was removed from the animal's left knee by first a vertical and then a 45° incision into the quadricep; a sample of subcutaneous fat was also removed from behind the knee at this time.

2.4. Histological analysis

Organs to be fixed were placed in Bouins (Triangle Biomedical Sciences Ltd. Lancashire, UK.) or Neutral Buffered Formaldehyde (NBF) for 2-6 hours depending on size, before being transferred to 70% ethanol for paraffin embedding. Organs used

for mRNA and/or protein analysis were snap frozen on dry ice and stored at -70°C. Tissues were either fixed in Bouins (Triangle Biomedical Sciences, Lancashire, UK) for six hours or NBF overnight before processing. An automated Leica TP-1050 processor (Leica Microsystems, Milton Keynes, UK) dehydrated the fixed tissue through a series of graded alcohol solutions over the course of 18 hours. After processing, the tissue was saturated and embedded in liquid paraffin wax and finished blocks left to cool. These were stored at room temperature until morphometric and histological analysis was required. Common solutions used in histological analysis are listed in Table 2.2.

Table 2.2: Common fixatives and immunohistochemistry washing and staining solutions used in histological experiments.

Solution type	Protocol	Quantity
4% NBF - normal buffered formaldehyde - 1 litre	40% formaldehyde Deionised H_2O Sodium dihydrogen phosphate monohydrate Disodium hydrogen phosphate anhydrous	100ml 900ml 4g 6.5g
Acid-Alcohol - 1 litre	1% conc. HCl 70% EtOH	10ml 700ml
Citrate buffer - 10 X (1.0M) - 2 litres - Used at 0.1M for antigen retrieval	Citric acid monohydrate (Sigma) Deionised H_2O *pH to 5.5 with NaOH* Deionised H_2O *pH to 6 with NaOH*	42.02g 1900ml - 100ml
Eosin	Triangle Biomedical Sciences Ltd. Lancashire, UK.	
Harris' Haematoxylin (HH)	Haematoxylin (Triangle Biomedical Sciences) Absolute alcohol *Combine and boil with:* Aluminium potassium sulphate Distilled water *Add* Mercury Oxide *Cool solution in ice then filter* *Add* glacial acetic acid for every 100ml HH	2.5g 25ml 50g 500ml 1.25g 4ml/100ml
Scott's tap water - 5 litres	Potassium chloride Magnesium sulphate Deionised H_2O	10g 100g 5000ml
TBS - Tris-buffered saline - 10 X - 1 litre - Use as X 1	Tris base NaCl HCl *Adjust to pH 7.5 with HCl then make up to 1 litre with deionised H_2O*	60.5g 87.6g 300ml ~700ml

EtOH=ethanol; HCl=hydrochloric acid; H_2O=water; g=grams; M=molar; ml=millilitres; g=grams; HCl=hydrochloric acid; H_2O=water; ml=millilitres; NaCl=sodium chloride NaOH=sodium hydroxide; NBF=neutral buffered formaldehyde

2.4.1. Sectioning

Tissue sections were cut at 5μm widths using a microtome (Lecia RM, 2135, Germany) and laid onto paper ready for mounting. This allowed for serial sectioning and for section ribbons to be stored if needed. This also allowed sections from treatment and control groups to be matched onto the same slide. Sections were floated onto coated slides (Superfrost ® plus, BHD Laboratory Supplies, Poole, Dorset, UK) and dried in an oven at 50°C overnight.

2.4.2. De-waxing and rehydrating

Slides were placed in racks of up to 25 and de-waxed in xylene (2 X 5minutes). Tissue sections were then rehydrated through two absolute alcohol troughs followed by graded 95% and 70% alcohol. At this point slides could be taken for immunohistochemistry (IHC) or stained with haematoxylin (a purple nuclear stain) and eosin (a pink cytoplasmic stain) for basic morphological characterisation. Slides were dipped in acet-alcohol to remove any excess haematoxylin staining before being eosin stained. Sections were then dehydrated through troughs of 70, 80 and 95% alcohol and two absolute alcohol troughs into xylene (2 X 5min) and finally mounted in pertex (Figure 2.1).

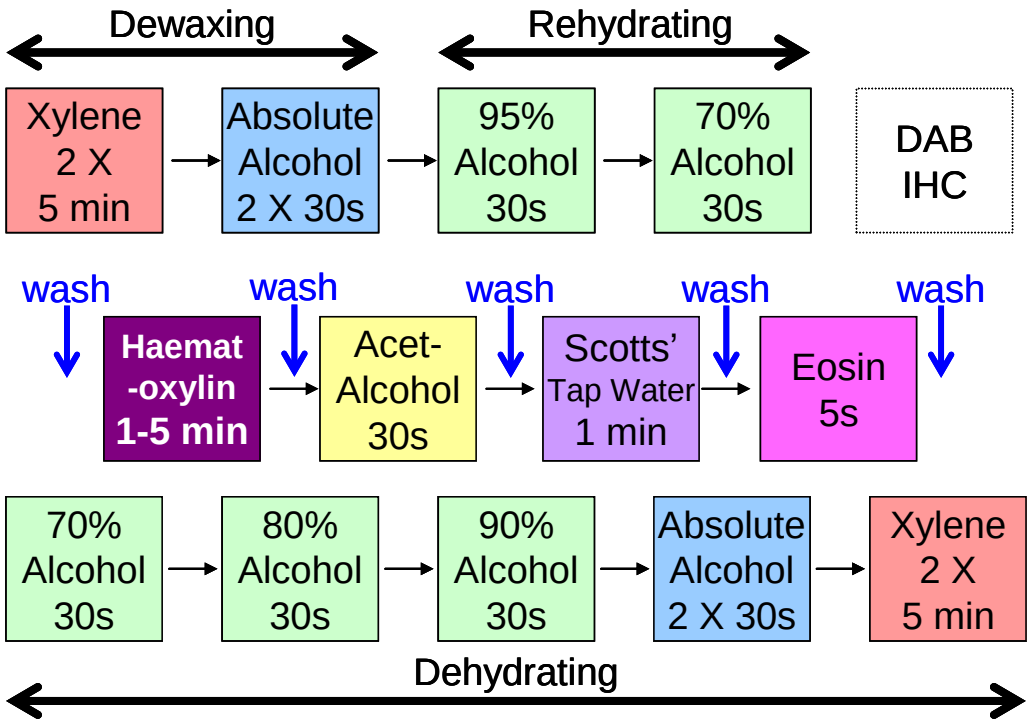

Figure 2.1: Schematic diagram of de-waxing, counterstaining and rehydrating slides during a typical staining run. Note, when performing DAB immunohistochemistry (IHC) the Eosin step was omitted.

2.4.3. Antigen retrieval

After hydration, sections for IHC underwent antigen retrieval; 1 litre of citrate buffer (0.01M) per slide rack was heated in a pressure cooker until boiling, the slide racks were placed in, the lid secured and pressure turned up to full. After five minutes of full pressure, the pressure valve was opened and the cooker was allowed to cool for at least 20 minutes before proceeding with subsequent IHC steps.

2.4.4. DAB-IHC

After antigen retrieval, endogenous peroxidise activity was blocked by washing slides for 30 minutes in 3% (v/v) hydrogen peroxide (Sigma) in 300ml methanol followed by a tap water rinse and two five minute washes in Tris-buffered saline (TBS). This was followed by a 15 minute block of endogenous avidin and biotin if required, according to the manufacturer's instructions (Vector Laboratories, Peterborough UK), with two TBS washes in after each block. Normal blocking serum was diluted 1:5 in TBS with 5% bovine serum albumin (BSA) and applied for 30 minutes to prevent nonspecific primary antibody binding. Meanwhile the primary

antibody was appropriately diluted in normal blocking serum and applied to the tissue for incubation in a humidity tray overnight at 4°C (Table 2.3).

Table 2.3: Primary and secondary antibodies used for DAB immunohistochemistry: Subsequent to the addition of a biotinylated secondary antibody at 1 in 250µl, slides were incubated with tertiary ABC-HRP antibody at 1 in 1000µl, followed by DAB at 1 in 100µl.

Primary Ab	Raised in	Block in	Dilution (µm)	Secondary AB	Source
PCNA	Mouse	NGS	1 in 1000	Goat anti mouse	Novocastra
VASA	Rabbit	NGS	1 in 200	Goat anti rabbit	AbCam
Caspase-3	Rabbit	NGS	1 in 200	Goat anti rabbit	Cell Signalling Technology
AR	Rabbit	NGS	1 in 750	Goat anti rabbit	Santa Cruz
AMH	Goat	NRS	1 in 500	Rabbit anti goat	Santa Cruz
Aromatase	Mouse	NGS	1 in 50	Goat anti mouse	Gift – Nigel Groome
17α OH	Rabbit	NGS	1 in 500	Goat anti rabbit	Gift – D. Hales
3β-HSD	Rabbit	NGS	1 in 1000	Goat anti rabbit	Gift – I. Mason
BrdU	Mouse	NGS	1 in 50	Goat anti mouse	Roche Diagnostics

AB=antibody; PCNA=proliferating cell nuclear antigen; AMH=Anti-Müllerian Hormone; AR=Androgen Receptor; 17αOH=17α hydroxylase; 3β-HSD=3β-hydroxysteroid dehydrogenase; BrdU= Bromodeoxyuridine; NGS/NRS=normal goat/rabbit serum.

Following at least 12 hours of incubation and two five minute TBS washes to remove excess primary antibody, an appropriate biotinylated secondary antibody in normal serum was incubated on sections for 30 minutes at a concentration of 1:500µl. A second wash cycle was then followed by addition of an avidin-biotin horseradish peroixdase complex (ABC-HRP; DAKO, High Wycombe, UK) diluted 1:1000µl TBS, which was applied for 30 minutes. After a final TBS wash, antibody localisation was determined by application of liquid diaminobenzidine (DAB)-substrate chromogen system (DAKO, High Wycombe, UK) for 30 seconds until the brown positive staining in control sections was optimal. Haematoxylin was used as a counter-stain (Figure 2.1), followed by submergence in acet-alcohol (5 seconds) and Scott's tap water (20 seconds) with water washes in-between. Slides were then dehydrated back through graded alcohols and xylene before finally mounting in pertex. Figure 2.2 illustrates the principles of epitope binding and how IHC uses this to visualise a protein expressed by a tissue.

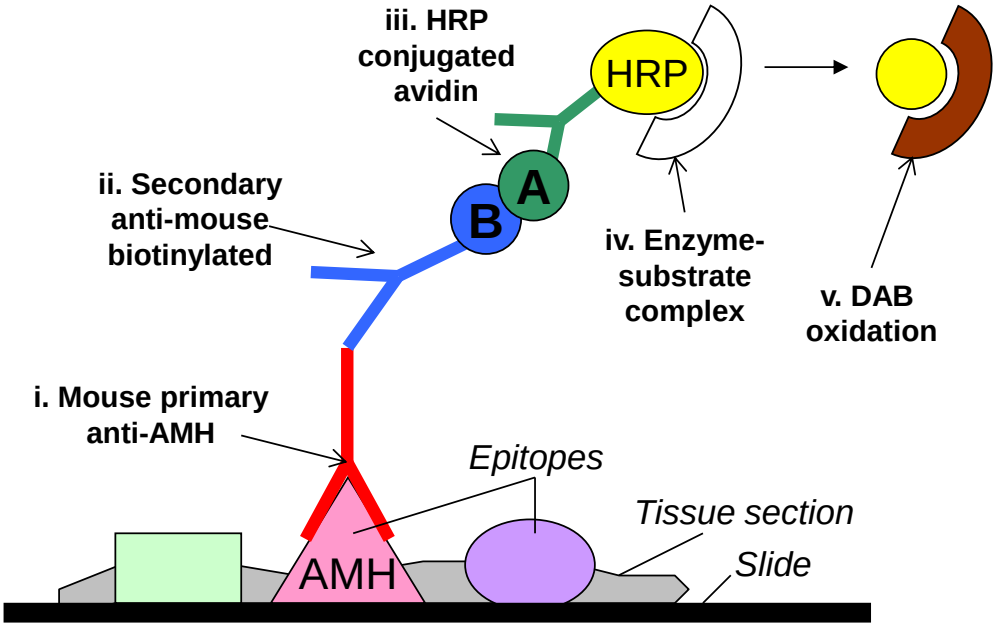

Figure 2.2: Antigen visualisation using DAB immunohistochemistry: (i) A primary antibody (AB), raised in mouse, recognises its complementary epitope AMH within the tissue; (ii) A secondary biotinylated AB specific for the mouse epitope is then added and binds to the primary AB; (iii) A third AB contains a complementary avidin molecule and conjugates to the biotin of the second AB; (iv) This tertiary AB contains a horseradish-peroxidase (HRP) conjugate, which in the presence of diaminobenzidine (DAB) substrate, oxidises to a brown colour (v).

2.4.5. Fluorescent IHC Protocol

Fluorescent IHC proceeded in much the same way as that of DAB-IHC, but washes were completed in phosphate buffer saline (PBS). The same primary antibodies could be used, but secondary/tertiary antibodies were conjugated to an alexa-fluorescent antibody (FAB) fragment; thus slide dishes were wrapped in foil to prevent bleaching of fluorescent fragments by light between stages. If HRP-linked or biotinylated complexes were not utilized, peroxidase or avidin-biotin blocking steps were not required. To enhance the fluorescence of some antibodies, red or green Tyramide was utilised at a dilution of 1:00µl after addition of secondary complexes for 10 minutes only. Slides were counterstained red with propidium iodide (1:1000µl), or blue toporo (1:500) and wet-mounted in permafluor for confocal laser image capturing (LSM-510).

2.5. Follicle Counting

Before commencing follicle counts, previous investigations into follicle numbers in rodents were assessed in order to decide the best method of quantifying the numbers and types of follicles present within the ovary. These methods are summarized in Table 2.4. The counting method used was that of Hirshfield and Midgley, since this method allows for a realistic estimate of follicle proportions, involves minimal data manipulation and is the study from which many others derive their follicle counting protocols, as shown in Table 2.4 (Hirshfield and Midgley 1978).

In this thesis, total follicle numbers are expressed alongside the proportions of follicles at each stage of follicle development; primordial, transitory, primary, secondary and antral, for analysis by two-way analysis of varience (ANOVA; see section 16 of this Chapter). Follicle numbers in these categories were also analysed by two-way ANOVA, but no further differences were seen between the number analysis compared to the percentage analysis and so these graphs are not reported.

Table 2.4: Summary of the various types of follicle counts performed on rodent ovaries: Follicle counts performed in this thesis were based on those of Hirshfield (1978).

Section Thickness	Sections Used	Data manipulation	Classification based on	Follicle count	Disadvantages	Advantages	Species	Reference
Serial 6 - 8µm	Every 10^{th}	None	GC morphology	Oocyte nucleus present	Cumbersome 3-11% error	Realistic estimate Doesn't use all tissue	Rat	(Hirshfield and Midgley 1978)
Serial 5µm	Every 10^{th}	X section number (10) Plus section thickness (5)	GC morphology	As in *Hirshfield 1978*	Using thickness correction factor is less accurate	As in *Hirshfield 1978*	Rat	(Flaws, Hirshfield et al. 2001)
Serial 5µm	Every 10^{th} & 11^{th}	None	GC morphology	Oocyte nucleus present in one but not in other section	As in *Hirshfield 1978*	Less likely to get duplicates by using two sections	Rat	(Myers, Britt et al. 2004)
Serial 5µm	All	None	Number of GC layers	As in *Hirshfield 1978*	Time consuming May overestimate	Whole ovary used	Rat	(Green, Mandl et al. 1951)
Serial 8µm	Every 5th	X section number (5)	GC morphology	As in *Hirshfield 1978*	As in *Hirshfield 1978*	As in *Hirshfield 1978*	Mouse	(Canning, Takai et al. 2003)
Serial 8µm	Every 5th	Not stated	GC morphology	As in *Hirshfield 1978*	As in *Hirshfield 1978*	As in *Hirshfield 1978*	Mouse	(Morita, Perez et al. 1999)
Serial 7µm	Every 4th	Oocyte nucleus X by inverse of sampling fractions	GC morphology & oocyte diameter	Oocyte nucleus present in a fraction of the thickness of each section	Assumes constant follicle distribution. Alters original data	Quick, overestimates corrected for using 'Abercrombie's method'	Mouse	(Britt, Drummond et al. 2001)

GC=granulosa cell; X=multiplied by

Only follicles containing a visible oocyte nucleus were included in the count and follicles were classified on the basis of their granulosa cell (GC) layering. A layer of flat squamous GCs indicated a primordial follicle. Two or more cuboidal GCs indicated a transitory follicle. If two or less than two layers of cuboidal GCs were present around the oocyte, the follicle was primary and if more than two layers of cuboidal GCs were present around the oocyte, the follicle was secondary. Finally if there were more than two layers of cuboidal GCs and an antrum had formed, the follicle was antral (Figure 2.3).

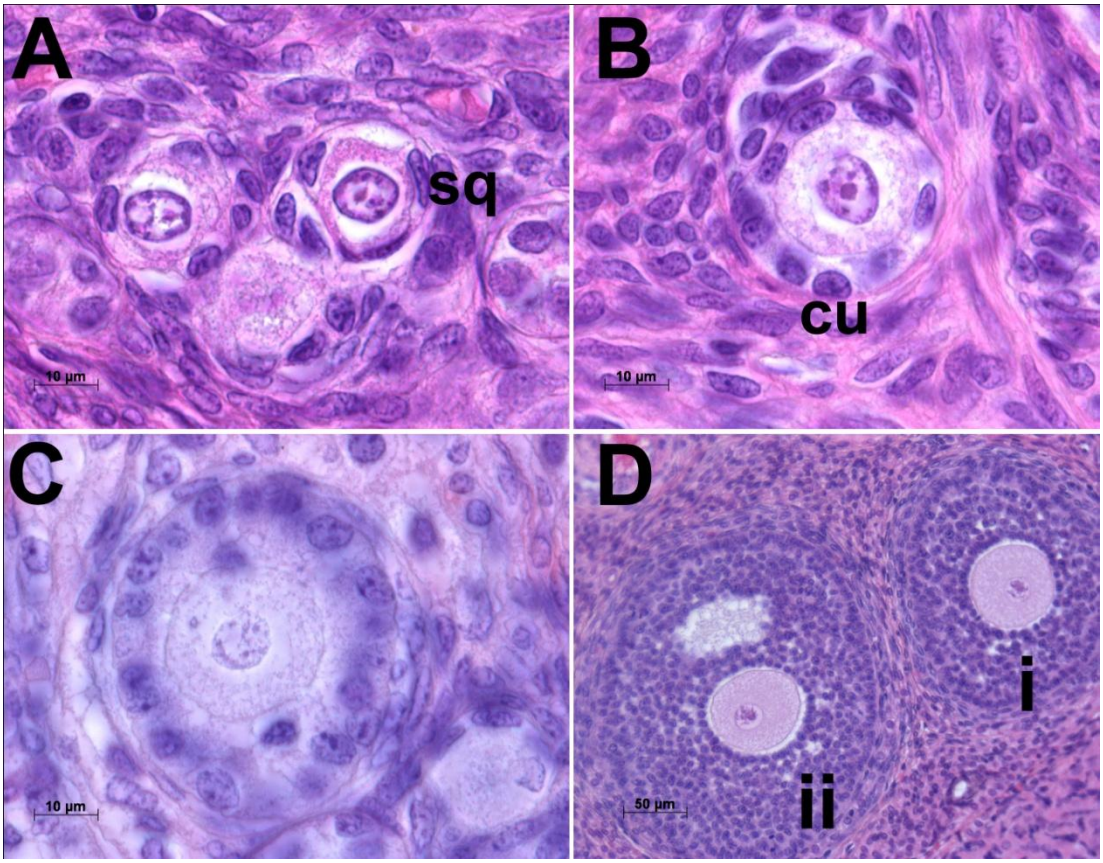

Figure 2.3: Follicle classifications exemplified as (A) Primordial; (B) Primary; (C) Secondary; (D) (i) Late pre-antral; (ii) Antral follicle: 'sq' and 'cu' designate squamous and cuboidal granulosa cells respectively. A-C are shown at X 40 and D at X 20 magnification.

2.6. Morphological and morphometric analysis

The number cells/follicles expressing a specific stain in addition to staining intensity were be used to assess follicle morphology in a semi-quantitative fashion. Morphometric analyses were also completed using stereological equipment comprising an Olympus BH-2 microscope fitted with a Prior automatic stage (Prior Scientific Instruments Ltd., Cambridge, UK). Image-Pro Plus version 6.2 with Stereologer-Pro 5 plug-in software (Media Cybernetics UK, Wokingham, Berkshire, UK) was used to count cells and measure areas in μm^2. The histological features and DAB stains quantified using a Stereologer are detailed in Table 2.5. Representative images shown in each chapter were taken with a Provis AX70 (Olympus Optical, London, UK) microscope fitted to a Canon DS6031 camera (Canon Europe, Amsterdam, The Netherlands).

Table 2.5: Summary of morphometric analyses performed using a Stereologer:

Marker	Area stained	Counts performed	Stereology performed
VASA	Germ cells	Germ cell count	Germ cell stain/μm^2
Caspase-3	Apoptotic cells	Apoptosis count	-
H&E stained sections	n/a	-	Antrum size (μm^2)
3βHSD	Strong in stroma, weak in theca interna, CL & mGCs	-	Area measured minus CL and mGCs (μm^2)
17α-hydroxylase	Theca interna, weak in mGCs	Follicle diameter	Stained area measured minus CL and mGCs (μm^2)
BrdU	Proliferating cells	Positive GCs across follicles of different sizes	Positive area in granulosa cells (μm^2)

H&E=haematoxylin and eosin; CL=corpus luteum; GCs=Granulosa Cells; OA=ovarian area; 3βHSD=3β-hydroxysteroid-dehydrogenase; 17αOH=17α-hydroxylase; BrdU=Bromodeoxyuridine.

Before starting any stereological analysis, the software was calibrated against the microscope objective so that all measurements were taken in µm or μm^2 and remained accurate. The ovarian section or follicle of interest was put into focus and

an experiment set up using Image ProPlus 6.2 software; this software was then used to tile an image of choice at a specific magnification. The final image file was then saved and used for any subsequent morphometric analysis of that image, for example, the measurement of ovarian area, follicle area, or follicle diameter. The proportion of cells stained positively with DAB IHC could also be measured within a particular area of interest, for instance 3β-hydroxysteroid dehydrogenase (3βHSD) positive stromal area, or BrdU staining of proliferating GCs. Examples of these types of morphometric analyses are illustrated in Figure 2.4. To select a DAB stained area, a reference colour range was taken from the brown stained region and all pixels within the stated colour range highlighted. Stained area below 10µm^2 was not included, in order to discount any background.

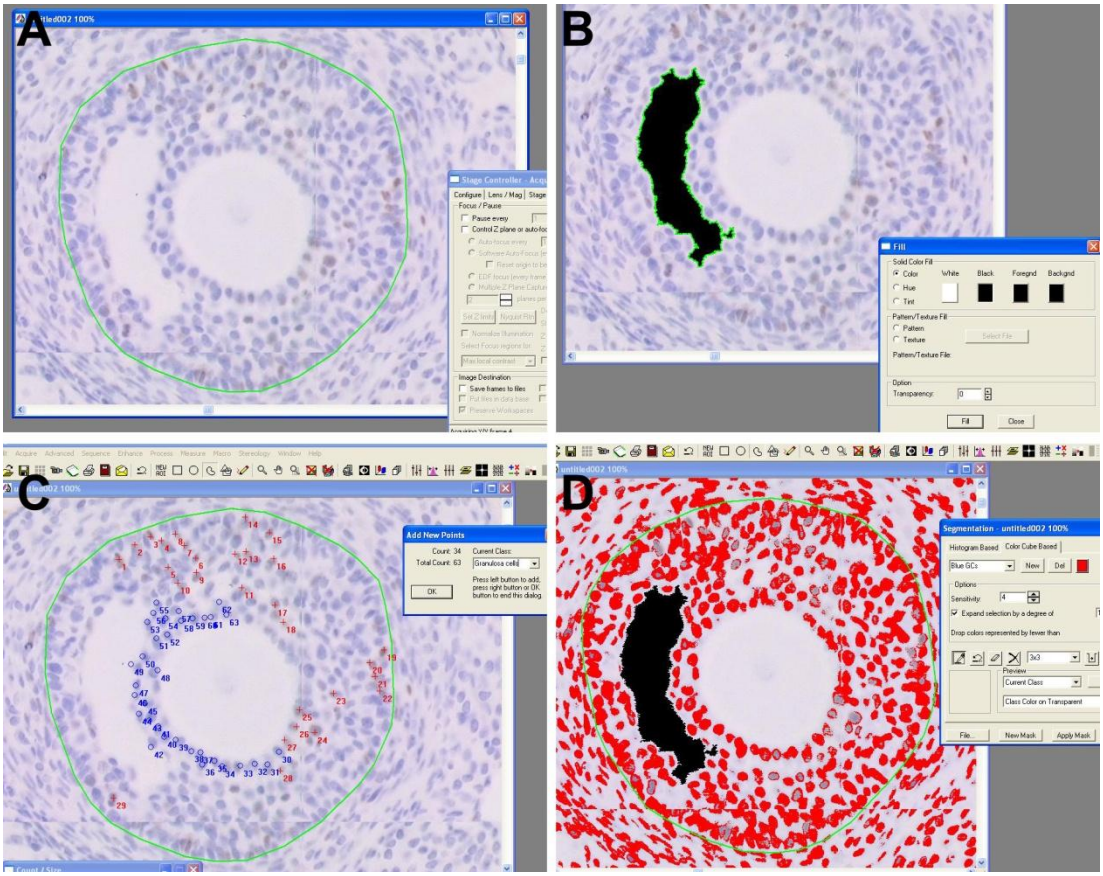

Figure 2.4: Stereological analysis of a follicle using Image ProPlus; (A) Tiled image of a follicle calibrated to the X 40 objective with a manual area of interest (AOI) drawn around this follicle in green. (B) This AOI may be filled in black, which here is the follicle antrum. The black area is measured in µm^2 and exported to an excel file. (C) Different cell types may be counted; here BrdU stained granulosa cells are counted in red and non-stained cells in blue. (D) DAB or haematoxylin staining may be specifically selected. In this case red staining to select the haematoxylin stained blue cells. Once again this stained area can be calculated in µm^2 within the AOI and the data exported for analysis to Microsoft excel.

2.7. Nucleic acid extraction

To guard against RNA degradation by ribonucleases, all solutions and instruments were autoclaved before use. The lab bench and all pipettes were wiped with 75% ethanol and RNase inhibitor before each RNA extraction run, and sterile plastic eppendorf tubes and pipette tips were used throughout. RNA was extracted using several different methods in this thesis, depending on the starting material (Table 2.6). For large amounts of easily homogenized or fatty starting material, for example Liver, a TRI-reagent protocol was used. For smaller amounts, for example pituitary tissue, a Qiagen RNA mini kit was used, and for all fat components a combination of the two was developed. Tissue was either homogenized using a rotor-starter mini-homogenizer, or in 2ml tubes run on a Tissue Lyser (Qiagen) at 25Hz for 2-3minutes.

Table 2.6: Tissues from which RNA was extracted: Methods of homogenization and extraction used and the typical mean yield of RNA for each tissue.

Tissue	Homogenisation method	RNA extraction method	Mean RNA yield (ng/µl)
Ovary	Tissue lyser	TRI reagent	241
Pituitary	Rotor Starter	Qiagen mini kit	1149
Liver	Tissue lyser	TRI reagent	3563
Mesenteric fat	Tissue lyser	TRI reagent extraction followed by Qiagen mini kit	883

TRI reagent= guanidinium thiocyanate and sodium acetate

The concentration of all eluted RNA was determined using a NanoDrop® ND-1000 Spectrophotometer (Nanodrop Technologies, Wilmington, DE, USA).

2.7.1. Tri-reagent method

This method uses the fact that RNA can be separated from DNA through tissue homogenization in 1ml of guanidinium thiocyanate and sodium acetate, otherwise known as TRI reagent (Chomczynski and Sacchi 2006). For each 1ml TRI reagent used, 0.2ml chloroform was added and mixed with the homogenate to complete the dissociation of nucleoprotein complexes. Upon centrifugation in these

acidic conditions, the RNA remained in an upper aqueous phase, leaving DNA in an interphase, and protein in an organic phase. Total RNA was then recovered by precipitation and centrifugation with 0.5ml isopropanol, which caused the RNA to form a pellet that was then washed with 75% ethanol solution. After air drying, the RNA was eluted at 60°C in an appropriate volume of water (30-50µl).

Contaminating genomic DNA was removed from TRI-extracted RNA using the Ambion® TURBO DNA-free DNase Treatment and Removal kit (Applied Biosystems). The DNase is then removed by incubation with a patented 'DNase Inactivation Reagent', which is then pelleted by centrifugation so that the supernatant containing DNA-free RNA can be removed to a fresh tube and stored at -70ºC for gene expression analysis.

2.7.2. RNeasy® column RNA extraction

This method takes advantage of the ability of nucleic acids to pH dependently adsorb onto silica/other solid phase set within an RNeasy® column (Qiagen) when tissue is homogenized in a buffer of high pH. For each 1ml of homogenization RLT buffer used, 10µl of β-Mecaptoethanol (β-ME) (Sigma) was added before starting. On-column DNase digestion was performed using a DNase digestion kit; for every column used, 70µl of Buffer RDD and 10µl of DNase stock solution were mixed gently.

Typically, 700µl RLT (+β-ME) was added to the tissue sample and homogenized before centrifugation at maximum speed to separate out the homogenate leaving a supernatant containing RNA (approximately 600-700µl depending on tissue). To this supernatant an equal volume of autoclaved 70% ethanol was added and the tubes mixed before adding 700µl of this lysate at a time to the RNeasy® columns. The columns were then spun at 10,000 rpm for 15 seconds and the flow-through discarded. To each column, 350µl of buffer RDD was added and the columns spun again at 10,000 rpm for 15 seconds, discarding flow-through. At this point DNase digestion step could be performed by addition of 80µl (70µl Buffer

RDD + 10µl DNase) DNase digestion mixture directly onto the column membrane for a 15 minute incubation at room temperature.

A further 350µl RDD buffer was next added and the columns spun at 10,000 rpm for 15 seconds, discarding flow-through and columns transferred to new collection tubes. Next, two 500µl loads of RNA wash buffer 'RPE' were pipetted onto the column and flow-through discarded; the first spun for 10,000 rpm for 15 seconds, the second for 2 minutes. Columns were next spun in a new collection tube (not supplied by the manufacturer) for 1 minute to thoroughly dry the membrane. RNA was then eluted by application of an appropriate volume of RNase free water, usually 30-50µl. This elute could then be passed through the column a second time to ensure the highest yield of RNA possible.

2.7.3. RNA extraction from fat

When extracting RNA from fat, the TRI-Reagent method alone produced between 3 and 70ng/µl RNA when tested on practice fat samples. Equally when even a small amount of tissue was extracted using the Qiagen mini-kit method, the column became clogged with fat and RNA yield was minimal. As a result of this, a combination of both methods was used, yielding between 300 and 2000ng/µl RNA per sample, depending on the fat depot under extraction. Initial homogenization and dissociation was completed with 1ml TRI-reagent and 0.2ml chloroform, and the resulting aqueous RNA phase added to an equal volume of 75% ethanol (approx 0.4ml). This solution was then applied to Qiagen mini-kit columns in 700µl aliquots, after which the Qiagen column protocol and DNase digestion steps were followed as detailed in Section 2.7.2

2.8. Reverse transcription, PCR and electrophoresis

Reverse transcription of copy DNA (cDNA) from total RNA was performed using the SuperScript® VILO™ cDNA Synthesis Kit (Invitrogen). The kit comprises a SuperScript® enzyme mix (the reverse transcriptase engineered from Moloney

murine leukaemia virus) and a 5 X VILO™ reaction buffer containing deoxyribonucleotides, random hexamer primers, and $MgCl_2$. Template RNA was used consistently at a concentration of 200ng/µl to allow to precise quantification of gene expression in downstream quantitative PCR reactions. Single reaction components are listed in Table 2.7. After preparation, the cDNA synthesis reaction was incubated according to the manufacturer's instructions at 42°C and then terminated at 85°C using a PTC200 (Thermo Cycler) PCR block. cDNA was stored short term at 4°C and frozen long term at -70°C.

Table 2.7: Single reaction components for SuperScript® VILO™ cDNA Synthesis Kit

Component	Volume (µl)
5 X Vilo™ reaction buffer	4
10 X SuperScript® enzyme mix	2
Nuclease free water	13
RNA template at 200ng/µl	1
	20

The Polymerase Chain Reaction (PCR) is a well documented tool for the detection and quantification of gene expression (Deepak, Kottapalli et al. 2007). To determine the presence or absence of a particular gene, primers specific to the sense and antisense of an amplicon within the gene of interest were used in a standard PCR with the resulting product run on 1% agarose gel. For 50ml agarose gel 0.5g agarose was dissolved in 1 X TAE buffer (A 1 litre solution of 10 X TAE was made by dissolving 242g Tris base in 842.9ml dH_2O with 57.1ml glacial acetic acid and 100ml 0.5M EDTA). Safeview (NBS Biologicals) was then added to warm liquid gel at 5µl per 100µl gel to allow safe visualisation of each gel under a UV Transilluminator. Samples were run next to an appropriate ladder (100bp interval) for band identification. In each run using cDNA, two controls were included; an RT-negative template control and a water control in place of cDNA template. When using extracted genomic DNA (Chapter 3) a water control only was included. All gels were run at 120 volts for at least half an hour before visualisation under a UV

transilluminator. All genes of interest were investigated in this way using 2 X Biomix Red PCR mix according to the manufacturer's instructions (Bioline, UK) as shown in Table 2.8.

Table 2.8: Single reaction components for a Biomix Red PCR

Component	Volume (µl)
Biomix Red	10
Distilled Water	8.6
Forward Primer	0.2
Reverse Primer	0.2
DNA template	1
	20

2.9. Quantitative PCR

Quantitative PCR (hereafter qPCR) allows analysis of the relative abundance of PCR products during the exponential phase of PCR when reagents are not limited. Most qPCR was performed using *Power* SYBR® Green PCR Master Mix (Applied Biosystems). Primers were designed using the online NCBI/Primer-BLAST tool. Specifications for primers used in qPCR included an amplicon length of 50 to 200 bases, a %GC content below or equal to 65% at most and a melting temperature of between 58° and 61°C. Table 2.9 lists the primers used for quantitative PCR for each gene of interest and the tissue(s) they were used to investigate.

Table 2.9 List of genes analysed by quantitative PCR for each tissue with primer sequences and locations for Syber Green chemistry; Control genes are in bold.

Gene Target	Primers used (5' → 3' direction)		Start	Stop	Amplicon size
Pituitary					
β-Actin	Fwd+	CCTGTGCTGCTCACCGAGGC	122	103	161
	Rev-	TGTGGGTGACCCCGTCTCCG	264	283	
αGSU	Fwd+	TTGCTTCTCCAGGGCATATC	293	274	178
	Rev-	GCGCTCAGAAGCTACGACTT	452	471	
FSHβ	Fwd+	GGACCCAGCTAGACCAAACA	196	177	152
	Rev-	TCTTACAGTGCAGTCGGTGC	329	348	
LHβ	Fwd+	ACACTGGCTATGTCCCAGG	65	47	181
	Rev-	GGCAGTACTCGAACCATGCTA	226	246	
Mesenteric Adipose					
β2-microglobuin	Fwd+	TCGCTCGGTGACCGTGATCTTT	34	13	98
	Rev-	AAGTTGGGCTTCCCATTCTCCGGT	109	132	
Adiponectin	Fwd+	ACTGCAACCGAAGGGCCAGG	98	79	97
	Rev-	TCTGCCATCACGGCCCGGTA	176	195	
Leptin	Fwd+	TCATTCCCGGGCTTCACCCCA	234	214	181
	Rev-	TCTGGCTTCTGCAGGCCACG	396	415	
Resistin	Fwd+	TGCTGTACCCTGCGGGTTGG	418	399	119
	Rev-	TTTCCTGCCCCCTGCGCTCT	518	537	
LPL	Fwd+	ACGCCTCCGGCTCAACCCTT	113	94	145
	Rev-	TCCGCGGAAGGCGGTCAAAC	239	258	
HSL	Fwd+	GTTTCCACCCACGGCGCTCA	3070	3051	173
	Rev-	TTCAGTCGCCGCGCGAACAT	3224	3243	
FAS	Fwd+	TCCTGGTGTGGTGCCTGCCT	2005	1986	159
	Rev-	GCAGCGTGGGGGCAATTCCT	2145	2164	
PPARγ	Fwd+	ACCCAGAGCATGGTGCCTTCG	138	118	79
	Rev-	CCGAAGTTGGTGGGCCAGAATGG	195	217	
Liver					
β-Actin	Fwd+	CCTGTGCTGCTCACCGAGGC	122	103	161
	Rev-	TGTGGGTGACCCCGTCTCCG	264	283	
PPARα	Fwd+	AGCGTGGTGCATTTGGGCGT	202	183	156
	Rev-	GCGGGCCACAGAGCACCAAT	339	358	
PEPCK	Fwd+	GCACCCCTGCCAGCCAATGT	1382	1363	171
	Rev-	ATGCTCTGCAGCAGCGGTGG	1534	1553	
GC receptor	Fwd+	TGGCCAAAGGCGATACCAGGC	1800	1780	128
	Rev-	TCAGGAGCAAAGCAGAGCAGGT	1907	1928	
5β-reductase	Fwd+	CGCCCAGCCCTGGAAAGGAC	351	332	144
	Rev-	GCCTCCCACGTGGCACACAG	476	495	

αGSU=common α gonadotrophin subunit; FAS=fatty acid synthase; FSHβ=follicle stimulating hormone subunit β; GAPDH=glyceraldehydes-3 phosphate dehydrogenase; GC=glucocorticoid; HSL=hormone sensitive lipase; LHβ=luteinising hormone subunit β; LPL=lipoprotein lipase; PEPCK=Phosphoenolpyruvate carboxykinase; PPAR=peroxisome proliferator activator protein; Fwd=forward primer; Rev=reverse primer.

2.9.1. SYBR Green Signal Generation

Most genes were analysed using a *Power* SYBR® Green PCR reaction according to the manufacturer's instructions. The chemistry of the SYBR® Green reaction means that both specific and non-specific dsDNA products are detected and so it was important for all primers to amplify only one product specifically. For this reason, each primer set and corresponding amplicon sequences were BLAST searched before ordering.

To validate primers for use with SYBR® Green, primer pairs first underwent standard PCR and gel electrophoresis in each chosen tissue to assess for the presence of a single PCR product, as shown for GAPDH in Figure 2.5. To further validate primers for use in *Power* SYBR® Green PCR, a set of standards was constructed by serially diluting a stock aliquot of cDNA from each tissue. Approximately six diluents were then run in triplicate for each target gene and a standard curve constructed using ABI7500 software (Version 2.0.1). RT Negative cDNA was diluted 1 in 10 and added to wells as a negative control for each target gene. For every PCR run, a master reaction mix was then made up for each gene under investigation and bulked up for the total number of individual well reactions. 9µl of master mix was pipetted into each well of a 96-well fast plate (Applied Biosystems) before adding 1µl of diluted cDNA template; individual reaction components are detailed in Table 2.10.

Table 2.10: Single reaction components for the *Power* SYBR® Green PCR reaction

Component	Volume (µl)
SYBR master mix 2X	5
Distilled Water	3
Forward Primer	0.5
Reverse Primer	0.5
cDNA template	1
	10

Primers were assessed using the criteria outlined by Figure 2.5. ABI7500 software calculated reaction efficiency as well as fit (R^2) and slope of a standard curve; a reaction efficiency of between 90-110% was considered acceptable, providing the R^2 value was between 0.95 and 1 (in accordance with the manufacturer's instructions). A melt (dissociation) curve was run by gradually increasing the temperature beyond that of cDNA melting temperature, in order to assess for the presence of a single reaction product. ABI7500 software records a melt curve of reporter fluorescence against temperature. Twin peaks on this melt curve would indicate the presence of non-specific/impure PCR product or primer-dimer formation. During each PCR plate run, RT negative samples appeared as small peaks before the major melt curve peak, due to the absence of any template cDNA.

For the amount of product to be doubling in the exponential phase, and assuming equal serial dilutions of cDNA were performed, the slope of a standard curve would be around -3.32. This was the main criterion used when evaluating and selecting primer sets for use in the quantification of gene expression. The primer validation criteria for each primer used in quantitative PCR throughout this thesis is shown in Figure 2.5 and Table 2.11.

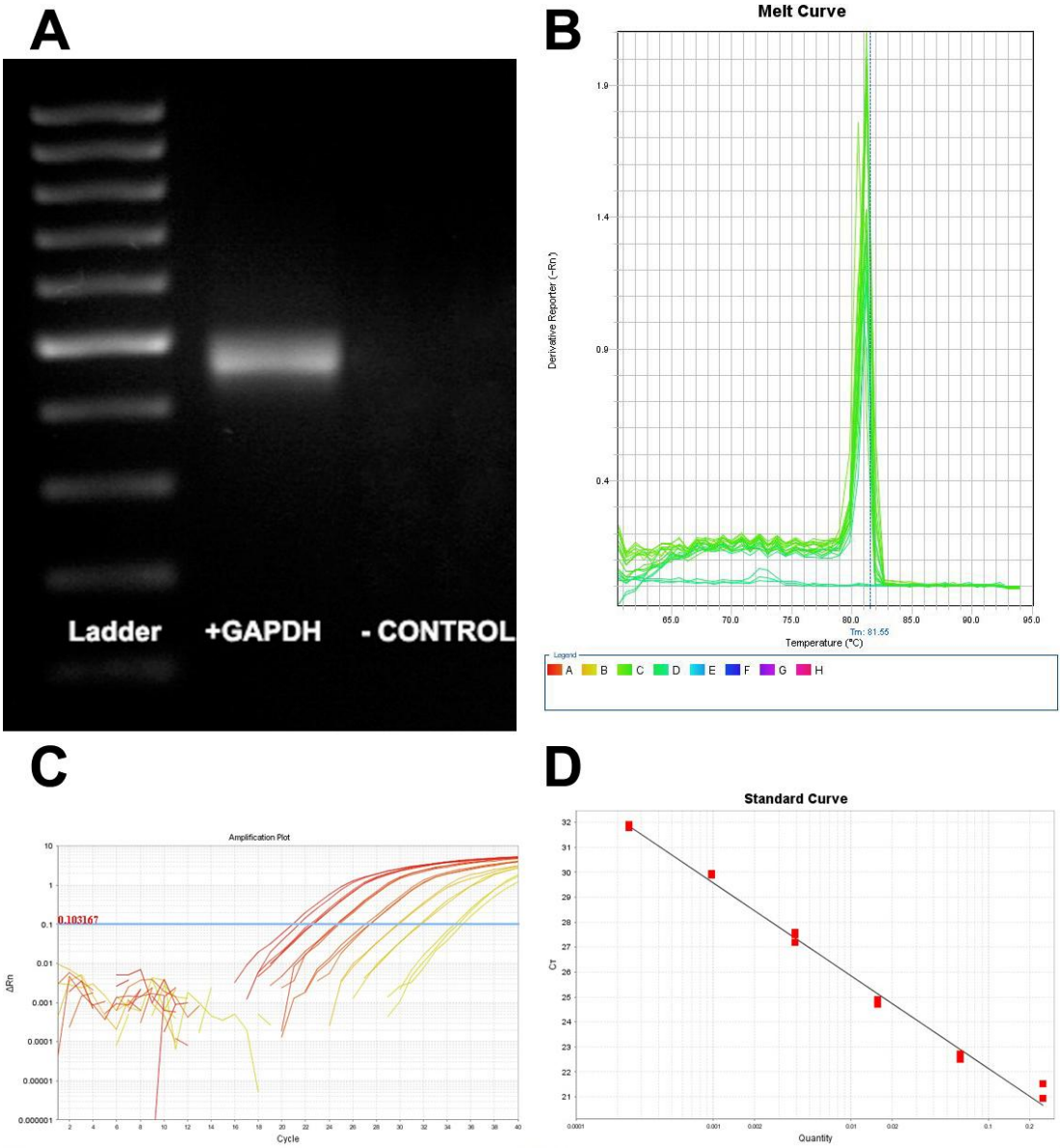

Figure 2.5: Gene expression validation: After initial validation using gel electrophoresis (A), serial diluents of a stock aliquot of cDNA at 1:4 nuclease free water were made up and run in triplicate on an ABI7500 machine. This generated (B) a dissociation (melt) curve to assess the purity of PCR product (C) an amplification plot with regular spacing between the CT value of the diluents which could be used to generate (D) a standard curve. The example shown here is for housekeeping gene GAPDH in the rat pituitary.

Table 2.11: Primer validation criteria for genes of interest in the designated tissues using SYBER Green PCR: Orange boxes denote control genes used; grey shading denotes use of Universal Probe Library (UPL) chemistry instead of SYBER green chemistry against the liver control gene cyclophillin (Chapter 5); *****denotes further control genes validated but not used for that tissue. Melt curves with more than one peak (✖) invalidated primers.

Tissue / Gene	Std curve dilution series	R^2	Efficiency (%)	Slope	Melt curve
Pituitary					
β-Actin	1:4	0.993	95	-3.48	✓
GAPDH*		0.988	94	-3.45	✓
αGSU		0.972	99	-3.35	✓
FSHβ		0.984	105	-3.20	✓
LHβ		0.858	103	-3.26	✓
Estrogen receptor		0.858	101	-3.21	✓
GR		0.992	107	-3.12	✓
Liver					
β-Actin	1:4	0.993	102	-3.25	✓
GAPDH		0.929	106	-3.19	✓
18-S*		0.996	60	-4.89	✓
β2-microglobulin*		0.998	101	-3.28	✓
TATA box binding protein*		0.977	102	-3.27	✖
PPARα		0.993	109	-3.12	✓
5β-reductase		0.999	98	-3.36	✓
PEPCK		0.999	100	-3.31	✓
PPARγ		0.947	86	-3.71	✖
Cyclophillin		0.997	104	-3.22	✖
5α reductase		✖	✖	✖	✖
11β-HSD type 1		0.624	637	-1.15	✖
Mesenteric fat					
B2-microglobulin	1:2	0.997	109	-3.12	✓
Cyclophillin*		0.971	107	-3.14	✖
Leptin		0.994	109	-3.13	✓
Resistin		0.984	107	-3.14	✓
Adiponectin		0.979	109	-3.13	✓
FAS		0.996	111	-3.08	✓
LPL		0.986	101	-3.21	✓
HSL		0.995	108	-3.13	✓
PPARγ		0.985	104	-3.02	✓

18-S=ribosome subunit 18; αGSU=common α gonadotrophin subunit; FAS=fatty acid synthase; FSHβ=follicle stimulating hormone subunit β; GAPDH=glyceraldehydes-3 phosphate dehydrogenase; GR=glucocorticoid receptor; HSL=hormone sensitive lipase; 11β-HSD=11β-hydroxysteroid dehydrogenase; LHβ=luteinising hormone subunit β; LPL=lipoprotein lipase; PEPCK=Phosphoenolpyruvate carboxykinase; PPAR=peroxisome proliferator activator protein.

2.9.2. Relative quantification

Gene expression was analysed by relative abundance to a reference gene as well as to control tissue gene expression and so the 2^ΔΔCT method was used. Sample cDNA was diluted 1 in 10µl in nuclease free water (1 in 5µl for cDNA derived from fat) and this diluent used in each for the PCR reaction for that specific tissue. After each run, the threshold was reset to 0.103 amplification units if required, and the data analysed by the ABI7500 software and exported into an Excel spreadsheet. Equation 1 below was used to work out the relative expression of the gene of interest. These results were then graphed and statistically analysed to assess any differences in gene expression.

(i) $\Delta CT = CT\ test\ gene\ (FSH\beta) - CT\ reference\ gene\ (\beta Actin)$

(ii) $\Delta\Delta CT = (Test\ tissue\ \Delta CT) - (Mean\ control\ tissue\ \Delta CT)$

(iii) $Relative\ expression = 2^{\wedge}\Delta\Delta CT$

Equation 1: 2^ΔΔCT method of analysis: (i) FSHβ analysed relative to βActin for the tissue of interest (ii) FSHβ expression analysed relative to mean control tissue ΔCT (iii) Assuming PCR is doubling the amount of the gene of interest every cycle, relative gene expression is calculated by taking 2 to the power of the ΔΔCT value.

2.9.3. Roche Light Cycler PCR (liver)

For liver genes which could not be optimized using SYBR green, for example 5α-Reductase, an alternative method of quantitative PCR was used. Primer-probe PCR involves addition of a fluorescent probe specific for the gene of interest which lies between the primer extension sites. Due to the presence of a probe complementary to the gene of interest, primer-probe PCR chemistry is highly specific at amplification and therefore measures no background primer-dimer formation. Analysis of the relative expression for each gene of interest in this instance was measured in relation to a control gene, using a standard curve method. For construction of a standard curve 1-2µl of cDNA from each sample were added together and serially diluted 1:3 in nuclease free water. These serial diluents were used to construct a standard curve for each gene, and were run on each 384 well plate (Roche, Welwyn, UK), in addition fluorescence was detected using a light cycler

(Roche, Welwyn, UK) and the data exported into Excel. CT values were then be used to calculate the expression of each gene in relation to the control gene cyclophillin using the ΔCT method. Details of universal probe library sequence designations are given in Chapter 5.

2.10. Steroid hormone plasma-extraction

To extract steroid hormone from plasma samples, 100-200µl rat plasma/qualitative plasma control was pipetted into large glass tubes, followed by 2ml of diethyl ether and these substances mixed using a multi-tube clamp vortex (Baxter Scientific Products) for 3 minutes. Industrial methylated spirit (IMS) was then poured over dry ice in a metal bath and the tube racks placed in the resulting "slurry" mixture. This process snap-freezes the bottom of the tubes leaving a fraction of the mixture containing liquid steroid hormone dissolved in ether. The unfrozen fraction containing steroid was decanted into corresponding 12x75 glass tubes and left to evaporate overnight in a fume hood. Steroid hormone was re-solvated in an appropriate volume of assay buffer to allow for subsequent RIA analysis in duplicate.

2.11. Radioimmunoassay

2.11.1. Radioactive handling and iodination

Radioactive substances were handled at an in-house 'hotlab' in accordance with local Health and Safety Rules and Radiation Protection Safety guidelines. Iodination of all tracers was carried out by Mr Ian Swanston. Tracers were stored in the hotlab and radioactive usage was documented in µCi. Before and after handling, a pre-iodination sweep check of the bench was carried out using a Geiger counter and any contamination reported to the Area Radiation Protection Officer. Contaminated glass and plastic were soaked in Decon detergent (Sigma, UK) after use.

2.11.2. RIA Protocol

Unless otherwise stated, RIA antibody reagents were provided by the National Institute of Diabetes and Digestive and Kidney Diseases (NIDDK, Bethesda, MD, USA) and have been made available to researchers for many years. RIA is therefore a well established standard technique for measuring hormone concentrations. Radioimmunoassay (RIA) is based on competition between a hormone, for example estradiol (E2) and a trace amount of radioactive E2 for binding sites on a primary antibody specific to E2.

In each assay a secondary antibody was added to binds the c-fragment epitope of the primary rabbit antibody. This formed a complex in the presence of normal rabbit serum γ-globulin (NRS). This complex precipitated upon addition of wash buffer (9g NaCl, 40g PEG 6000, Triton-X 0.2% 1ml dissolved in 1 litre dH_20) and was pelleted by centrifugation at 4ºC at 1400rpm for half an hour. Any "free" ^{125}I-steroid was poured off, leaving a pelleted 'bound' ^{125}I-steroid fraction, which was measured using a γ-counter machine. Thus, the greater the amount of standard/unknown steroid competing with the ^{125}I-steroid, the lower the resulting counts.

The concentration of steroid in the unknown sample is interpolated from a standard curve using standard solutions with known concentrations of steroid. The typical standard curves obtained for each RIA described in this thesis are shown in Figure 2.6; a semi log plot where the y-axis is conferred by the ratio of bound to free ligand, against a logarithmic x-axis of standard concentrations.

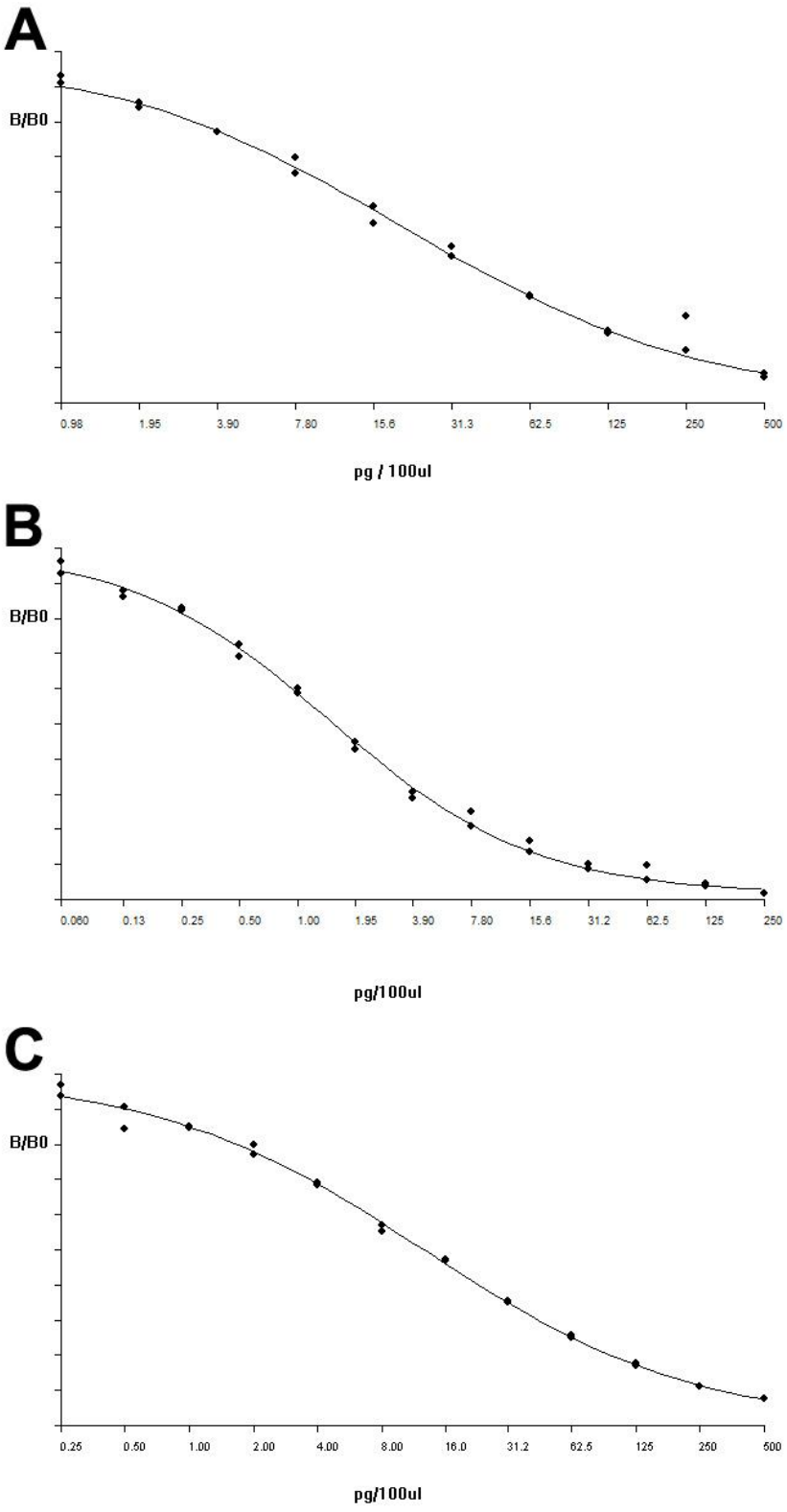

Figure 2.6: Standard curves from (A) Androstenedione (B) Estradiol and (C) Testosterone RIA experiments: Relative binding against known standard quantities for n=1 curve per assay.

Tubes were labelled in duplicate and set up with a standard curve followed by unknown samples for assay, as shown in Table 2.12.

Table 2.12: Reagent volumes (µl) used in a typical RIA experiment

Sample	Buffer	Primary antiserum	Tracer	Secondary antiserum	NRS
Total counts	-	-	100	-	-
NSB	100	-	100	100	100
B_0	100	100	100	100	100
Standards/samples	100	100	100	100	100

NRS=normal rabbit serum; NSB=non specific binding

Tracer was defrosted inside a lead protector and then added to the required amount of assay buffer until 100µl of buffer/tracer mix was read at 10-15,000 counts on a mini-γ-counter. Primary antibody, tracer and secondary antibody/NRS were added over several time courses (between 1-3 days) depending on the sensitivity of the assay (Table 2.13).

Table 2.13: Protocol and reagent summaries for RIAs performed: all tracers were made up to between 10-12,000 counts per minute for each assay.

Assay:	Androstenedione	Estradiol	Testosterone
Tracer	A4- I^{125} (MP Biomedicals) Code 07-109226	E2 MAIA kit (Biostat Diagnostics, Cheshire, UK)	T- I^{125} (MP Biomedicals) Code 07-189126
Standard range	Top: 5000pg/ml Bottom: 9.8pg/ml (Sigma)	Top: 2500pg/ml Bottom: 0.6pg/ml (MAIA kit)	Top: 5000pg/ml Bottom: 2.5pg/ml (Sigma T1268)
Primary AB	Rabbit α-A4 Use at 1:320,000 (MP Biomedicals)	Rabbit α-E2 1:5 (MAIA kit)	Rabbit α-T Use at 1:600,000 (AMS Biotech)
Primary incubation	Overnight	n/a	n/a
Sample incubation	Overnight in fridge		
Secondary AB serum	Donkey α Rabbit Use at 1:1000 (Diagnostic Scotland)	Goat α Rabbit Use at 1:200 (Diagnostic Scotland)	Donkey α Rabbit Use at 1:60 (Diagnostic Scotland)
NRS	Use at 1:200	Use at 1:200	Use at 1:600
Secondary/NRS incubation	1 hour on bench	4 hours on bench	

AB=antibody; NRS=normal rabbit serum; α=anti; A4=androstenedione; E2=estradiol T=testosterone

Phosphate gelatinous buffered saline (PGBS) was used as an assay buffer. PGBS was made by dissolving 11.46g of $Na_2HPO_4.2H_2O$, 2.61g of NaH_2PO_4, 9g NaCl, 1g of gelatine and 0.1g thiomersalate in 1 litre dH_2O and altering the pH to 7.4 using HCl.

2.11.3. RIA Analysis

To analyse the raw γ-count data, a specialist software program, AssayZap (Biosoft, Cambridge, UK) was used. AssayZap allows the user to program in standard curve, quality control and unknown samples, which it then utilizes to construct standard curves; the B_0 and NSB values are used to estimate the upper and lower curve limits. Each standard curve was saved to a 'graveyard' for future reference. The programme then calculates the data for quality controls and quantities of hormone present in each unknown, and the resulting data can be exported into Microsoft Excel for statistical analysis.

2.12. Enzyme Linked Immunosorbent Assay (ELISA)

An ELISA operates using similar principles of antigen binding as RIA and is a well established technique for measuring hormone levels in small quantities of plasma or media. In the ELISA kits used for insulin and inhibin B analysis, microplate wells were pre-coated with a capture antibody for the protein of interest. Gonadotrophin ELISAs were developed my Mr Ian Swanson. These used adsorbent plastic plates (Nunc Biologicals) which were coated by incubating the adsorbent plates with 50µl capture antibody at a specified concentration overnight at 4ºC. Capture antibodies were diluted in coating buffer made by dissolving the contents of one carbonate-bicarbonate capsule (Sigma, code C3041) in 100ml deionised water. The plate was then washed the next day and blocked with assay buffer for at least one hour. After blocking and two consecutive washes, the standards, qualitative controls and unknown samples were added to the plate and again incubated overnight at 4ºC. ELISA protocols are summarised in Table 2.14. ELISA wash buffer was made as a X 25 concentrate by dissolving 302g tris base, 450g sodium chloride

(NaCl), 25ml tween20 in dH_2O. The pH was adjusted to 7.5 using hydrochloric acid (HCl) and the volume made up to 2 litres. Gonadotrophin ELISA assay buffer, in which ELISA reagents were dissolved was made by dissolving 6g tris base, 9g NaCl, 10g BSA (Sigma A3294), 1g bovine-γ globulin, 0.1ml tween20, 0.05g thiomersalate in dH_2O. The pH was adjusted to 7.5 with HCl and buffer volume made up to 1 litre.

Table 2.14: Protocol and reagent summaries for ELISAs performed:

ELISA	FSH	LH	Insulin Kit	Inhibin-B Kit
	In house	**In house**	**Crystal Chem. Inc.**	**DSL Inc.**
Stock protein	Mouse FSH 2.5µg/vial (NIDDK AFP5308D)	Mouse LH 2.5µg/vial (NIDDK AFP5306A)	Rat Insulin 25.6ng/ml	N/A
Standard Range	0.78 to 50µg/ml	0.078 to 25µg/ml	0.1 to 12.8 ng/ml	10 to 1000pg/ml
Capture antibody (4°C)	Anti-β chain Mab (Medix 6602) 4µg/ml overnight	Anti-β chain Mab (Gift, code 518B7) 2µg/ml overnight	Pre-coated plates	Pre-coated plates
Sample incubation	Overnight		2 hours	Overnight
Signal biotin-conjugate antibody (RTP)	Anti-rat α subunit IC1 (NIDDK AFP66P9986) 0.5µg/ml 2 hours	Anti-β chain Mab (Medix 5303) 1µg/ml 2 hours	Anti-insulin enzyme conjugate 30 min	Anti-inhibin α-subunit 20min
Detection HRP conjugate antibody (RTP)	Anti-rabbit HRP (Thermo #31458) 1:10,000, 30min	Amdex Strep-HRP (GE Healthacre RPN4401V) 1:10,000, 30min	Included in step above	Strep-HRP 20 min
Chromogen solution	TMB Microwell Peroxidase (KPL) 30 min		Enzyme substrate 10 min	TMB in citrate with H_2O_2 40 min
Stop Solution	6% H_3PO_4		0.5M H_3PO_4	0.2M H_3PO_4
Wash Solution	ELISA wash buffer		Provided by manufacturer	

FSH=follicle stimulating hormone; H_3PO_4= phosphoric acid; HRP=horseradish peroxidase; LH=luteinising hormone; RTP=at room temperature and pressure; Strep=streptavidin; TMB=tetramethylbenzidine chromogen reagent.

After incubation with samples, ELISA plates were washed before addition of 100µl/well antibody-biotin conjugate against the protein of interest, followed by a further wash and addition of 100µl/well streptavidin conjugated horseradish peroxidise (HRP) antibody, which attaches to the biotin conjugate. A further wash cycle removed unbound conjugate, after which 100µl/well TMB (3',5,5'-tetramethylbenzidine), was added and oxidised by the conjugated HRP, generating a blue coloured product. Oxidation was stopped by 100µl/well phosphoric acid

solution, turning each well yellow. The absorbance was read at λ 450nm and λ 600-620nm. The second reading was subtracted from the first to eliminate any background from the results. For the gonadotrophins a standard curve was plotted using AssayZap standard values of absorbance (nm) against their known concentration (ng/ml), and the values of unknown samples interpolated (Figure 2.7).

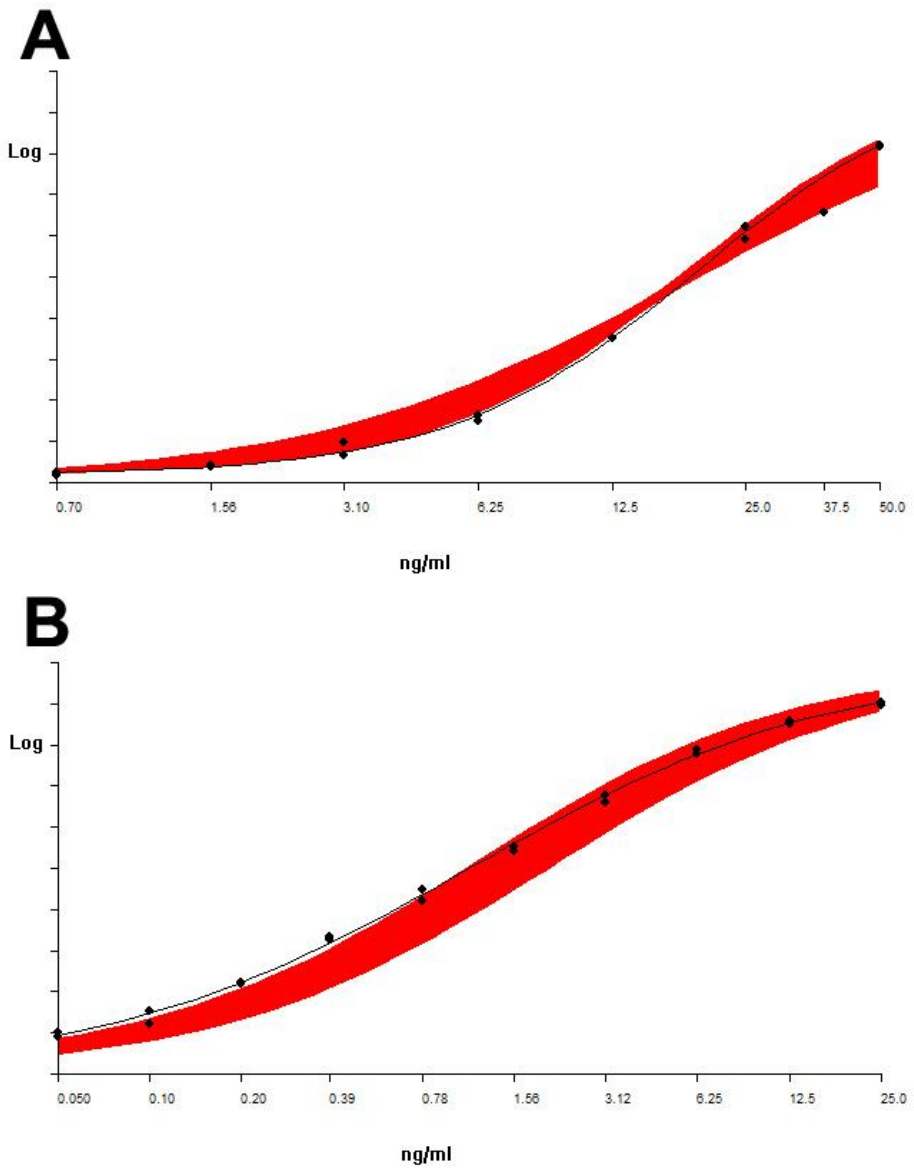

Figure 2.7: Standard curves for (A) FSH and (B) LH in-house ELISA plates (*n*=10 each): Typical curves are shown against a range (red) of other standard curves. Unknown values were interpolated using AssayZap.

For the insulin and inhibin ELISAs linear regression was performed according to the manufacturer's instructions and the values of any unknown samples interpolated from this standard curve. Inhibin B levels were interpolated using AssayZap (Figure 2.8) and insulin levels using GraphPad Prism (Figure 2.9).

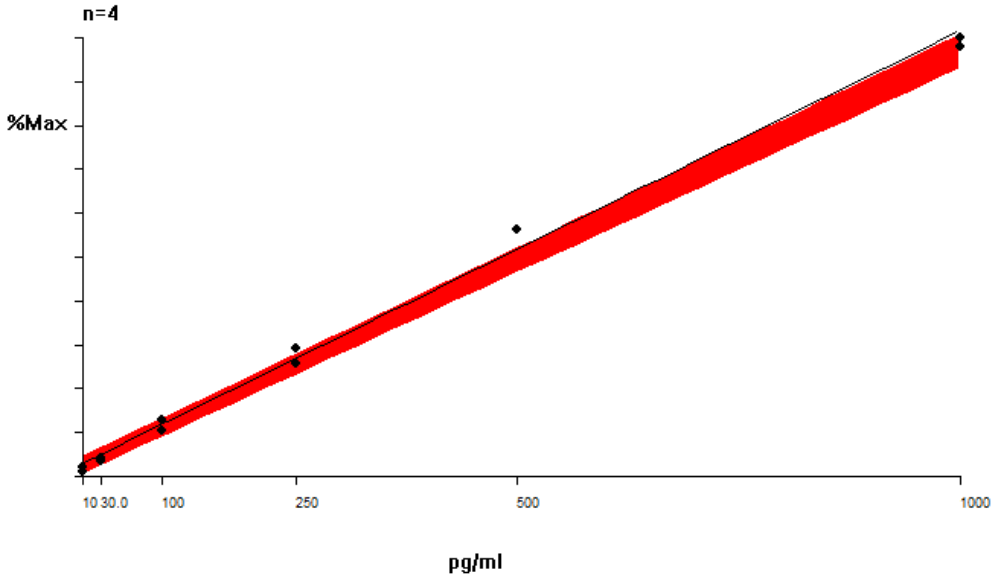

Figure 2.8: Standard curve for *n*=4 Inhibin B ELISAs: Unknown values were interpolated using AsssayZap linear regression analysis.

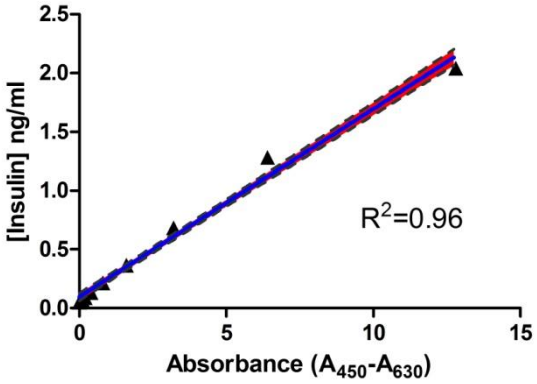

Figure 2.9: Standard curve for *n*=9 Insulin ELISAs: Unknown values were interpolated using GraphPad Prism linear regression analysis. Blue line is the mean linear relationship between insulin concentration and absorbance, with shading indicating the 95% confidence limit of the assay.

2.13. Glucose assay

A glucose assay was used to determine the blood glucose levels of rats undergoing glucose tolerance testing. Unlike the ELISAs which rely on antibody binding, a glucose assay relies on a naturally redox reaction where addition of hexokinase enzyme, catalyses the phosphorylation of glucose, the product of which is further oxidized to 6-phosphogluconate, simultaneously reducing NAD+ to NADH. The amount of NADH formed is proportional to the concentration of glucose in the sample, and is then measured by an increase in absorbance at 340nm.

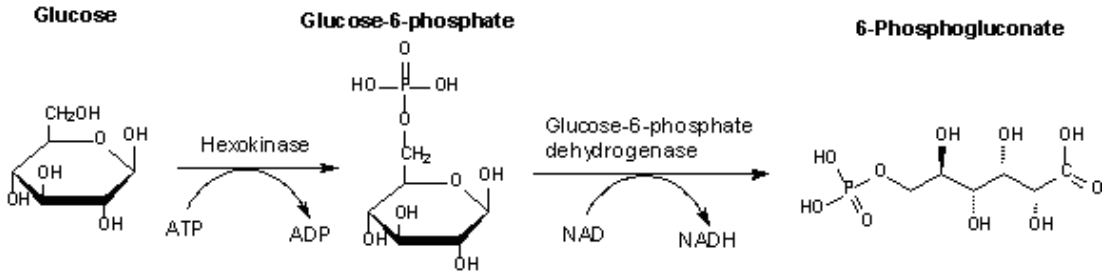

Figure 2.10: Reactions occurring in the glucose assay system: Hexokinase catalyses the phosphorylation of glucose by ATP into glucose-6-phosphate (G6P) and ADP. G6P is subsequently oxidized to 6-phosphogluconate through the reduction of NAD+ to NADH by Glucose-6-Phosphate dehydrogenase. The amount of NADH formed is equimolar to the amount of glucose in the initial sample and is measured by spectrophotometer at 340nm.

200mg/dl glucose standard (TR15923 Thermo Scientific) was used to make up the standards listed in Table 2.15. To each well 200µl of infinity glucose hexokinase liquid stable reagent (TR15421, Thermo Scientific) was added and covered for precisely 10 minutes before measuring the absorbance at 340nm.

Table 2.15: Standard concentrations and volumes used for constructing glucose assay standard curves: 200mg/dl glucose standard was diluted in distilled water as shown for each standard up to 150mg/dl. 2µl of each standard was added in duplicate to the assay and 3-5µl added to give the higher standard values (blue).

[Standard] (mg/dl)	Distilled water (µl)	Glucose Standard (µl) at 200mg/dl
Blank	100	0
25	87.5	12.5
50	75	25
100	50	50
150	25	75
200	-	**2**
300	-	**3**
400	-	**4**
500	-	**5**

Linear regression was used to form a straight line from which unknown samples and were be interpolated (Figure 2.11).

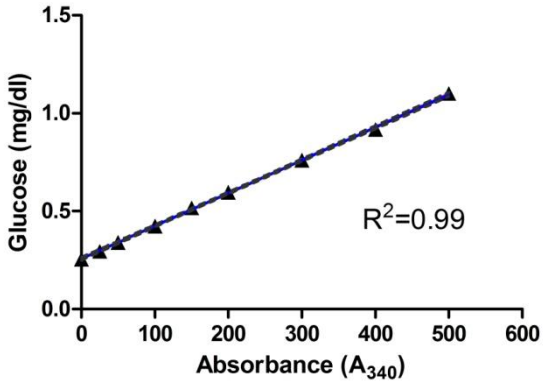

Figure 2.11: Standard curve for *n*=9 glucose assay plates: Unknown values were interpolated using GraphPad Prism linear regression analysis. Blue line is the mean linear relationship between insulin concentration and absorbance, with shading indicating the 95% confidence limit.

2.14. Statistical analyses

All raw data was collated in a Microsoft Office Excel 2003 spreadsheet and exported to GraphPad Prism 5 for statistical analysis. Two-way analysis of variance (ANOVA) was performed between any grouped data, for example follicle counts, with a Bonferroni post-hoc to assess for specific in-group differences. Unless otherwise states, a two-tailed unpaired student's t-test was used to evaluate differences between rodent treatment groups in all other circumstances.

Another analysis used was the Mann-Whitney test for non-parametric comparisons. A Kolmagorov-Smirnov test was also employed to assess the distribution of follicle percentage data (Chapters 4 and 7). This test showed that distribution of follicles in the ovary is not Guassian in control animals, likely due to large proportions of primordial follicles. However, the distribution of percentages/proportions between control and treated groups was similar in all experiments. However, it should be noted that higher *n* numbers than those employed in these experiments are usually required for distribution analysis and KS test to be robust.

To measure correlation between two sets of data (X and Y), Pearson product-moment correlation (PPMC) was used. A PPMC is a type of linear regression for normally distributed data. As shown in Equation 2 a correlation coefficient, '**r**' or '$\mathbf{R^2}$'is calculated; a value close to 1 or -1 denotes a positive or negative correlation, and a value of 0 denotes no correlation.

$$r = \frac{1}{n-1}\sum_{i=1}^{n}\left(\frac{X_i - \bar{X}}{s_X}\right)\left(\frac{Y_i - \bar{Y}}{s_Y}\right)$$

Equation 2: Pearson-product moment correlation (PPMC): the covariance of the two variables (X and Y) divided by the product of their standard deviations. *r*=correlation coefficient, n=number of measurements, *S* / ð=standard deviation, Ẋ=mean

To assess for differences between two correlation coefficients, a Fisher *r*-to-*Z* transformation was performed and applied to the sample correlation coefficients (r) calculated by a PPMC. A Fisher transformation is shown in Equation 3. In statistical packages like GraphPad, a P value for a Fisher transformation can also be calculated to test for the significant differences between two sets of overlapping correlative data.

$$z = 0.5[\ln\{1+r\} - \ln\{1-r\}]$$

$$\sigma_{z1\text{-}z2} = \sqrt{[\{1/N1-3\} + \{1/N2-3\}]}$$

Equation 3: Fisher r-to-*Z* transformation: A PPMC correlation coefficient 'r' is transformed to a normally distributed Fisher coefficient, 'z' for each PPMC, where ln is the natural logarithm. The next formula calculates the differences between each fisher coefficient ($\sigma_{z1\text{-}z2}$) for the number of data points from each sample group (N).

Data is expressed in graph format where appropriate with control bars/lines in red and error bars denoting the standard error of the mean value (SEM) where possible. Data was considered significantly different if the resulting *P* value of a statistical test was ≤0.05 (denoting a 95% confidence of significance) and the levels of significance are expressed throughout this thesis as per the rules in Table 2.16.

Table 2.16: Significance levels pertaining to all data analysis within this thesis.

Significance	Star Value	*P* value
Not significant (NS)	n/a	> 0.5
95% significance	*	≤ 0.5
99% significance	**	≤ 0.1
99.9% significance	***	≤ 0.01

2.15. General solutions

Reagents for other solutions used in the lab are summarised in Table 2.17.

Table 2.17: General solutions used:

Solution type	Protocol	Quantity
EDTA - 500ml - 0.5M	EDTA disodium salt Deionised H_2O *pH to 8 with NaOH, top up to 500ml*	93.05g 400ml
Agarose gel - 1% - Electrophoresis	Agarose Deionised H_2O TAE 1X	0.5g 45ml 5ml
TAE - Tris acetate EDTA - 1 litre - X 50	Tris base Deionised H_2O Glacial acetic acid EDTA (0.5M)	242g 842.9ml 57.1ml 100ml
TE Tween	Tris-HCl EDTA 0.5M Tween Deionised H_2O *(make up to 50ml)*	2.5ml 100µl 250µl ~47.15ml

EDTA=ethylendiamine tetra-acetic acid; g=grams; HCl=hydrochloric acid; H_2O=water; ml=millilitres.

Chapter 3. Generation of a Granulosa Cell specific Androgen Receptor Knockout (GCARKO)

3.1. Introduction

Over the past 20 years, genetic manipulation has been an invaluable tool when investigating physiological processes *in vivo* (Andersson and Skalhegg 1998). Global mouse knockouts of growth differentiation factor-9 (GDF-9KO), estrogen receptor β (ERβKO) and the androgen receptor (ARKO) to mention a few have illustrated the essential role of these genes and their protein products not only in female reproduction, but in many areas of mammalian physiology (Reviewed in Matzuk 2000). Classical gene targeting has been refined, and now both tissue specific and developmentally timed knockouts are possible. Instead of disrupting the target gene in embryonic stem (ES) cells directly, a gene of interest is now flanked or 'floxed' at introns by two *lox*P sites. A knockout is derived through Cre recombinase action at these sites when the *lox*P mouse line is bred with a second line which expresses the *Cre recombinase* gene (Figure 3.1)**.**

Within a Cre-*loxP* system, Cre recombinase can be driven by an upstream promoter of choice, which allows the researcher to direct Cre expression, and therefore the knockout, in a cell lineage specific manner. Furthermore, the Cre-*loxP* system overcomes embryonic and neonatal lethality problems which can arise from global knockouts, and recent generation of floxed fluorescent protein transgenes allows researchers to visualise Cre activity within live cells and organs in real-time. One disadvantage lies in the selection of a promoter able to drive Cre expression with sufficient precision and activity that it completely excises the target gene. In addition geneticists must rely on the *lox*P sites to be sufficiently accessible to the Cre recombinase protein (Davey and MacLean 2006).

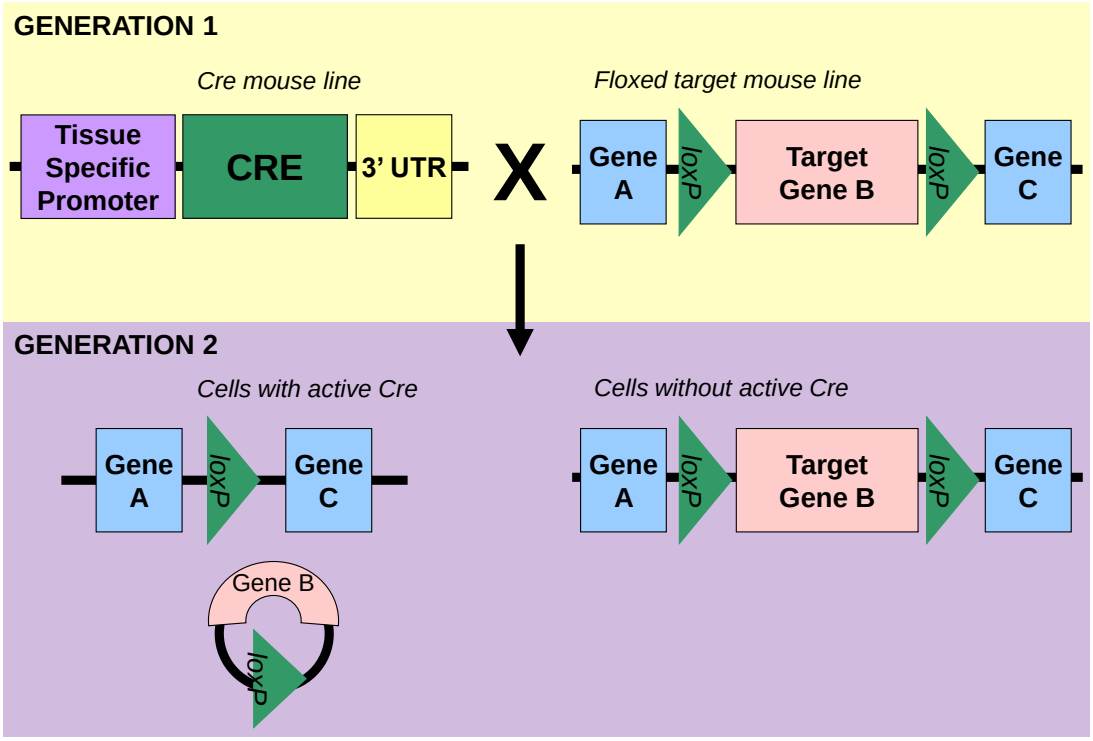

Figure 3.1: The Cre-*lox*P system of transgenic derivation: In generation 1 Cre recombinase expression is driven by a cell/tissue specific promoter within the genome of a first mouse line. The genome of a second mouse line contains the target gene flanked by two 34 base pair *loxP* sites. When these two mouse lines are mated together, the resulting offspring (generation 2) contain both the tissue specific Cre recombinase and ubiquitously expressed *loxP* sites flanking the gene of interest. The cell specific Cre recombinase recognises the *loxP* sites, excises the DNA between them, so that they recombine, removing the gene of interest (Adapted from Davey and MacLean 2006).

Global AR knockout (ARKO) female mice exhibit reduced follicular maturation, and upon stimulation with hCG these ARKO females produce fewer CL and exhibit increased levels of GC apoptosis, thus the AR appears necessary for folliculogenesis (Hu, Wang et al. 2004). The use of Cre-*lox*P technology to ablate the AR in a cell or tissue specific manner would allow more informative conclusions to be drawn as to its role within the ovary. In male mice, generation of AR Cre-*lox*P knockouts is a straightforward process in comparison to female mice, since the AR gene is located on the X chromosome; a single generation cross of a floxed female ($Cre^{-/-}$ $AR^{f/f}$) with a Cre positive male ($Cre^{-/+}$ $AR^{+/y}$) will theoretically produce a knockout in half of the male F1 offspring. Conversely generation of female ARKO animals, with the exception of the global knockout previously described, is considerably more difficult. The F1 generation must first be genotyped to ensure that

a second generation F2 derivation can potentially produce a knockout animal. The main issue that arises when knocking out a gene on the X-chromosome in female animals is that of dosage compensation and XCI (discussed in Chapter 1, Section 11.2). In the derivation of male embryos with a floxed X-linked gene of interest, one Y chromosome and one X chromosome only are present, thus XCI does not take place and the floxed gene is expressed and can excised by Cre in the F1 generation when the male is bred with a Cre positive female. By comparison, in female embryos with a floxed gene of interest, dosage compensation processes inactivate one unaltered chromosome in 50% of cells, and the other floxed chromosome the other 50% of cells of the P1 generation. The resultant female offspring of the F1 generation will therefore, in theory, exhibit a mosaic pattern of floxed cells. In order to successfully flox 100% of cells in the next generation of female animals, this female must be bred with another male that also contains a floxed X-linked gene of interest. Recent research using AR-floxed mice has therefore yielded little insight regarding the involvement of the AR in female fertility with publications focused upon the more accessible effect of cell specific ARKO upon male fertility (Table 3.1).

Table 3.1: Summary of novel reproductively relevant ARKO publications to date: ARKO studies are either global knockouts or they target male tissues.

Cre promoter	Target cells	Gender studied	Reference(s)
β-Actin	Global	♂ and ♀	*(Yeh, Tsai et al. 2002)*
hCMV	Global	♂ and ♀	*(Matsumoto, Takeyama et al. 2003; Notini, Davey et al. 2005)*
PGK	Global	♂ and ♀	*(Venken, De Gendt et al. 2006)*
AMH	Sertoli cells	♂ only	*(Chang, Chen et al. 2004; De Gendt, Swinnen et al. 2004)*
AMHR-II	Leydig cells	♂ only	*(Xu, Lin et al. 2007)*
Transgelin	Peritubular Myoid cells	♂ only	*(Zhang, Yeh et al. 2006)*
Scyp1	Germ cells	♂ only	*(Simanainen, Allan et al. 2007)*

♂=male physiology; ♀=female physiology; hCMV=human cytomegalovirus minimal promoter; PGK=phosphoglycerate kinase-1; AMH=Anti-Müllerian Hormone.

A successful SCARKO model has since been described using a Cre-*lox*P system, with *Cre* driven off the Sertoli-cell specific AMH promoter (Chang, Chen et

al. 2004; De Gendt, Swinnen et al. 2004). In the female mouse, AMH is produced by GCs of growing follicles and functions to inhibit the recruitment of primordial follicles into the activated follicle pool through an as yet unknown mechanism (Visser, Durlinger et al. 2007). For this reason, a granulosa cell specific androgen receptor knockout mouse (GCARKO) has been attempted in order to elucidate the specific role of AR in granulosa cell function more clearly. AR is expressed throughout the tissues of the mammalian ovary and non-aromatisable androgens such as DHT have been shown to augment GC FSH production *in vitro* (Hillier and De Zwart 1981). However, the molecular mechanisms by which AR affects GC function *in vivo* remain to be documented. This chapter will describe an attempt to generate a GCARKO model using the sisters of SCARKO animals and breeding them for a further generation.

3.2. Objectives

- To derive a GC specific ARKO (GCARKO) mouse using the SCARKO breeding line as previously described (De Gendt, Swinnen et al. 2004).

- To verify Cre activity by mating AMH-Cre positive males to females with a floxed enhanced yellow fluorescent protein (EYFP) transgene.

- To verify AR knockout in the GCs of second generation AMH-Cre X ARflox crosses using IHC and IHF techniques.

- Identify any differences in the estrus cycles and reproductive organs of knockout and mosaic knockout female animals.

- Identify the role of AR in follicle development using this model, through ovarian, follicle and GC cultures.

3.3. Methods

3.3.1. Transgenic Line Husbandry

Experiments were conducted at a University of Edinburgh animal house facility, Western General Site, Edinburgh. All animal studies were carried out in accordance with the Animal (Scientific Procedures) act 1986 and were approved by the Home Office. BRR staff were responsible for daily mouse husbandry and smears were performed by Ms Linda Baker on site, stored in a humidity box and couriered to the author for examination at the end of two weeks. Experimentation operated through personal licence PIL 60/10682 and project licence PPL 60/3544 held by Professor Philippa Saunders. Mice were housed in clear solid-bottomed cages, containing bedding of wood shavings, corn cob and cardboard tubing.

3.3.2. ARflox and AMH-Cre transgenic mouse breeding

GCARKO line females were bred utilizing the same transgenics used when obtaining a Sertoli-cell ARKO (SCARKO); full details of transgenic mouse generation can be found in Figure 1 of the original paper (De Gendt, Swinnen et al. 2004). Briefly, ES cells from a 129/SvJ BAC library were used to isolate a fragment containing the first two exons of the murine AR gene, the sequence of which was confirmed using Southern blot techniques. Next a targeting vector was constructed and electroporated into male R1 ES cells. Antibiotic cultures were used to isolate any recombined cells and successful homologous recombination was confirmed by further digestion and Southern blotting. In addition, an internal probe was used as a check against random vector integration. The recombined clones were subsequently transfected with a Cre-expressing plasmid and exon 2 excision verified by Southern blot.

ES cells containing the target vector were injected into blastocysts from Swiss-Webster (SW) females and implanted into pseudo-pregnant dams; chimeric male offspring were identified by agouti coat colour and mated to SW females as a test for germ line transmission. Germ line offspring were again identified by their

agouti phenotype and were subsequently genotyped using genomic DNA from tail-tip biopsies. Two chimeric males demonstrating 100% germ line transmission were used as founders of the ARKO and SCARKO transgenic lines (De Gent et al. 2004). To generate a SCARKO male, knockout female $Cre^{-/-}AR^{f/f}$ from a 129/Swiss background were mated to C57BL/6 males $Cre^{+/-}$ $AR^{+/y}$, shown in Figure 3.2.

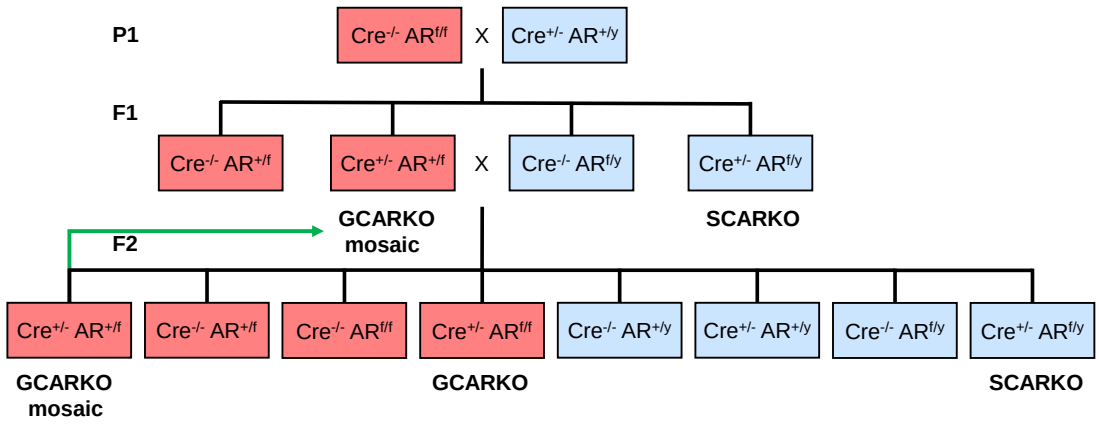

Figure 3.2: Schematic diagram showing the generation of the male F1 SCARKO transgenic line which were then used to derive the GCARKO second F2 generation: First (P1), second (G1) and third (G2) animals were genotyped at each stage to assess the allelic status of the floxed AR and for the presence or absence of Cre. Hemifloxed F2 GCARKO mosaic animals could be used to continue GCARKO line generation (green arrow). Female animals are shown in red and male animals in blue.

F1 $Cre^{+/-}AR^{+/f}$ females could not be bred with F1 $Cre^{+/-}AR^{f/y}$ SCARKO males as the SCARKO mouse is infertile.

3.3.3. AMH-Cre X EYFPflox

To test for the expression of Cre protein C57BL/6 $Cre^{+/-}AR^{+/y}$ males were mated to females containing a floxed enhanced yellow fluorescent (EYFP) protein. This EYFP strain was derived as described for the ARKO line (Chapter 3, Section 3.2), but here the EYFP transgene was inserted into the ubiquitously expressed *ROSA26 locus* on autosome 6, not AR exon 2 locus on the X chromosome (Srinivas, Watanabe et al. 2001). The *ROSA26 locus* is a commonly used and easily targeted location for transgene insertion. It highly expresses inserted genes and is not apparently subject to gene silencing events (Irion, Luche et al. 2007). The EYFP

transgene was inserted downstream of a stop codon, that becomes excised by Cre recombinase, allowing expression of EYFP in the Cre positive cells EYFP floxed mice (Figure 3.3).

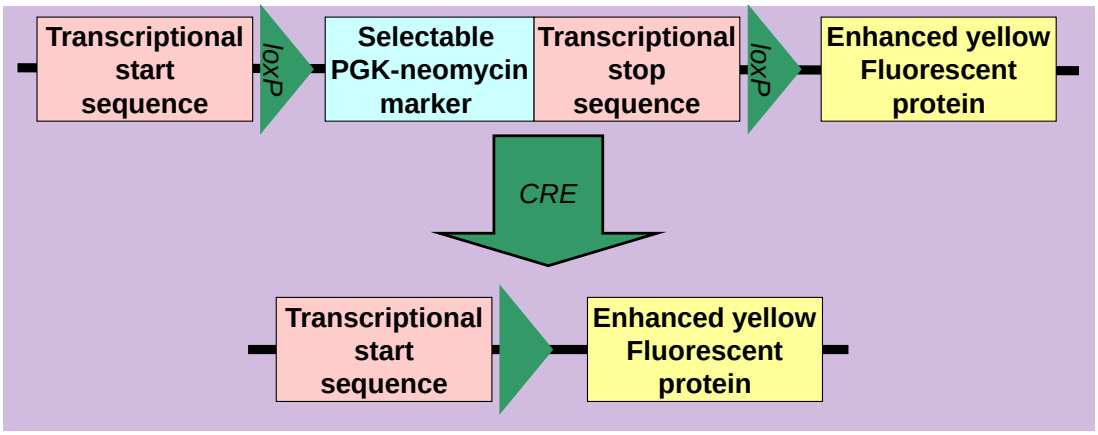

Figure 3.3: Structure and function of the EYFP transgene: Cre activity excises at two *loxP* sites removing a transcriptional stop sequence (tpA) and allowing expression of EYFP within the target cell or tissue (Adapted from Srinivas, Watanabe et al. 2001).

Female offspring of AMH-Cre X EYFP crosses were killed at weaning by cervical dislocation and their ovaries removed and placed in PBS (as described in Chapter 2, Section 3). Whole ovaries were then viewed under a filter on a light microscope to see if GCs expressed EYFP. These ovaries were also fixed to be used as positive controls in IHC for AR, Cre and YFP (Chapter 2, Section 4).

3.3.4. Genotyping

Mice were identified by ear clips which could then be used as a tissue sample for subsequent genotyping. F1 generation mice were genotyped for the allelic status of the AR (i.e. presence of a floxed transgene) and for the presence or absence of Cre using primer pairs (Table 3.2). Primers were designed to span exon 2 of the AR gene. Thus animals with one floxed allele and one non-floxed allele ('hemifloxed') could be identified by two PCR products, and would in theory be mosaic GCARKO animals.

Table 3.2: Details of primers used to genotype GCARKO line animals: Animals were genotyped for the presence/absence of Cre. The AR primers designated the allelic status of the floxed AR, with a band at 644bps in wild type animals, and a band at 675bp in floxed animals. Hemifloxed animals had both these bands. GAPDH was run as a positive control gene.

Gene Target	Primers used (5' → 3' sequence)		Length (bp)	Tm (°C)	%GC
AR	Fwd+	AAGCAGGTAGCTCTGGGACA	20	54	55%
	Rev-	CGTTTCTGCTGGCACATAGA	20	54	50%
Cre	Fwd+	GATCGCTGCCAGGATATACG	20	54	50%
	Rev-	AGGCCAGGTATCTCTGACCA	20	54	60%
GAPDH	Fwd+	CTGCACCACCAACTGCTTAGC	20	54	55%
	Rev-	ATGCCAGTGAGCTTCCGTTC	20	54	55%

F2 generation animals were genotyped in the same way. However, only the presence or absence of Cre could be used as a marker for potential GCARKO animals and was only fully assessed by ovarian immunohistochemistry for the AR to identify these animals after sacrifice.

To genotype generation F1 and F2 animals, DNA extraction from ear clip samples was used. To extract, 25µl TE Tween solution (Method: 250µl TRIS-HCl, 19µl 0.5M EDTA, plus 25µl Tween) and 2µl of a proteinase-K (pK) digestion enzyme were added tp each ear clip in a 0.2ml PCR tube. Samples, including pK negative controls, were then lysed at 55°C for two hours on a PTC200 (Thermo Cycler) PCR block, with a second step of 95°C for seven minutes to denature the pK.

Lysed samples were then vortexed and centrifuged at 4000 rpm for five minutes; 10µl of DNA was then removed from the top aqueous layer and diluted in 90µl of autoclaved distilled water. Subsequent PCR was then performed for each gene using standard Biomix Red (Thermogenics) master mix (Table 3.3).

Table 3.3: PCR master mix components used in genotyping.

Component	Volume (µl)
Biomix Red	10
Nuclease Free Water	7.6
Forward Primer	0.2
Reverse Primer	0.2
DNA template	2
TOTAL	**20**

Samples were subsequently run on a cycle PCR program (Table 3.4) and visualised next to a 100 base pair interval ladder on 1% agarose TAE gel, examples of which are shown for each genotype (Figure 3.4).

Table 3.4: Thermo Cycler PCR program used in genotyping: After step 1, steps 2 to 4 are repeated 30 times before final extension of the PCR product

Step	Component	Temperature (ºC)	Time (min)
1	Initial Denaturation	95	2
2	Denaturation	95	0.5
3	Annealing	54	0.5
4	Extension	72	1
5	Final Extension	72	5

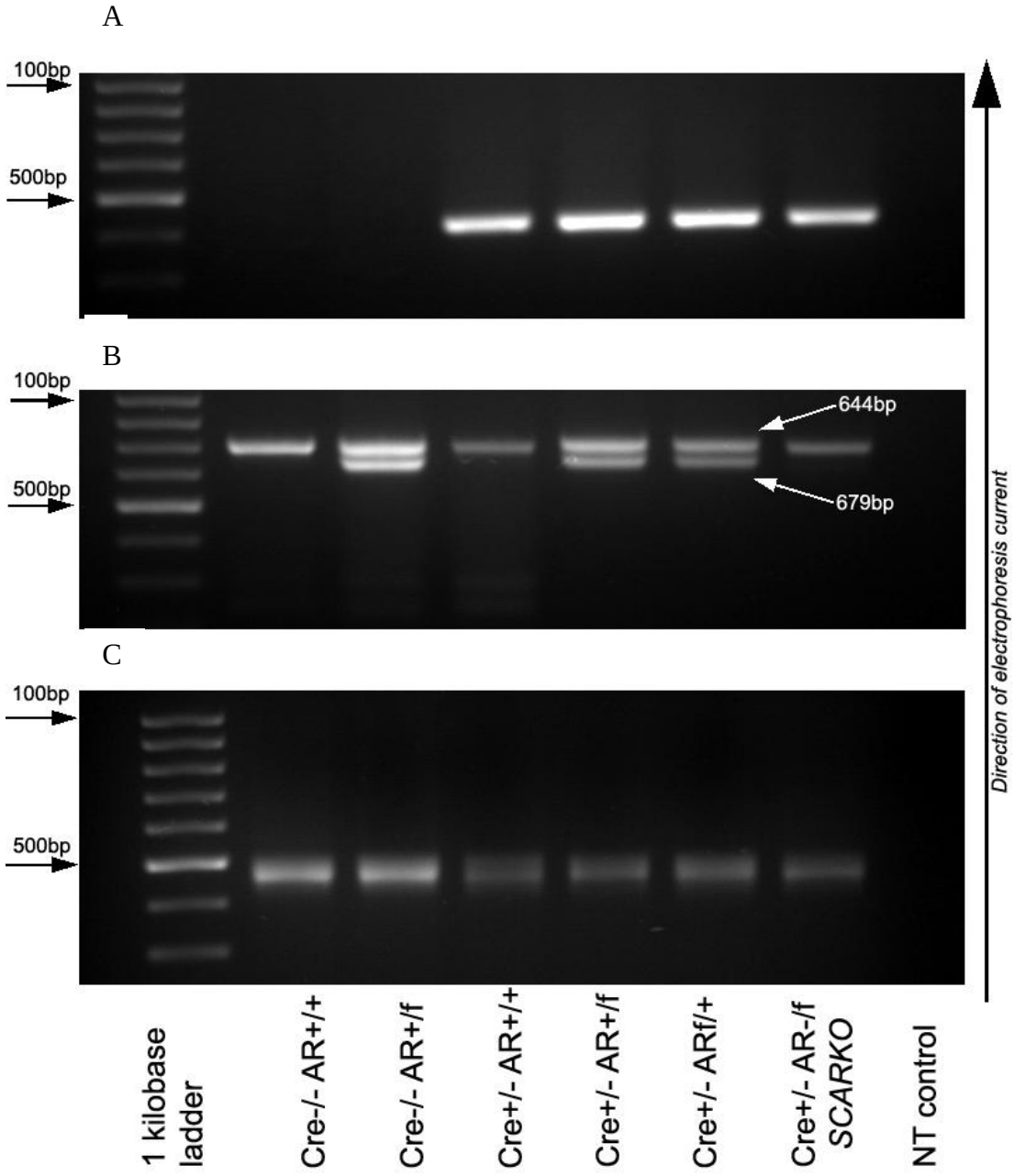

Figure 3.4: Image of a standard gel showing the results of a typical PCR performed when genotyping F1 and F2 generation GCARKO line: Panel (A) shows the presence or absence of Cre, panel (B) the allelic status of the floxed AR and (C) GAPDH control for the same six animals. Potential knockouts yielded the same apparent genotype as $Cre^{+/-}$ $AR^{+/+}$ and thus were identified using IHC. In each PCR gel run, negative (water no-template (NT) control) and positive (DNA from a SCARKO male) controls were included.

3.3.5. Immunohistochemistry and immunofluorescence

For histological analysis, colour co-immunolocalisation was performed using alexa-fluorophore antibodies (Table 3.5). Fluorescent staining was optimised for each individual antibody prior to dual staining optimisation. Dual staining took place over three days with relevant blocking steps between antibody additions as previously described (Chapter 2, Section 4).

Table 3.5: Antibodies used in immunofluorescence (IHF): All tissues were blocked with and all antibodies were diluted in block serum, either normal goat or rabbit serum (NGS/NRS).

Primary antibody	Raised in	Block	Dilution	Secondary Antibody	Tertiary Antibody	Tyramide	Source
Cre	Rabbit	NGS	1 in 2500	Goat α Rabbit Peroxidase FAB	-	1 in 10	Abcam
GFP	Mouse	NGS	1 in 250	Goat α Mouse Peroxidase FAB	-	1 in 10	Abcam
AMH	Goat	NRS	1 in 100	Rabbit α Goat Biotinylated	Streptavidin alexafluor 488	-	Santa Cruz
AR	Rabbit	NGS	1 in 200	Goat α Rabbit Biotinylated	Streptavidin alexafluor 546	-	Santa Cruz

IHF runs were counterstained by either Toporo blue (at 1:500µl) or propidium iodide red (at 1:1000µl) and finally mounted wet (i.e. without dehydration through alcohols and xylene) using permafluor for laser confocal microscopy across three colour wavelengths; red at λ 546nm, green at λ 488nm and blue at λ 623nm.

3.4. Results

3.4.1. Cre is driven off the AMH promoter in $Cre^{-/+}$ $EYFP^{-/+}$ F1 mice

To verify that the AMH promoter was driving Cre sufficiently, Cre positive females from AMH-$Cre^{-/+}$ X EYFPflox crosses were culled and their ovaries examined in PBS under a fluorescent filter. Results showed that Cre successfully drives EYFP expression in ovaries from $Cre^{-/+}EYFP^{-/+}$ animals, and no EYFP expression was observed in ovaries from $Cre^{-/-}$ $EYFP^{-/+}$ (Figure 3.5).

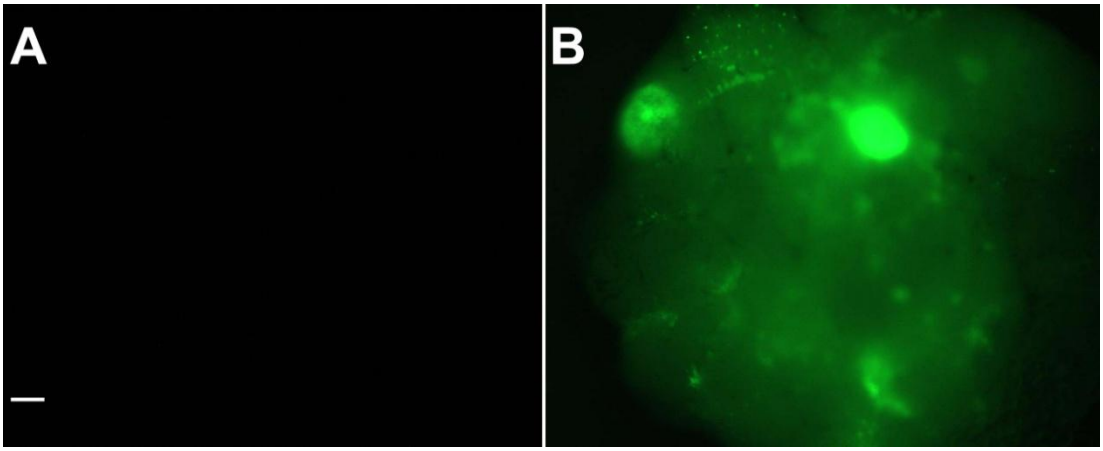

Figure 3.5: EYFP (green) is expressed by Cre recombinase activity, driven off the AMH promoter in the rat ovary: (A) Control $Cre^{-/-}EYFP^{+/-}$ ovary **(B)** $Cre^{-/+}EYFP^{+/+}$ ovary. Whole ovaries were dissected out into PBS and examined under a fluorescent filtered microscope before fixing for use as Cre positive controls. Bar=100µm

To determine more precisely where EYFP expression was occurring in the ovaries of $Cre^{-/+}EYFP^{+/+}$ animals, a GFP-antibody against the common fluorescent form of the GFP and YFP proteins was used to detect the location of EYFP expression (Figure 3.6).

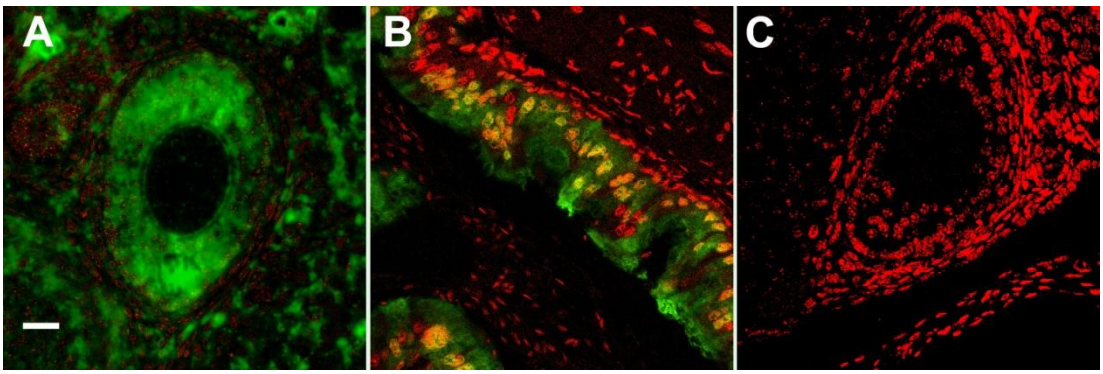

Figure 3.6: EYFP expression (green) brought about by Cre recombinase action: (A) $Cre^{-/+}EYFP^{-/+}$ ovaries **(B)** positive control $Cre^{+/-}EYFP^{+/-}$ epididymus[*] **(C)** negative control $Cre^{-/-}$ $EYFP^{-/-}$ ovary. Sections were counterstained with propidium iodide red. Bar=50µm.

To prove that AMH was driving Cre expression, the pattern of Cre expression was assessed using an antibody against Cre itself. This antibody exhibited extensive nonspecific staining using DAB IHC, and so IHF was employed to assess Cre expression. In ovaries from $Cre^{-/+}EYFP^{-/+}$ animals, Cre was expressed in the granulosa cells of developing follicles (Figure 3.7B-C).

Additionally, both Cre and EYFP expression within individual follicles lacked uniformity and although present, varied between GCs (Figures 3.6 and 3.7). This uneven expression of EYFP and Cre is probably attributable to the uneven expression and subsequent transcription, translation and secretion of AMH by follicle GCs.

[*] Acknowledgement and thanks to Laura O'Hara for supplying epididymus sections from EYFP male mice for use as positive controls in Cre IHF.

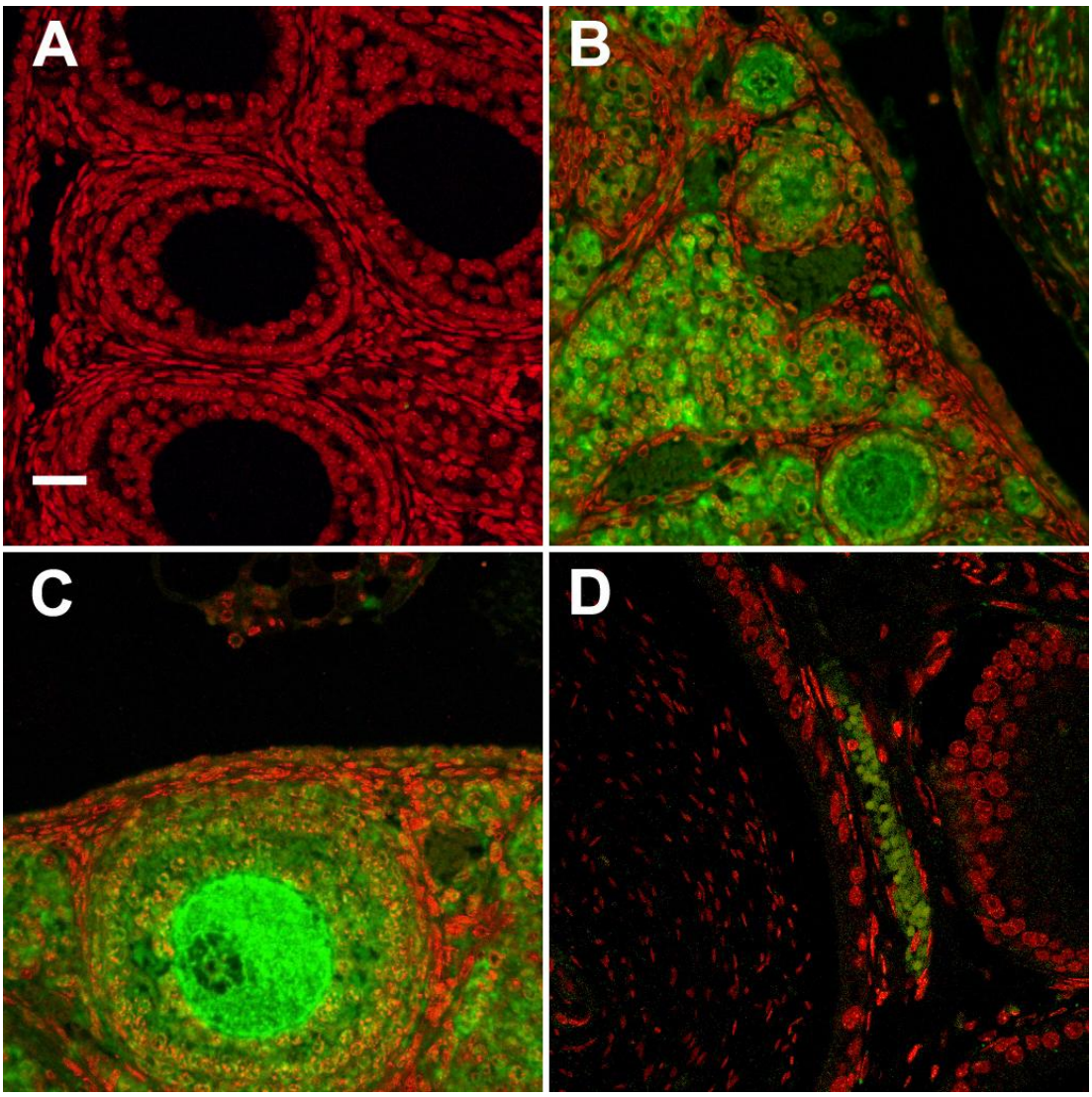

Figure 3.7: Ovarian Cre expression (green) in EYFP and GCARKO line mice: (A) Negative control $Cre^{-/-}EYFP^{+/-}$ ovary **(B)** $Cre^{+/-}EYFP^{+/-}$ **(C)** GCARKO line AMH-$Cre^{+/-}AR^{+/f}$ ovary **(D)** positive control† $Cre^{+/-}EYFP^{+/-}$ epididymus Sections were counterstained with propidium iodide red. Bar=50µm.

To assess for effects of Cre upon AMH or AR expression, dual IHF was performed for these proteins on the same sections, and the histological phenotype of Cre $^{+/-}AR^{+/+}$ control ovaries compared with that of Cre $^{+/-}AR^{f/f}$ ovaries and ovaries from potential knockout animals. As a second control, sections from ovaries of $Cre^{-/+}$ $EYFP^{-/+}$ animals were also used (Figure 3.8).

† Acknowledgement and thanks to Laura O'Hara for supplying epididymus sections from EYFP male mice for use as positive controls in Cre IHF.

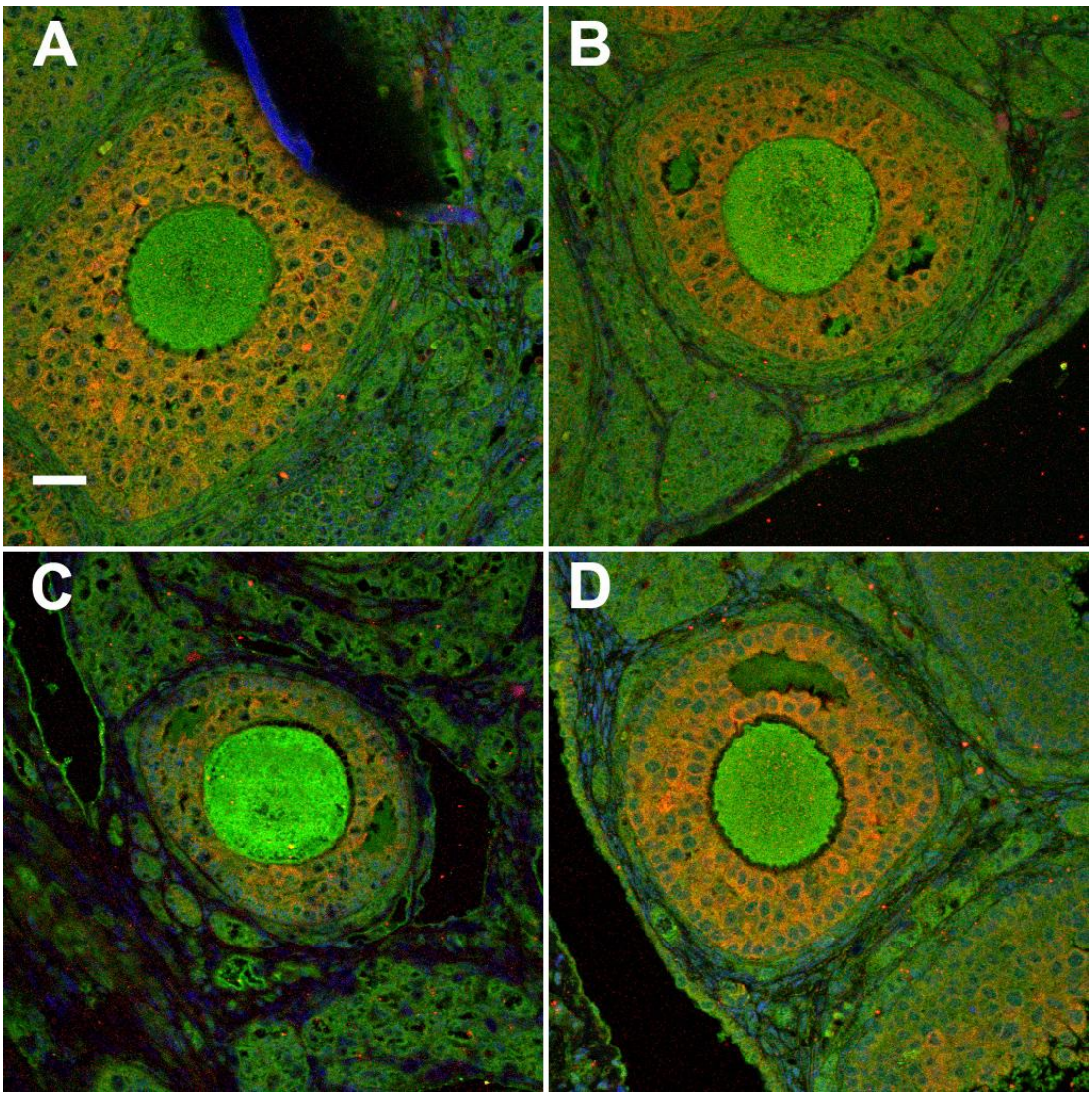

Figure 3.8: Ovarian AMH (red) and AR (green) immunocolocalisation: (A) Control Cre $^{+/-}$ AR$^{+/+}$ ovary, **(B)** Control Cre $^{+/-}$EYFP$^{+/-}$ ovary, **(C)** Hemifloxed Cre $^{+/-}$ AR$^{f/f}$ ovary and **(D)** ovary from a potential knockout animal. Sections were counterstained with toporo blue. Bar =50µm.

AMH expression was evident in the GCs of developing follicles, and while AR expression was evident in all ovarian compartments, including GCs, stroma, theca and CL (Figure 3.8). No difference was observed in either AMH or AR expression between Cre $^{+/-}$AR$^{+/+}$ control animals or Cre $^{+/-}$EYFP$^{+/-}$ control animals. Moreover, IHF for AR (green) within hemifloxed ovaries and potential knockout ovaries remained uniform. The predicted mosaic pattern of AR expression in hemifloxed animals was not observed using IHF.

3.4.2. AMH-Cre X ARflox to produce a GCARKO

As expected, parental generation P1 ovaries from $Cre^{-/-}AR^{f/f}$ exhibited normal expression of AR (Figure 3.9).

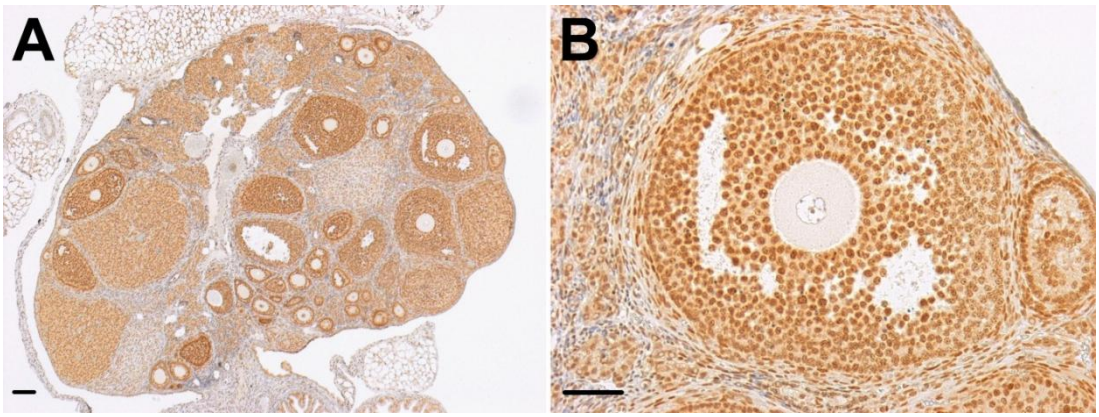

Figure 3.9: DAB IHC for AR expression in parental generation (P1) $Cre^{-/-}$ $AR^{f/f}$ ovaries: Shown at **(A)** X 2 magnification, bar=200µm and **(B)** X 20 magnification, bar=50µm.

Although a mosaic pattern of AR expression was expected in F1 hemifloxed $Cre^{+/-}AR^{+/f}$ females, the F1 generation exhibited normal expression of both AR and AMH in control $Cre^{-/-}AR^{f/f}$ and hemifloxed $Cre^{+/}AR^{+/f}$ females (Figure 3.10), presumably due to the presence of a single wild type AR allele.

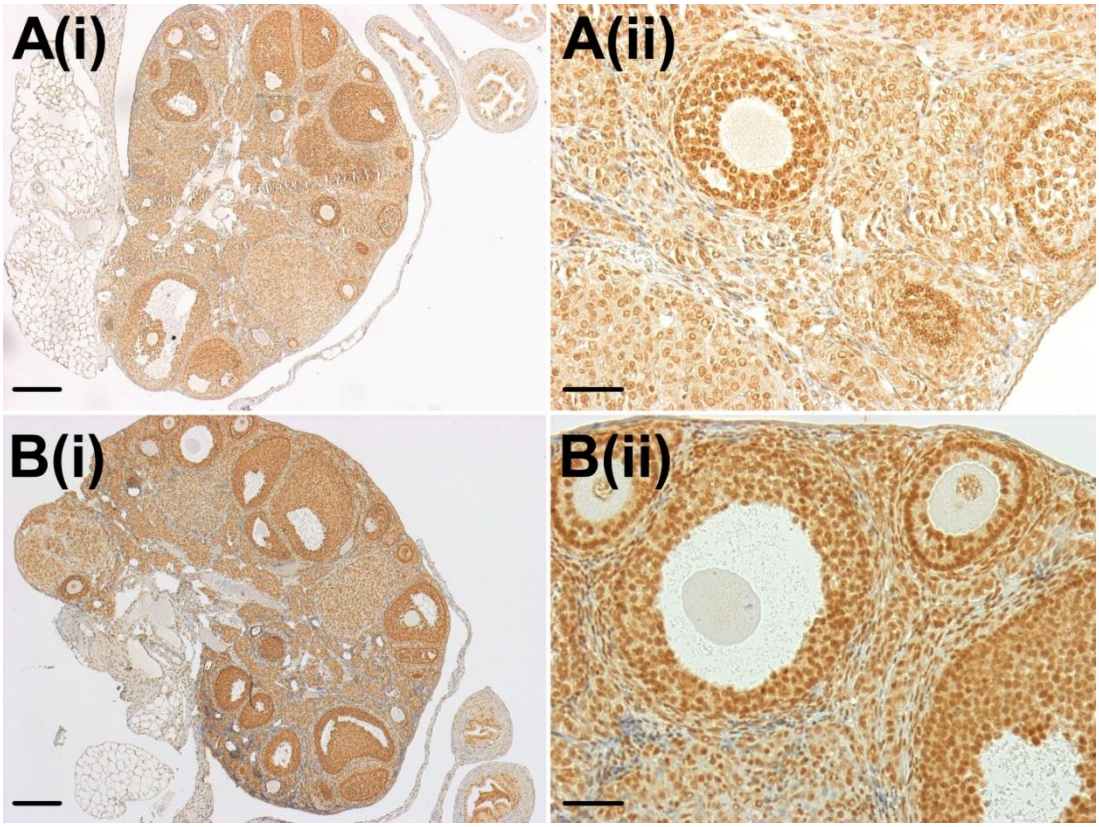

Figure 3.10: DAB IHC for AR expression in first generation (F1) (A) $Cre^{-/-}$ $AR^{f/f}$ and **(B)** $Cre^{+/-}$ $AR^{+/f}$ ovaries: Shown at (i) X 2 magnification, bar=200µm and (ii) X 20 magnification, bar=50µm

Fixed ovaries from F2 animals (*n*=72) were collected for histological examination of AR and AMH expression. In theory 10% of total offspring should present with a granulosa cell knockout phenotype and 10% with a mosaic phenotype as predicted by the inheritance pattern of Mendelian genetics (Figure 3.2). Animals were genotyped prior to sacrifice in order to identify hemifloxed $Cre^{+/-}AR^{+/f}$ that could be used to breed further generations and maintain the colony. Cre positive animals with a single PCR gel band for the AR gene were designated as potential knockouts (either genotype $Cre^{+/-}AR^{+/+}$ or $Cre^{+/-}AR^{f/f}$). Their phenotype was only identified upon histological examination for the presence/absence of AR in ovarian GCs. If the ovarian phenotype did not match the designated genotype, the PCR was repeated at least twice.

Despite repeated genotyping for $Cre^{+/-}AR^{+/f}$, no F1 or F2 hemifloxed $Cre^{+/-}AR^{+/f}$ animals exhibited a mosaic pattern of AR expression in their ovaries (Figure 3.11). In addition, of the animals designated as potential knockouts ($Cre^{+/-}AR^{+/+}$ or $Cre^{+/-}AR^{f/f}$, only one F2 exhibited some mosaic GCARKO, even though repeated genotyping did not indicate a hemifloxed $Cre^{+/-}AR^{+/f}$ animal.

Ovaries from $Cre^{+/-}AR^{+/f}$ generation F1 and $Cre^{+/-}AR^{f/f}$ generation F2 animals were further investigated for Cre expression using IHF (Figure 3.12). Cre expression appears sufficiently driven off the AMH promoter in both generations and thus does not account for the mosaic pattern of AR expression observed in one F2 animal.

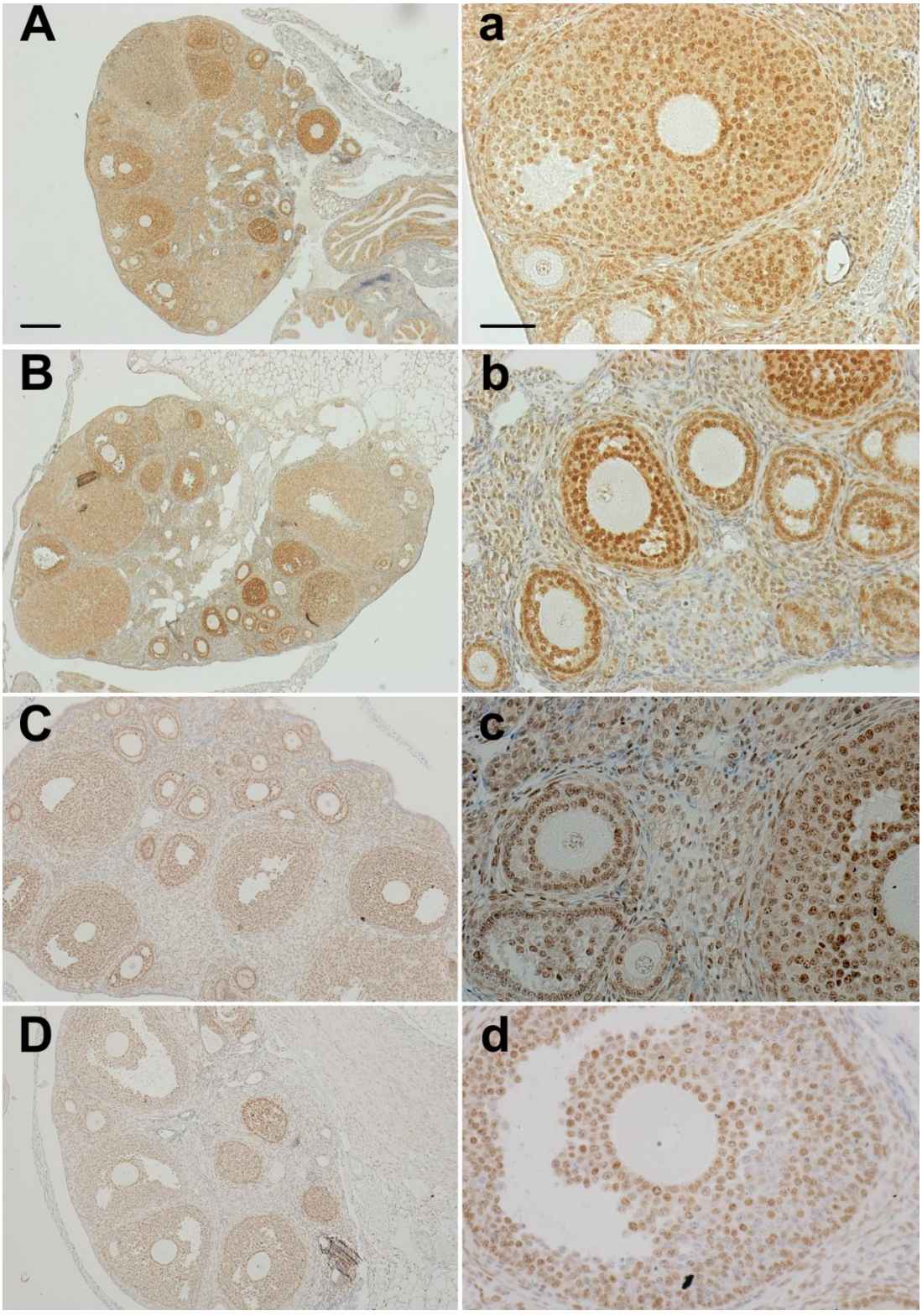

Figure 3.11: AR expression in second generation (F2) ovaries: (A) $Cre^{-/-}AR^{f/f}$ (B) $Cre^{-/-}AR^{f/+}$ (C) $Cre^{+/-}AR^{f/+}$ and (D) $Cre^{+/-}AR^{f/f}$. Uppercase lettered images bar=200µm, lowercase lettered images bar=50µm. Images D and d illustrate the only F2 animal to exhibit mosaic AR expression within GCs.

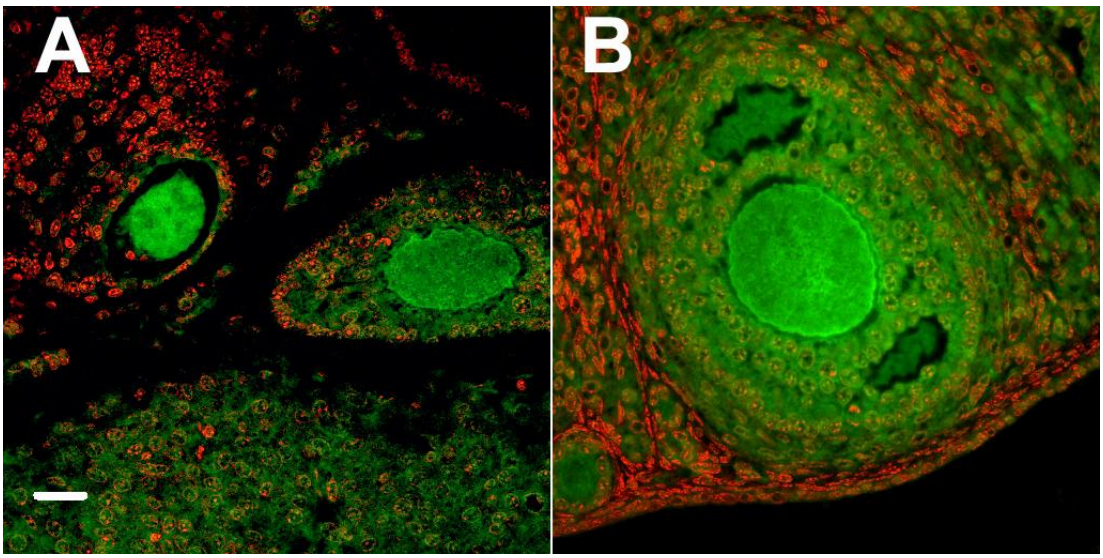

Figure 3.12: Cre (green) is expressed in (A) $Cre^{+/-}AR^{+/f}$ F1 and (B) $Cre^{+/-}AR^{f/f}$ F2 ovaries. Sections were counterstained with propidium iodide red. Bar=50µm.

During the generation of the GCARKO transgenic line, Mendelian genetics were used to predict the likely proportions of each genotype observed with each generation. Table 3.6 illustrates the proportions expected alongside those observed, which were scored with each course of AR IHC for each animal. While a mosaic AR pattern was expected in $Cre^{-/+}AR^{f/+}$ F2 animals, none were seen except in one animal genotyped several times over as a potential F2 GCARKO (Table 3.6).

Table 3.6: Expected proportions of female GCARKO animals across litters compared to those actually identified using a combination of genotyping and IHC techniques.

Genotype (symbols)	Genotype (words)	Experimental Outcomes		Predicted Occurrence (%)	Actual Occurrence (%)
		Genotype	AR IHC		
$Cre^{-/-}$ $AR^{f/f}$	Control floxed	Cre negative	AR positive	18 (25%)	33 (47%)
$Cre^{-/-}$ $AR^{f/+}$	Control hemifloxed	Cre negative	AR positive	18 (25%)	19 (26%)
$Cre^{-/+}$ $AR^{f/+}$	Mosaic hemifloxed	AR hemifloxed	AR positive, no mosaic	18 (25%)	19 (26%)
$Cre^{-/+}$ $AR^{f/f}$	GCARKO	Cre positive, potential KO	One mosaic	18 (25%)	1 (<1%)
TOTAL				**72 (100%)**	**72 (100%)**

AR=androgen receptor; Cre=cre recombinase; GCARKO=granulosa cell androgen receptor knockout.

3.5. Discussion and conclusion

In $Cre^{-/+}EYFP^{-/+}$ F1 mice, Cre recombinase activity drove EYFP expression sufficiently for detection under a fluorescent filter and through the use of IHF, although GC Cre expression was uneven. This irregular pattern of Cre expression was also observed by the laboratory where the AMH-Cre transgenic line was developed (Lecureuil, Fontaine et al. 2002). Furthermore despite confirmed Cre activity in F1 $Cre^{+/-}$ $AR^{+/f}$ animals, Cre recombinase did not result in a mosaic ARKO in $Cre^{+/-}AR^{+/f}$ F1 animals, nor a full GCARKO in $Cre^{+/-}AR^{f/f}$ F2 animals as was predicted and therefore it is likely that Cre is not well driven off the AMH reporter in the female animal.

Several aims of this transgenic project have been met; Cre activity was verified by EYFP expression in rodent granulosa cells, AR expression in the GCARKO line was verified using IHC and IHF. However, the ultimate aim of this project was to derive a GCARKO animal in order to understand the role of AR within folliculogenesis through more novel means, and in this case the knockout was unsuccessful.

It is likely that the penetrance of Cre was not strong enough to fully excise the AR. Indeed, no other published studies have used the AMH-Cre line to drive a knockout in the female. Furthermore, the Cre recombinase protein itself may have had insufficient access to the floxed AR transgene in the female animal, although this is unlikely since a successful GCARKO has recently been generated using the AMHR2 driven Cre line. Preliminary results from a recently published GCARKO model indicate that AR is essential for proper primordial follicle activation, since in the absence of GC AR expression there is a reduction in the population of primordial follicles (Sen and Hammes 2010). GCARKO animals in this study exhibited a reduced proportion of primordial follicles in GCARKO animals, indicating that AR may be necessary for proper follicle recruitment in the rodent. In this study animals

remained fertile although they ovulated with fewer numbers of CL (Sen and Hammes 2010).

The AMH-type II receptor (AMHR2)-Cre reporter mouse line has since produced several GC specific knockout models to study the involvement of certain molecules in GC and ovarian development; for example the ribonuclease Dicer-1 (Lei, Jin et al. 2010), the tumour suppressor Pten (Fan, Liu et al. 2009), and other key developmental proteins that include hedgehog signalling molecules (Ren, Cowan et al. 2009) and Wnt4 (Boyer, Paquet et al. 2009). To drive future GC knockout studies, the AMHR2 Cre line would therefore be a superior choice over the AMH-Cre reporter.

In conclusion, an alternative avenue of identifying the role of androgens regarding the ovary must be pursued.

Chapter 4. Effects of fetal and postnatal testosterone exposure on the rat reproductive tract

4.1. Introduction

Clinical studies show that LH levels in PCOS women are frequently raised (Welt, Taylor et al. 2005), and an increased stromal compartment has been documented in the PCO (Fulghesu, Ciampelli et al. 2001). There is also evidence to suggest that developing follicles in ovaries from PCOS women have increased 17α-hydroxylase (17αOH) activity within the theca interna layer (Nelson, Legro et al. 1999). Together these steroidogenic ovarian cell types, under the influence of LH hypersecretion, may contribute to the ovarian hyperandrogenaemia observed in PCOS patients (Kaaijk, Sasano et al. 2000). However, it remains unclear whether these hormonal imbalances are due to defects at the ovarian, pituitary or even the hypothalamic level of the reproductive axis (Abbott, Dumesic et al. 2002).

The hyperandrogenic status of many women with PCO is hypothesised to be one cause of the anovulation associated with the disorder, since the functional status of follicles within the PCO is altered; PCO are typified by the presence of an increased number of follicles (12 or more) which are between two and nine mm in diameter (Dewailly, Catteau-Jonard et al. 2007; Fulghesu, Angioni et al. 2007). These features could well be the result of suppression of pituitary FSH, below the levels required to stimulate adequate folliculogenesis (Franks, Stark et al. 2008). Thus an altered LH to FSH ratio impairs follicle selection and dominance, as a result of which few follicles rarely grow to greater than nine mm, reducing hormonal feedback to the hypothalamus/pituitary, and preventing the GnRH/LH surge that would normally induce ovulation (Taylor, McCourt et al. 1997). However, this does not rule out a defect in hypothalamic or pituitary sensitivity to hormonal feedback. Indeed the sheep model of PCOS has shown a reduction in feedback sensitivity to E2 in fetally androgenised ewes (Veiga-Lopez, Astapova et al. 2009). The vicious cycle

of PCOS is one reason the source of the disorder has been difficult identify despite decades of research.

Previous research into the fetal and neonatal programming of male rats by testosterone proprionate (TP) (Welsh, Saunders et al. 2008; Welsh, MacLeod et al. 2010) has now been extended as this chapter investigates the consequences of fetal and neonatal exposure of female rats to TP, examining immature animals at postnatal day pnd 25 and adult animals at pnd 90. No rodent studies have performed in-depth validation of the neonatally androgenised animal as a model for PCOS, and few have documented the plethora of reproductive and metabolic consequences which result from fetal and/or neonatal androgen exposure (Chapter 1, Section 11). This chapter examines the effects of different windows of exposure to TP on ovarian development and aspects of metabolism, and seeks to determine if the alterations in ovarian, pituitary and metabolic function (that are a feature of PCOS in women), could occur independently at different times during fetal and/or neonatal life. Furthermore this chapter will focus upon the validation of the neonatal androgenised rat as a model for PCOS, using the clinical features described herein.

4.2. Objectives

- To determine which windows of neonatal TP treatment induce an altered reproductive phenotype in the adult animal and to what extent if any, the resulting phenotype mimics human reproductive pathophysiologies such as PCOS or POF.

- To determine if the alterations in ovarian, pituitary and metabolic function (that are a feature of PCOS in women), could occur independently at different times during fetal and/or neonatal life.

- To validate postnatal TP exposed animals as a rat model of PCOS in line with clinical criteria.

4.3. Methods

Animals were housed and maintained as described in Chapter 2, Section 2.

4.3.1. Study outline

In this study e.0.5 was defined by the presence of a vaginal plug and a minimum of four litters were used for each treatment group. For treatment during embryonic development, pregnant dams were injected with 20mg/kg TP in 0.4ml of corn oil. However, TP exposure during late fetal life has been shown to induce dystocia, significantly increasing the mortality of both pups and mother. To prevent this, animals from these treatment groups which received fetal TP were delivered by caesarean at e21.5 and cross-fostered to untreated dams that had delivered their own pups within six hours of caesarean. Animals treated during postnatal life received injections corresponding to pup weight every three days; those in the TP treatment group received a dose of 20mg/kg TP while those in the control litters received a comparable volume of corn oil (Welsh, Saunders et al. 2008; Welsh, MacLeod et al. 2010). The windows of TP treatment are outlined in Figure 4.1 and are hereafter designated as fetal, late postnatal, fetal plus postnatal and postnatal windows. The numbers of animals used in each treatment group are outlined in Table 4.1.

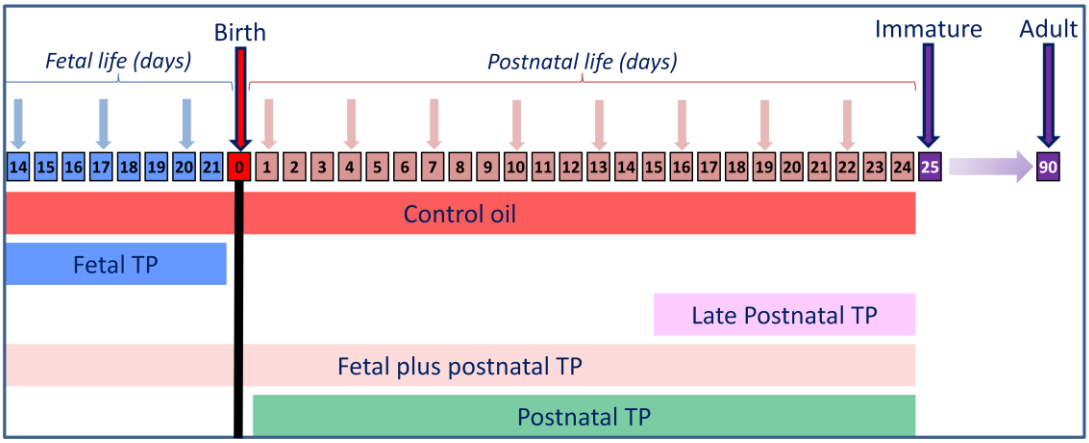

Figure 4.1: Schematic diagram to illustrate the windows of TP exposure in rats: Downward blue and orange arrows indicate the days of TP injection at 20mg/kg during fetal and postnatal life respectively. The downward red arrow indicates the day of birth, and purple arrows the days of sacrifice for immature (pnd 25) and adult (pnd 90) animals. Treatment groups are designated control, fetal, late postnatal, fetal plus postnatal, and postnatal TP hereafter.

Table 4.1: The number of animals in each experimental control and TP treatment group (outlined in Figure 4.1) in addition to their sampling ages.

Group Name	TP exposure	Immature pnd 25		Adult pnd 90	
		Male	Female	Male	Female
Control	Oil: e14.5-pnd24	18	9 (20*)	21	9 (11*)
Fetal	e14.5-e21.5	8	5 (7*)	9	3
Fetal plus postnatal	e14.5-pnd24	8	4 (8*)	6	6 (9*)
Late postnatal	pnd15-24	9	5	7	5
Postnatal	pnd1-24	5	6	4	4 (6**)

*red in brackets indicates the original sample number before litters were discounted due to suspected human error. **blue in brackets indicates the correct sample number but where three animals in the fetal plus postnatal group had dysgenic ovaries unsuited to follicle counting, and where two animals in the postnatal group developed large ovarian cysts and so were excluded from follicle analysis.

Certain litters were excluded from this study, namely two control litters, one fetal TP litter and one fetal plus postnatal TP litter. These litters were discounted due to suspected human error when administering the TP doses and control vehicle.

4.3.2. Necropsy

Two or more litters from each treatment window were culled and weighed at each time point for immature pnd 25 and adult pnd 90 (Chapter 2, Sections 2-3). Plasma was collected by cardiac puncture using heparinised syringes for gonadotrophin and estradiol analysis. The uterus and ovaries were subsequently dissected out and weighed before fixing in bouins, followed by paraffin embedding and serial sectioning (Chapter 2, Section 4).

4.3.3. Follicle counts and IHC

One ovary from each animal was serial sectioned and every 10th section H&E stained for follicle count analysis under a light microscope at X 20 magnification. The intervening sections were serially mounted onto the same slides, where possible with a control section, and DAB stained for various immunohistochemical markers used in morphometric analysis, described in Table 4.2.

Table 4.2: IHC markers used on cohorts of serial sections, every 10th section: In the staining protocols requiring stereological measurements, weak staining was excluded by tracing round the area of interest as previously described in Section 2.5.

IHC type	Marker	Area stained	Counts performed	Stereology performed	Group analysed	Age Analysed
H&E	Nuclear & cytoplasmic	Whole ovary	Follicle count	-	All	Day 25 & Day 90
DAB	VASA	Germ cells	Germ cell count	Germ cell stain/μm^2	Fetal TP	e21.5
DAB	PCNA	Nuclei of proliferating cells	Qualitative	-	All	Day 90
DAB	Caspase-3	Apoptotic cells	Apoptosis count	-	Control & Fetal TP	e21.5
DAB	AMH	GCs of activated follicles up to the large antral stage	Growing follicle counts	-	Control, Postnatal TP and Fetal plus Postnatal TP	Day 90
DAB	Aromatase	mGCs of large antral & dominant follicles	Stain intensity scored, positively stained follicles counted	-	Control, Postnatal TP and Fetal plus Postnatal TP	Day 90
DAB	3βHSD	Strong in stroma, weak in theca interna, CL & mGCs	-	Measured as % ovarian area (-CL)	Control and Postnatal TP	Day 90
DAB	17α-hydroxylase	Theca interna, weak in mGCs	Positively stained follicles counted	Measured as % ovarian area; thecal thickness (μm)	Control and Postnatal TP	Day 90

IHC=immunohistochemistry; H&E=Haematoxylin & Eosin; PCNA=Proliferating cell nuclear antigen; (m)GCs=(mural) granulosa cells; CL=Corpus Luteum; AMH=Anti-Müllerian Hormone; 3βHSD=3β-hydroxysteroid-dehydrogenase.

4.4. Results

4.4.1. Effects of TP administered during late fetal life

The effects of fetal TP were first assessed at e21.5 using serial DAB IHC for VASA, a germ cell secretagogue (Figure 4.2). Using the stereological methods described in Chapter 2 Section 6, germ cells were counted for ovaries from both control and fetal TP treated animals. Additionally, the ovarian area was measured to allow quantification of germ cell density.

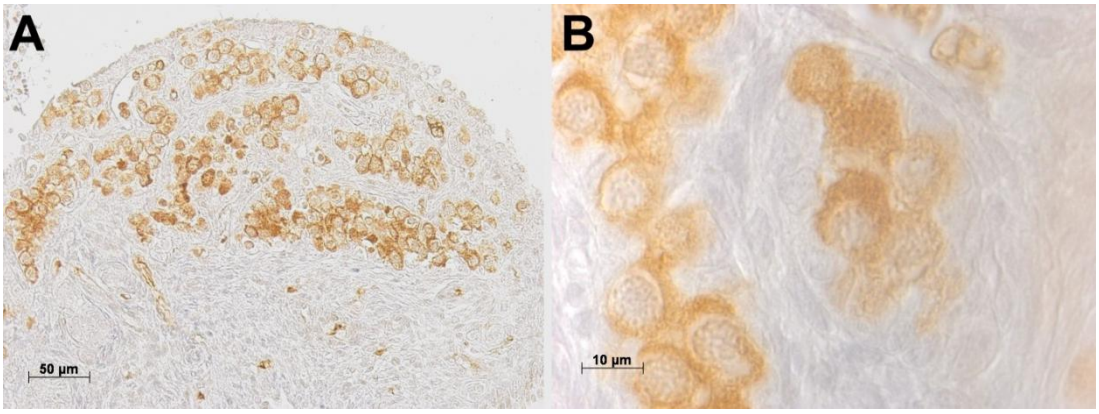

Figure 4.2: Germ cell clusters stained with VASA within the rat ovary at e21.5. Germ cells are shown at (A) X 20 and (B) X 40 magnification.

Morphometric analysis of germ cell populations, both the total numbers and proportion of germ cells per μm^2 area, showed no significant differences between treatment groups (Figure 4.3).

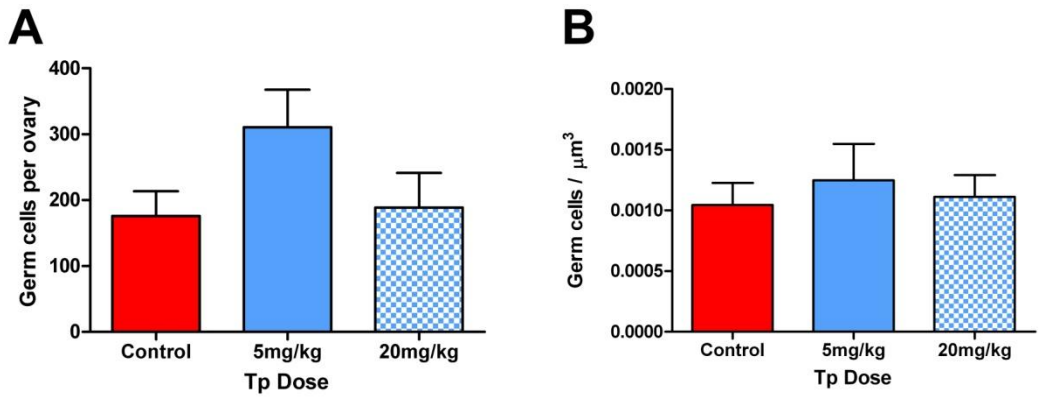

Figure 4.3: (A) Total germ cell numbers per ovary and (B) number of germ cells per µm^2 ovary at birth (e21.5/pnd0): Shown for control (n=4), and animals treated with 5mg/kg TP (n=4) or 20mg/kg TP (n=4) during the fetal window. Values are expressed as the mean ±SEM and were analysed by student's t-test.

Cleaved caspase-3 (CC3) protein was used to assess for the effects of fetal TP upon germ cell apoptosis within the ovary at e21.5 by using a further DAB stain for this apoptotic marker, illustrated in Figure 4.4. There were no differences in apoptosis occurring between ovaries from control and fetal TP treated animals (Figure 4.5).

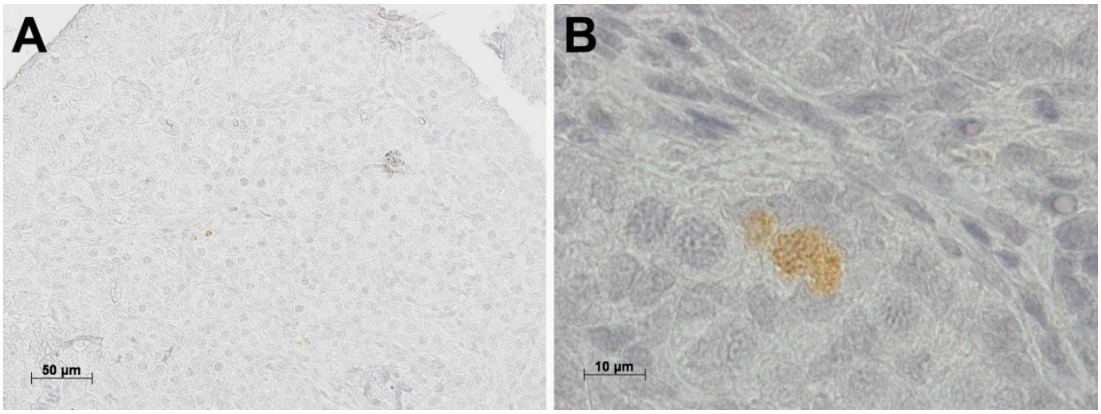

Figure 4.4: Cleaved caspase-3 staining showing germ cell apoptosis occurring in the rat ovary at birth (e21.5): visualized at (A) X20 and (B) X40 magnification

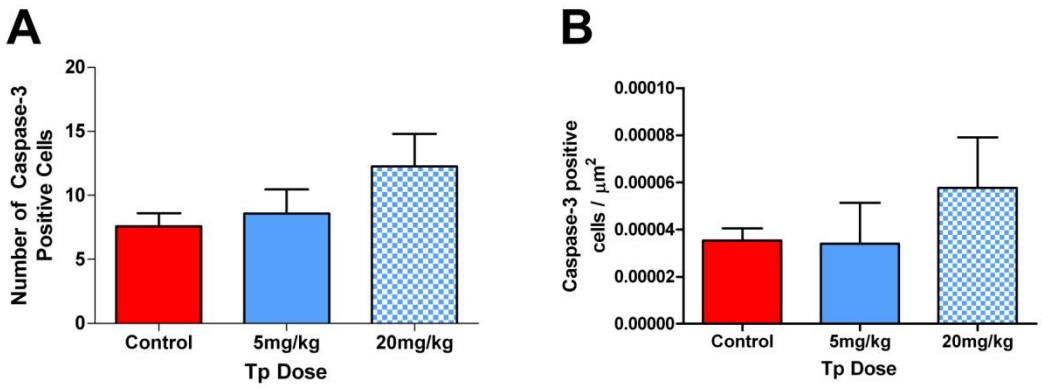

Figure 4.5: Quantitative analysis of apoptosis occurring in the rat ovary at birth (e21.5) with (A) number of cleaved caspase-3 positive germ cells and (B) number of cleaved caspase-3 positive germ cells per µm^2 ovary: Shown for control (n=4), and animals treated with 5mg/kg TP (n=4) or 20mg/kg TP (n=4) during the fetal window. Values are expressed as the mean ±SEM and were analysed by student's t-test.

Examination of gross ovarian morphology and was performed for both control and fetal TP treated animals at immature pnd 25 and adult pnd 90. No differences in ovarian morphology were observed in immature fetal TP animals or in adult animals (Figure 4.6).

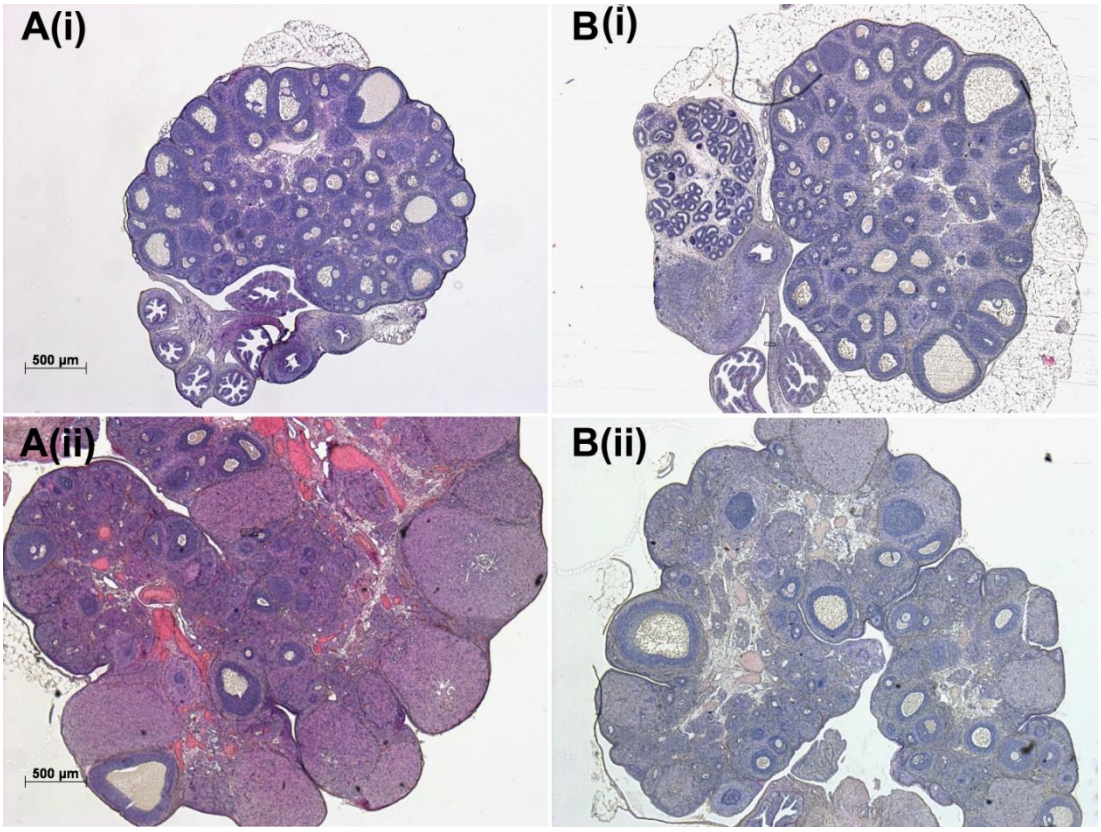

Figure 4.6: Representative images of gross ovarian morphologies seen in (A) control and (B) fetal TP treated animals (i) at immature day 25 and (ii) at adult day 90; Normal morphology was observed at both ages; control animals and adult fetal TP animals both exhibit CL. Images were taken at X 2 magnification.

Adult animals in the fetal TP treatment group developed a vaginal opening and ovulated with normal numbers of CL. In addition, there were no significant differences in follicle numbers and proportions between control and fetal TP treatment groups in both immature and adult animals (Figure 4.7).

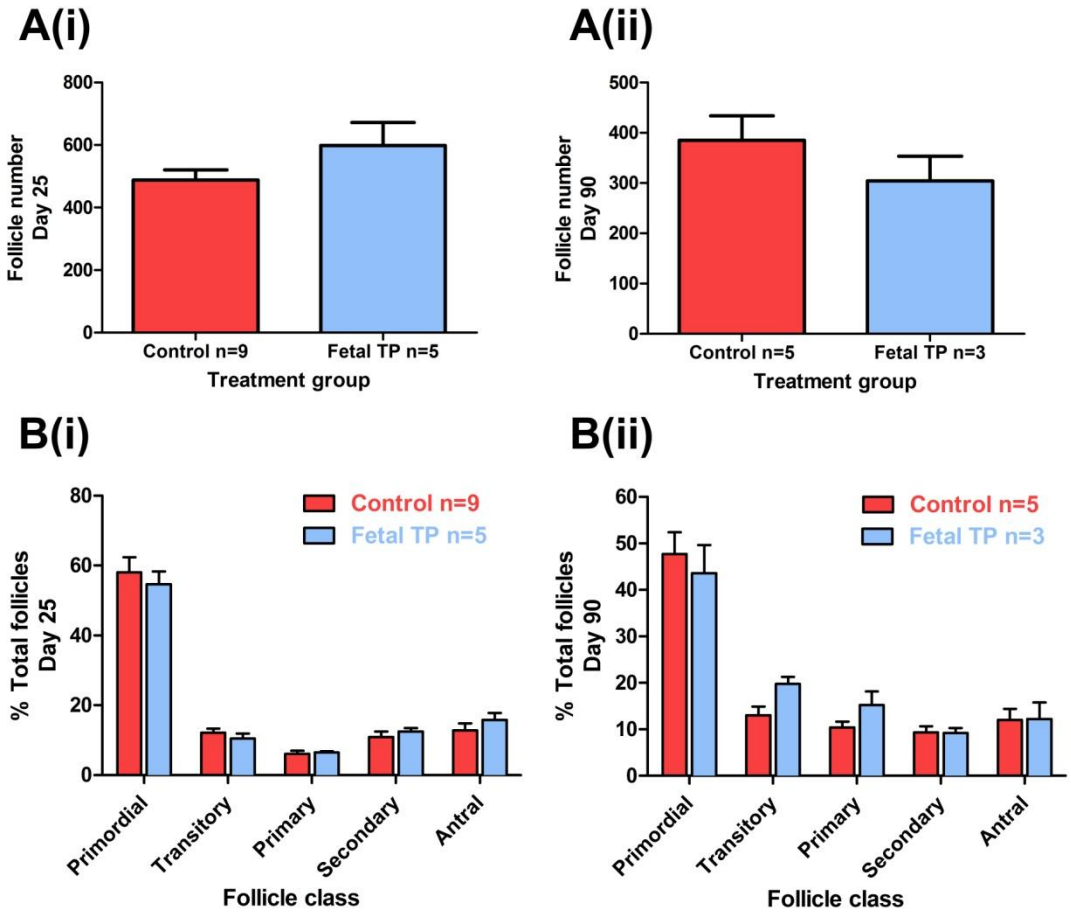

Figure 4.7: Total follicle counts (A) and follicle proportion analysis (B) of control and fetal TP treated animal groups at (i) immature day 25 and (ii) adult day 90. Values are expressed as the mean ± SEM, (A-B) were analysed using a student's unpaired t-test and (C-D) were analysed by two-way ANOVA with Bonferroni post-hoc test.

4.4.2. Effects of TP administered during late postnatal life

The ovarian morphologies of control and late postnatal TP treated animals were compared in immature animals (Figure 4.8) show follicle antra lined by pyknotic GCs, a sign of follicle atresia.

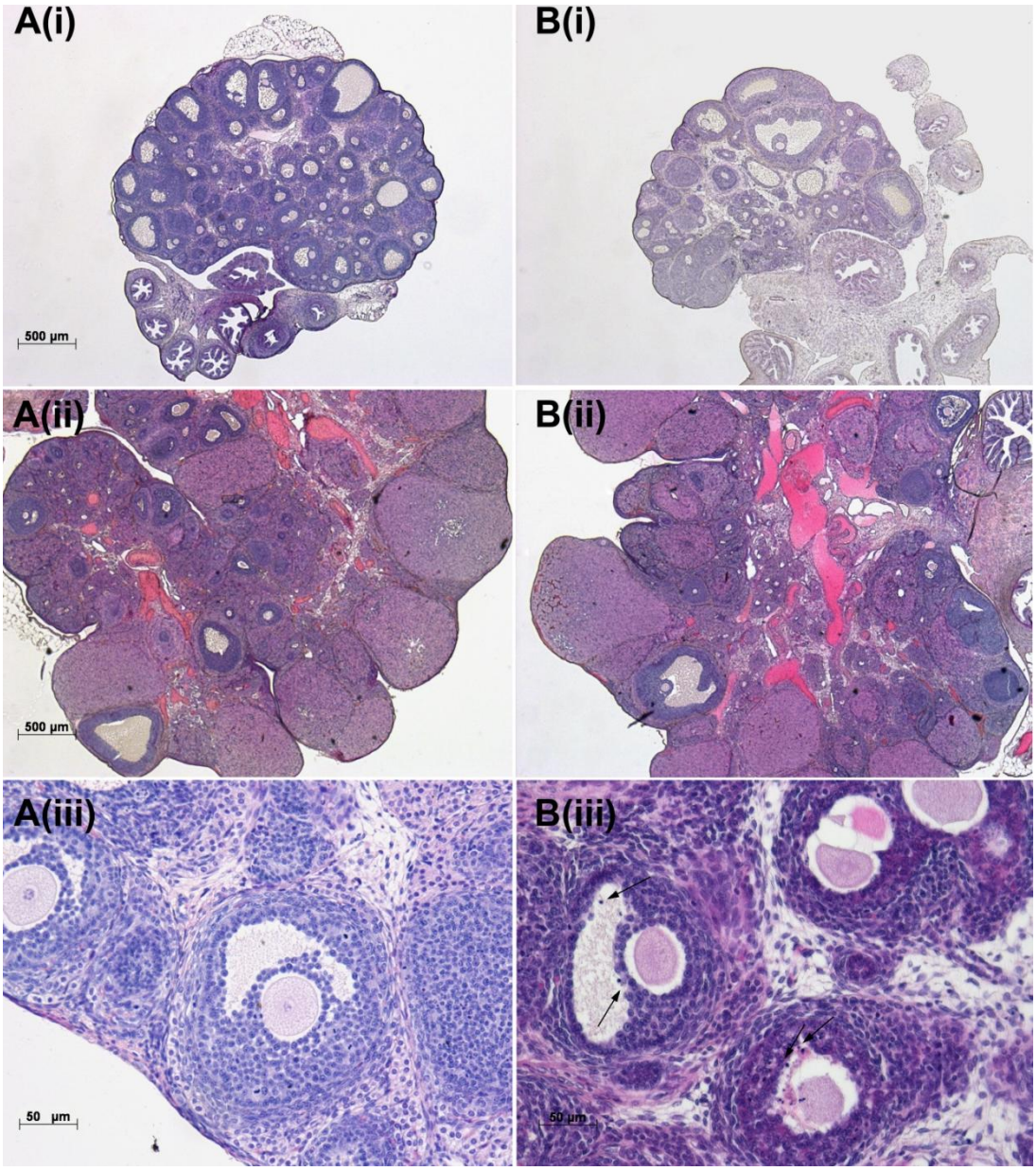

Figure 4.8: Representative images of gross ovarian morphologies seen in (A) control and (B) late postnatal TP treated animals (i) at immature day 25 and (ii) at adult day 90; Images were taken at (i-ii) X 2 and X 20 (iii) magnification. (iii) Illustrates follicle atresia evidenced by granulosa cells with pyknotic nuclei (arrowheads) at pnd 25 by TP in the late postnatal treatment group. Note the normal morphology observed at pnd 90 where like control animals, adult late postnatal TP animals exhibit CL.

Adult females treated with late postnatal TP developed a vaginal opening and, like fetal TP treated animals, exhibited morphologically normal ovaries which ovulated with normal numbers of CL.

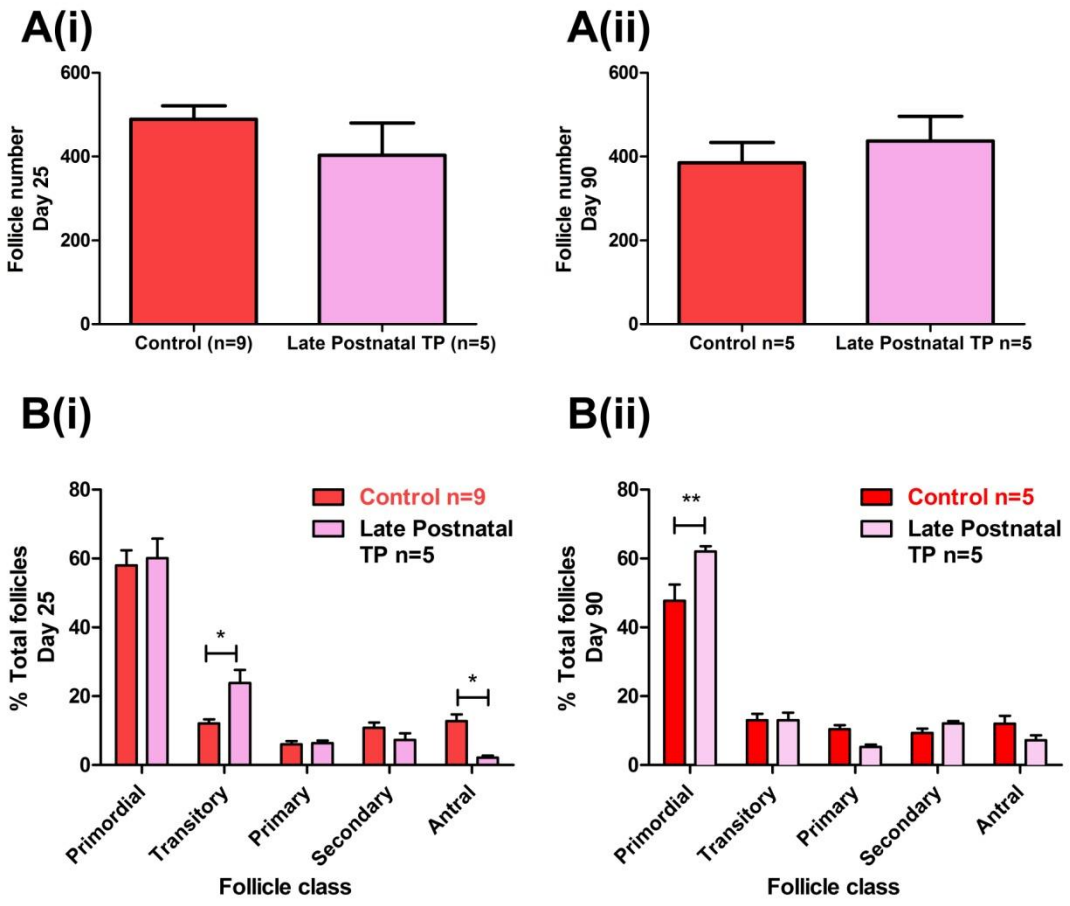

Figure 4.9: Total follicle counts (A) and follicle proportion analysis (B) of control and late postnatal TP treated animal groups at (i) immature day 25 and (ii) adult day 90: Values are expressed as the mean ± SEM. (A-B) were analysed using a student's unpaired t-test and (C-D) using two-way ANOVA with Bonferroni post-hoc test (* P≤0.05; ** P≤0.01).

Examination of follicle numbers and proportions in immature and adult animals treated with late postnatal TP revealed no significant differences in total follicle numbers (Figure 4.9). However, immature animals treated with late postnatal TP exhibited an increase (P≤0.05) in the proportion of transitory follicles, and a decrease (P≤0.05) in the proportion of antral follicles. Furthermore adult animals

treated with late postnatal TP exhibited a significant increase ($P \leq 0.01$) in the proportions of primordial follicles.

4.4.3. Effects of TP administered during both fetal and postnatal life

Animals treated with TP for the fetal plus the postnatal period displayed morphologically dysgenic ovaries at immature pnd 25. By contrast adult pnd 90 animals treated with fetal plus postnatal TP lacked a vaginal opening and developed dysgenic "streak" ovaries (Figure 4.10).

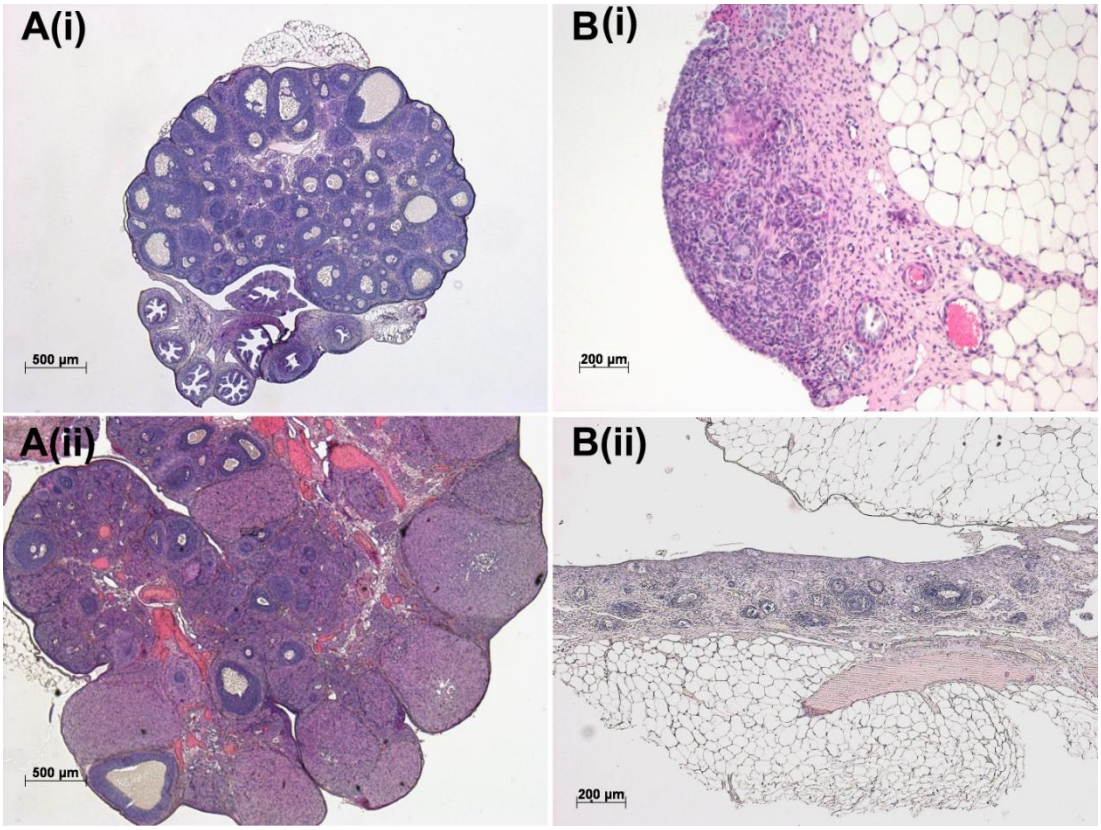

Figure 4.10: Representative images of gross ovarian morphologies seen in (A) control and (B) fetal plus postnatal TP treated animals (i) at immature day 25 (ii) at adult day 90: Note the dysgenic morphology found in both immature and adult animals from the fetal plus postnatal TP treatment group. Images were taken at (A) X 2 and (B) X 10 magnification.

Follicle population analyses of these ovaries (Figure 4.11) confirmed no differences in follicle numbers in the immature animal. However there existed a

greater proportion of transitory follicles (P≤0.001), and a lower proportion of antral follicles (P≤0.05) in comparison to controls at pnd 25. In adult animals treated with fetal plus postnatal TP there were significantly fewer ovarian follicles (P≤0.05) when compared to controls, and analysis of follicle proportions found a greater proportion of primordial follicles (P≤0.001) at this age.

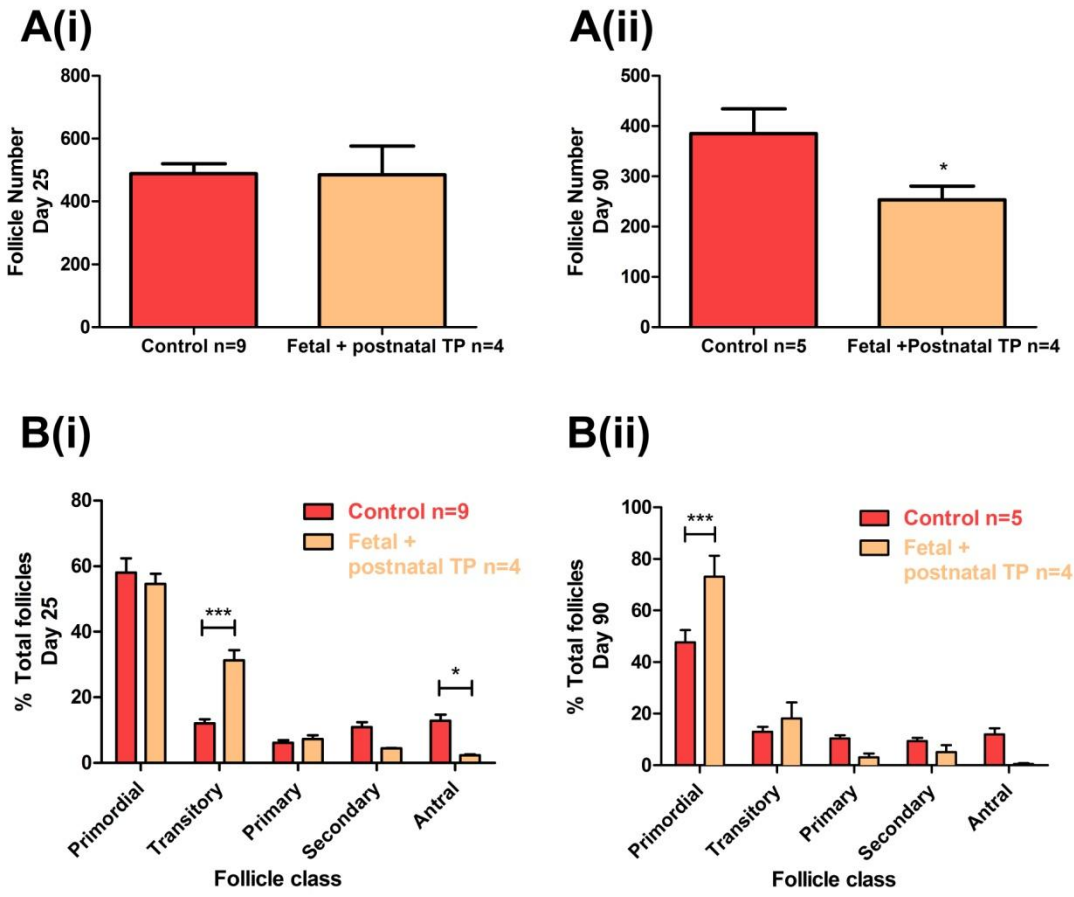

Figure 4.11: Total follicle counts (A) and follicle proportion analysis (B) of control and fetal plus postnatal TP treated animal groups at (i) immature day 25 and (ii) adult day 90. Values are expressed as the mean ± SEM, (A-B) were analysed using a student's unpaired t-test and (C-D) were analysed by two-way ANOVA with Bonferroni post-hoc test (*P≤0.05; *** P≤0.001).

To investigate the effects of fetal plus postnatal TP treatment upon the adult ovary, 5µm ovary sections of ovaries from these animals were mounted on the same slide as a control ovary section and underwent IHC staining for various ovarian

markers of ovarian and follicular functional status. One marker included proliferating cell nuclear antigen (PCNA), a cell cycle protein involved in DNA replication and repair which is strongly expressed in the GC of growing follicles as they progress from small to medium size (El-Hefnawy and Zeleznik 2001). PCNA expression is reduced in atretic follicles irrespective of their size, and shows expression in the non-proliferating corpus luteum (Baravalle, Salvetti et al. 2007). PCNA expression in "streak" ovaries from adult animals treated with fetal plus postnatal TP was subjectively weaker when compared to PCNA expression in control ovaries (Figure 4.12). Interestingly, the GCs around the antra of the cystic follicles showed reduced PCNA expression.

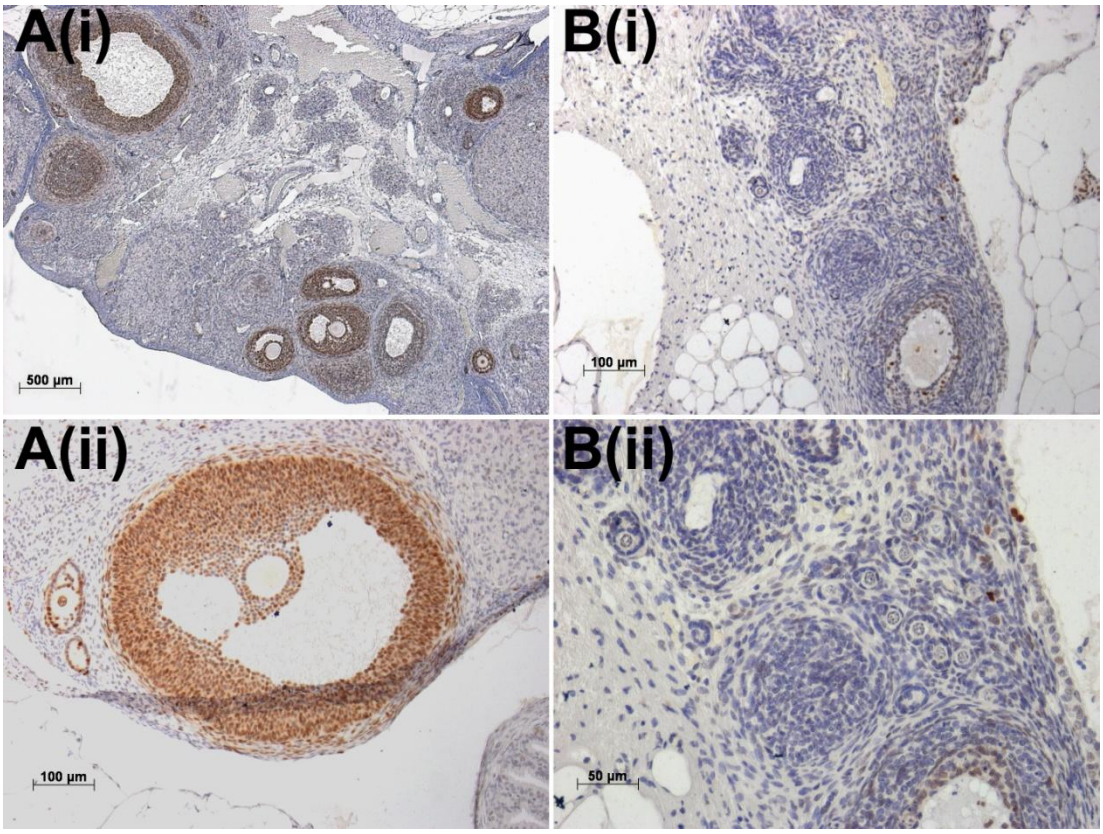

Figure 4.12: PCNA expression in adult (A) control and (B) "streak" ovaries from animals treated with fetal and postnatal TP; expression is reduced in "streak" ovaries as there is a marked absence of larger proliferating follicles, like those depicted in A(ii).

To quantitatively assess the functional status of follicles within dysgenic "streak" ovaries and to compare them to controls, further IHC for AMH, a GC secretagogue known to inhibit further follicle recruitment was performed (Figure 4.13). Subsequent analysis of the number of follicles expressing AMH illustrated that there were significantly fewer activated follicles ($P \leq 0.05$) within the dysgenic "streak" ovaries of fetal and postnatal TP animals (Figure 4.14).

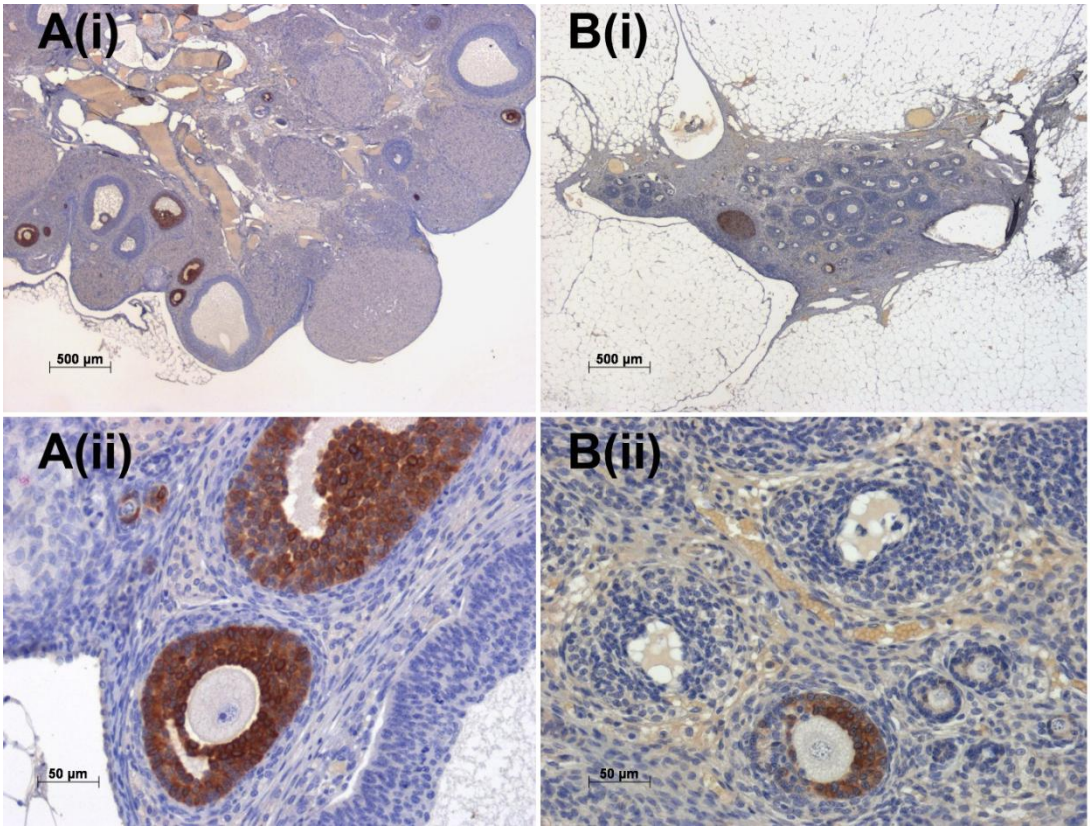

Figure 4.13: AMH expressing follicles in adult (A) control and (B) "streak" ovaries: Shown at (i) X 2 and (ii) X 20 magnification respectively. Note the absence of AMH expression in newly activated follicles within the "streak" ovary (B).

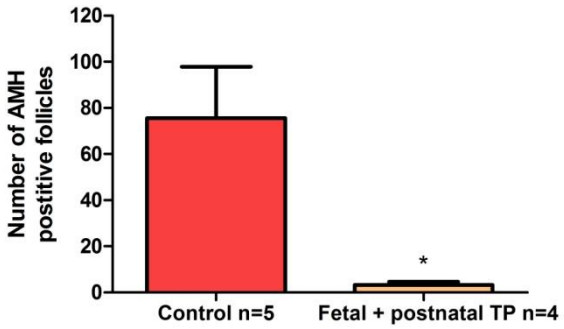

Figure 4.14: Follicle population analysis – the number of AMH positive follicles in control (n=5) and "streak" (n=4) ovaries: Values are expressed as the mean ± SEM, and were analysed using a student's unpaired t-test (* P≤0.05).

Additionally, IHC for cleaved caspase-3 was performed on serial sections of ovaries. Very little staining was observed in both control ovaries and "streak" ovaries making semi-quantitative analysis of apoptosis in these sections unfeasible.

4.4.4. Effects of TP administered during postnatal life

Immature animals treated with TP for the postnatal period displayed morphologically normal ovaries while adult females of this treatment group lacked a vaginal opening and exhibited an anovulatory ovarian phenotype, as shown by the absence of CL (Figure 4.15).

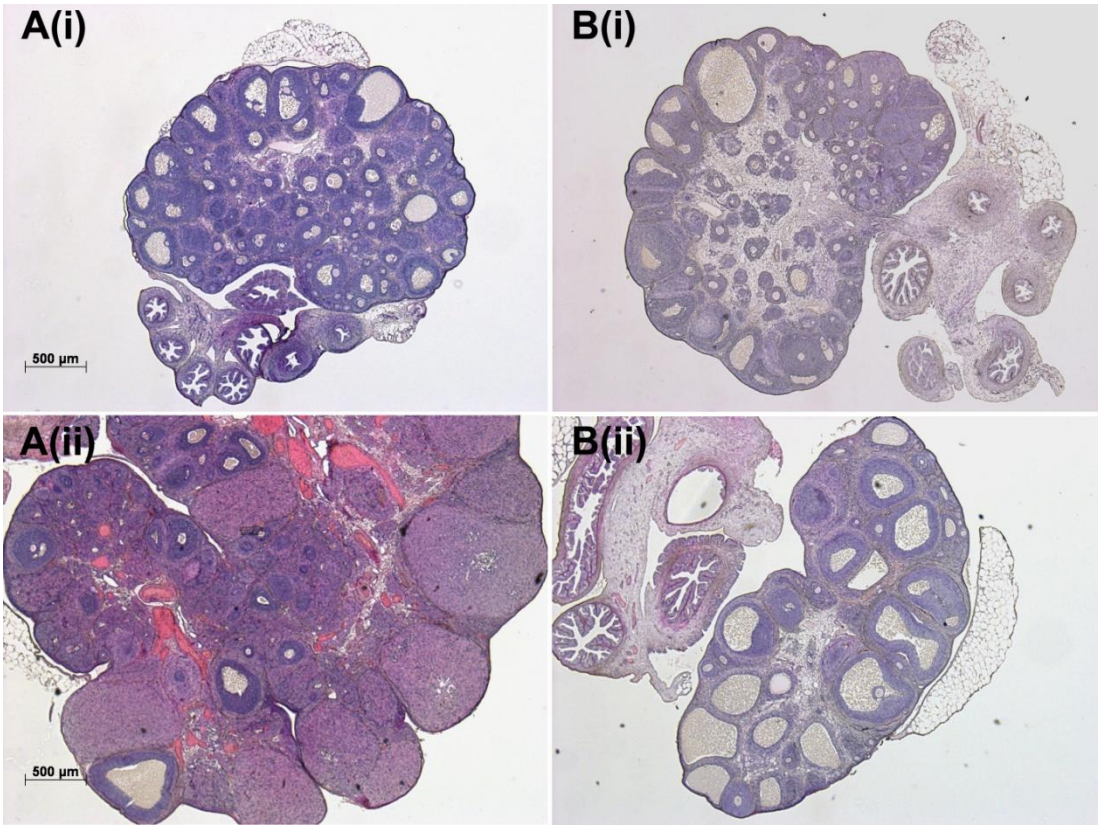

Figure 4.15: Representative images of gross ovarian morphologies seen in (A) control and (B) postnatal TP treated animals (i) at immature day 25 (ii) at adult day 90; Note the relatively normal morphology of animals treated with postnatal TP at pnd 25 (Bi) and the anovulatory 'cystic'-like morphology found in adult animals of the same treatment group. Images were taken at X 2 magnification.

It is of note that 2 out of 6 adult animals in the postnatal TP treatment group developed large fluid filled cysts around one of their ovaries. These large cysts were fixed in bouins for later microscopic examination (Figure 4.16).

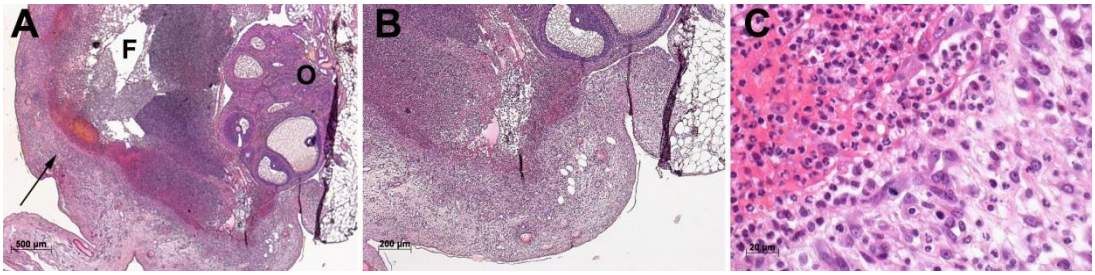

Figure 4.16: Postnatal TP produces large fluid filled cysts in the adult (pnd 90) animal: O=ovary and F=fluid filled cyst in panel (A) with an arrow indicating the capsule surrounding the cyst at X 2 magnification. (B) and (C) show this area further magnified area at X 20 and X 40 respectively.

Follicle population analysis of animals treated with postnatal TP revealed no significant differences in total follicle numbers at either pnd 25 or pnd 90, and no differences in follicle proportions at immature pnd 25. In adult animals treated with postnatal TP there was a significant increase in the proportion of primordial ovarian follicles (P≤0.01) when compared to controls (Figure 4.17).

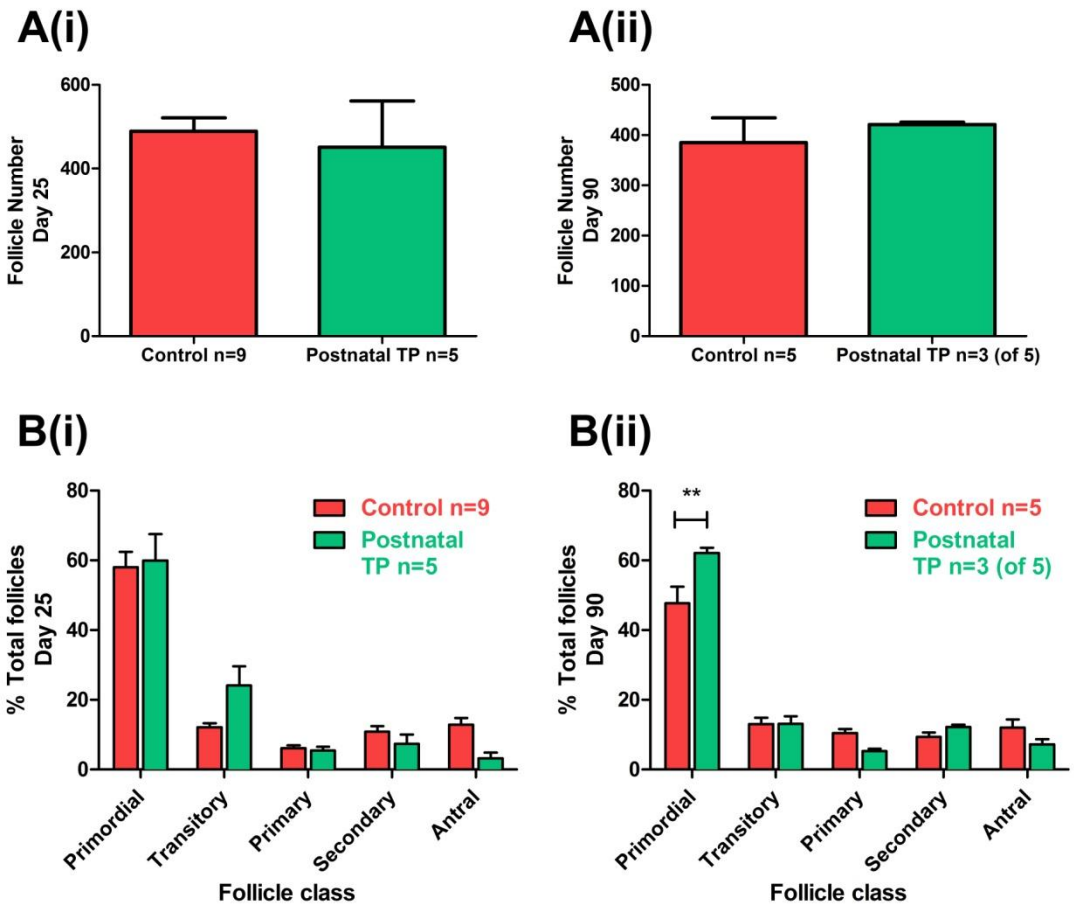

Figure 4.17: Total follicle counts (A) and follicle proportion analysis (B) of control and postnatal TP treated animal groups at (i) immature day 25 and (ii) adult day 90. Values are expressed as the mean ± SEM, (A-B) were analysed using a student's unpaired t-test and (C-D) were analysed by two-way ANOVA with Bonferroni post-hoc test (** P≤0.01).

4.4.5. Effects of TP upon metabolic and hormonal parameters

To investigate the effects of the various TP treatment windows upon hormonal parameters, E2 and gonadotrophin levels from animals at the time of sacrifice were measured (Figure 4.18). Although there is an apparent trend for higher LH levels in adult animals from the postnatal TP treatment group compared to controls, this was not significant. When gonadotrophin levels were below the detectable range of the assay (LH in pnd 25 late postnatal and postnatal TP and FSH in pnd 90 postnatal TP treated animals), non-parametric analysis found there to be a significant reduction in gonadotrophin levels ($P \leq 0.05$). Otherwise, no significant differences in LH or FSH levels across treatment groups were found, in either immature or adult animals.

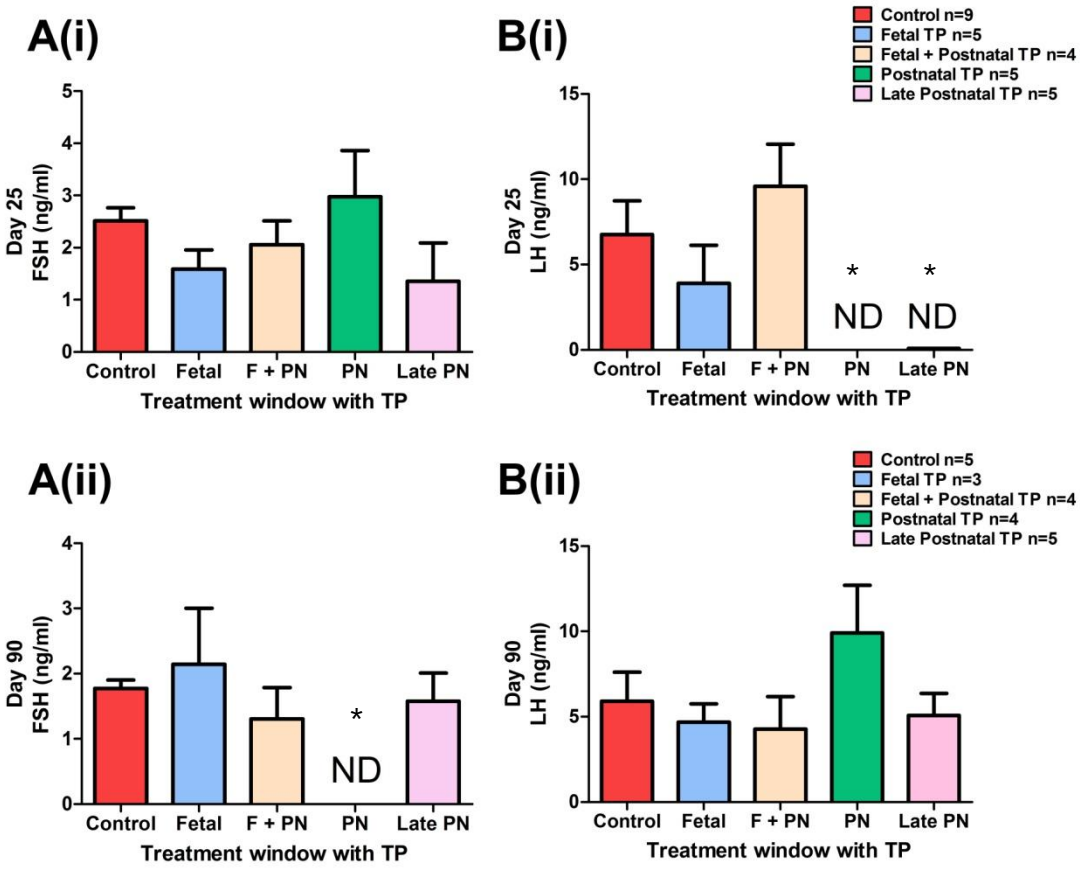

Figure 4.18: Plasma (A) FSH levels and (B) LH levels in (i) immature day 25 animals and (ii) adult day 90 animals, shown across treatment groups with n numbers as indicated. Values are expressed as the mean ± SEM and were analysed using a student's unpaired t-test. **ND**=not detectable levels <0.1ng/ml FSH and <0.2ng/ml LH; these groups were compared to controls using a non-parametric Mann Whitney test (* P≤0.05).

As previously detailed in Chapter 1, Sections 5 and 6, circulating E2 released by the ovary not only feeds back to the hypothalamic-pituitary axis to induce the GnRH/LH surge that stimulates ovulation, but it also acts to prepare the uterine endometrium for implantation of a potential embryo. Thus one biological marker of E2 levels in female mammals is uterine weight. Ovarian and uterine weights for each treatment group are shown in Figure 4.19 and are illustrated together with plasma E2 levels.

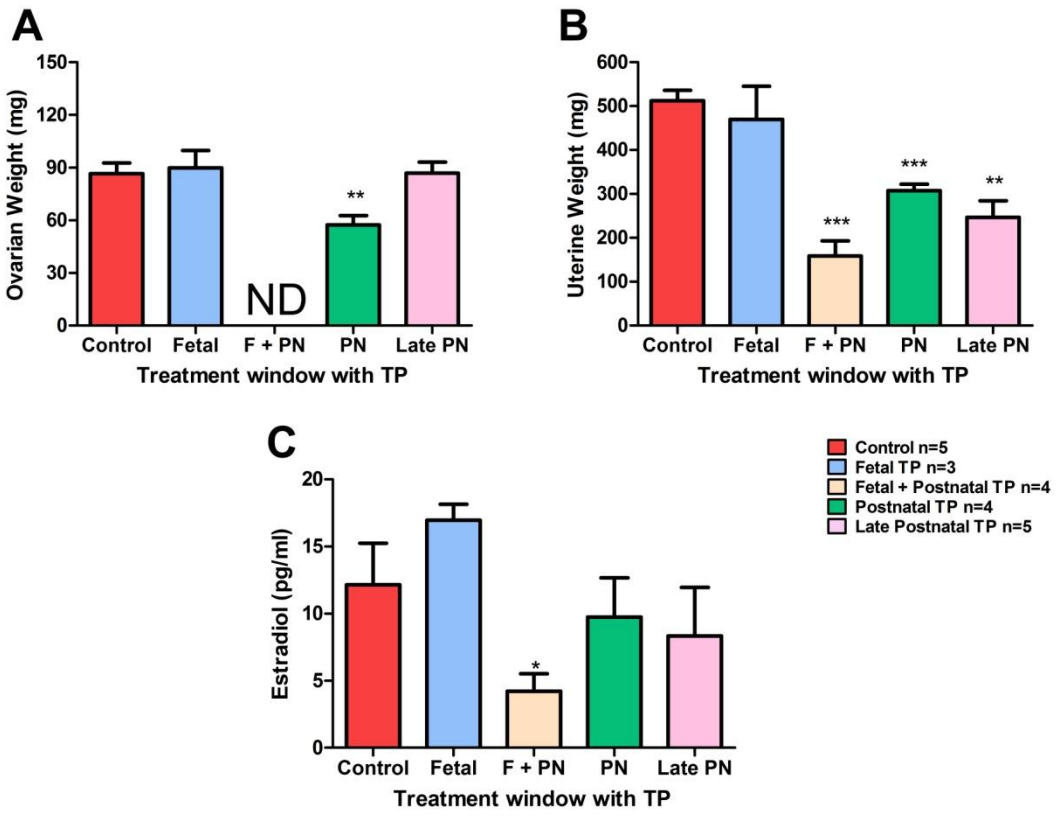

Figure 4.19: (A) Ovarian weights (B) uterine weights and (C) estradiol (E2) levels across treatment groups in adult animals with n numbers as indicated: Values are expressed as the mean ± SEM and were analysed using a student's unpaired t-test (*P≤0.05; ** P≤0.01; *** P≤0.001), **ND**=ovaries were not detectable in the gonadal fat pad, so the whole area was removed and fixed without weighing.

Ovaries from animals treated with postnatal TP weighed significantly less (P≤0.01) than those from control animals, presumably due to the absence of CL.

Ovaries from animals treated with fetal or late postnatal TP were not significantly different in weight compared to controls and had CL present (Figure 4.19).

Due to the dysgenic nature of the ovaries from the fetal plus postnatal TP treatment group, these ovaries could not be located within the gonadal fat pad to be weighed. This data supports the fact that significantly lower E2 levels ($P \leq 0.05$) were found in this treatment group, in addition to significantly smaller uteri ($P \leq 0.001$). Furthermore, uteri from the postnatal and late postnatal treatment groups were also significantly lighter ($P \leq 0.01$) when compared to those of control animals. However these treatment groups exhibited no significant differences in plasma E2 levels when compared to controls.

In addition to the reproductive phenotypes observed in animals exposed to TP during various windows of fetal and postnatal life, a metabolic phenotype was also seen in animals receiving TP postnatally. By day 25 of life, immature animals in the fetal plus postnatal TP, postnatal TP and late postnatal TP treatment groups were all significantly heavier compared to control animals ($P \leq 0.05$, $P \leq 0.001$ and $P \leq 0.001$ respectively, Figure 4.20).

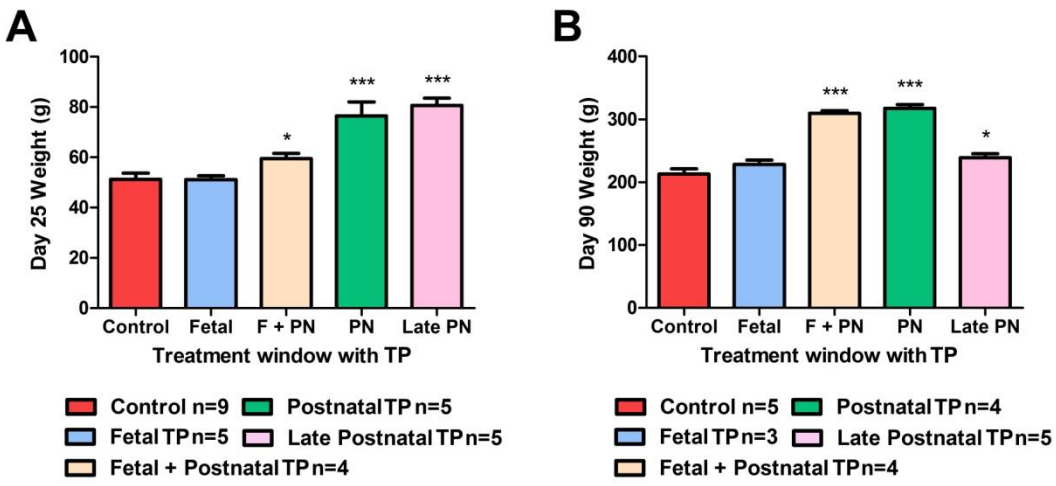

Figure 4.20: Animal body weights at (A) immature day 25 and (B) adult day 90, shown across treatment groups, with n numbers as indicated: Values are expressed as the mean ± SEM and were analysed using a student's unpaired t-test (* P≤0.05; ***P≤0.001).

At adult day 90 this weight gain was even more apparent, with fetal plus postnatal TP treated animals and postnatal TP treated animals growing to approximately 35% heavier than controls ($P \leq 0.001$). Furthermore at this age, late postnatal TP treated animals remained significantly heavier than controls, however only by a margin of around 8% ($P \leq 0.05$). There was no effect of fetal TP exposure upon weight gain in either immature or adult animals of this treatment group.

The significant weight gain induced by postnatal TP exposure in adult animals coupled with the cystic anovulatory phenotype of the ovaries within this treatment group led to further investigations into this window of postnatal TP exposure as a rodent model for PCOS.

4.4.6. Validation of a PCOS model

To investigate whether the cystic appearance of follicles observed in ovaries of animals treated with postnatal TP was due to the absence of CL and extra accumulation of follicle fluid into the antral space, antrum size of individual follicles with a nucleus was measured in every 10th 5µm section from the ovaries of both the control postnatal TP animals (Figure 4.21).

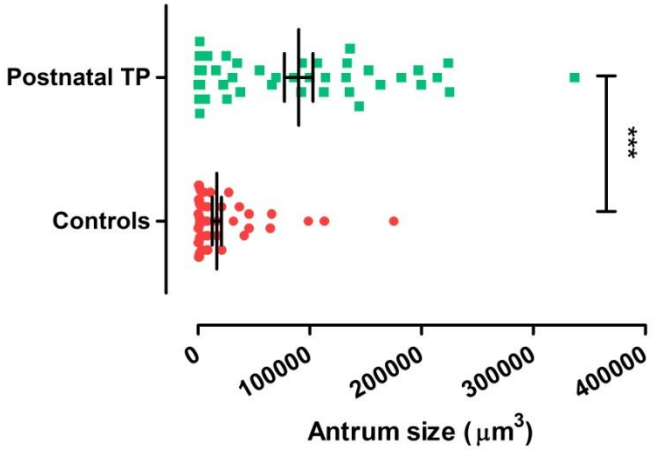

Figure 4.21: Antrum size in follicles from control (n=6) and postnatal TP treated (n=4) animals: Values are shown for every antral follicle with a nucleus in every 10th 5µm section of each ovary. Black lines illustrate the mean ±SEM and differences were analysed using a student's unpaired t-test (*** P≤0.001).

Given that ovaries from the postnatal TP group had on average significantly larger antra (P≤0.001) when compared to control ovaries, follicular functional status was investigated further using DAB IHC for AMH and aromatase on two additional cohorts of adjacent serial sections.

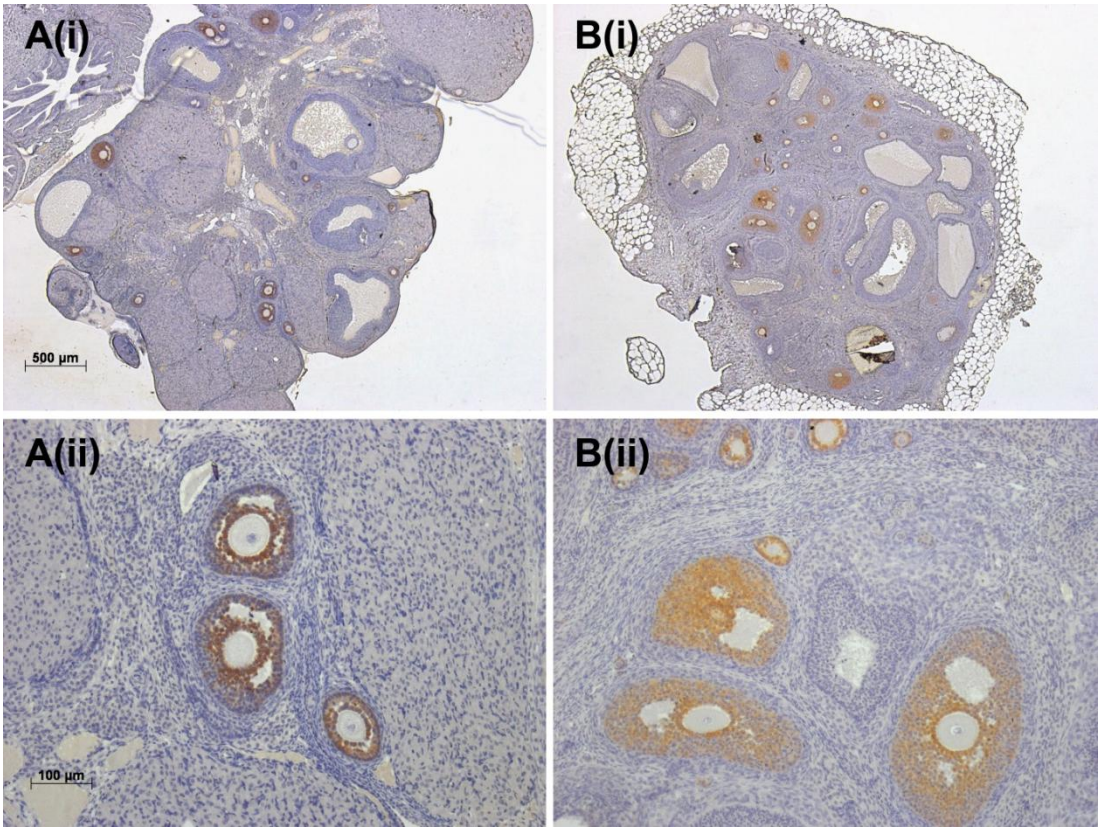

Figure 4.22: AMH staining in ovaries from (A) control and (B) postnatal TP treated animals. Images are shown at (i) X 2 and (ii) X 20 magnification.

Ovaries of the postnatal TP group showed similar AMH staining to those of the control group (Figure 4.22); AMH is secreted from the GCs closest to the oocyte in activated growing follicles at the various levels of folliculogenesis. It was not secreted by any non-growing primordial follicles or by any very large antral follicles in either control or postnatal TP group ovaries. AMH positive follicles were counted and classified according to their size in order to perform a more quantitative morphometric analysis (Figure 4.23).

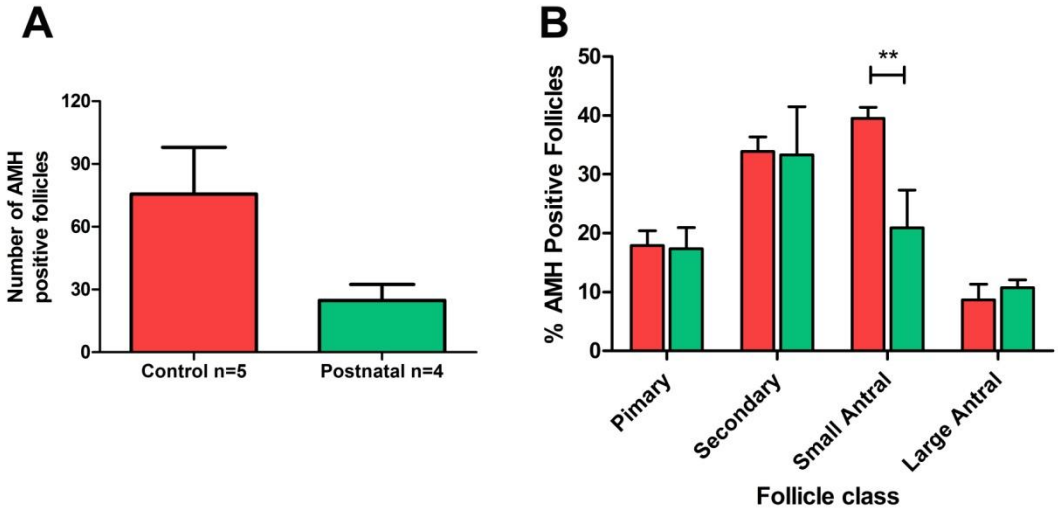

Figure 4.23: Follicular functional status through AMH serial staining to show (A) the number AMH positive follicles per ovary, and (B) AMH positive follicles classed and calculated as a percentage of AMH positive follicle numbers: Shown for control (n=5) and postnatal TP (n=4) ovaries. Values are expressed as the mean ± SEM and (A) was analysed using a student's unpaired t-test and (B) using two-way ANOVA with Bonferroni post-hoc test (** P≤0.01).

AMH staining was used to identify the number of activated follicles present in control and postnatal TP group ovaries. There was no significant difference in the total number of activated AMH positive follicles. However a significantly lower proportion of AMH positive small antral follicles (P≤0.01) in ovaries from postnatal TP treated animals were found, when compared to those from controls. During these experiments the number of GC layers secreting AMH was also documented and categorised by follicle type to determine if the level of AMH secretion was affected by postnatal TP. No significant differences between treatment groups were observed (data not shown).

Adjacent serial sections were stained for aromatase, the enzyme present in mGCs which, in large antral follicles, converts A4 and T produced by the theca cells of the follicle into estrogens (Figure 4.24). The number of aromatase positive follicles was counted in every 10^{th} section for each ovary, and these follicles were subsequently classified to have strong, weak or negative staining for aromatase (Figure 4.25). Despite significantly more aromatase positive follicles per ovary from

the postnatal TP treated group compared to controls (P≤0.05), no significant differences were found when large antral follicles were classified based on their aromatase staining.

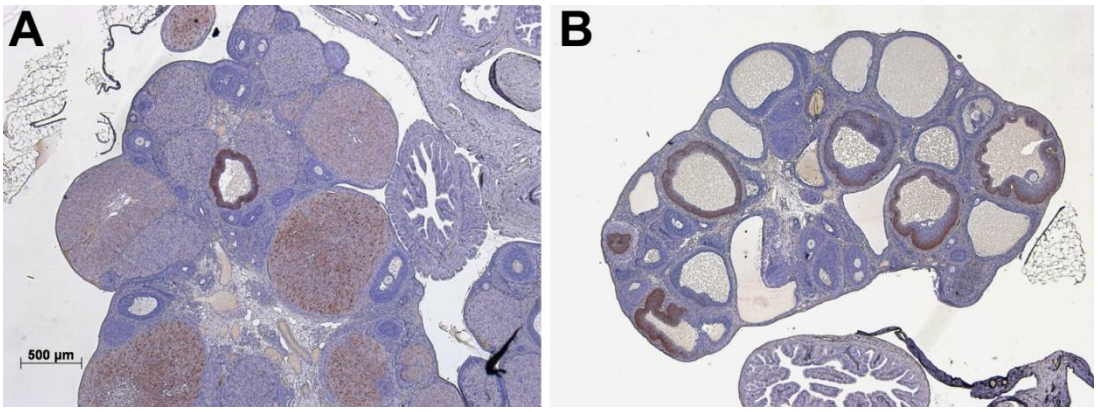

Figure 4.24: Aromatase staining in ovaries from (A) control and (B) postnatal TP treated animals: Images are shown at X 2 magnification.

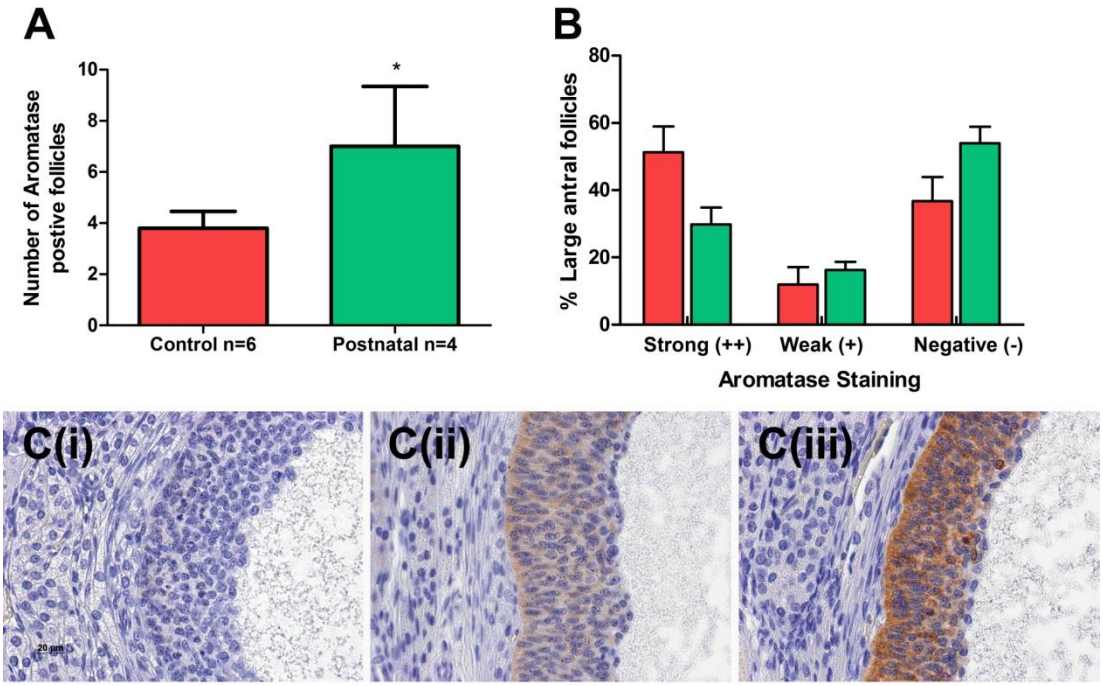

Figure 4.25: Follicular functional status inferred using aromatase serial staining in control (n=5) and postnatal TP (n=4) ovaries: (A) Number of aromatase positive follicles and (B) % large antral follicles classified on aromatase staining intensity; (C) i) strong, ii) weak, iii) negative aromatase staining. Values are expressed as the mean ± SEM with (A) analysed using a student's unpaired t-test and (B) using two-way ANOVA with Bonferroni post-hoc test (* P≤0.05).

Clinical studies have observed an increased stromal compartment and an increased thecal thickness in the ovaries of women with PCOS (Nelson, Legro et al. 1999). These cellular compartments of the mammalian ovary are highly steroidogenic and may contribute towards hyperandrogenic status documented in many women with PCOS. To assess whether there was an increase in the stromal compartment and steroidogenic activity of theca interna in this rat model, serial DAB IHC using antibodies specific for these ovarian compartments was employed. Morphometric stereological analysis allowed the relative contribution of each of these ovarian compartments to be individually calculated.

The stromal compartment was quantified using morphometric stereological analysis for 3β-hydroxysteroid-dehydrogenase (3βHSD), as previously described in Chapter 2, Section 6, illustrated in Figure 4.26. This enzyme is an isomerase that converts 5,3-βhydroxysteroids to 4,3-ketosteroids; notably (17-hydroxy) pregnenolone to (17-hydroxy) progesterone, androstenediol to T and dehydroepiandrosterone to A4 within both the adrenal and ovary.

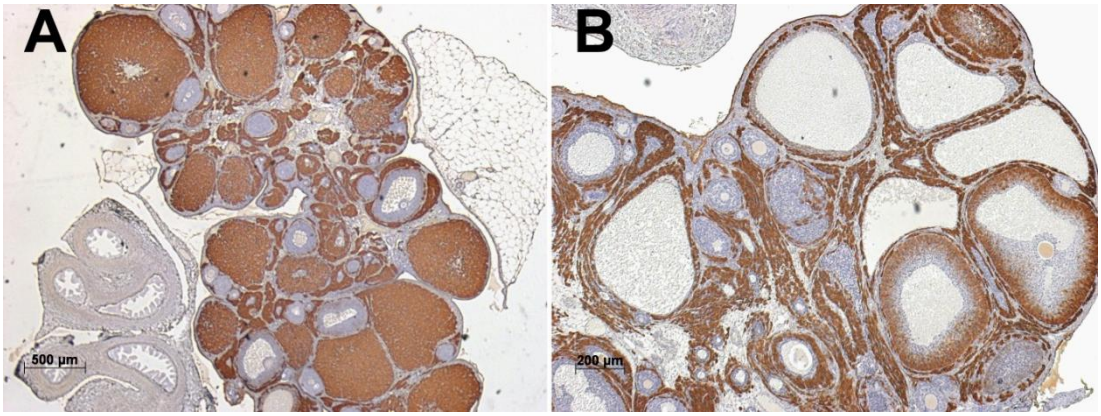

Figure 4.26: Stromal 3β-HSD staining in ovaries from (A) control and (B) postnatal TP treated animals. CL staining (controls) and mural GC staining was excluded from the area of interest before analysis. Images are shown at X 2 and X 4 magnification respectively.

In a cohort of serial sections, the ovarian area was determined in each section for ovaries from postnatal TP treated animals and control oil animals (excluding CL).

The 3βHSD DAB stained area was determined in the same sections and taken as a percentage of ovarian area, again excluding CL and any mGC staining. When compared to controls, ovaries from postnatal TP treated animals presented a significantly greater area of 3β-HSD positive stroma (P≤0.05), and in addition these ovaries contained a larger proportion of stromal tissue (P≤0.001), illustrated in Figure 4.27.

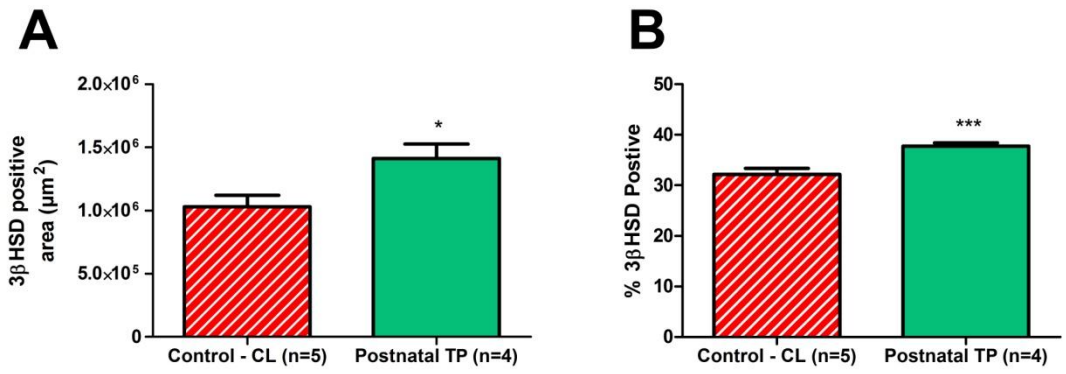

Figure 4.27: Stromal compartment measured as (A) overall 3β-HSD staining and (B) proportion of 3βHSD staining relative to ovarian area, in ovaries from control (n=5) and postnatal TP treated animals (n=4)[‡]. Control ovarian area excludes CL area. Values are expressed as the mean ± SEM and were analysed using a student's unpaired t-test (*P≤0.05; *** P≤0.001).

The thecal compartment was measured in a similar fashion, using serial staining for 17α-hydoxylase (17α-OH), an enzyme primarily localised to the theca interna of the rodent ovary (Figure 4.28). The enzyme 17α-OH is a cytochrome p450 monooxygenase which, in the ovary converts pregnenolone and progesterone to their 17-hydroxy counterparts. The enzyme subsequently acts as a lyase upon these two compounds to form dehydroepiandrosterone and androstenedione respectively, making 17α-OH an important enzyme in the generation of ovarian androgens.

[‡]The measurement and analysis of data presented in Figure 4.27 was carried out by Marie Broyde, an honours student under the author's supervision.

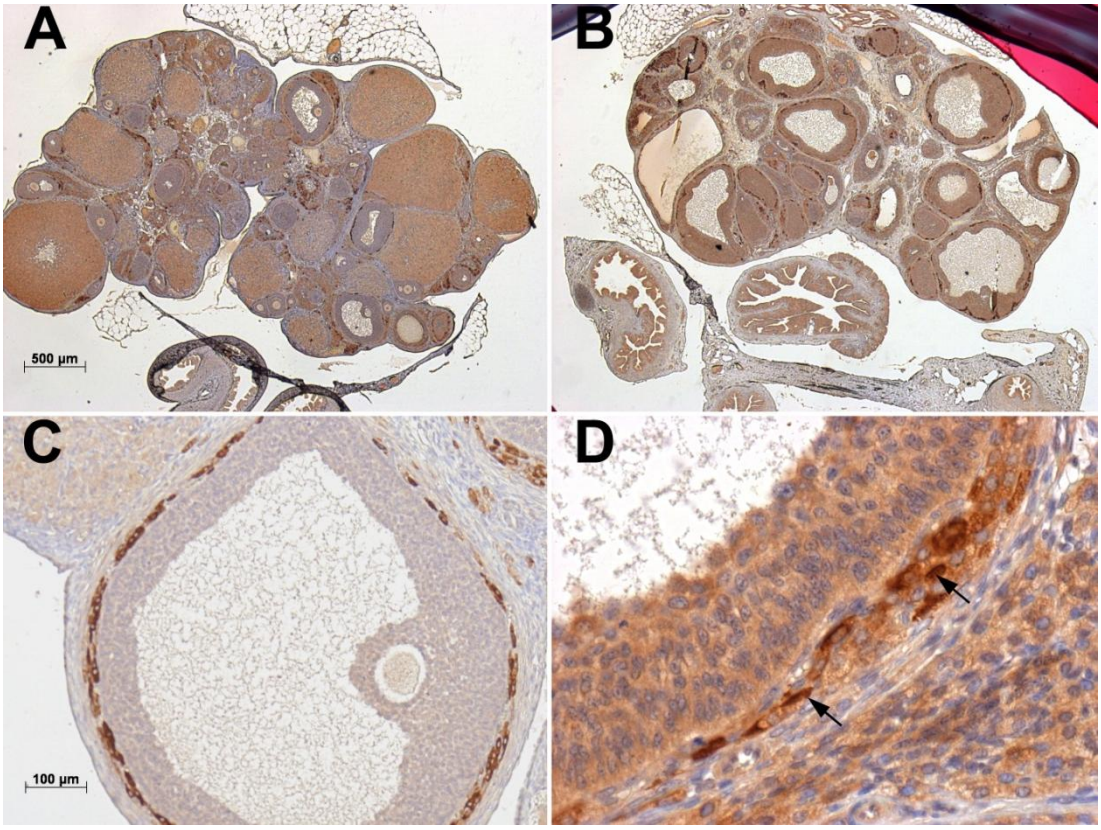

Figure 4.28: Theca interna 17α-hydroxylase staining in ovaries from (A) control and (B) postnatal TP treated animals. CL staining (controls) and stromal background staining (D) was excluded from the area analysis by only including strong 17α-OH staining in the analysis, as exemplified by the follicle in panel C and indicated by arrowheads in panel D.

The 17αOH positive compartment was measured using the stereological methods described in Chapter 2, Section 6. The compartment was first selected and measured in μm^2, and then taken as a % of ovarian area excluding the CL area, shown in Figure 4.29. There was a significantly reduced overall 17αOH area in ovaries from the postnatal TP treatment group compared to controls ($P \leq 0.05$), however this difference was absent when whole ovarian area (excluding CL) was accounted for.

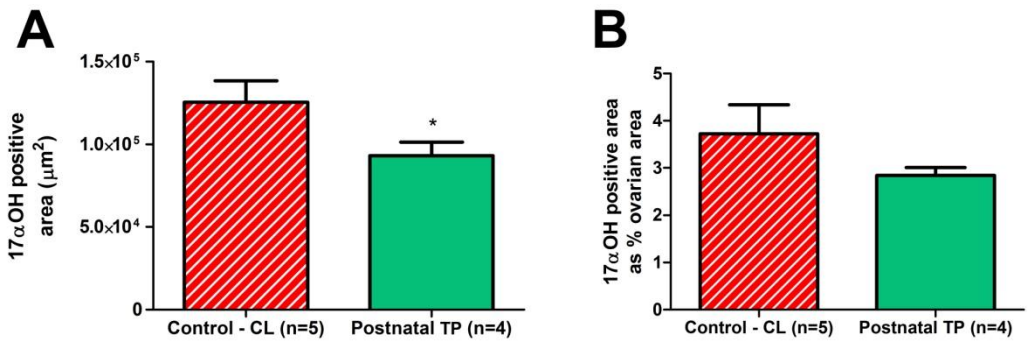

Figure 4.29: Thecal compartment analysis using serial 17αOH staining in ovaries from control (n=5) and postnatal TP treated (n=4) animals[§]: (A) Total 17αOH stained area (B) 17αOH staining as a % of ovarian area (excluding. CL). Values are expressed as the mean ± SEM and were analysed using a student's unpaired t-test (* P≤0.05).

Additionally, follicles expressing 17αOH in their theca were classified and counted and their theca interna thickness measured individually during whole morphometric ovary analysis for 17αOH expression in each section. Again CL area and background stromal/mGC staining was excluded from this analysis, by only selecting the area with strong 17αOH staining, as indicated in Figure 4.28. As shown by Figure 4.30, there were no significant differences in the proportions of follicles expressing 17αOH in their theca interna between ovaries from control and postnatal TP treated animals. Furthermore there were no significant differences in mean theca interna thickness. There was however a direct correlation between thecal area and follicle size within ovaries from control animals as well those from postnatal TP treated ovaries. These two correlations were not significantly different from one another.

[§] The measurements and analysis for data in Figure 4.29 were carried out by Marie Broyde, an honours student under the author's supervision.

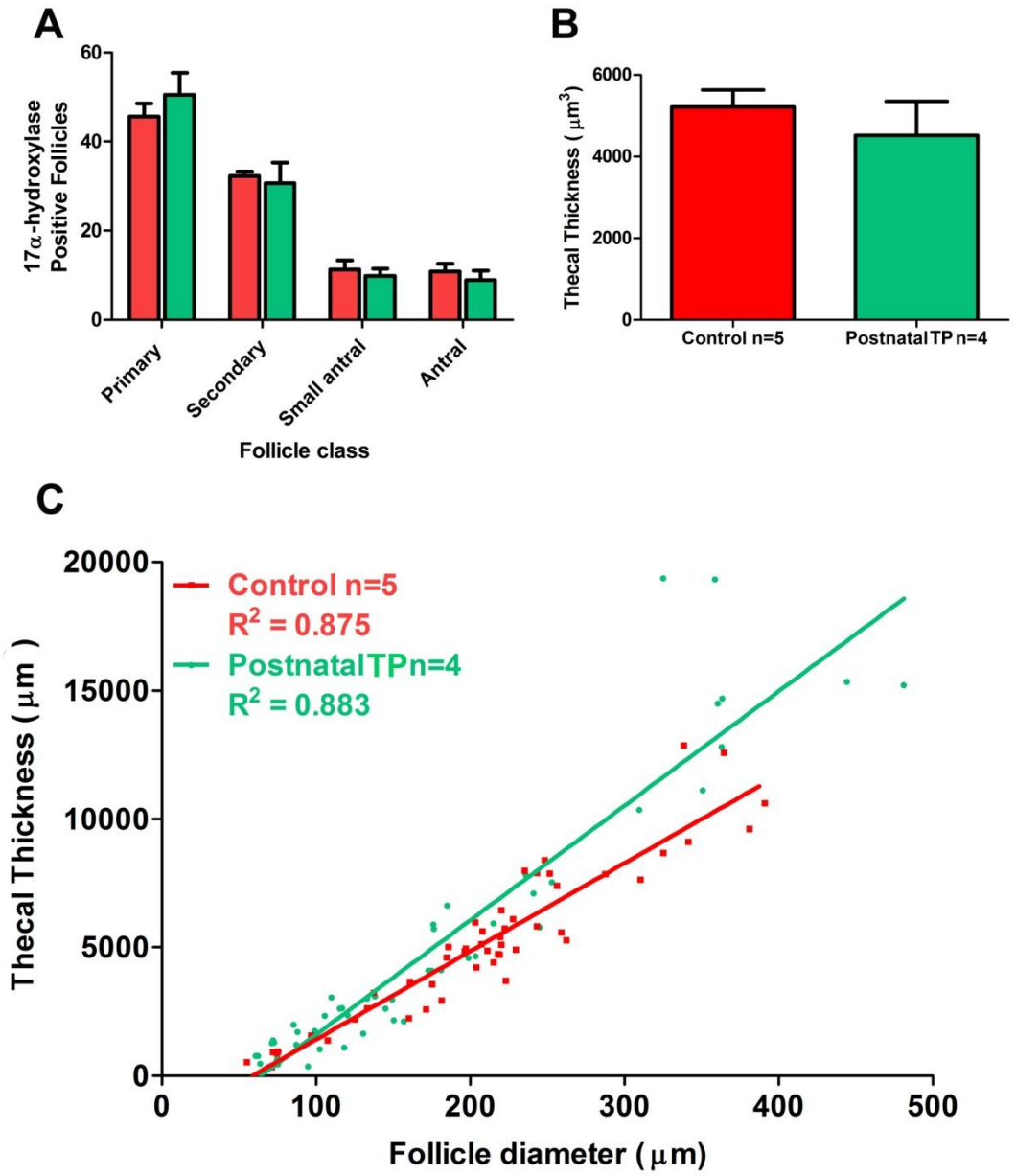

Figure 4.30: Further thecal compartment analysis using serial 17αOH staining in ovaries from control (n=5) and postnatal TP treated (n=4) animals: (A) Proportions of 17α-OH positive follicles[**]; (B) Theca interna area for individual follicles; (C) Relationship between thecal area and follicle size. For (A-B) values are expressed as the mean ± SEM; (A) analysed by two-way ANOVA with Bonferroni post-hoc test; (B) analysed using a student's unpaired t-test; (C) analysed first by linear regression (control R^2=0.875, postnatal R^2=0.883); a Fisher-*Z* transformation tested for differences between these two correlations - Control n=43 follicles and postnatal TP n=44 follicles yielded P=0.876.

[**] The measurements and analysis for data in Figure 4.30 part A only were carried out by Marie Broyde, an honours student under the author's supervision.

4.5. Discussion

Current rat models of PCOS employ the chronic administration of steroids/steroidogenic inhibitors during postnatal life to produce an altered reproductive phenotype in the adult. For example steroids used include T (Beloosesky, Gold et al. 2004), DHEA (Anderson and Lee 1997; Anderson, Lee et al. 1997), estradiol valerate (Brawer, Munoz et al. 1986; Rosa, Guimaraes et al. 2003), DHT and letrozole (Manneras, Cajander et al. 2007). Other models use a single bolus injection of testosterone or estradiol on or just after the day of birth to produce a PCO-like phenotype in the adult animal (Barraclough 1961; Brawer, Naftolin et al. 1978; Ota, Wakizaka et al. 1986; Grossmann, Diez-Guerra et al. 1987; Alexanderson, Eriksson et al. 2007). In addition, relatively few rodent models have fully examined the reproductive phenotype in the adult animal and contrasted it with the clinical situation (Ota, Wakizaka et al. 1986; Manneras, Cajander et al. 2007). The main objective of these investigations was therefore to determine which windows of neonatal TP treatment induce an altered reproductive phenotype in the adult animal and to what extent if any, the resulting phenotype mimics human reproductive pathophysiologies such as PCOS or POF.

4.5.1. Fetal TP has no discernable effects upon the female rat

Within the fetal TP treatment group, no effect was observed at any stage of measurement upon the formation and natural apoptosis of germ cells at birth. In addition i*n vitro* cultures of fetal chicken ovaries have shown that androgens may act to promote germ cell proliferation rather than affect atresia (Anderiesz and Trounson 1995).

No effect of fetal TP exposure upon folliculogenesis or potential fertility occurred in adult life, as evidenced by the presence of healthy CL formation in addition to normal follicle numbers and proportions within the ovaries of these animals at both immature pnd 25 and pnd 90. Immature and adult body weights were normal, and gonadotrophin and E2 levels were comparable to those seen in controls at each stage of investigation for this TP treatment group. These findings corroborate

previous investigations into the effects of fetal TP upon female reproductive development (Smith 1970; Slob, den Hamer et al. 1983). It is worth noting that there may be species differences in the response to fetal androgen exposure as fetal TP administration in Sprague-Dawley (SD) rats in one study reduced both immature and adult animal body weight (Wolf, LeBlanc et al. 2004). Fetal TP treated female rats develop masculinised features of the urogenital tract, for example an increased ano-genital distance (AGD), as described in the original paper upon which these studies were based (Welsh, Saunders et al. 2008; Welsh, MacLeod et al. 2010).

4.5.2. Postnatal TP treatment leads to changes in ovarian follicle composition in the immature animal

At pnd 25, in late postnatal TP and fetal plus postnatal TP ("streak" ovary) treatment groups, a higher proportion of activating transitory follicles and lower proportion of small antral follicles was observed, with no effect seen on total follicle numbers at this age. These results may demonstrate the mitogenic effects of testosterone upon folliculogenesis, whereby androgens stimulate GC proliferation of smaller newly activated transitory and primary follicles. These findings are supported by elegant experiments using ruminant follicles pre-exposed to testosterone then grafted into chick ovaries; the grafts were shown to selectively increase the proportion of growing primary follicles (Qureshi, Nussey et al. 2008). The same graft study found androgens to have a protective effect upon follicle survival, which is at odds with the reduced proportion of small antral follicles found in the late postnatal and fetal plus postnatal TP treatment groups of the current investigation. In the rat, ovarian AR expression is reduced in GCs of FSH responsive follicles (Tetsuka, Whitelaw et al. 1995) and previous studies involving exogenous administration of androgens to rats have shown that at the later stages of gonadotrophin-dependent folliculogenesis, exogenous androgens can facilitate follicular atresia (Drummond 2006; Honnma, Endo et al. 2006). Indeed the small antral follicles present in the immature rat ovary will not express sufficient mGC aromatase for the production of estrogen (Mahesh, Mills et al. 1987). Thus in the current study TP likely acts to promote GC atresia in more advanced follicles, accounting for the reduction in small antral follicle proportions within these TP treatment groups at pnd 25.

A similar but insignificant trend was observed in the postnatal TP (PCO-like) treatment group at pnd 25. This lack of significance is most likely due to a reprogramming of the hypothalamic-pituitary-ovarian/adrenal (HPO/HPA) axes by early neonatal TP exposure, reducing the mitogenic actions of TP from exerting their influence. This explanation is the most plausible as animals in the late postnatal TP treatment group will have completed neonatal HPA and HPG organogenesis, while those in the fetal plus postnatal TP treatment group may have an increased sensitivity to postnatal TP exposure as a result of fetal TP treatments, as evidenced from other investigations (Hoepfner and Ward 1988).

4.5.3. Fetal plus postnatal TP treatment leads to the formation of dysgenic "streak" ovaries

TP administered during both fetal and postnatal life resulted in dysgenic "streak" ovaries within both immature and adult animals, which by pnd 90 of life had fewer follicles, fewer activated AMH expressing follicles and consequential lower circulating E2 levels with significantly reduced uterine weights. Secretion of AMH by GCs of growing follicles is known to inhibit further follicle activation (Rey, Lukas-Croisier et al. 2003). Following the ovulation of larger growing follicles, AMH levels dip and a further group of follicles activate, allowing regular follicular recruitment during the rodent estrus cycle (Rey, Lukas-Croisier et al. 2003). The deficit of AMH expressing follicles in these '"streak"' ovaries would indicate unimpeded follicular recruitment, which accounts for the reduction in follicle numbers within the adult animals at pnd 90. However, it remains unclear why these ovaries were dysgenic in immature animals. Changes to "streak" ovary tissue structure cannot be ruled out as one potential cause of the low levels of AMH/PCNA expression observed subjectively in these ovaries. Indeed, ovaries could not be properly located in the gonadal fat pad during dissection. Alterations in tissue structure might impede the breaking open of cross-linked proteins (such as collagens, biotins and fibrins) during IHC antigen retrieval and may subsequently affect IHC appearance. However, AMH expression, when it was observed in "streak" ovaries, was just as strong as that in control ovaries. This supports the notion that the changes

in AMH (and potentially PCNA) expression observed are due to differences in the tissue itself and are not an artefact of the IHC process.

Formation of "streak" ovaries at both pnd 25 and pnd 90 implicates a combined effect of TP exposure during late fetal life together with the TP administered during early postnatal life, especially considering no effect was found in fetal TP treated animals and a different effect observed in postnatal TP treated animals. The TP dose administered during this study (20mg/kg) was designed to remain within the effective range for three days post-injection, minimizing the need for daily injections and thus reducing the number of stressful events pups and dams experienced. It is possible that the levels of circulating E2 (resulting from the placental aromatization of TP) and/or TP within animals of the fetal plus postnatal TP group at birth were high enough to persist into early neonatal life.

It is known from other studies that neonatal E2 exposure in rodents prevents germ cell nest breakdown in the ovary (Kezele and Skinner 2003; Jefferson, Newbold et al. 2006). Since fetal E2/TP exposure was followed by TP administration the day after birth, the action of fetal TP may have increased the sensitivity of the postnatal animal to further androgen exposure. This notion is supported by another study in which TP administered to Sprague-Dawley rats during the late fetal period (e17-e18), had a priming effect upon female animals, leading to the masculinisation of female behaviour and physiology in animals which subsequently received a small postnatal dose of 5µg TP (Hoepfner and Ward 1988). Only one other study involving neonatal thymectomy at pnd 3 has resulted in the complete dysgenesis of ovarian function from such a young age in the rat, with ovaries histologically comparable to those observed in this study (Scalzo and Michael 1988). It is of course possible that combined fetal and neonatal TP treatment is able to reprogram thymocyte function, and further study into the effects of thymectomy upon ovarian development are therefore required (Deshpande, Chapman et al. 1997; Chapman, Min et al. 2009).

Further investigation into the reproductive consequences of combined late fetal and early neonatal testosterone, DHT or estradiol exposure in the rat is therefore warranted, as the effects of such treatments should be assessed at earlier time points in neonatal life, for example as germ cell nest breakdown completes on day one of life, after primordial follicles have finished forming on day five of life, and after formation of the first primary follicles by and ten of life, in addition to *ex-vivo* studies.

One additional point of note is that fetal TP administration can lead to dystocia, associated with delayed littering and pup loss (Wolf CJ 2002). Animals in the fetal and fetal plus postnatal TP treatment group were cross-fostered to untreated dams that had recently littered. There is evidence to suggest that inadequate maternal care, in addition to differences litter size, during the rodent neonatal development period can affect hypothalamic-pituitary axis development (Champagne, Francis et al. 2003; Roma, Huntsberry et al. 2007). Cross fostering of certain litters (fetal and fetal plus postnatal TP) and not others (postnatal and late postnatal TP) may therefore have had an additional environmental effect upon endocrine development and function in animals from different litters, and could partially account for the differences in ovarian morphology and reproductive dysfunction observed between the postnatal and fetal plus postnatal treatment groups, although the mechanisms remain unknown.

4.5.4. Postnatal TP treatment leads to weight gain in adult animals

Significant weight gain was observed at immature pnd 25 and adult pnd 90 within all treatment groups receiving TP postnatally. This indicates that the window of postnatal androgen exposure which can produce a metabolic phenotype extends further than two weeks of age. Furthermore, these findings are corroborated by other investigations, whereby regular neonatal administration of androgens (DHT) or aromatase inhibitors (Letrozole) have been shown to lead to weight gain and increased adiposity in adult animals (Manneras, Cajander et al. 2007; Manneras,

Jonsdottir et al. 2008). No studies have fully assessed the metabolic consequences of early neonatal programming of rat metabolism by testosterone, although rat models of the metabolic syndrome involve the fetal administration of the synthetic glucocorticoid, dexamethasone (Seckl 2001), since maternal stress is a known programming cause of adult disease (Cottrell and Seckl 2009).

4.5.5. Postnatal TP treatment leads to changes in ovarian follicle composition in the adult animal

One novel finding of these investigations was the increased primordial follicle proportion consistently observed in all animals that received TP postnatally. At present it is unclear clear how neonatal TP affects the rat follicle pool in this way, although recent research in mice has shown that estrogen acting via both ERα and ERβ can affect primordial follicle populations by inhibiting oocyte apoptosis and proper germ cell nest breakdown before birth, and after birth acting to prevent germ cell nest breakdown (Chen, Breen et al. 2009). Thus aromatisation of TP into E2 within the neonate could account for the effects seen, as aromatase activity has been shown in the neonatal pituitary of female rats (Carretero, Vazquez et al. 2003). Additionally, reduced primordial follicle recruitment could play a part in the conservation of the primordial pool documented in these studies. These findings also corroborate with those of the primate model of PCOS, where increased proportions of primordial follicles were observed in infant animals following fetal exposure to TP (Abbott 2010).

4.5.6. The postnatally androgenised rat as a PCOS model

Postnatal TP administered between days 1-25 of life induced a PCOS-like phenotype in the adult rat by day 90. This potential PCOS model was subsequently evaluated by examining whether the ovarian and endocrine abnormalities associated with the clinical symptoms of the syndrome, namely a cystic ovarian phenotype, anovulation, high circulating levels of LH, low levels of E2, altered functional status of follicles and follicular persistence, increase in ovarian stromal compartment, increased theca interna 17αOH activity and finally obesity were present.

Animals from the postnatal TP group had reduced ovarian weights due to anovulation and lack of CL in addition to low uterine weights which, as a bioassay for estrogens in the rat, could have been due to low estrogen levels, although it should be noted that plasma E2 levels were comparable to controls in this group. Additionally, these animals exhibited a slight but insignificantly raised level of plasma LH, with no effect upon circulating FSH. One explanation for this is the fact that control animals were not culled at proestrus when E2 and FSH levels in the rodent are at their highest prior to the LH surge and ovulation. In addition other neonatally androgenised rat studies have shown E2 levels in the adult animal to be comparable to those at control proestrus with gonadotrophin levels comparable to met/diestrus (Ota, Wakizaka et al. 1986).

Histological examination of ovaries from postnatal TP treated animals showed them to be anovulatory, with large fluid filled antral follicles apparent on subjective inspection. Alongside control ovaries, these PCO-like ovaries underwent serial section analysis for AMH and the results showed a reduction in the proportion of small antral AMH positive follicles. This may have contributed towards a larger mean number of antral follicles staining positive for aromatase found in adjacent sections, and supports the idea that the functional status of follicles within the rat PCO was altered. This argument is supported by the fact that follicles within the ovaries of adult postnatal TP treated animals had larger mean antrum sizes. Together, these observations add weight to the conclusion that although the postnatally TP treated female rat does not necessarily exhibit the hormonal aspects associated with PCOS such as raised LH and depressed FSH, some ovarian and metabolic aspects are recapitulated in the adult animal, namely weight gain, an anovulatory cystic phenotype, follicular persistence and altered follicular functional status.

The effect of postnatal TP treatment upon the ovarian thecal and stromal compartments was also investigated. No difference was observed between ovaries from postnatal TP treated animals or control animals with regard to the status of the

theca; the thecal compartment was of a comparable size, enveloped a comparable number of follicles and the 17αOH stained area was similar between control and TP treated animals. A novel finding of this study was the increased amount and proportion of 3βHSD positive stroma found in postnatal TP treated animals, which further recapitulates clinical observations in women with PCOS (Fulghesu, Ciampelli et al. 2001; Fulghesu, Angioni et al. 2007). The increased stromal compartment observed may be a contributing factor to the resulting hyperandrogenism and anovulation seen in both this model and PCOS women. As no differences in circulating gonadotrophins were observed in adult postnatal TP treated animals, this would indicate that the increased stromal compartment could be due to epigenetic programming of the ovarian endocrinology, as hypothesized by other investigators studying the disease aetiology (Franks 2010).

4.6. Conclusions

The results from the fetal plus postnatal TP group, in addition to the findings of other studies (Hoepfner and Ward 1988), demonstrate that fetal TP is able to reduce the threshold of sensitivity to neonatal testosterone exposure in female animals, providing one explanation for the ovarian dysgenesis observed in this treatment group.

In the rodent, birth instigates a loss of maternal E2 for the offspring and subsequently oocyte apoptosis and nest breakdown occur (Chen, Breen et al. 2009). In rats that received fetal TP, oocyte apoptosis and nest breakdown could still occur subsequent to caesarean delivery. However animals which received postnatal TP in addition to fetal TP would have maintained their oocyte quotient and undergone disrupted cyst breakdown, which can account for their dysgenic phenotype. In animals receiving postnatal TP alone, TP (either as aromatised E2 or as TP) could only affect cyst breakdown resulting in a PCO-like ovarian phenotype. In late postnatal TP animals, cyst breakdown would already have initiated yet the level of TP exposure at this time point may still have been enough to conserve the proportion of primordial follicles. Exposure to TP during the first 25 days of rat life additionally led to a significant increase in both immature and adult body weight through an as yet unknown mechanism.

To conclude further, TP administration during the first 15 days of rat life leads to a valid PCOS-like phenotype in the female that is overweight, anovulatory, has 'cystic' follicles, and an increased ovarian stromal compartment. Although this model does not recapitulate the hormonal abnormalities associated with PCOS. Neonatal exposure to TP has potent effects in the adult animal and thus warrants further investigation into the windows of exposure necessary to produce a PCOS-like phenotype, as well as a more detailed examination of the hormonal and metabolic consequences of this treatment. These aspects of the neonatally androgenised rat as a model of PCOS are further examined in Chapter 5.

Chapter 5. Windows of postnatal testosterone exposure which alter the rat HPG axis

5.1. Introduction

PCOS is significantly associated with obesity in both the clinical setting (Sathyapalan and Atkin 2010), as well as in primate (Abbott 2010), sheep (Padmanabhan, Veiga-Lopez et al. 2010), and rodent (Manneras, Cajander et al. 2007) models of this reproductive endocrinopathy. Obesity is an increasing problem for Western society, and likely results through a combination of three factors (1) more sedentary lifestyles, (2) increases in calorific intake, and (3) a genetic background predisposed to energy storage (Patel, Srinivasan et al. 2009). Development of glucose intolerance and/or insulin resistance alongside obesity gives rise to a metabolic syndrome, which according to the World Health Organisation, carries with it an increased risk of CVD, certain cancer development, arthritis, stroke, and T2DM, in addition to placing huge logistical and financial strain on medical services (W.H.O. 2006).

Women are increasingly likely to develop PCOS as the result of obesity, and weight reduction can serve to ameliorate symptoms and restore fertility (Reviewed in Norman, Noakes et al. 2004; Pasquali and Gambineri 2004). However, not all obese women will develop PCOS and not all PCOS patients gain weight (ESHRE Group 2006). Although this discrepancy can be explained to some extent by the inherent heterogenic nature of PCOS, given that some women diagnosed with PCOS ovulate regularly (Chapter 1 Section 11), researchers are still left with the quandary as to why weight gain in some women negatively impacts fertility, while others remain unaffected. The heterogeneity of PCOS likely results from a combination of genetic risk factors, environmental factors and potentially developmental programming by nutrition or steroid hormones during fetal and/or infant life (Qi and Cho 2008; Lee 2009; Patel, Srinivasan et al. 2009). It is therefore reasonable to hypothesize that more than one endocrine system may be programmed by aberrant hormonal exposure

simultaneously with the reproductive system. This chapter will examine the effects of various windows of postnatal (testosterone proprionate) TP exposure upon rat ovarian physiology, and in addition investigate further the metabolic aspects which are associated with infertility in the rat PCOS model, previously defined in Chapter 4.

5.1.1. Programming windows

Previous investigations in neonatally androgenised rodents have not defined whether the reason for PCO-like formation and/or anovulation is due to a defect at the ovarian level, pituitary level, hypothalamic level or indeed is a combination of all three. However, it is known that a PCO-like ovary will result in the adult rat treated with TP between the day of birth (pnd 0) and pnd 5 (Barraclough 1961; Hoepfner and Ward 1988). To delineate which period of postnatal life in rats is the most sensitive to TP treatment and taking into account the ovulatory phenotype which results from TP exposure after pnd 15 (Chapter 4), the first 15 days of postnatal life were broken up into treatment windows corresponding to different windows of ovarian development. Firstly an early window of exposure, when primordial follicle formation completes between pnd one and six, secondly a late window of exposure after formation of primary follicles has begun between pnd seven and 15, finally a full window of exposure across both these time periods from pnd one to 15 (Kezele and Skinner 2003).

Historic studies in rodents examined LH pulsatility in relation to hypothalamic GnRH release using bilateral pre-optic area stimulation (Barr and Barraclough 1978). The same scientists had documented lordosis behaviour and reported that neonatally androgenised female rats were unreceptive to male mating behaviours (Barraclough and Gorski 1962). In addition, they identified the hypothalamic POA as an area modulated by neonatal TP (Barraclough 1961; Barraclough and Gorski 1961; Gorski and Barraclough 1962; Gorski and Barraclough 1962). The investigations described in this chapter extend these findings by Barraclough, Gorski and colleagues to examine in greater detail the pituitary-ovarian axis of the sterilised female rat as a model of PCOS. Although the first five days of postnatal life have already been

identified as a key developmental time period in rodent endocrinology (Barraclough 1961), no studies have examined the effects of various windows of neonatal TP upon multiple endocrine organ systems at a molecular level.

During the designated early window of rodent postnatal life, it is not just ovarian primordial follicles which complete their development. Sexually dimorphic areas of the neuroendocrine system are also modulated by the circulating hormonal milieu at this time (Morris, Jordan et al. 2004), discussed in Chapter 1, Section 2. Furthermore, in rodents a postnatal leptin surge occurs after pnd seven, the role of which remains unclear, but this increase in leptin is known to occur independently of body fat mass and may well be involved in neuroendocrine development (Ahima, Prabakaran et al. 1998). The HPAA has also shown sensitivity to neonatal steroid exposure, with one laboratory reporting that TP given to female rats at birth leads to hyperplasia and increased zona reticularis proliferation in the adult rat adrenal in addition to a lower 'male-like' corticosteroid response to stress (Seale, Wood et al. 2005; Seale, Wood et al. 2005; da Silva, Lopes-Costa et al. 2007; da Silva, Lopes-Costa et al. 2009). Additionally, programming of liver reductase activity in the rat occurs in response to circulating steroid hormones, leading to differential expression of these enzymes between the sexes (Gustafsson and Stenberg 1974; Gustafsson and Stenberg 1974). In a more recent study, neonatally androgenised female rats developed indicators of NAFLD (Demissie, Lazic et al. 2008), a pathology frequently associated with prolonged obesity in women with PCOS (Chapter 1, Sections 9 and 11; Fassnacht, Schlenz et al. 2003; Setji and Brown 2007).

Rat models of the metabolic syndrome have focussed upon early postnatal life as a key period of development, when both pancreatic islets and neurons are undergoing the final stages of development (Patel, Srinivasan et al. 2009). Such models range from fetal treatments with synthetic corticosteroids to investigate the effects of maternal stress (O'Regan, Kenyon et al. 2004; Seckl 2004; Drake, Livingstone et al. 2005), to high fat/high carbohydrate diets administered to mother and/or pups (Srinivasan, Dodds et al. 2008; Srinivasan, Mitrani et al. 2008). Indeed many studies

in both rodent and human have shown that abnormal calorific intake during both fetal and early postnatal development can lead to the development of metabolic syndrome-like features in the adult mammal (Patel, Srinivasan et al. 2009).

Chapter 4 illustrated that TP given throughout the first 15 days of rat postnatal life produces a PCOS-like phenotype in the adult which is both anovulatory and overweight. However, it is unclear at which time during these 15 days TP can affect rodent physiology and to what extent TP is able to alter reproductive development. Moreover, the metabolic characteristics associated with the weight gain, observed in these animals still lack full definition in female animals, as do the precise effects upon the pituitary. This chapter will focus upon the effects of different windows of TP administration within the first 15 days of postnatal life, from pnd 1, the day after birth, to pnd 15. This study will examine not only the pituitary-ovarian axis, but also animal growth and fat distribution alongside mesenteric adipose adipokine expression, in addition to the programming effect of neonatal TP upon hepatic factors involved in the regulation of metabolism.

5.2. Objectives

- To investigate which windows of TP exposure within the first 15 days of postnatal life produce a PCOS-like phenotype in the female rat, by splitting TP exposure into three windows: full, from pnd one to 15; early, from pnd one to six; late, from pnd one to 15.

- To further explore the effect that these windows of TP exposure have upon proportions of activated follicles within the ovaries of adult TP exposed animals and compare them to those of control oil treated animals.

- To ascertain the effects of these windows of TP exposure upon the pituitary through assessment of both plasma and pituitary gonadotrophin content in addition to mRNA expression levels of the three gonadotrophin subunits.

- To elucidate the effects of TP exposure upon endocrine organs such as liver, adrenal and fat depot weights.

- To investigate the effect of TP exposure upon the liver by analysing mRNA expression levels of proteins involved in insulin/glucose homeostasis and glucocorticoid metabolism, and relate these findings to the metabolic status of the animals.

- To further investigate the effect of TP exposure upon growth and adipogenesis by analysing mRNA expression levels of proteins involved in adipogenesis and lipolysis within mesenteric fat, and then relate these findings to the metabolic status of the animals.

5.3. Methods

5.3.1. Treatment windows

To elucidate which window of postnatal TP treatment would produce a PCOS-like phenotype, the first fifteen days of rat postnatal life were divided into three main treatment windows. For continuity between studies, the same dose of 20mg/kg TP was used in this study as was used in the original study described in Chapter 4. The first treatment window was for the full fifteen days, with injections on days one, four, seven, ten and 13. A litter of control animals were correspondingly injected with the same volume of oil at these time points. Secondly an early window treatment for the first six days of life exposed animals to TP through injections on pnd one and four. Finally, a late window of treatment, for pnd seven to 15, exposed animals to TP through injections on pnd seven, ten and 13. These full, early and late windows of treatment are schemed in Figure 5.1 and the colours used in this figure will correspond to the same treatment groups throughout this chapter.

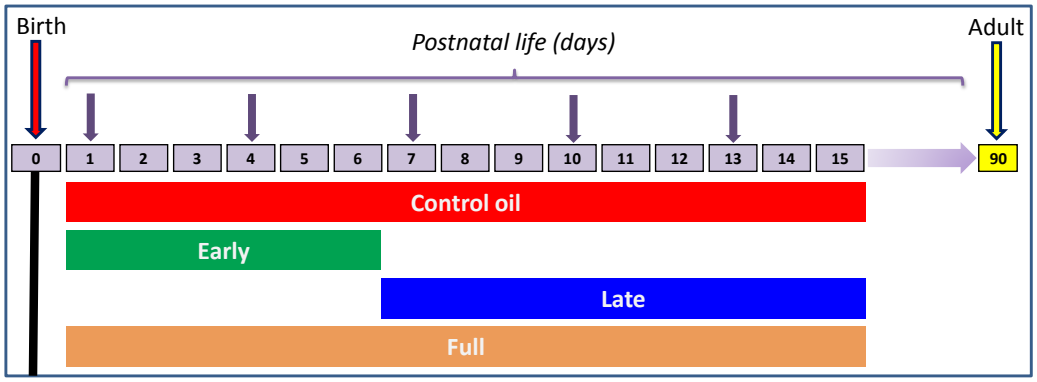

Figure 5.1: Schematic diagram to illustrate the windows of postnatal TP exposure in rats: Downward purple arrows indicate the days of TP injection at 20mg/kg postnatal life. The downward red and yellow arrows indicate the days of birth and sacrifice respectively. Treatment groups are designated control, early, late and full TP treatment windows hereafter.

One litter of animals was used for control full and early treatment groups and two smaller litters were amalgamated at weaning for the late window treatment group. Five dams underwent timed-mating overnight with stud males. After birth

(pnd 0) all litters were sacrificed down to an *n*=8 animals to prevent any differences in suckling litter size from masking/causing a metabolic phenotype in the adult female animals. At weaning (day 21) any male litter mates were sacrificed and as many females as possible kept in each treatment group (Table 5.1).

Table 5.1: The number of animals in each experimental control and TP treatment group: These groups correspond to those outlined in Figure 5.1. Birth litter numbers are divided by sex, animals were sacrificed to an *n=8* in each litter on the day of birth with males sacrificed at weaning (pnd21).

Group name	TP exposure	Number of pups at birth		Group *n* number
		Male	Female	(With animal designations)
Control	Oil: pnd 1 - 15	8	5	**5 (A-E)**
Early	pnd 1 – 6	4	6	**6 (A-F)**
Full	pnd 1 – 15	6	8	**8 (A-H)**
Late (litter 1)	pnd 7 – 15	8	4	**7 (A-G)**
Late (litter 2)	pnd 7 – 15	5	3	

TP=testosterone proprionate; pnd=postnatal day.

Animals were checked for a vaginal opening and underwent smears to assess both ovarian cyclicity and which cycle stage they were at. This allowed sacrifices to take place at proestrus when estrogen levels in the female rodent are at their highest (Chapter 1, Section 5). After weaning and vaginal opening formation, crude chow consumption was assessed in tandem with ovarian cyclicity for two weeks. Litters were split up into cages of two or three animals, depending on the group *n* number. Chow was weighed and topped up for each cage every two days and normalised for the number of animals in each cage, and the number of days. For example, the chow in a cage of three control animals weighed 96g less two days later and so the formula (96 X 0.5)/3 gave a result of 16g chow consumption per day for that period.

5.3.2. Necropsy

In this study additional tissues to those described in Chapter 4 were removed and weighed along with the ovary and uterus: Pituitary, liver, adrenal, retroperitoneal

adipose, and mesenteric adipose. The hypothalamic area, a portion of sub-cutaneous adipose and a portion of skeletal quadricep muscle were also removed but not weighed. Before sacrifice, animals underwent 8-13 days of smears to observe cyclicity and ensure that cycling animals were sacrificed at proestrus. Animals were sacrificed on or just after pnd 80 in week 10 of life, one week earlier than in the previous study (Chapter 4).

5.3.3. Immunohistochemistry

One ovary from each animal of each treatment group was fixed in Bouins and paraffin embedded. Standard IHC protocols were adhered to as previously described (Chapter 2 Section 4). Ovaries were embedded together to allow sectioning of multiple ovaries at the same time, and mounting on the same slide (Table 5.2).

Table 5.2: Ovaries from different treatment groups were embedded together and sectioned at the same time. The control ovary was always embedded at the base of the block and the others in an upwards clockwise direction to enable easy identification of which ovary came from which animal. Letters indicate animal designation (Table 5.2).

Block designation	Position in block (where 1=base of block)				
	1	2	3	4	5
090444	Control A	Early A	Full A	Late A	Early F
09-0445	Control B	Early B	Full B	Late B	Full F
09-0446	Control C	Early C	Full C	Late C	Late F
09-0447	Control D	Early D	Full D	Late D	Full G & H
09-0448	Control E	Early E	Full E	Late E	Late G

Serial sections were taken from all blocks and every 10th section mounted onto a clearly labelled slide for proliferating cell nuclear antigen (PCNA) DAB IHC (Chapter 2 Section 4). These sections were stained for PCNA in order to identify which follicles were activated. PCNA staining identifies proliferating GCs and so

only follicles from the primary to dominant stages of follicle development were considered for analysis. A follicle with 80% or more GCs surrounding it expressing PCNA was considered a primary; follicles with less than 80% of surrounding GCs expressing PCNA were designated transitory or primordial and for the purposes of these investigations were not counted (Chapter 2, Section 5). Secondary follicles were divided into groups of small (two to four layers of GCs) or large (five or more layers of GCs). Small antral follicles were classed as having an antrum which did not extend around most of the oocyte, and large antral follicles were classed as having an antrum which extended around most of the oocyte with clear cumulus and mural GC formation

5.3.4. RIA and ELISA

Blood samples taken at the time of sacrifice were processed as described in Chapter 2, Section 2. Samples were defrosted and analysed in duplicate for LH, FSH, E2 and the ovarian androgens A4 and T. Gonadotrophins were measured by ELISA and steroid hormones measured by RIA (Chapter 2, Sections 11 and 12). Pituitaries were additionally quartered and homogenised in 500µl PBS to assess pituitary gonadotrophin content. This was normalised to pituitary protein content using a Bradford assay.

5.3.5. Gene expression analysis

RNA was extracted from samples of pituitary, liver and mesenteric fat taken from each animal. The RNA was measured using a Nanodrop, reverse transcribed into cDNA, which as then used to quantify the levels of mRNA present for each gene of interest using quantitative PCR (Chapter 2, Sections 7 and 8). The genes analysed, along with the PCR chemistry used and the tissues in which they were investigated are listed in Tables 5.3 and 4.4. Gene expression was calculated by the ΔΔCT method when using SYBER green chemistry (Chapter 2, Section 9). When using universal primer-probe library PCR, a standard curve for each gene was included on

every plate and for each sample, expression of gene of interest was subtracted from a validated control gene for that tissue.

Table 5.3: List of genes analysed by quantitative PCR for each tissue with primer sequences and locations for Syber Green chemistry. Control genes are in bold.

Gene Target	Primers used (5' → 3' direction)		Start	Stop	Amplicon Length (bp)
Pituitary					
β-Actin	Fwd+	CCTGTGCTGCTCACCGAGGC	103	122	161
	Rev-	TGTGGGTGACCCCGTCTCCG	283	264	
αGSU	Fwd+	TTGCTTCTCCAGGGCATATC	274	293	178
	Rev-	GCGCTCAGAAGCTACGACTT	471	452	
FSHβ	Fwd+	GGACCCAGCTAGACCAAACA	177	196	152
	Rev-	TCTTACAGTGCAGTCGGTGC	348	329	
LHβ	Fwd+	ACACTGGCTATGTCCCAGG	47	65	179
	Rev-	GGCAGTACTCGAACCATGCTA	246	226	
Mesenteric Adipose					
β2-microglobuin	Fwd+	TCGCTCGGTGACCGTGATCTTT	13	34	96
	Rev-	AAGTTGGGCTTCCCATTCTCCGGT	132	109	
Adiponectin	Fwd+	ACTGCAACCGAAGGGCCAGG	79	98	97
	Rev-	TCTGCCATCACGGCCCGGTA	195	176	
Leptin	Fwd+	TCATTCCCGGGCTTCACCCCA	214	234	182
	Rev-	TCTGGCTTCTGCAGGCCACG	415	396	
Resistin	Fwd+	TGCTGTACCCTGCGGGTTGG	399	418	119
	Rev-	TTTCCTGCCCCCTGCGCTCT	537	518	
LPL	Fwd+	ACGCCTCCGGCTCAACCCTT	94	113	145
	Rev-	TCCGCGGAAGGCGGTCAAAC	258	239	
HSL	Fwd+	GTTTCCACCCACGGCGCTCA	3051	3070	173
	Rev-	TTCAGTCGCCGCGCGAACAT	3243	3224	
FAS	Fwd+	TCCTGGTGTGGTGCCTGCCT	1986	2005	159
	Rev-	GCAGCGTGGGGGCAATTCCT	2164	2145	
PPARγ	Fwd+	ACCCAGAGCATGGTGCCTTCG	118	138	77
	Rev-	CCGAAGTTGGTGGGCCAGAATGG	217	195	
Liver					
β-Actin	Fwd+	CCTGTGCTGCTCACCGAGGC	103	122	161
	Rev-	TGTGGGTGACCCCGTCTCCG	283	264	
PPARα	Fwd+	AGCGTGGTGCATTTGGGCGT	183	202	156
	Rev-	GCGGGCCACAGAGCACCAAT	358	339	
PEPCK	Fwd+	GCACCCCTGCCAGCCAATGT	1363	1382	171
	Rev-	ATGCTCTGCAGCAGCGGTGG	1553	1534	
GC receptor	Fwd+	TGGCCAAAGGCGATACCAGGC	1780	1800	127
	Rev-	TCAGGAGCAAAGCAGAGCAGGT	1928	1907	
5β-reductase	Fwd+	CGCCCAGCCCTGGAAAGGAC	332	351	144
	Rev-	GCCTCCCACGTGGCACACAG	495	476	

αGSU=common α gonadotrophin subunit; bp=base pairs; FAS=fatty acid synthase; FSHβ=follicle stimulating hormone subunit β; GAPDH=glyceraldehydes-3 phosphate dehydrogenase; GC=glucocorticoid; HSL=hormone sensitive lipase; LHβ=luteinising hormone subunit β; LPL=lipoprotein lipase; PEPCK=Phosphoenolpyruvate carboxykinase; PPAR=peroxisome proliferator activator protein; Fwd=forward primer; Rev=reverse primer.

Table 5.4: List of genes analysed by quantitative PCR for liver tissue using Roche light cycler chemistry. Primers and probes were sourced from Applied Biosystems.

Gene Target	ABI primer/probe code
Liver	
Cyclophillin A	**Rn00690933_m1**
PPARγ	Rn00440945_m1
5α-Reductase	Rn00567064_m1
11β-HSD Type 1	Rn01415034_m1

11β-HSD=11β-hydroxysteroid dehydrogenase; PPAR=peroxisome proliferator activator protein.

5.4. Results

5.4.1. Effects of postnatal windows of TP exposure upon the rat ovary

Full and early window TP treated animals did not develop vaginal openings, but in late window TP treated animals vaginal openings were present four days earlier than in the control group. Persistent estrus was observed in late window TP animals in contrast to the normal cycling controls. Furthermore, full, early and late TP treated animals all developed PCO- like ovaries (Figure 5.2).

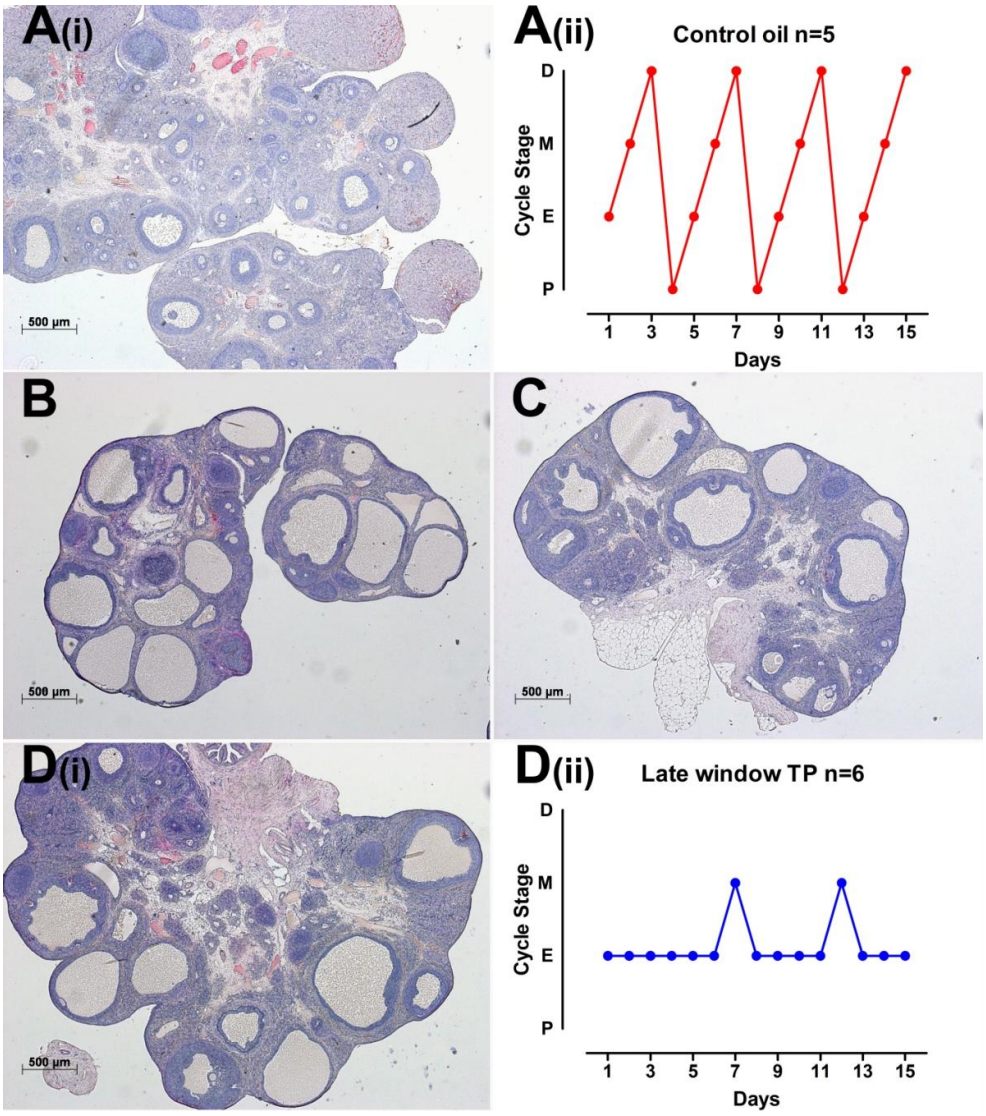

Figure 5.2: Ovarian morphologies (i) and estrus cyclicity (ii) shown where possible for (A) control (B) early (C) full and (D) late postnatal TP treated animals. Note, early and full postnatal testosterone treated animals developed pin hole vaginal openings and could not be smeared. Bar=500µm.

With greater *n* numbers than the previous study (Chapter 4), the changes in activated follicle proportions were next investigated. Each ovary was serial sectioned and every 10th section underwent DAB staining for PCNA (Figure 5.3). This enabled follicles from the primary to antral stages of folliculogenesis to be considered in the analysis.

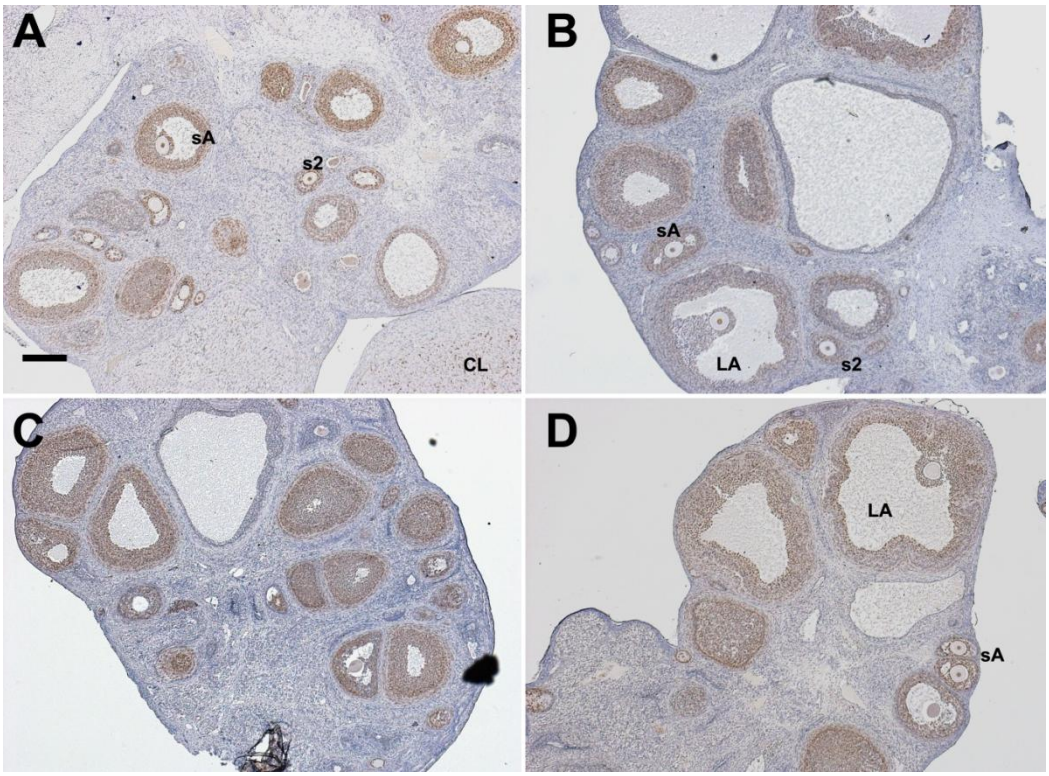

Figure 5.3: PCNA DAB staining in (A) control (B) early (C) full and (D) late postnatal TP treated animals: Follicle types are labelled; s2=small secondary; sA=small antral; LA=large antral follicle; CL=corpus luteum. Shown at X 4 magnification, bar=200µm.

A follicle exhibiting more than 80% PCNA positive GCs surrounding the oocyte was considered a primary; follicles with less than 80% PCNA positive GCs were not counted. This follicle population analysis is illustrated in Figure 5.4.

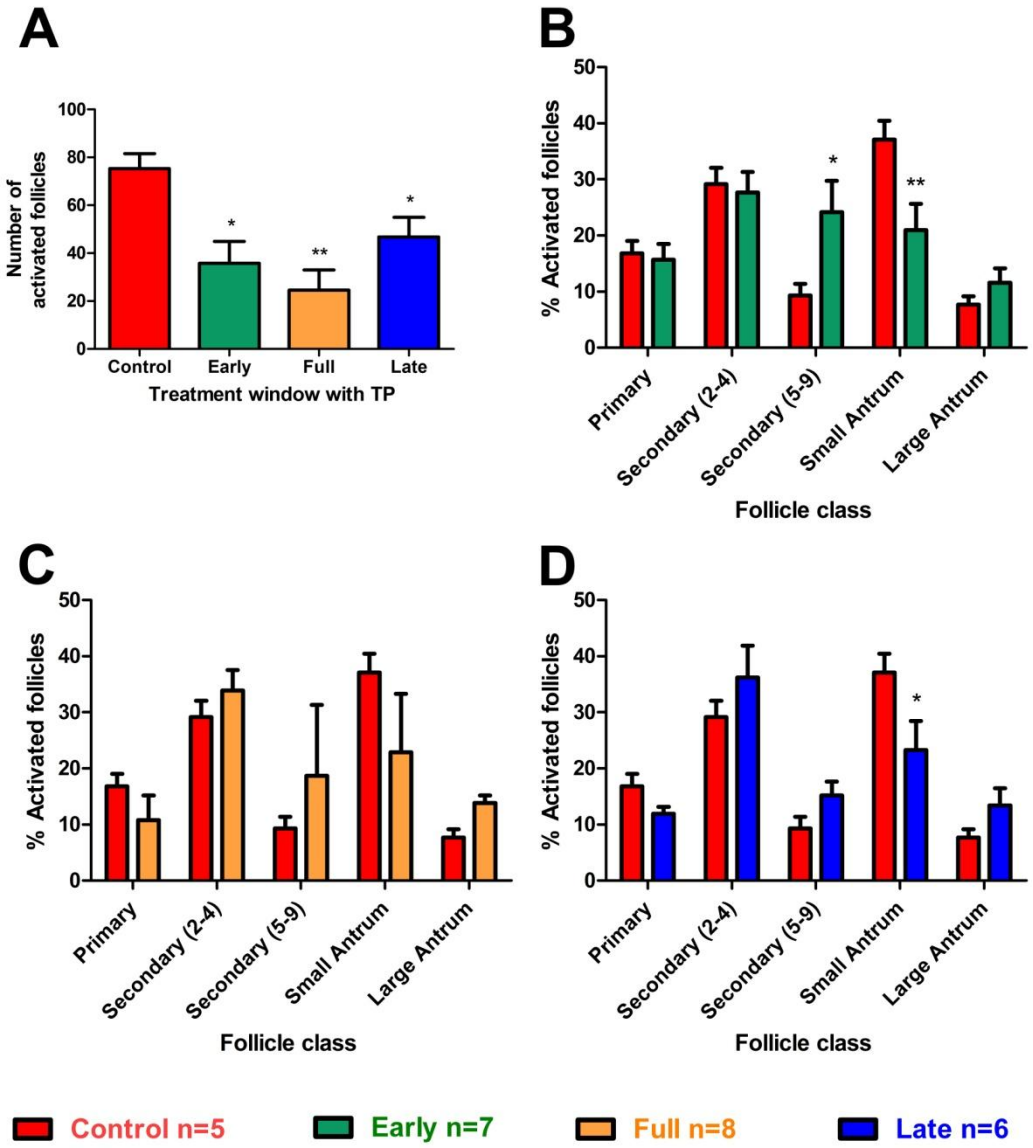

Figure 5.4: Follicle population analyses across treatment window groups: (A) Total number of activated follicles alongside the percentage proportions of activated (growing non-primordial) follicles in control (n=5) versus (B) early window (n=7) (C) full window (n=8) and (D) late window (n=6) TP treated animals. Values are expressed as the mean ±SEM with (A) analysed by student's unpaired t-test and (B-D) analysed by two-way ANOVA with Bonferroni post-hoc test (* P≤0.05; **P≤0.01).

Animals treated with TP in the early, full and late windows had significantly fewer activated follicles when compared to control ovarian follicle counts (P≤0.05 P≤0.01 and P≤0.05 respectively). In contrast, early window TP treated animals had ovaries with a significantly higher proportion of large secondary follicles (P≤0.05) and a significantly lower proportion of small antral follicles (P≤0.01) when

compared to controls. Similarly ovaries from the late window TP group had a significantly lower proportion of small antral follicles (P≤0.05); however none of these results were recapitulated in ovaries from full window TP treated animals.

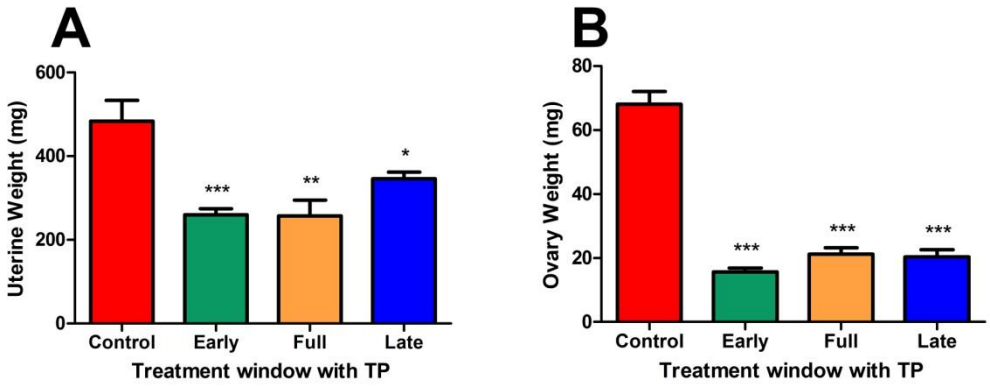

Figure 5.5: The effect of various windows of TP treatment upon (A) ovary and (B) uterine weight: Shown for control (n=5) versus early (n=6), full (n=8) and late (n=7) window TP treatment groups. Values are expressed as the mean ±SEM values and were analysed by student's unpaired t-test (* P≤0.05; **P≤0.01; *** P≤0.001).

Uterine weights were significantly reduced in early, full and late TP treatment groups (P≤0.001, P≤0.01 and P≤0.05 respectively), as were ovarian weights (P≤0.001) again due to the absence of CL (Figure 5.5). Subsequent analysis of circulating ovarian feedback hormones (Figure 5.6) showed inhibin B feedback to be reduced in all TP treated animals (all at least P≤0.01). However, the interpretation of E2 levels is slightly more complex, as 2 of 5 control animals exhibited E2 levels below those seen at proestrus. Despite smearing the control animals in order to sacrifice at proestrus, it is possible they were sacrificed too late to catch the high levels of E2 and were instead sacrificed at the beginning of estrus. E2 levels across TP treatment window groups were significantly lower than proestrus controls (P≤0.01; Figure 5.6).

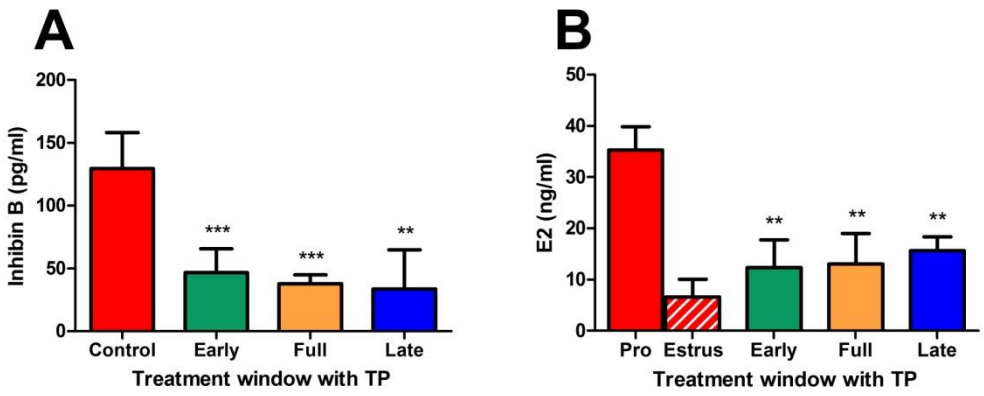

Figure 5.6: The effect of various windows of TP treatment upon ovarian feedback hormones: (A) Inhibin B (B) Estradiol (E2) shown for control (n=5) versus early (n=6), full (n=8) and late (n=7) window TP treatment groups. Control E2 results are broken down into red proestrus (control n=3) and striped estrus (control n=2) respectively. Values are expressed as the mean ±SEM values and were analysed by student's unpaired t-test against control proestrus values only (** P≤0.01; *** P≤0.001).

No differences in circulating ovarian androgens T or A4 were found in either the early, full or late TP treatment groups when compared to controls (Figure 5.7).

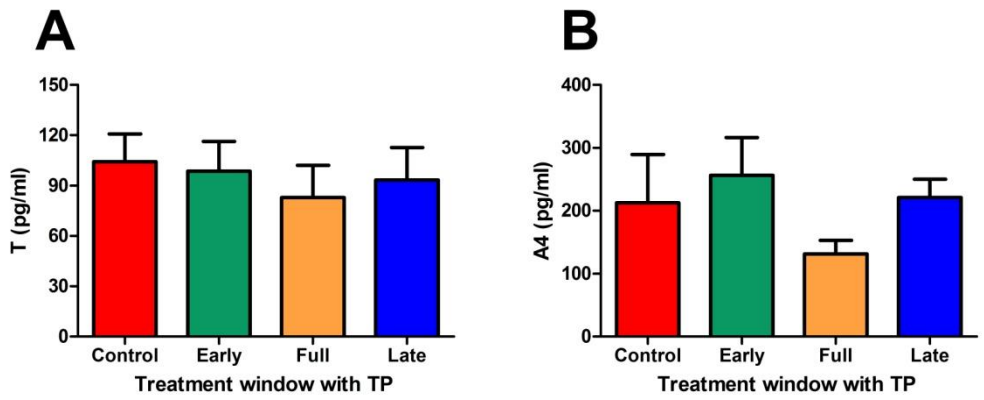

Figure 5.7: The effect of various windows of TP treatment upon (A) testosterone (T) and (B) androstenedione (A4): Shown for control (n=5) versus early (n=6), full (n=8) and late (n=7) window TP treatment groups. Values are expressed as the mean ±SEM values and were analysed by student's unpaired t-test.

5.4.2. Effects of postnatal windows of TP exposure upon the rat pituitary

To assess whether the reduction in inhibin B/E2 feedback released from the ovary affected pituitary gonadotrophin secretion, rat pituitary weight and plasma and pituitary gonadotrophin contents were investigated. No differences in pituitary weight were observed across treatment groups although a larger range of pituitary weights were observed in the early window TP treatment group when compared with the other groups (Figure 5.8A).

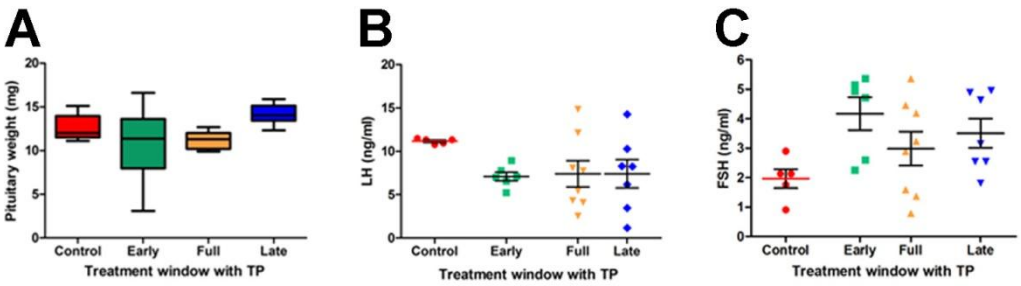

Figure 5.8: Effects of various windows of TP exposure upon the female rat pituitary weight and plasma gonadotrophin levels: (A) Pituitary weight (B) Plasma LH (C) Plasma FSH levels, for control (n=5) early (n=6), full (n=8) and late (n=7) window TP treatment groups. Values are expressed as (A) median range box plot and (B-C) a whisker dot plot and were analysed by student's unpaired t-test (* P≤0.05; ** P≤0.01; *** P≤0.001).

Plasma gonadotrophin analysis yielded complex results; roughly half of animals across TP treatment groups had significantly raised FSH levels when compared to controls (P≤0.01) (Figure 5.8B), while others had circulating FSH levels comparable to controls. Animals from the early window TP treatment group had reduced levels of LH compared to controls (P≤0.001), while of the animals in the full window TP treatment group, two had significantly raised LH (P≤0.05) and six had reduced LH (P≤0.001). In the late window TP treatment group, five animals showed reduced LH (P≤0.001) and three animals had levels of LH comparable to controls. The differences in gonadotrophin levels are best shown as a scatter diagram (Figure 5.8D), where unlike the gonadotrophin levels of TP treated animals, control animals

occupy a distinct area of the plot with relatively high LH and low FSH, typical of animals at proestrus.

To assess the effects of postnatal TP upon pituitary gonadotrophin storage, homogenised quartered pituitaries underwent gonadotrophin analysis at both the protein (Figure 5.9) and mRNA level (Figure 5.10). No significant differences in pituitary FSH or LH content were found in the early and full TP treatment groups when compared to controls. Animals in the late TP treatment group expressed a range of LH protein contents with three animals showing stored LH levels significantly higher than those of control animals ($P \leq 0.001$).

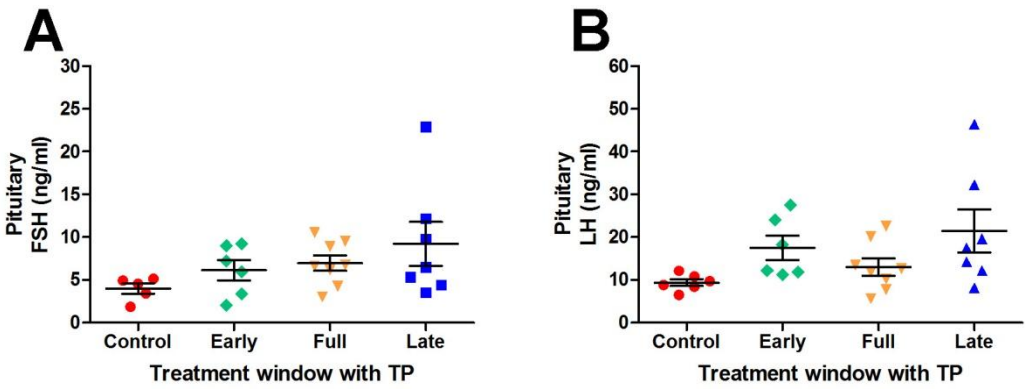

Figure 5.9: Pituitary gonadotrophin protein content across treatment groups: (A) FSH (B) LH levels for control (n=5), early (n=6), full (n=8) and late (n=7) window TP treatment groups with the late window group broken up into high and low outliers (*n* numbers in white boxes). Values expressed are actual with the mean ±SEM and analysed by student's unpaired t-test (*** P≤0.001).

The levels of pituitary mRNA expression for the common αGSU subunit were not significantly different between TP treated and control animals (Figure 5.10), whilst early and full postnatal TP significantly increased FSHβ subunit mRNA with no effects upon LHβ subunit mRNA. There was a trend in pituitaries from the late postnatal TP treatment group for increased transcription of both FSHβ and LHβ subunits.

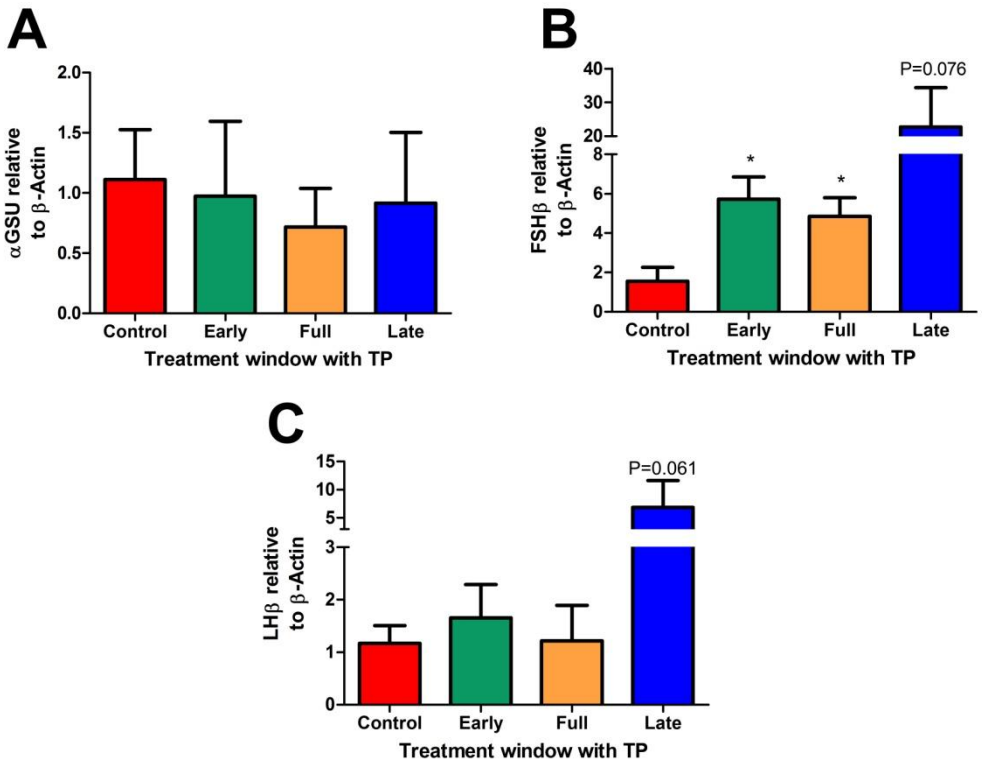

Figure 5.10: Expression of pituitary gland (A) αGSU (B) LHβ and (C) FSHβ gonadotrophin subunits: Shown for control (n=5) versus early (n=6), full (n=8) and late (n=7) window TP treatment groups. Values are expressed as the mean ±SEM and analysed by student's unpaired t-test (* P≤0.05).

5.4.3. Effects of postnatal testosterone upon growth and fat deposition

By pnd 33 there was a significant increase in the body weight of animals from the early (P≤0.001), full (P≤0.01) and late (P≤0.001) postnatal TP treatment groups when compared to control animals (Figure 5.11). These differences in body weight remained constant until animals were sacrificed.

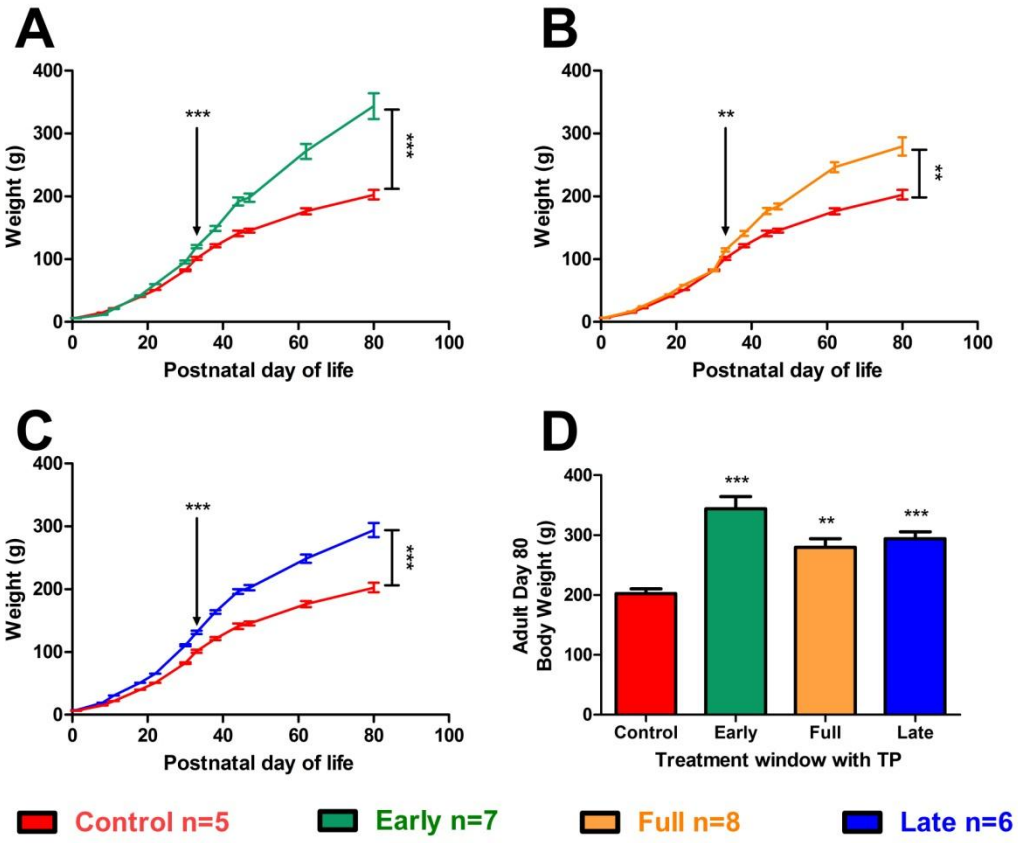

Figure 5.11: Effects of postnatal testosterone upon pup growth for control versus (A) early (n=7), (B) full (n=8) and (C) late (n=6) window TP treated animals, with (D) adult weight at pnd 80. Note, each group of animals significantly gains weight after weaning around pnd 33 (arrows). Values are expressed as the mean ±SEM, analysed by student's unpaired t-test (** P≤0.01; *** P≤0.001).

At pnd 33 the food consumption of each litter was measured over two-day intervals for two weeks. Chow consumption fluctuated in the same way for each litter during these weeks of postnatal life and no differences in the daily chow consumed nor the average chow consumption for each treatment group were found (Figure 5.12).

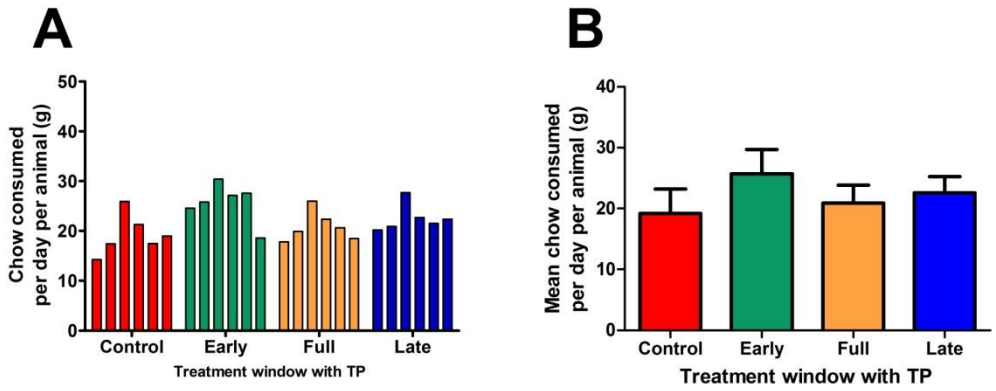

Figure 5.12: Effects of postnatal TP on animal chow consumption: (A) Absolute values by day analysed by two way ANOVA with Bonferroni post-hoc test (B) Mean daily chow consumption ±SEM, analysed by student's unpaired t-test. Shown for control oil (n=5) early (n=7), full (n=8) and late (n=6) window TP treated animals during early adulthood. Chow was weighed every two days for two weeks. Differences in chow weight at each interval were divided by the number of animals per cage.

To assess for the effects of postnatal TP upon fat deposition, mesenteric and retroperitoneal fat pads were dissected out and weighed at sacrifice. The mesenteric and retroperitoneal adipose depots were both significantly heavier in early window ($P \leq 0.001$), full window ($P \leq 0.01$ and $P \leq 0.05$ respectively) and late window ($P \leq 0.001$) TP exposed animals (Figure 5.13, A&C). These differences could not be normalised to body weight at the time of sacrifice (Figure 5.13, B&D).

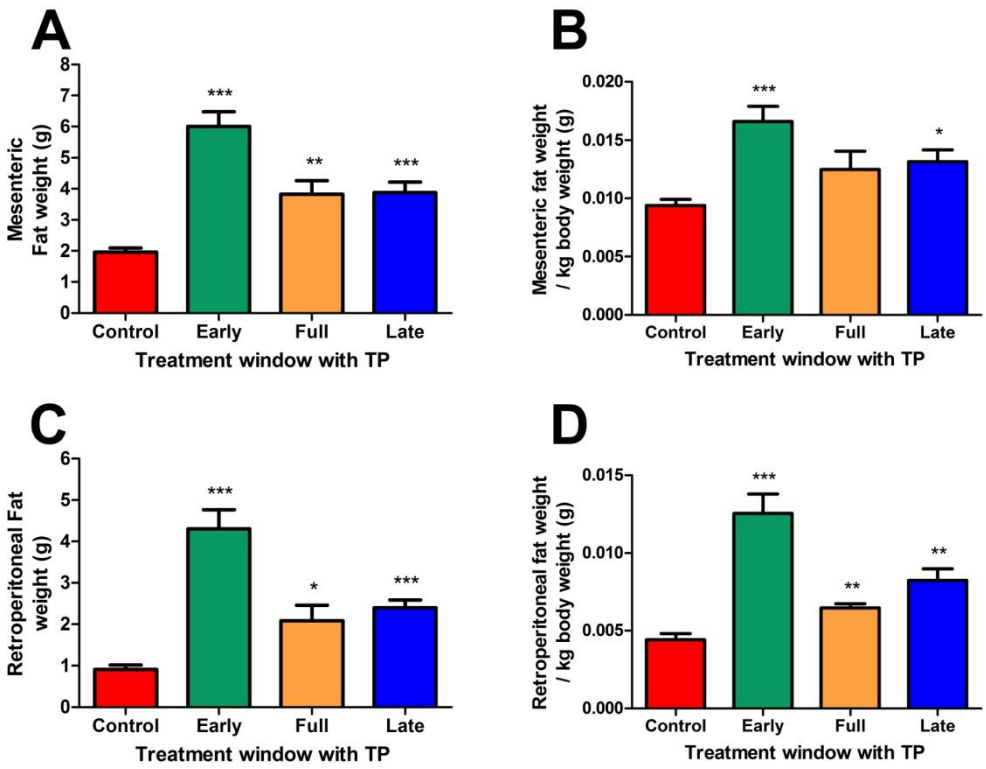

Figure 5.13: Fat deposition in adult female rats across treatment window groups: (A) Mesenteric fat weight (B) adjusted to body weight and (C) Retroperitoneal fat weight (D) adjusted to body weight for control oil (n=5), early (n=7), full (n=8) and late (n=6) window TP treated animals. Values are expressed as the mean ±SEM, analysed by student's unpaired t-test (* $P \leq 0.05$; ** $P \leq 0.01$; *** $P \leq 0.001$).

A sample of mesenteric adipose was underwent mRNA expression analysis for various adipogenic and lipolytic markers (Figure 5.14 and Figure 5.15 respectively). Early postnatal TP had no effect upon leptin or adiponectin expression and led to a significant decrease ($P \leq 0.05$) in resistin expression. Likewise full window postnatal TP had no effect upon expression of these three adipokines. Late

window TP significantly increased mesenteric adipose leptin expression (P≤0.05) and showed a non significant trend for higher adiponectin and resistin levels (Figure 5.14).

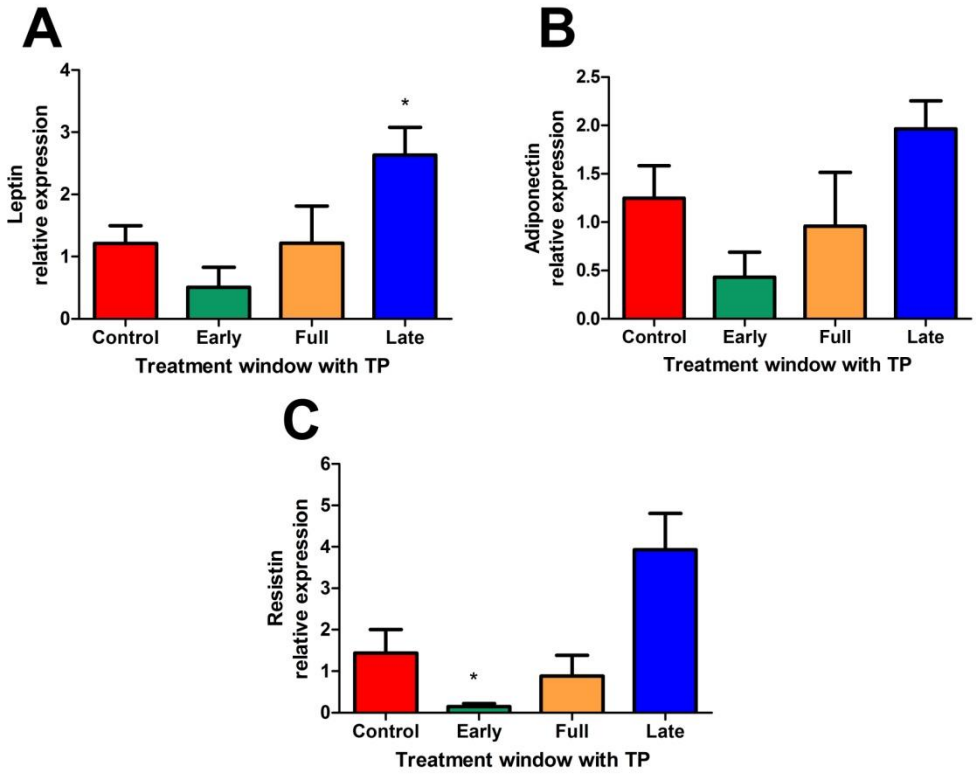

Figure 5.14: Expression of mesenteric fat adipokines (A) Leptin, (B) Adiponectin, and (C) Resistin: Shown for control oil (n=5), early (n=7), full (n=8) and late (n=6) window TP treated animals. Values are expressed as the mean ±SEM, analysed by student's unpaired t-test (* P≤0.05).

Examination of genes involved in lipolysis showed late window TP to have no effect upon expression of lipoprotein lipase (LPL), hormone sensitive lipase (HSL), fatty acid synthase (FAS) or peroxisome proliferator activator protein-γ (PPARγ). Conversely early window TP exposure significantly reduced the expression of these molecules ($P \leq 0.05$), with the exception of LPL, for which only a trend reduction was seen. Full window TP led to a significant reduction in mesenteric FAS expression ($P \leq 0.001$), with only a trend reduction in LPL and PPARγ expression. For this treatment group HSL expression was comparable to that of control mesenteric adipose.

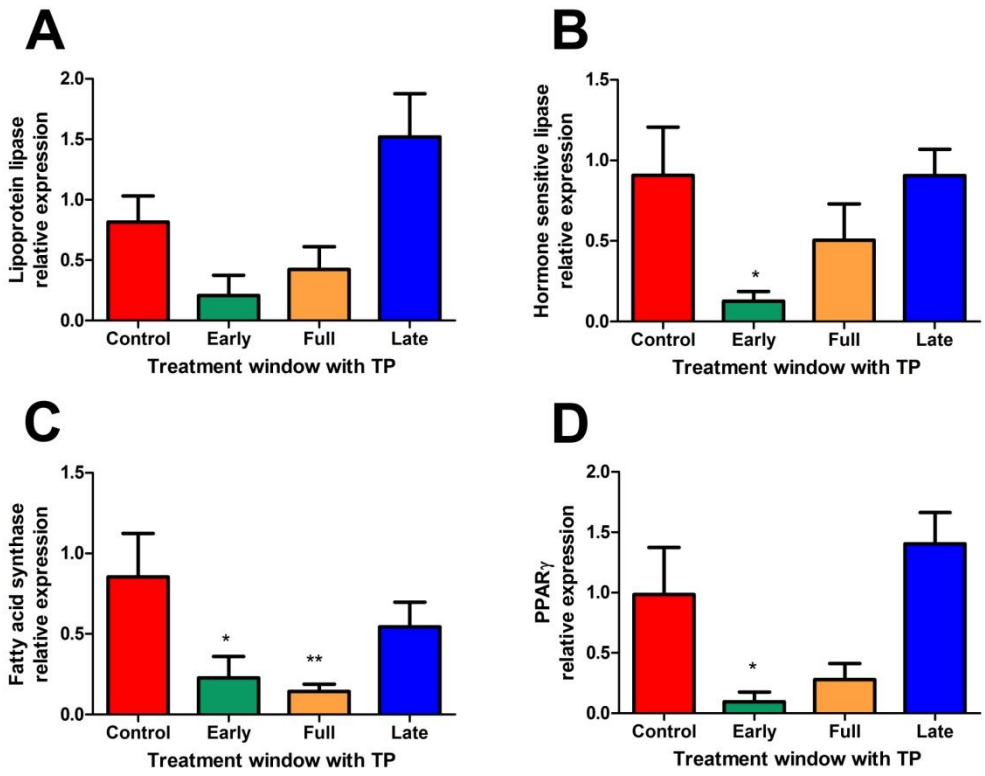

Figure 5.15: Expression of mesenteric fat lipolytic factors (A) LPL, (B) HSL, (C) FAS, and (D) PPARγ: Shown for control oil (n=5), early (n=7), full (n=8) and late (n=6) window TP treated animals. Values are expressed as the mean ±SEM, analysed by student's unpaired t-test (* P≤0.05; ** P≤0.01).

5.4.4. Effects of postnatal testosterone upon other endocrine organs

Only early window postnatal TP significantly increased adrenal weight (P≤0.01, Figure 5.16), while early (P≤0.001), full and late (P≤0.01) window TP treatment led to significant increases in liver weight which normalised to body weight (Figure 5.17).

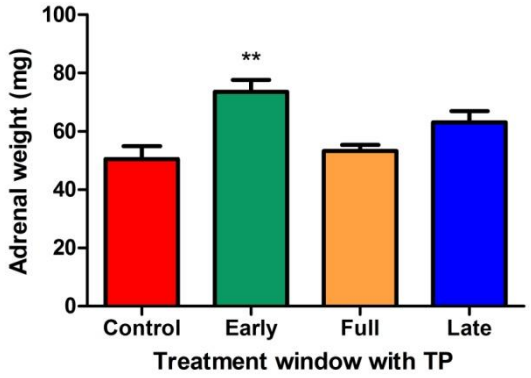

Figure 5.16: The effect of various windows of TP treatment upon adrenal weight: Shown for control (n=5) versus early (n=6), full (n=8) and late (n=7) window TP treatment groups. Values are expressed as the mean ±SEM values and were analysed by student's unpaired t-test (* P≤0.05; ** P≤0.01; *** P≤0.001)

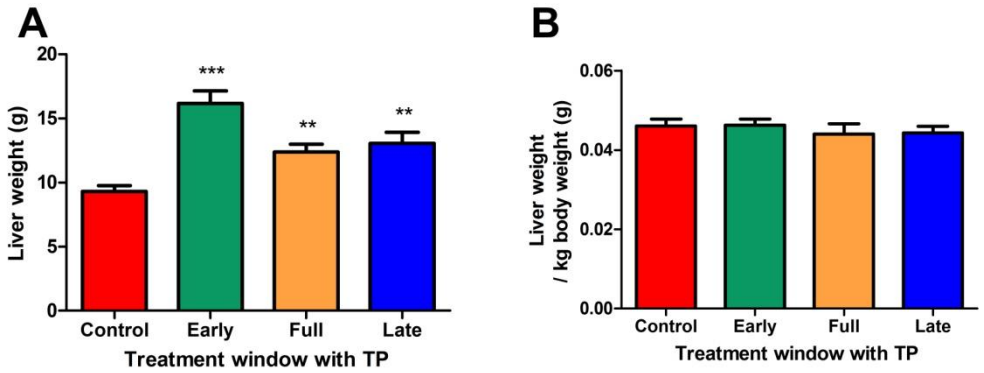

Figure 5.17: The effect of various windows of TP treatment upon liver weight: (A) Gross liver weight (B) liver weight normalised to body weight for control (n=5) versus early (n=6), full (n=8) and late (n=7) window TP treatment groups. Values are expressed as the mean ±SEM values and were analysed by student's unpaired t-test (**P≤0.01; ***P≤0.001)

Furthermore, livers from all TP treatment groups appeared fatty upon dissection and analysis of gene expression for molecules involved in insulin and glucose homeostasis (Figure 5.18), in addition to genes involved in glucocorticoid metabolism (Figure 5.19), was subsequently undertaken. Relative expression of liver PPARα was significantly increased in early window TP exposed animals (P≤0.05), with a non significant trend increase in expression for full window TP exposed animals. Liver PPARγ and PEPCK expression were not affected by postnatal TP exposure, although there appeared a trend increase in PEPCK expression within livers from the late window TP treatment group.

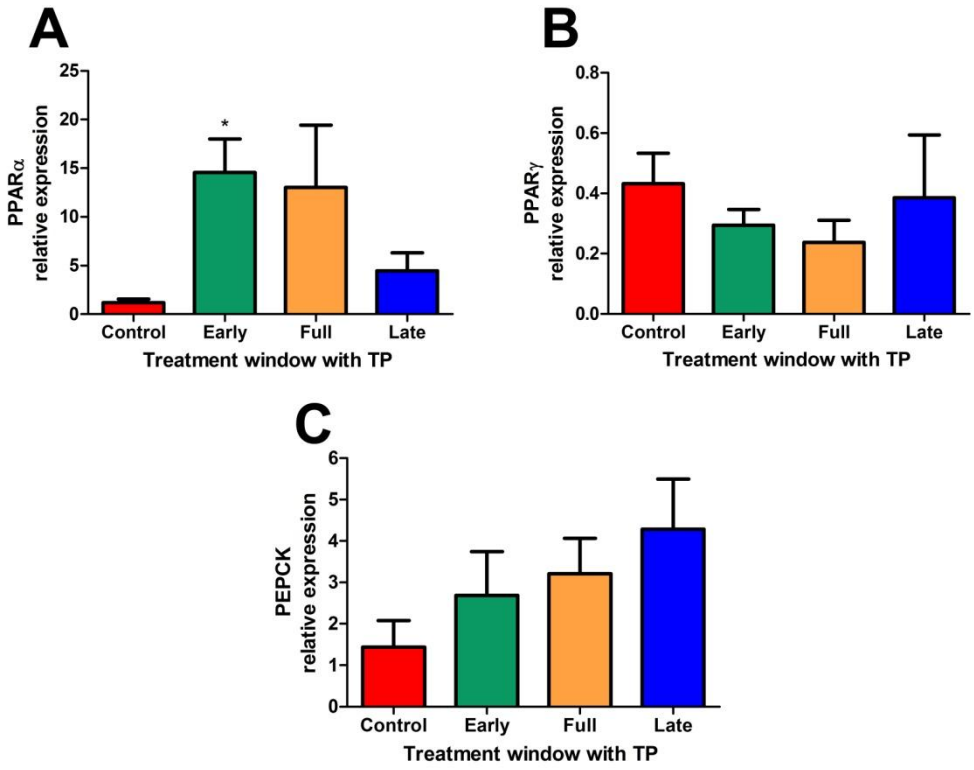

Figure 5.18: Expression of liver (A) PPARα (B) PPARγ and (C) PEPCK genes involved in insulin/glucose homeostasis: Shown for Control oil (n=5), early (n=7), full (n=8) and late (n=6) window TP treated animals. Values are expressed as the mean ±SEM, analysed by student's unpaired t-test (* P≤0.05).

Liver expression of 11β-hydroxysteroid dehydrogenase type 1 (11βHSD1), 5β-reductase and glucocorticoid receptor (GR) was significantly increased (P≤0.05) in all groups of TP exposed animals (with the exception of the late window TP group for GR expression, which showed only a non significant trend increase compared to controls). Expression of 5α-reductase was significantly reduced in the livers of both early and full window TP treated animals (P≤0.05), while 5α-reductase expression in the livers of late window TP treated animals was comparable to the expression in control animal liver.

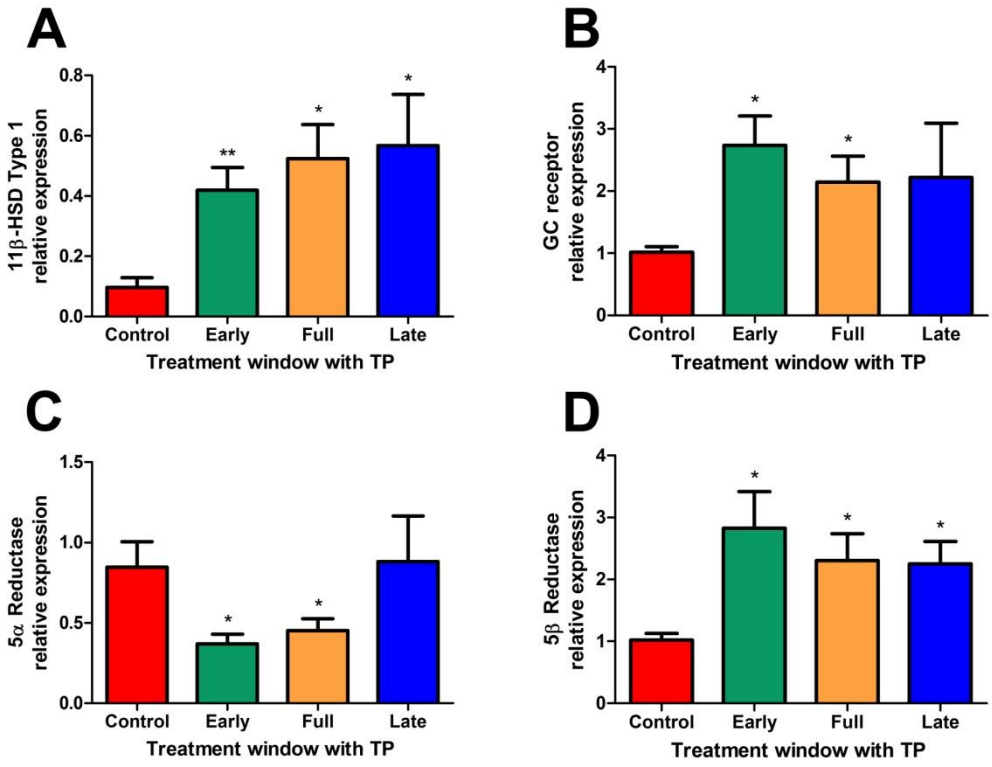

Figure 5.19: Expression of liver (A) 11β-HSD-1, (B) Glucocorticoid Receptor, (C) 5α-Reductase (Type 1), and (D) 5β-Reductase genes involved in glucocorticoid metabolism: Shown for control oil (n=5), early (n=7), full (n=8) and late (n=6) window TP treated animals. Values are expressed as the mean ±SEM, analysed by student's unpaired t-test (* P≤0.05; ** P≤0.01).

5.5. Discussion

It is known from these studies and others that exposure to TP during neonatal life in the rat leads to an anovulatory ovarian phenotype in the adult animal (Chapter 4). With the exception of experiments by Barraclough, Gorski and colleagues, few investigations have focused upon which key windows of postnatal life produce alterations in the various endocrine axes of the rodent; these studies demonstrated a hormone sensitive period of development in the rat occurring between birth and day 10 of life (Barraclough and Leathem 1954; Barraclough 1955; Barraclough 1961).

Specific examination of neonatal TP and the programming effects it exerts upon the rodent ovary, pituitary, adrenal, liver and adipose tissue has therefore been examined in this chapter.

5.5.1. Windows of neonatal TP exposure, the ovary and hormones

All windows of TP treatment in this study produced adult animals which had PCO-like ovaries, within which there was a reduction in activated follicle numbers. This may be due to the increases in secondary and small antral follicle proportions within early and late TP treatment groups; as with more follicles activated, so more may undergo atresia, although individual follicle proliferation and atresia were not measured in this study.

As yet no other rodent models of PCOS have been examined at the level of follicle activation. Studies on ovaries from androgenised non-human primates and anovulatory PCOS women show a higher number of preantral and small antral follicles in these ovaries when compared to controls (Hughesdon 1982; Vendola, Zhou et al. 1998; Webber, Stubbs et al. 2003; Maciel, Baracat et al. 2004). To some extent these findings corroborate with the increased preantral and small antral follicle proportions described in the current study. However, although these types of follicles were more prevalent proportionately, they were fewer in number. Normal levels of circulating ovarian androgens T and A4 were also found in the current study,

whereas high levels have been found in some PCOS women and androgenised primates. An increase in circulating androgens could act to increase follicular recruitment, and would therefore account for the increased numbers of transitory and small preantral follicles observed in human and adult androgenised primate investigations (Vendola, Zhou et al. 1998; Jonard and Dewailly 2004; Maciel, Baracat et al. 2004). A primate model of PCOS in which animals received TP *in utero* showed a reduction in activated follicle numbers and an increase follicle proportions at the secondary and small antral level (Abbott 2010). The results of the activated follicle analysis in the rat could therefore be a direct consequence of androgen exposure during ovarian development, rather than a specific feature of PCOS itself. These changes in follicle populations could potentially result through disrupted germ cell nest breakdown/primary follicle formation by early postnatal TP exposure, though whether this is an effect mediated by androgens or estrogens through aromatisation remains to be seen (Pepling and Spradling 2001; Chen, Jefferson et al. 2007; Chen, Breen et al. 2009).

No differences in circulating ovarian androgen levels (T and A4) were found between control and TP treated animals, and other studies contribute conflicting evidence regarding the neonatally androgenised rat as a PCOS model; with one study reporting a decrease in circulating T levels by pnd 100 after injection with 1mg TP at birth (Alexanderson, Eriksson et al. 2007), while another describes an increase in circulating T levels at pnd 63 after androgenisation between pnd one and five (vom Saal and Bronson 1978; vom Saal and Bronson 1980). Indeed normal circulating levels of ovarian androgens, in particular testosterone are found in ovulatory women diagnosed with PCOS, but are less frequently documented in anovulatory PCOS patients (Abbott, Tarantal et al. 2009; Guastella, Longo et al. 2010).

Reduced E2 and inhibin B production by the ovary was also observed, which indicates insufficient hormonal feedback to induce FSH release in preparation for ovulation. This data was supported by a reduction in ovarian weights (due to absence

of CL) in addition to a reduction in uterine weights (a physiological marker of estrogen levels) across treatment groups.

5.5.2. Windows of neonatal TP exposure and the pituitary

Pituitary weight was comparable to controls across treatment window groups, although early TP treatment in contrast to that of full and late window treatment resulted in a greater range of pituitary weights. Despite reduced inhibin B and E2 feedback to the pituitary gland in all TP treated animals, only some animals showed the significantly raised levels of FSH expected to result from this reduction in negative feedback. Other animals had FSH levels comparable to proestrus control animals. The plasma gonadotrophin profiles of each animal from each TP treatment group were highly variable in contrast to those of the control group. A high variability in gonadotrophin secretion patterns has also been found in women with PCOS, with LH pulse frequency increasing across all types of the syndrome, but LH pulse amplitude increasing in obese PCOS patients only (Arroyo, Laughlin et al. 1997). Since neither LH pulse frequency, nor amplitude, was assessed in these experiments, the effect of neonatal TP upon LH pulsatility cannot currently be determined.

In the late window TP treatment group a trend for higher pituitary FSHβ and LHβ expression, when taken together with the raised level of stored pituitary LH protein in some animals, indicates that the pituitary glands of the late window TP treatment group may have had some physiological response to the reduced circulating inhibin B and E2 – by synthesising and storing more FSH. This is further supported by the reduction in circulating LH levels and concomitant increase in gonadotrophin storage and transcription within the late window TP group. A recent pituitary specific insulin receptor knockout mouse model (PitIRKO) has shown that feeding a HFD to control animals led to normal serum LH with an increase in αGSU and LHβ pituitary expression. Conversely PitIRKO animals on a HFD had low serum LH and no transcriptional response to the diet induced obesity (Brothers, Wu

et al. 2010). This evidence supports a potential role for insulin in the pathogenesis of PCOS-like features in the rodent, especially since animals treated with TP during late window postnatal life gained significant weight.

Animals in early and full window TP treatment groups showed no differences in gonadotrophin storage when compared to controls, despite increases in FSH secretion and decreases in LH secretion in some animals. This paucity of pituitary response to low levels of inhibin B and E2 could indicate that early neonatal TP is able to reprogram the hypothalamic-pituitary axis and alter the pituitary response to steroid positive and negative feedback. Indeed, in male rats prenatal and postnatal androgen surges program the neuroendocrine axis, including the feedback loops which regulate gonadotrophin secretion in response to testicular androgens (Welsh, MacLeod et al. 2010; Scott, Hutchison et al. 2008). Since androgen levels in TP treated animals were comparable to those of control animals, this could explain why no apparent response was seen in gonadotrophin transcription, storage or secretion from the pituitary.

It is worth noting that not all animals exhibited the patterns described. Research in sheep has shown that androgens can disrupt the negative feedback sensitivity of the pituitary through alterations in GnRH receptor and gonadotrophin subunit expression (Manikkam, Thompson et al. 2008; Veiga-Lopez, Astapova et al. 2009). Future experiments could therefore assess the hypothalamic-pituitary gonadotrophin response to sex steroids T and E2. In addition to examining the expression of hypothalamic-pituitary genes involved in the regulation of gonadotrophin secretion. An increase in gonadotrophin secretion could be observed in response to exogenous T, if indeed the neuroendocrine axis had been reprogrammed to a male-like phenotype.

5.5.3. Windows of neonatal TP exposure and other endocrine organs

Early neonatal TP has previously been shown to masculinise the HPAA (Seale, Wood et al. 2005), which could account for the heavier adrenals documented in animals from the early window TP treatment group, a consequence of neonatal TP also observed in a separate study (Barraclough 1961). Moreover developmental studies in male rats show that both estrogen and androgen action in the neonate are required for suitable adrenal function in the adult animal (Seale, Wood et al. 2005). Programming of the neonatal adrenal may occur at the level of the zona reticularis of the adrenal cortex, although no concurrent investigations into the hypothalamic-pituitary component of the HPAA or hormonal milieu have been performed. Morphometric analyses of adult female rat adrenals show that a thicker, more proliferative zona reticularis compartment results from TP exposure shortly after birth (da Silva, Lopes-Costa et al. 2007; da Silva, Lopes-Costa et al. 2009).

Certain clinical studies have shown that adrenal steroid production inferred by ACTH challenge in women with PCOS is slightly but significantly higher when compared to that of control women (Puurunen, Piltonen et al. 2009). Whether this is the result of increased adrenal sensitivity, a reduction in feedback sensitivity, or an increase in zona reticularis activity, remains to be elucidated, although the non human primate model of PCOS has shown some evidence in support of the latter (Zhou, Bird et al. 2005). It is worth noting that reduced adrenal activity in rats is secondary to a lack of circulating E2 (Seale, Wood et al. 2005), as was also observed across treatment window groups in this study, thus the effects of neonatal TP upon the rodent HPAA, particularly the rodent stress response, warrant further investigation.

Fatty livers were observed in animals treated with TP and liver weight was greater in all treatment window groups, although these values normalised to body weight, implying that hepatic mass may have grown larger in response to the metabolic requirements of the heavier animals. Characteristics of NAFLD, such as the fatty livers observed in this study at the time of sacrifice, can also be caused by a

HFD in rodents. These features result through neonatal androgen exposure, but are not compounded by the presence of a HFD (Demissie, Lazic et al. 2008). This suggests that NAFLD may be a consequence of increased adiposity rather than the result of hepatic programming by postnatal steroidal milieu, which potentially explains why NAFLD is associated with prolonged obesity in PCOS sufferers (Fassnacht, Schlenz et al. 2003; Setji and Brown 2007).

From the patterns in hepatic gene expression observed, it is reasonable to deduce that early window TP exposure may act to program an increase in glucocorticoid turnover, through the increases in hepatic 11βHSD-1 and 5β-reductase expression observed. It should also be noted hepatic expression of these genes is heightened in other rodent models of obesity (Drake, Livingstone et al. 2005). Investigations into the effects of diet upon enzymes involved in glucocorticoid turnover have shown that male rats up-regulate both 11βHSD-1 and 5β-reductase expression in response to an acute high fat diet, although this response subsides after long term HFD feeding (Morton, Ramage et al. 2004; Drake, Livingstone et al. 2005).Taken together with the results described in this study, these investigations support the hypothesis that increased glucocorticoid turnover (whether epigenetically programmed or raised in response to nutrition/diet) could play a role in the pathogenesis of female obesity, particularly since the animals described in the current study gained weight without consuming greater amounts of food. Investigation of steroid urinary metabolites in PCOS women has documented an increase in glucocorticoid clearance (Chin, Shackleton et al. 2000). However, a more recent study has also shown cortisol production to be elevated in obese women, independent of PCOS diagnosis (Roelfsema, Kok et al. 2010). Collectively these studies indicate that further investigations into the neonatal programming of obesity and glucocorticoid metabolism by androgens should include the measurement of corticosteroid hormones and 11βHSD enzyme expression in mesenteric adipose.

The GR is known to undergo epigenetic modification and expression has been shown to increase in the presence of higher levels of corticosteroids, as

occurred in livers from animals that received late window TP treatment (Lillycrop, Slater-Jefferies et al. 2007). However, this was not the case in the early or full window TP treatment groups and therefore only neonatal TP administered before pnd six might act to reprogram liver GR expression. Furthermore, early window TP led to an apparent decrease in hepatic 5α-reductase expression in the adult. This is at odds with studies in human females which show 5α-reductase as well as 11β-HSD1 expression to both be elevated in insulin resistant women (Tomlinson, Finney et al. 2008). Moreover, neonatal TP has been shown to masculinise hepatic function in female rats and reduce 5α-reductase activity in female animals (Pak, Tsim et al. 1985). In PCOS although 5α-reductase activity within the liver may be reduced, one investigation has demonstrated an up-regulation of activity within peripheral tissues (Fassnacht, Schlenz et al. 2003). Other studies have shown PCOS to correlate with high levels of 5α-reduced metabolites, in addition to up-regulated 5α-reductase activity within the PCO itself (Jakimiuk, Weitsman et al. 1999).

At this point it is worth remembering that neonatally androgenised animals in this study did not exhibit raised levels of either T or A4, and so full analysis of steroid metabolites in the plasma/urine of neonatally androgenised females could in future prove useful when assessing rodent models of PCOS, particularly when differentiating between ovarian and adrenal hyperandrogenism.

The expression profile of genes involved in liver catabolism of fatty acids under the regulation of nutrition and gluconeogenic hormones showed that early window TP exposure led to raised PPARα transcription factor expression in the adult liver. Regulation of PPARα and PEPCK genes by gluconeogenic hormones and glucocorticoids is well described (Panadero, Herrera et al. 2000; Panadero, Vidal et al. 2001). Thus the increase in PPARα expression may be secondary to the increases in glucocorticoid turnover observed. A similar trend was shown in PEPCK expression but was not significant. As only diminutive differences are apparent in catabolic gene expression profiles between postnatal TP exposed rats and their control counterparts, further investigation into the nutritional status of the neonatally

androgenised rodent is warranted, potentially through glucose tolerance and insulin resistance testing.

In human metabolic syndrome and in the Zucker rat model of obesity, a reduction in liver 11βHSD-1 expression and a concomitant increase in expression of both 5α and 5β reductase occurs (Stimson, Lobley et al. 2010). Such discordances may be explained through differences between species and experimental design. However, to some extent these findings support the notion that a different obese pathophysiology may develop in women with PCOS, as well as in rodent models where steroid programming is at work during development.

5.5.4. Windows of neonatal TP exposure, growth and adipose tissue

By 12 days post-weaning, animals from all TP treatment windows were significantly heavier than controls, with early TP treatment having the strongest impact by pnd 80. These animals became approximately 50% heavier than controls. Despite such weight increases, there were no differences in crude chow consumption after weaning between animals in the control litter and those of the TP treatment groups. The weight gain observed could therefore be due to a combination of several factors; a decrease in physical activity and thus calorie expenditure or an increase in calorie absorption, either of which may result through programming by neonatal TP exposure. Onset of weight gain occurred after weaning in all groups, suggesting that either a change in diet at puberty may result in the metabolic changes documented, or that activation of the GnRH pulse generator may be involved in the pathogenesis of adult onset obesity in neonatal TP treated rats.

Steroid treatments and altered nutrition can lead to HPAA abnormalities in conjunction with obesity; fetal administration of corticosteroids or a high fat neonatal diet have previously been used to model metabolic syndrome in the rodent (Plagemann, Heidrich et al. 1992; Armitage, Taylor et al. 2005; Drake, Livingstone

et al. 2005). Only one study has thus far investigated in detail the effects of exogenous corticosteroid during the neonatal period upon the ovary, where fetal dexamethasone in the five days before birth reduced follicle numbers by pnd five (Ristic, Nestorovic et al. 2008). Evaluation of the effects of corticosteroids upon female reproductive axis development have yet to be undertaken, although some investigations have shown that dexamethasone administered to adult rodents can increase the number of eggs ovulated (Tohei, Sakamoto et al. 2000; Rockwell and Koos 2009). In current studies postnatal TP led to significant weight gain in line with that of rodent models of the metabolic syndrome (Armitage, Taylor et al. 2005).

At sacrifice, all TP window treatment groups showed significantly greater mesenteric and retroperitoneal fat masses, which did not normalise to body weights. This indicates that the weight gain observed in animals which received TP was due to increased adiposity. While several rodent studies into the developmental programming of female reproduction by both androgens and estrogens have documented weight gain in the adult animals (Barraclough 1961; vom Saal and Bronson 1978; Alexanderson, Eriksson et al. 2007), none have related this adult obesity to increases in fat deposition at specific sites. However, rat models where a PCOS-like phenotype is induced by chronic steroid administration, have demonstrated that androgens or estrogens can lead to increased central obesity (Beloosesky, Gold et al. 2004; Wang, Sun et al. 2004; Alexanderson, Eriksson et al. 2007). One study went on to show that high circulating androgens led to an increase in adipocyte size and reduction in insulin sensitivity in adult animals receiving long term DHT treatment (Manneras, Cajander et al. 2007).

It may well be that the changes adipose distribution documented are an adaptive response to neonatal TP and its influence upon the developing metabolic axes. It is well documented that animals over-nourished during early postnatal life have shown steeper growth trajectories, potentially as an adaptive response to over nutrition (Gluckman and Hanson 2004). This predictive adaptive response is hypothesised to occur where a mismatch exists between the ‘expected’ post-

developmental nutritional environment and the actual one (Chapter 1, Section 9; Gluckman and Hanson 2004; Gluckman, Cutfield et al. 2005; Ikenasio-Thorpe, Breier et al. 2007). Further investigation is therefore warranted into the spatiotemporal expression and secretion of lipolytic factors and adipokines across female rodent development within the various adipose tissue depots. Other endocrine influences upon adipokine expression also need to be taken into account, given that a change in postnatal environment in rodents has been shown to induce alterations in adult metabolism, including both central and peripheral insulin and leptin sensitivities (Krechowec, Vickers et al. 2006).

As a known predictor of insulin resistance and metabolic syndrome in humans, the mesenteric (central) fat mass was chosen to assess expression of various adipokines and lipolytic factors involved in adipogenesis and the pathogenesis of obesity (Stevens 1995; Liu, Chan et al. 2006). During the early window of rodent postnatal life, organ development is still occurring (Armitage, Taylor et al. 2005). Given the differences between treatment groups in the expression of some adipogens and adipokines, it is reasonable to speculate that administration of TP prior to the postnatal leptin surge (early window) may to some extent program the metabolic response to obesity in a different way to TP administered after the postnatal leptin surge (late window).

The reduction in expression levels of lipolytic factors (FAS, HSL, LPL, PPARγ) and adiponectin in animals receiving TP during the early window may be due to a reduction in lipolysis. FAS is known to be involved in the synthesis of fatty acids and is transcriptionally regulated by insulin/feeding via a sterol regulatory element binding protein (SREBP) pathway (Gosmain, Dif et al. 2005). A reduction in FAS expression might therefore indicate the development of insulin resistance. The involvement of HSL and LPL in lipolysis indicates that a reduction in HSL and LPL expression may lead to increased adipogenesis, triglyceride storage and as a result, adiposity. Low HSL expression has also been documented in obese women with PCOS which may partly explain the association of PCOS with increased

atherosclerotic risk (Seow, Tsai et al. 2009). Furthermore, adiponectin has been shown to inversely correlate with insulin resistance in studies of human obesity, therefore the lower levels observed here could indicate the development of insulin resistance in early window TP treated animals. In addition, low adiponectin levels have been documented in NAFLD models (Pagano, Soardo et al. 2005), as well as in PCOS patients, independently of their body mass index (Toulis, Goulis et al. 2009). Future investigations into the metabolic status of rats receiving neonatal TP could therefore examine plasma, liver and adipose triglyceride levels to further evaluate changes in adipogenesis and metabolism.

Late window TP exposure led to increased leptin and trend increases in resistin and adiponectin levels, as may be expected in animals with increased adiposity, shown by other studies aiming to recapitulate features of the metabolic syndrome in rodents (Cleasby, Kelly et al. 2003). However, no differences in lipolytic factor expression were observed. In other investigations, leptin has been shown to reduce adipose FAS and LPL expression (Cleasby, Kelly et al. 2003; Gallardo, Bonzon-Kulichenko et al. 2007). Thus it can be deduced that an increase in leptin activity could function to restrict lipolysis in already overweight animals. Plasma and adipocyte leptin protein levels were not analysed in this study and so cannot currently be related to lipolytic factor expression.

Few models of PCOS have performed analysis of genes involved in adipogenesis, although one recent study in fetally androgenised sheep has shown that the adult animals have reduced hepatic HSL and PPARγ expression, but increased adipose PPARγ expression (Padmanabhan, Veiga-Lopez et al. 2010). While these findings are distinct to those documented in this study, they provide support to the notion that transcriptional function in adipose tissue can be altered in adult animals as a result of neonatal steroid exposure. Whether these effects are directly the result of epigenetic programming by steroids, or occur indirectly through an alternate mechanism remains to be seen.

5.6. Conclusions

The investigations described herein show that the first 15 days of postnatal life in the rat is a steroid-sensitive period of development, and this finding is supported by the prior work of others (Barraclough and Leathem 1954; Barraclough 1961). Moreover the results of this chapter show that TP exposure between pnd 1 and 6 is potentially able to reprogram the female neuroendocrine axis so that there is reduced negative feedback from the ovary to hypothalamic-pituitary centres.

Taken together, these results allow further evaluation of the neonatally androgenised rat PCOS model which although anovulatory and overweight, does not exhibit high levels of circulating androgen, nor an increased number of activated follicles. Furthermore the results demonstrate that neonatal TP exposure may reprogram hepatic glucocorticoid turnover, in addition to adipose lipolysis, potentiating an obese phenotype. Whether the changes in gene expression observed result through an epigenetic mechanism or via changes in calorie absorption or nutrition/diet remains to be seen, although the early window of postnatal development (pnd 1-6) before the postnatal leptin surge appears to be the key window during which the programming of both the hypothalamic-pituitary neuroendocrine and metabolic axes occurs.

Collectively these results indicate that the PCOS-like phenotype which develops in the rat as a consequence of neonatal TP exposure may be a useful model for non-ovulatory PCOS with normal androgen levels and impaired hypothalamic-pituitary ovarian feedback mechanisms, in addition to features of the metabolic syndrome. Furthermore, examination of the metabolic changes which result from early neonatal steroid treatment warrant further investigation.

Chapter 6. Dose of postnatal TP required to alter the rat hypothalamic-pituitary gonadal axis

6.1. Introduction

In early rat postnatal development there exists a time period between pnd one (the day after birth) and pnd six, during which the HPG and metabolic axes can be developmentally reprogrammed by aromatisable androgens such as TP (Barraclough 1961; Beloosesky, Gold et al. 2004; Alexanderson, Eriksson et al. 2007). This results in anovulatory infertility and a metabolic syndrome-like phenotype in adult animals (Chapter 5). In addition to rodents, this key window of reproductive and metabolic development also exists at corresponding time periods in sheep (Clarke, Scaramuzzi et al. 1976; Wood and Foster 1998; Steckler, Herkimer et al. 2009; Veiga-Lopez, Astapova et al. 2009) and non human primate fetal life (Dumesic, Abbott et al. 2007; Abbott, Tarantal et al. 2009; Abbott 2010). Studies in rats suggest that a single dose above 0.5mg/kg TP is required for effective reprogramming at both the reproductive and metabolic levels (Gorski and Barraclough 1963). However, it remains unknown whether the dose of TP administered during this key period of development affects the resulting severity of reproductive and metabolic disorders in the adult animal.

Investigations into the aetiology of PCOS, the most common cause of infertility in women, indicate that PCOS may result from epigenetic programming by abnormal steroid exposure during development, in addition to environmental and genetic influences (Chapter 1, Section 11; Abbott, Dumesic et al. 2002). Mono-ovulatory PCOS animal models use fetal androgen treatment to induce a reproductive and metabolic phenotype in the adult. These animals become anovulatory, show increased LH pulse amplitude and develop features of the metabolic syndrome which include an increased central fat mass that correlates with insulin resistance and glucose intolerance (Abbott, Dumesic et al. 1998; Manikkam, Thompson et al. 2008; Abbott 2010). Furthermore, granulosa cells (GCs) taken from women with PCOS show increased in proliferation rates when in culture (Stubbs, Stark et al. 2007; Das, Djahanbakhch et al. 2008). Bidirectional communication operates between the oocyte and surrounding GCs throughout follicle development (Eppig 2001; Knight

and Glister 2003; Edson, Nagaraja et al. 2009). Disruption of GC proliferation by a mitogenic factor, such as androgens, may help explain why follicle development appears dysregulated in PCOS; the PCO typically presents on an ultrasound scan with an increased number of follicles (12 or more) that are between two and nine mm in diameter (Dewailly, Catteau-Jonard et al. 2007; Fulghesu, Angioni et al. 2007). Furthermore, culture studies have shown androgens may induce GC atresia in larger antral follicles (Hagen, McNatty et al. 1976; Harlow, Hillier et al. 1986; Harlow, Shaw et al. 1988; Honnma, Endo et al. 2006). It is therefore reasonable to deduce that the high levels of ovarian androgens seen in many women with PCOS may impact follicle development through their mitogenic and/or atretic actions upon GCs.

A potential rat model of polycystic ovarian syndrome (PCOS) has previously been described (Chapters 4 and 5), in which the neonatally androgenised animal developed follicles with larger antra, as well as ovaries with a greater proportion of stroma in comparison to control ovaries, like those observed in PCOS (Fulghesu, Ciampelli et al. 2001; Fulghesu, Angioni et al. 2007). However, whether these abnormalities are due to the effects of neonatal TP upon GC atresia or proliferation remain to be seen. Thus in this chapter the functional status of GCs within the various ovarian follicle types will be investigated by examining BrdU incorporation in GCs and through this the level of GC proliferation. Metabolic abnormalities resulting from neonatal TP exposure have also been documented at the transcription level (Chapter 5), although glucose intolerance and insulin resistance have yet to be demonstrated in this particular PCOS model.

The current study expands previous investigations into the window of neonatal TP exposure required to induce a PCOS-like phenotype in the adult animal (Chapter 5), and aims to assess whether TP dose affects the severity of the reproductive and/or metabolic phenotype seen in adult animals. In addition, administration of a single dose of TP on pnd one of life will further delineate the window of steroid exposure necessary to produce a PCOS-like phenotype in the adult animal.

6.2. Objectives

- To investigate which doses of TP administered during the early window of postnatal life produce a PCOS-like phenotype in the female rat; 1, 5 or 20mg/kg.

- To ascertain the effects of these doses of TP exposure upon reprogramming of the hypothalamic-pituitary axis through measurement of both plasma and pituitary gonadotrophin content in addition to mRNA expression levels of the three gonadotrophin subunits.

- To further explore the effect of each TP dose upon GC proliferation in the ovaries of the neonatally androgenised rat using IHC for BrdU incorporation.

- To elucidate the effects of different TP doses upon other endocrine organs such as liver, adrenal and fat depot weights.

- To further investigate the effect of TP exposure upon the pancreas through glucose tolerance testing and subsequent analysis of insulin and glucose plasma levels.

- To investigate whether the effects of a single injection of TP on the day after birth produces a PCOS-like phenotype in the female rat, and if this treatment results in any significant differences in reproductive or metabolic abnormalities when compared to those observed in early window TP exposed animals.

6.3. Methods

6.3.1. Experimental outline

To elucidate which dose of postnatal TP treatment would produce a PCOS-like phenotype, two litters of rats per treatment group were given either 1, 5 or 20mg/kg TP. The same dose of 20mg/kg as well as the same timing of TP exposure during the early window of postnatal life (with TP injections on pnd 1 and 4) were used in this study in accordance with previous studies (Chapters 4 and 5). In addition to investigate the effects of TP dose, one extra litter was used to further delineate the window of steroid exposure necessary to produce a reproductive phenotype in the adult animal by administering a single dose of 20mg/kg TP on the day after birth (pnd 1). Two control litters were correspondingly injected with the same volume of oil during the early window time point. The varying doses and windows of treatment are schemed in Figure 6.1 and the colours used in this figure will correspond to the same treatment groups throughout this chapter.

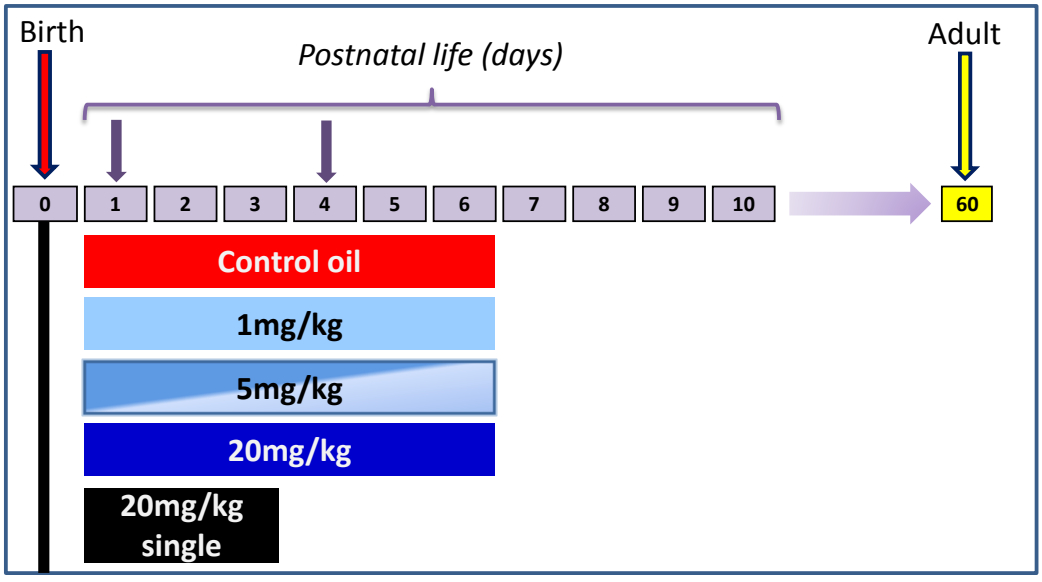

Figure 6.1: Schematic diagram to illustrate the windows of postnatal TP exposure in rats: Downward purple arrows indicate the days of TP injection postnatal life. The downward red and yellow arrows indicate the days of birth and sacrifice respectively.

Two litters of Wistar rats were used for each treatment dose group, except for the 20mg/kg single group which used only one litter. Initially, ten dams underwent timed-mating overnight with stud males. After birth (pnd 0) one newborn litter was killed by the dam (this litter was originally designated to the 20mg/kg single group), bringing the total number of litters used in this study down to nine with *n* numbers detailed in Table 6.1. Subsequently all litters were sacrificed down to an *n*=8 animals at pnd 1 to prevent any differences in suckling and litter size from masking/causing a metabolic phenotype in the adult female animals (Champagne, Francis et al. 2003; Roma, Huntsberry et al. 2007). At weaning (pnd 21) any male litter mates were sacrificed and as many females as possible kept in each treatment group.

Table 6.1: The number of animals in each experimental control and TP treatment dose group: These groups correspond to those outlined in Figure 6.1. Birth litter numbers are divided by sex, animals were sacrificed to an *n=8* in each litter on the day of birth with males sacrificed at weaning (pnd21);

Group name	TP exposure	Number of pups		Final group *n* number	
		Male	Female	Animal designations	Group *n*
Control	Oil: pnd 1 - 6	8	7	**06 A – G**	*n=15*
		6	8	**07 A – H**	
1mg/kg	pnd 1 - 6	8	7	**08 A – G**	*n=14*
		8	7	**10 A – G**	
5mg/kg	pnd 1 - 6	10	7	**11 A – G**	*n=14*
		6	7	**12 A – G**	
20mg/kg	pnd 1 - 6	7	4	**09 A – D**	*n=10*
		10	6	**13 A – F**	
20mg/kg single	pnd 1 - 3	6	7	**06 A – G**	*n=7*

TP=testosterone proprionate; pnd=postnatal day.

Crude chow consumption was assessed in tandem with smears for ovarian cyclicity for two weeks after puberty although it should be noted that only control litters developed vaginal openings. Litters were split up into cages of two or three animals, depending on the group *n* number. Chow was weighed and topped up for each cage every two days and normalised for the number of animals in each cage and

the number of days. For example, the chow in a cage of three control animals weighed 96g less two days later and so the formula (96 X 0.5)/3 gave a result of 16g chow consumption per day for that period.

6.3.2. Insulin resistance and glucose tolerance

Insulin resistance and glucose tolerance were assessed after chow consumption measurements during this study. In week eight of life, animals underwent glucose tolerance testing (GTT). Briefly, rats were fasted overnight from 6pm, tail nick blood samples were taken over three time (*t*) points (*t*=0, *t*=30 and *t*=120 minutes) with the *t*=0 sample taken before gavage[††] with a 50% (2g/kg) glucose solution. These blood samples were used for both insulin and glucose assays (Chapter 2, Sections 12 and 13).

6.3.3. Necropsy

Animals were injected intra-peritonealy with 100mg/kg of the synthetic nucleoside BrdU at 6pm the evening before sacrifice. BrdU is a thymidine analogue and incorporates into the DNA of replicating cells during the mitotic S-phase. An antibody against the BrdU epitope was therefore used to assess cell proliferation using IHC.

The same tissues as in the previous study (Chapter 5) were removed and weighed along with the ovary and uterus: Pituitary, liver, adrenal, retroperitoneal adipose, and mesenteric adipose tissue. The hypothalamic area, a portion of subcutaneous adipose tissue and a portion of skeletal quadricep muscle were also removed but not weighed. One ovary and adrenal was frozen and the second was fixed in 4% NBF before processing and embedding (Chapters 2, Section 4). Animals were sacrificed on or just after pnd 60 in week eight of life. Blood samples taken at

[††] Special thanks to Mr Mark Fisken for performing glucose gavages.

sacrifice by cardiac puncture were spun down and plasma stored at -20ºC for future investigation of plasma gonadotrophin and hormone levels (Chapters 2, Sections 11 and 12).

6.3.4. Immunohistochemistry and stereological analysis

Ovaries from each litter were embedded together and serial sectioned at 5µm intervals. H&E staining was performed on some mounted sections to examine ovarian morphology. Every 10th section from each treatment group underwent DAB staining for BrdU. Briefly, BrdU antibody (Roche) was diluted in NGS at 1:50µl and slides incubated overnight at 4ºC in a humidity tray before standard DAB visualisation (Chapter 2, Section 4)

Measuring the proportion of BrdU staining occurring in the GCs of various follicles, the number of GCs present within a follicle would in theory relate to follicle area. For this reason follicles of different classes in the control group had both area and the number of visible GCs measured; a correlation between these two factors was performed for follicles both with and without an antrum to ensure the presence of a linear relationship (Figure 6.2).

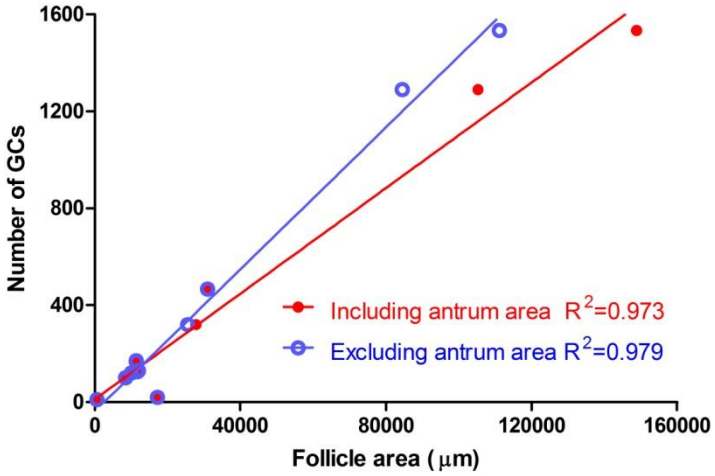

Figure 6.2: The number of granulosa cells (GCs) within a follicle is directly proportional to the follicle area. This linear relationship remains even when antrum area is excluded from the follicle area measured, analysed by linear regression.

BrdU staining in individual follicles from each treatment group was subsequently assessed using Image ProPlus 6.2 software connected to a stereological microscope. Follicles were tiled individually at X 40 magnification. The basement membrane of each follicle assessed was drawn around using Image ProPlus allowing only the GC and oocyte (and an antrum if present) to be selected as an area of interest (AOI), described in detail in Chapter 2, Section 6. Within the selected AOI, the overall brown stained GC area (BrdU positive) or blue stained GC area (BrdU negative) area could be selected and taken as a proportion of the AOI. In antral follicles the antrum area was additionally measured so that it could be excluded from the AOI. The proportion of BrdU incorporation within GCs increased in line with follicle size, although no significant differences between the levels of proliferation in follicles of various sizes were observed. As the largest range in levels of GC proliferation measured by BrdU incorporation were observed in antral follicles, this group of follicles was split into small and large antral follicles (Figure 6.3).

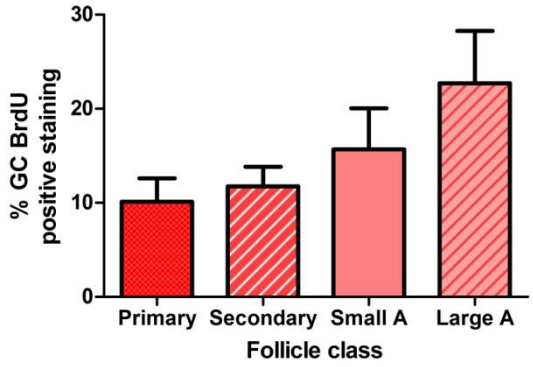

Figure 6.3: Granulosa cell BrdU proliferation index in different sized follicles from ovaries of control animals. A=antral. Values are expressed as the mean ±SEM and were analysed by student's unpaired t-test.

Small antral follicles were classed as having an antrum which did not extend around most of the oocyte, and large antral follicles were classed as having an antrum which extended around most of the oocyte with clear cumulus and mural GC formation (Figure 6.4).

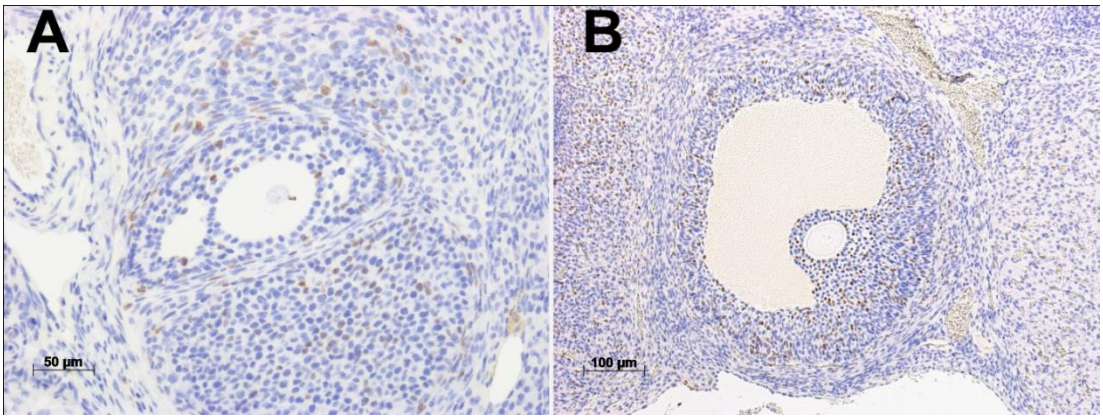

Figure 6.4: Images typical of (A) small antral follicles and (B) large antral follicles stained with BrdU: Small antral follicles were classed as having an antrum which did not extend around most of the oocyte, and large antral follicles were classed as having an antrum which extended around the oocyte with clear cumulus and mural GC formation. Images are shown at (A) X 20 and (B) X 10 magnification.

6.4. Results

6.4.1. Effects of TP dose upon reproductive tract and hormones

Control animals demonstrated regular estrus cycles, whilst all animals that received TP did not develop vaginal openings and thus their estrus cyclicity could not be assessed. Ovaries from all animals that received TP were anovulatory and had no CL (Figure 6.5).

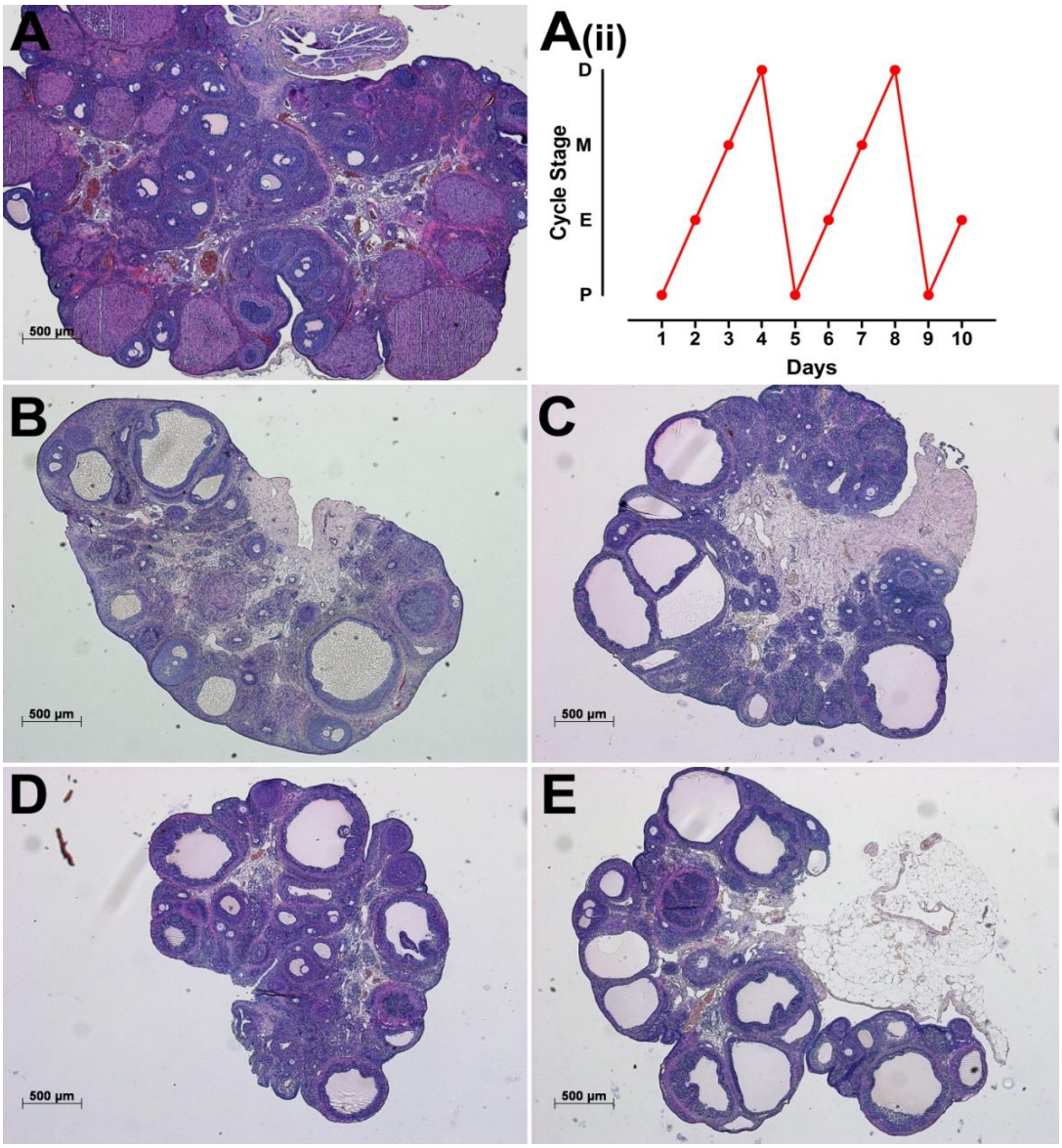

Figure 6.5: H&E stained ovaries and estrus cyclicity documented where possible in (Ai) Control (B) 1mg/kg TP (C) 5mg/kg TP (D) 20mg/kg and (E) single dose 20mg/kg TP dosage groups. Note the cystic phenotype seen across all TP treatment doses and that no animals other than controls (Aii) developed vaginal openings. Images at X 2 magnification.

Every 10th section from each ovary underwent DAB staining for BrdU incorporation (Figure 6.6) followed by stereological analysis to assess the proportion of GCs which incorporated BrdU (stained brown) relative to the proportion of GCs which did not (Figure 6.7).

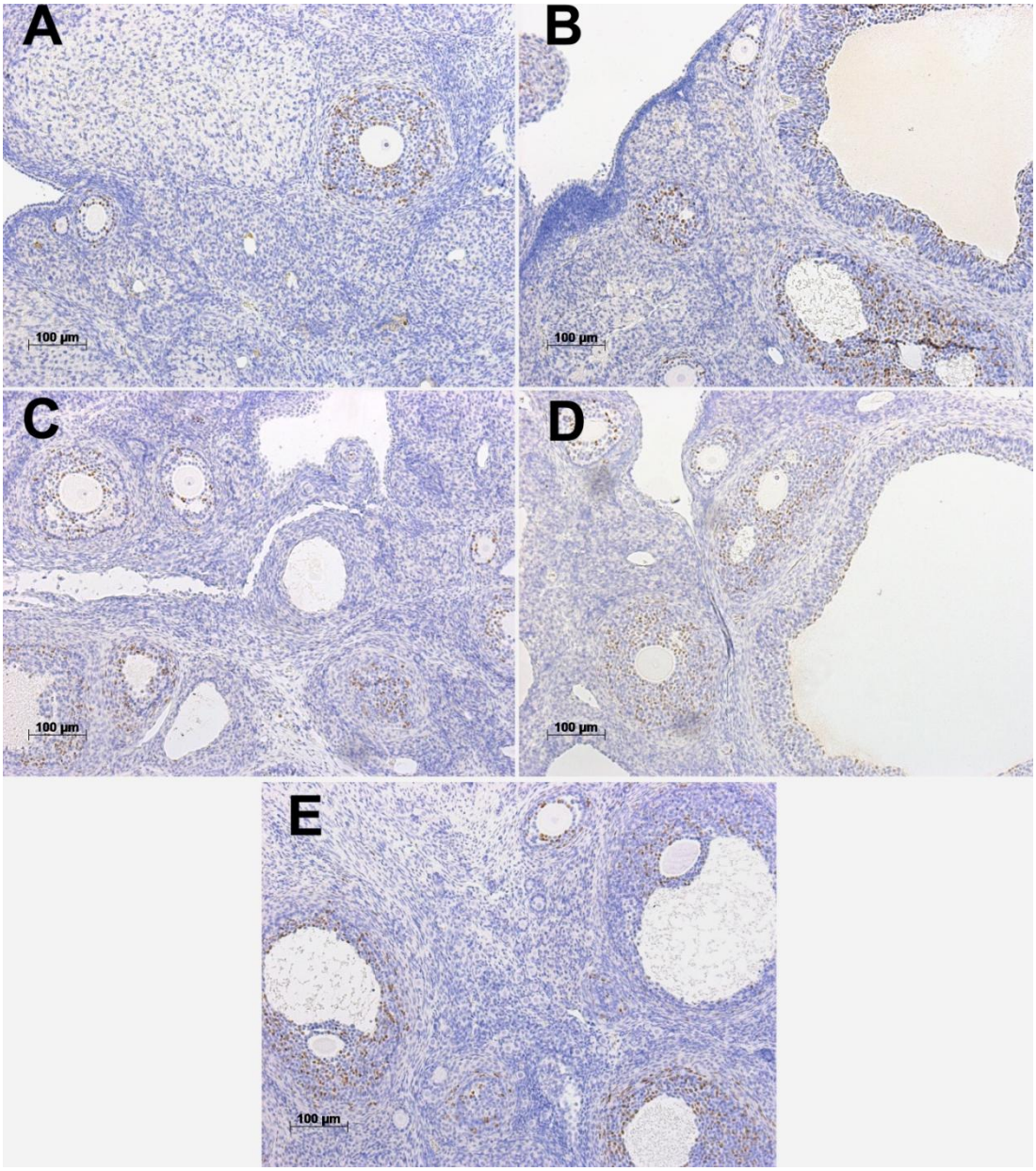

Figure 6.6: DAB immunohistochemistry for BrdU in follicles of (Ai) Control (B) 1mg/kg TP (C) 5mg/kg TP (D) 20mg/kg and (E) single dose 20mg/kg TP dosage groups: Images are shown at X 10 magnification.

No difference in the incorporation of BrdU into GCs during proliferation was observed across treatment groups for primary, secondary and antral follicle classes (Figure 6.7).

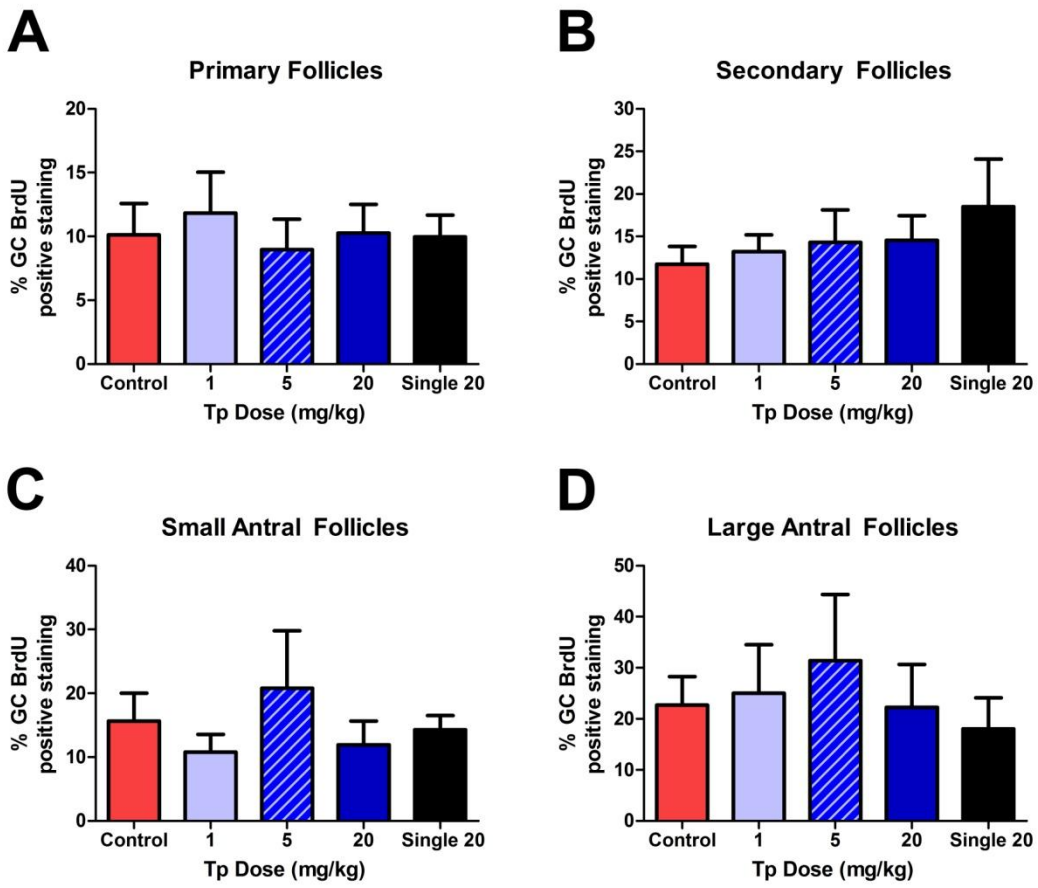

Figure 6.7: Granulosa cell BrdU proliferation index for (A) primary (B) secondary (C) small antral and (D) large antral follicles: BrdU staining is taken as a percentage of granulosa cell area. Counts were performed in every 10th 5µm section for ovaries from control (n=15), 1mg/kg TP (n=14), 5mg/kg TP (n=13), 20mg/kg TP (n=10), and single dose 20mg/kg TP (n=7) treated animals. Values are expressed as the mean ±SEM and were analysed by student's unpaired t-test.

Uterine and ovarian weights were significantly reduced in animals from all TP treated dose groups when compared to controls ($P \leq 0.05$ and $P \leq 0.001$ respectively), most likely due to the absence of CL (Figure 6.8).

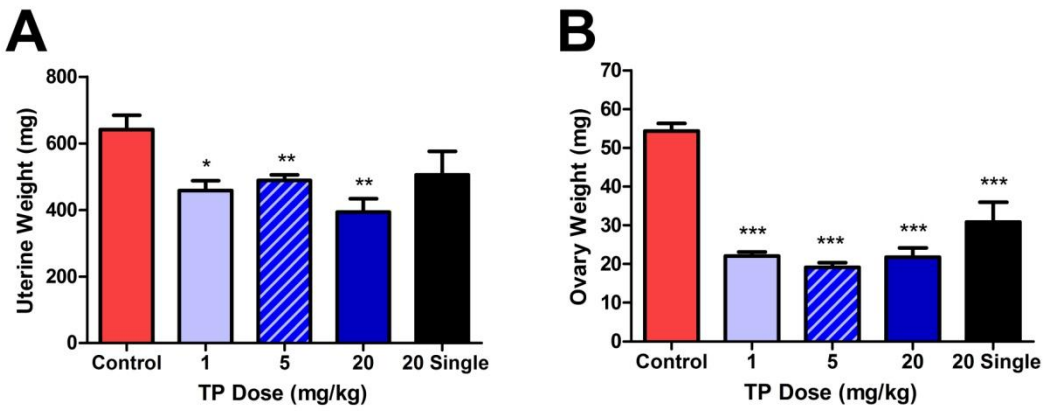

Figure 6.8: Effects of various doses of TP upon (A) uterine and (B) ovarian weight: Shown for control (n=15), 1mg/kg TP (n=14), 5mg/kg TP (n=13), 20mg/kg TP (n=10), and single dose 20mg/kg TP (n=7) treated animals. Values are expressed as the mean ±SEM and were analysed by student's unpaired t-test (* P≤0.05; ** P≤0.01 *** P≤0.001).

Subsequent analysis of circulating ovarian feedback hormones (Figure 6.9) showed both inhibin B and E2 feedback to be reduced in all TP treated animals (P≤0.01 and P≤0.05 respectively) compared to control proestrus levels, except for animals from the single 20mg/kg TP dose group, which despite low levels of circulating inhibin (P≤0.01), had E2 levels comparable to those of control animals.

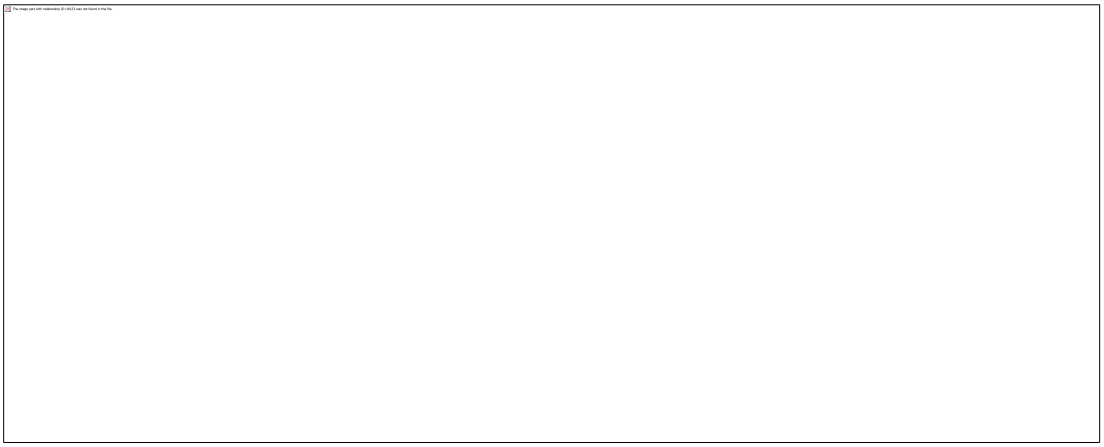

Figure 6.9: Effects of various doses of TP upon ovarian feedback hormones (A) Inhibin B and (B) Estradiol (E2): Shown for control (n=15), 1mg/kg TP (n=14), 5mg/kg TP (n=13), 20mg/kg TP (n=10), and single dose 20mg/kg TP (n=7) treated animals. Values are expressed as the mean ±SEM and were analysed by student's unpaired t-test (* P≤0.05; **P≤0.01 *** P≤0.001).

No differences in circulating ovarian androgen levels T or A4 were found between TP treated animals of any dose group, except for the single injection 20mg/kg dose group which had significantly greater levels of T ($P \leq 0.01$) when compared to controls (Figure 6.10).

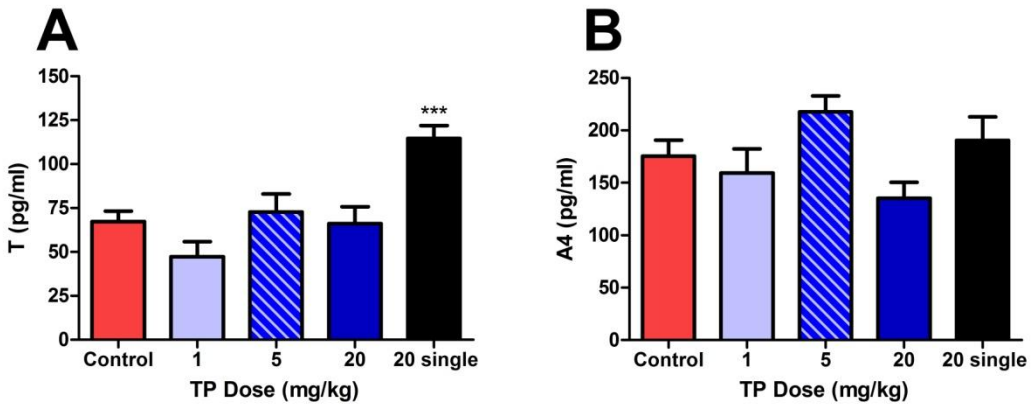

Figure 6.10: Effects of various doses of TP upon plasma (A) testosterone (T) and (B) Androstenedione (A4) levels: Shown for control (n=15), 1mg/kg TP (n=14), 5mg/kg TP (n=13), 20mg/kg TP (n=10), and single dose 20mg/kg TP (n=7) treated animals. Values are expressed as the mean ±SEM and were analysed by student's unpaired t-test (*** P≤0.001).

6.4.2. Effects of TP dose upon the pituitary

Pituitary weights (Figure 6.11) were significantly greater in animals treated with single 20mg/kg and 5mg/kg TP doses (P≤0.05), while animals in the 20mg/kg TP dose group showed a significant reduction in pituitary weight (P≤0.05). Plasma FSH levels were not significantly different between dose groups, and LH levels were significantly reduced in the 5mg/kg and 20mg/kg dosage groups (P≤0.001). There were no significant differences in pituitary gonadotrophin protein levels between treatment groups, although a trend increase in pituitary FSH and LH levels was observed in the 5mg/kg TP treatment group (Figure 6.12)

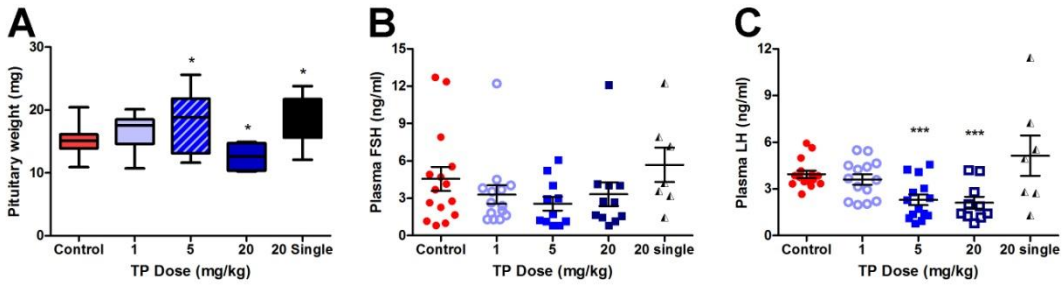

Figure 6.11: Effects of various doses of TP exposure upon plasma gonadotrophin levels: (A) Pituitary weight (B) Plasma FSH (C) Plasma LH levels, shown for control (n=15), 1mg/kg TP (n=14), 5mg/kg TP (n=13), 20mg/kg TP (n=10), and single dose 20mg/kg TP (n=7) treated animals. Values are expressed as (A) the mean ±SEM and (B-C) dot plot, and were analysed by student's unpaired t-test (* P≤0.05; *** P≤0.001).

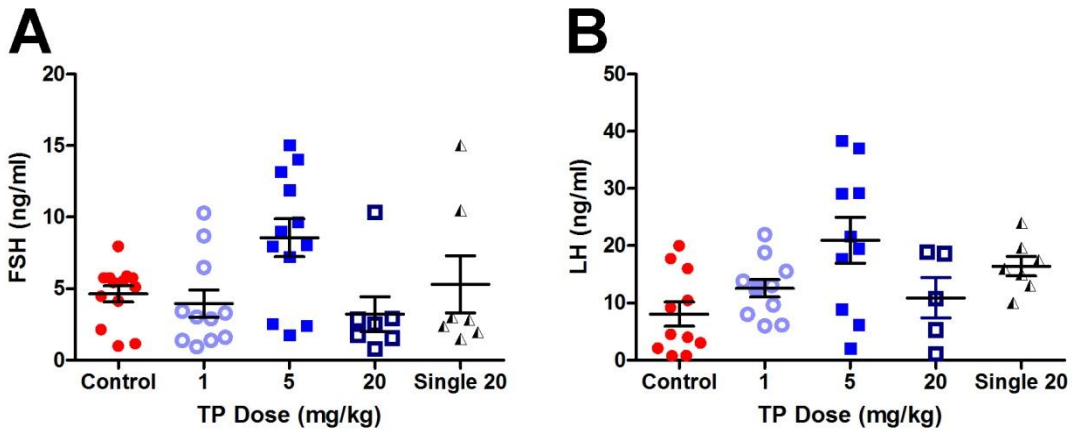

Figure 6.12: Pituitary gonadotrophin protein levels across dosage groups (A) FSH levels (B) LH levels: Shown for control (n=15), 1mg/kg TP (n=14), 5mg/kg TP (n=13), 20mg/kg TP (n=10), and single dose 20mg/kg TP (n=7) treated animals. Values are expressed as the mean ±SEM and were analysed by student's unpaired t-test.

Pituitary gland expression of gonadotrophin subunits αGSU, FSHβ and LHβ was not significantly different to controls across TP dosage groups (Figure 6.13). However, a trend of increased LHβ expression was observed in the 5mg/kg and single 20mg/kg dose groups.

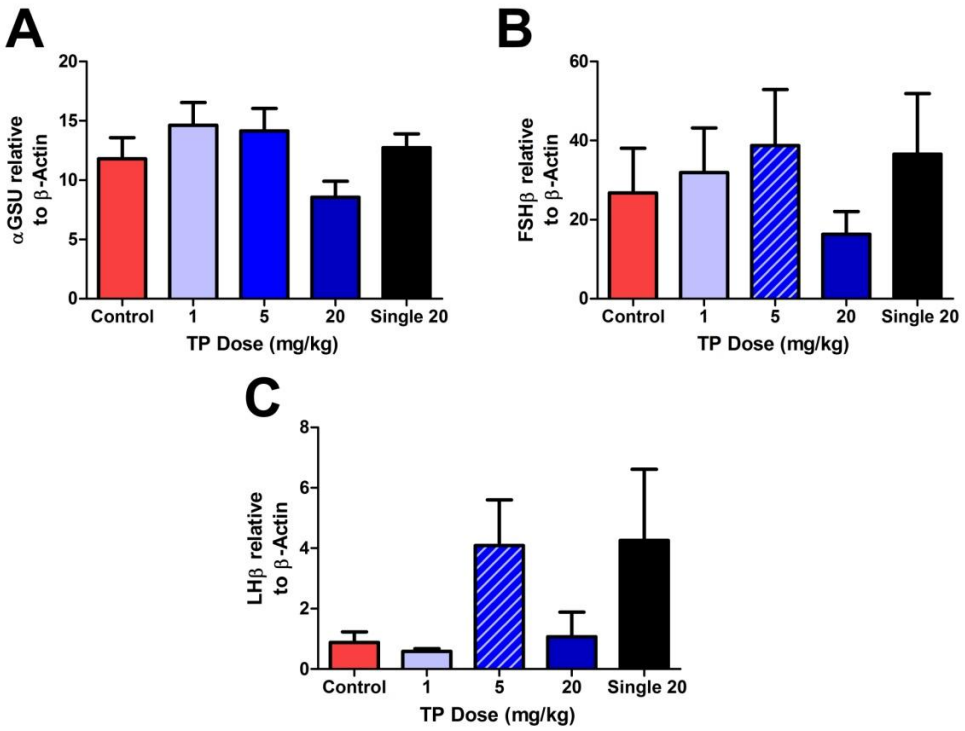

Figure 6.13: Expression of pituitary (A) αGSU (B) FSHβ and (C) LHβ gonadotrophin subunits: Shown for control (n=15), 1mg/kg TP (n=14), 5mg/kg TP (n=13), 20mg/kg TP (n=10), and single dose 20mg/kg TP (n=7) treated animals. Values are expressed as the mean ±SEM and were analysed by student's unpaired t-test.

6.4.3. Effects of postnatal TP doses upon other endocrine organs

No effect of neonatal TP exposure upon adrenal weight was observed across TP dose groups (Figure 6.14).

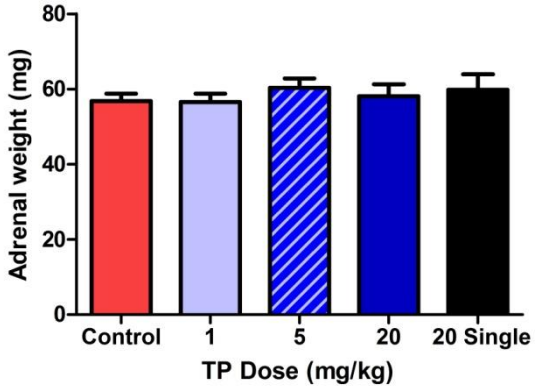

Figure 6.14: Effects of various TP doses upon adrenal weight: (A) Shown for control (n=15), 1mg/kg TP (n=14), 5mg/kg TP (n=13), 20mg/kg TP (n=10), and single dose 20mg/kg TP (n=7) treated animals. Values are expressed as the mean ±SEM and were analysed by student's unpaired t-test.

Liver weight at sacrifice was significantly raised in the 5mg/kg TP dose group (P≤0.001) when compared to control liver weight, this difference was removed when liver weight was divided by body weight (Figure 6.15).

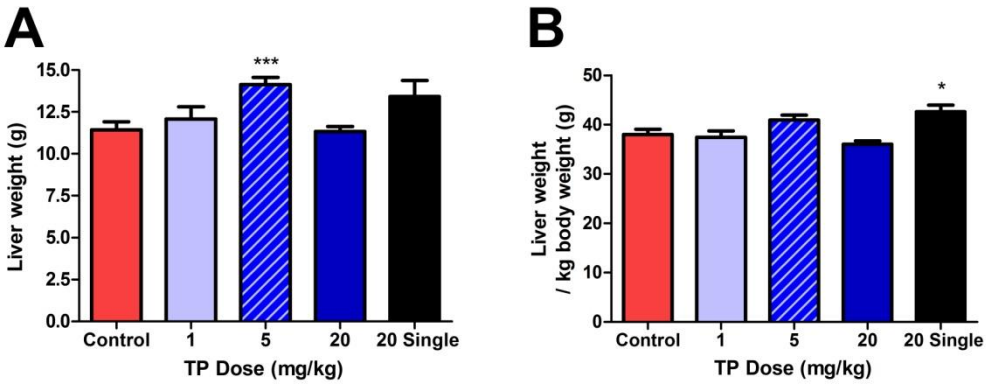

Figure 6.15: Effects of various TP doses upon liver weight: (A) Gross liver weights (B) liver weights normalised to body weight for control (n=15), 1mg/kg TP (n=14), 5mg/kg TP (n=13), 20mg/kg TP (n=10), and single dose 20mg/kg TP (n=7) treated animals. Values are expressed as the mean ±SEM and were analysed by student's unpaired t-test (* P≤0.05; ***P≤0.001).

6.4.4. Effects of early window TP dose upon fat deposition

Animals which received different doses of TP during the early window of postnatal development became significantly heavier after pnd 47 ($P \leq 0.01$). At sacrifice (pnd 60) these animals remained significantly heavier in each dose group; 1mg/kg ($P \leq 0.01$), 5mg/kg ($P \leq 0.001$) and 20mg/kg ($P \leq 0.05$). In contrast, animals which received a single dose of 20mg/kg on pnd one of life had significantly gained weight shortly after weaning by pnd 26 ($P \leq 0.001$). However, from pnd 32 up until the point of sacrifice at pnd 60, these animals had body weights comparable to those of controls (Figure 6.16).

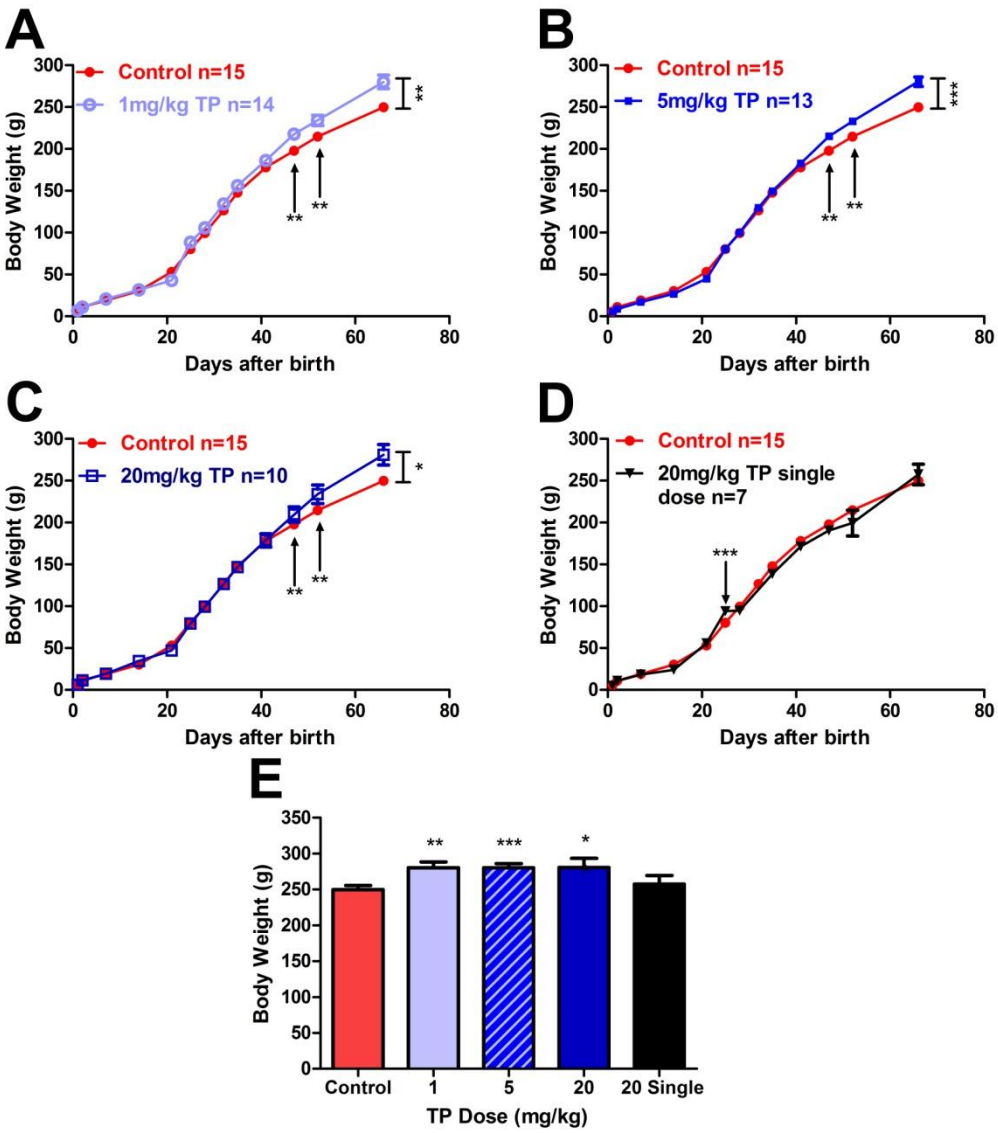

Figure 6.16: Effects of postnatal testosterone doses upon pup growth: Growth curves for control (n=15) versus (A) 1mg/kg TP (n=14), (B) 5mg/kg TP (n=13), (C) 20mg/kg TP (n=10), and (D) single dose 20mg/kg TP (n=7) treated animals. (E) Adult weight at cull. Values are expressed as the mean ±SEM and were analysed using a student's unpaired t-test (*P≤0.05; ** P≤0.01; ***P≤0.001).

Gross chow consumption was measured during weeks six and seven of life before glucose tolerance tests took place (Chapter 6.3.1). No differences in chow consumption between control litters and those from TP treatment groups were observed (Figure 6.17).

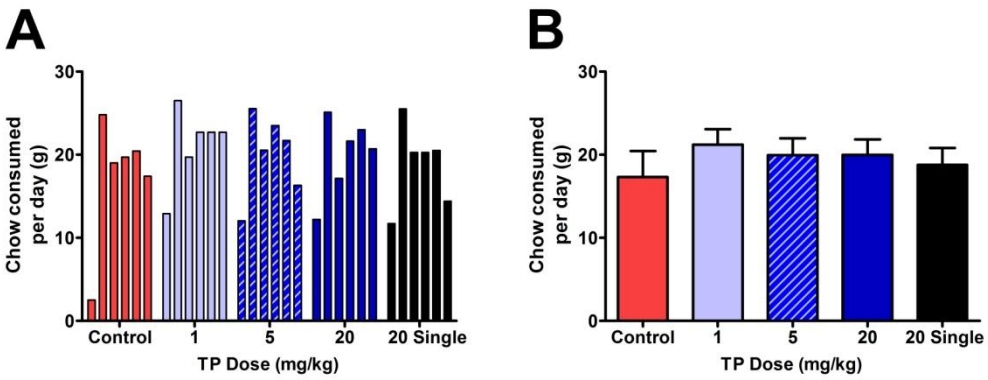

Figure 6.17: (A) Chow was weighed at two day intervals for two weeks with (B) mean ±SEM chow consumption: Shown for Control (n=15), 1mg/kg TP (n=14), 5mg/kg TP (n=13), (D) 20mg/kg TP (n=10), and single dose 20mg/kg TP (n=7) treated animals. Chow weight differences between intervals were divided by the number of animals per litter for each dosage group. Values in B represent the mean ±SEM, analysed by student's unpaired t-test.

At sacrifice both the mesenteric and retroperitoneal adipose depot were dissected and weighed to assess for differences in fat distribution (Figure 6.18). A significantly heavier mesenteric adipose depot was observed in 1mg/kg ($P \leq 0.001$), 5mg/kg ($P \leq 0.001$), 20mg/kg ($P \leq 0.01$) and single dose 20mg/kg ($P \leq 0.01$) TP dose groups, and these differences were not normalised by adjusting for body weight. In contrast, the retroperitoneal adipose depots across treatment groups were not significantly heavier than that those of control animals.

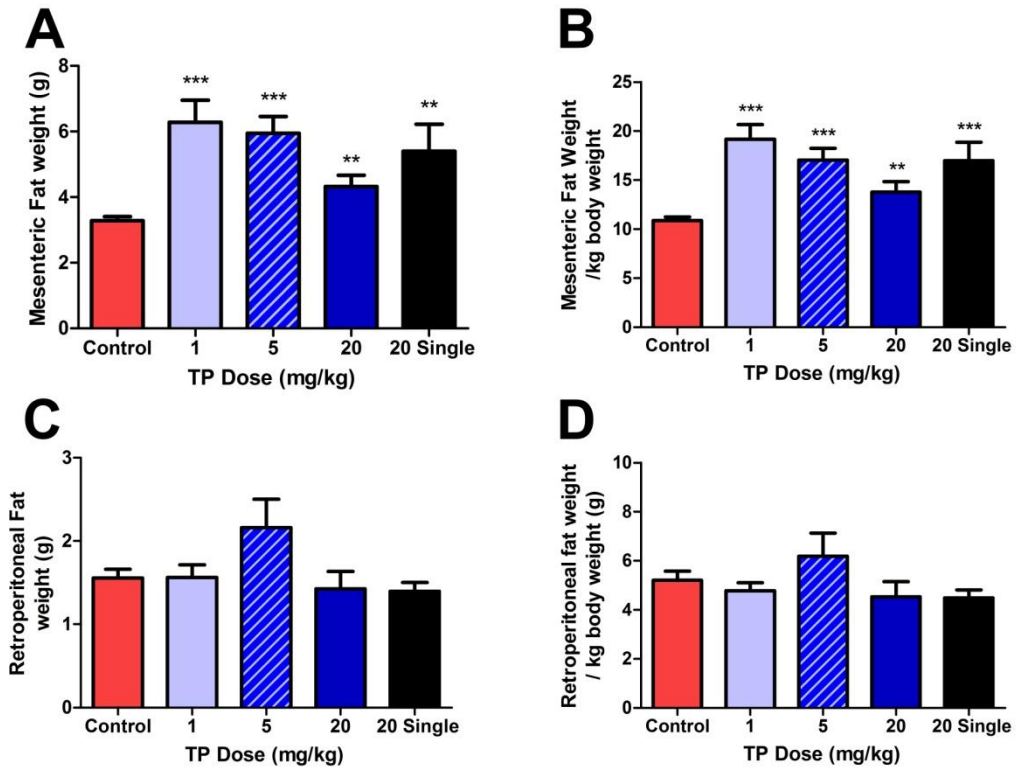

Figure 6.18: Fat deposition in adult female rats across dosage groups: (A) Mesenteric fat weight (B) adjusted by body weight with (C) Retroperitoneal fat weight (D) adjusted for body weight for (A) Control (n=15) (B) 1mg/kg TP (n=14), (C) 5mg/kg TP (n=13), (D) 20mg/kg TP (n=10), and (E) single dose 20mg/kg TP (n=7) treated animals. Values represent the mean ±SEM, analysed by student's unpaired t-test (**P≤0.01; *** P≤0.001).

6.4.5. Effects of TP dose upon insulin and glucose metabolism

Plasma samples taken at *t*=0, 30 and 120 minutes after glucose gavage were used to analyse insulin and glucose levels. The mean insulin response to glucose over two hours is shown for each TP treatment group in Figure 6.19. Analysis of plasma insulin *t*=0 was used to determine the fasting insulin levels, whilst area under the curve analysis of the insulin response to glucose was undertaken to determine if animals were insulin resistant (Figure 6.20). All animals which received TP had significantly higher (P≤0.01) fasting AM plasma insulin levels and were insulin resistant (P≤0.01).

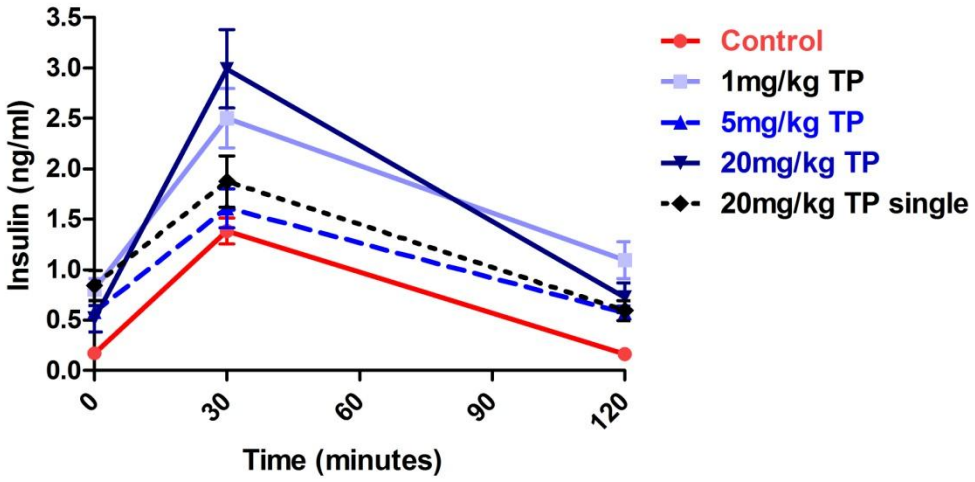

Figure 6.19: Rat insulin responses to glucose gavage over time: Measured at *t*=0, 30 and 120 minutes with mean ±SEM values shown for control (n=15), 1mg/kg TP (n=14), 5mg/kg TP (n=13), 20mg/kg TP (n=10), and single dose 20mg/kg TP (n=7) treated animals.

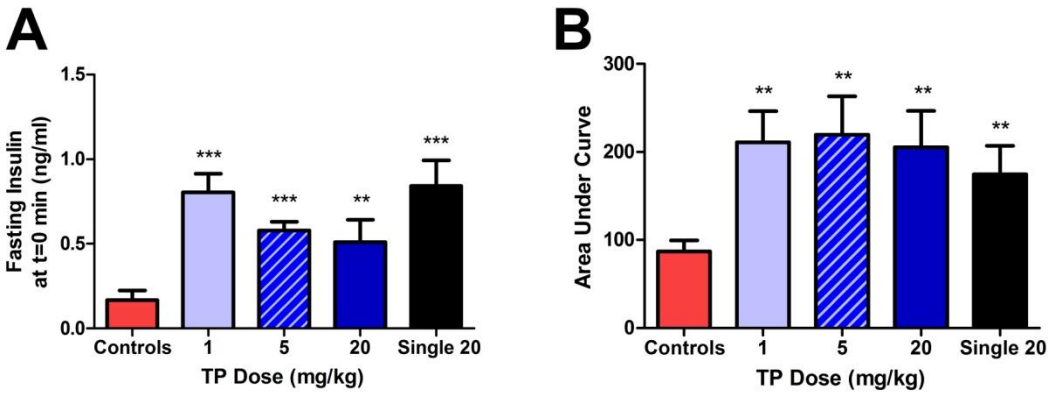

Figure 6.20: (A) Fasting insulin levels at *t*=0 minutes and (B) Area under the curve (AUC) analysis of insulin response to glucose gavage after overnight fast: Shown across dosage groups for control (n=15), 1mg/kg TP (n=14), 5mg/kg TP (n=13), 20mg/kg TP (n=10), and single dose 20mg/kg TP (n=7) treated animals. Values are expressed as the mean ±SEM, and were analysed by student's unpaired t-test (**P≤0.01; *** P≤0.001).

The mean blood glucose levels after glucose gavage are shown for each treatment group in Figure 6.21. Analysis of plasma glucose at *t*=0 was used to determine fasting glucose levels, whilst area under the curve analyses of the blood glucose levels after gavage were undertaken to determine if animals were glucose tolerant (Figure 6.22). Animals in the 5mg/kg, 20mg/kg and single dose 20mg/kg TP

treatment groups all had raised fasting AM glucose levels (P≤0.01). Area under the curve analysis of blood glucose levels however showed no glucose intolerance in these groups. Fasting glucose levels in the 1mg/kg TP treatment group were comparable to those of controls and area under the curve analysis of blood glucose levels in this treatment group showed these TP treated animals to have significantly better clearance of glucose than control oil treated animals (P≤0.05)

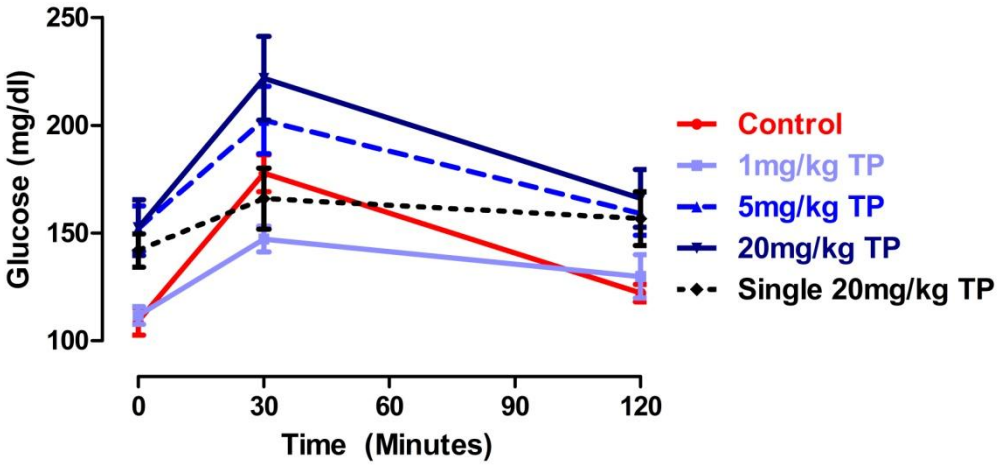

Figure 6.21: Mean blood glucose levels after glucose gavage over time: Measured at *t*=0, 30 and120 minutes with absolute values shown for control (n=15), 1mg/kg TP (n=14), 5mg/kg TP (n=13), 20mg/kg TP (n=10) and single dose 20mg/kg TP (n=7) treated animals. Lines show the mean ±SEM insulin response values for each treatment group.

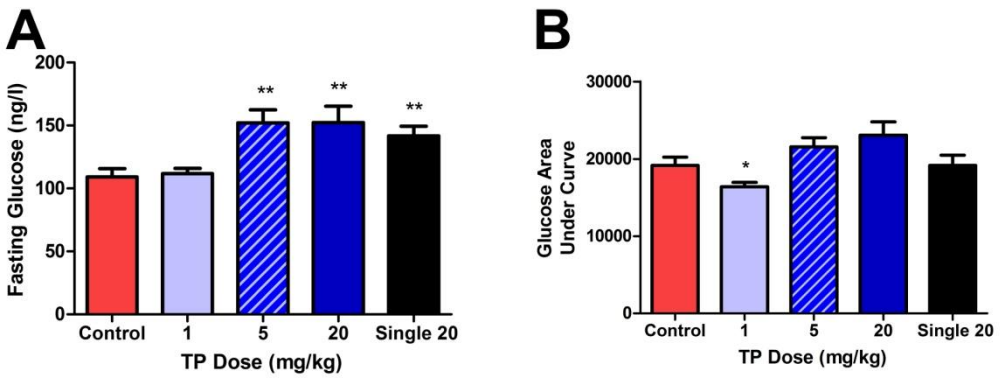

Figure 6.22: (A) Fasting blood glucose levels and (B) area under curve (AUC) analysis of glucose tolerance response after overnight fast: Shown across dosage groups at t=0 minutes. Shown for control (n=15), 1mg/kg TP (n=14), 5mg/kg TP (n=13), 20mg/kg TP (n=10), and single dose 20mg/kg TP (n=7). Values are expressed as mean ±SEM, analysed by student's unpaired t-test (* P≤0.05; ** P≤0.01; *** P≤0.001).

6.5. Discussion

This chapter sought to investigate whether the dose of TP administered during early postnatal development in the rat affects the resulting severity of reproductive and metabolic dysfunction in the adult animal. To expand previous investigations into the neonatally androgenised rat as a model for PCOS, effects of TP dose upon ovarian GC proliferation, the HPG axis and insulin resistant aspects of the metabolic syndrome were studied.

6.5.1. Effects of TP dose upon HPG axis and infertility

In line with previous investigations (Chapters 4 and 5), ovaries from all animals which received neonatal TP were PCO-like and had reduced ovarian weights due to a lack of ovulation and formation of CL. Furthermore, there was no apparent effect of TP dose upon the severity of PCO formation. These results are in line with previous reports that a TP dose above 0.5mg/kg (10μg of TP on the day of birth) is required for anovulation to result in the adult animal (Gorski and Barraclough 1963).

No differences in GC proliferation between controls or TP treated animals were documented at any stage of follicular development for any TP dosage group. This finding is at odds with those of human studies using cultured GCs which found that GCs of preantral follicles from PCOS women had increased levels of proliferation. In one study, a concurrent reduction in cleaved caspase-3 mediated atresia was also observed (Stubbs, Stark et al. 2007; Das, Djahanbakhch et al. 2008). However, it should be noted that there are both experimental (*in vivo* vs. *in vitro*) and species differences between these investigations. In addition, the GC cultures in the described studies were from women with high levels of circulating androgens. This may partly explain why increased levels of GC proliferation were observed, as androgens have shown mitogenic properties when added to GC cultures (Harlow, Shaw et al. 1988; Drummond 2006; Stubbs, Stark et al. 2007; Das, Djahanbakhch et al. 2008; Qureshi, Nussey et al. 2008). This could further explain why no effect upon

GC proliferation was observed in the current study, since no TP dose treatment group had high levels of circulating T or A4.

However, raised circulating levels of T were found in the single 20mg/kg dose group of this study and no differences in GC proliferation were seen through the assessment of BrdU incorporation. Although, it may be that these raised levels of T were not sufficiently high for an effect upon GC proliferation to be observed.

All animals which received TP neonatally had reduced inhibin B and E2 feedback levels from the ovary to the hypothalamic-pituitary axis by pnd 60, with the exception of animals in the single 20mg/kg dose group, who had E2 levels comparable to those of controls. There were no significant changes in pituitary gonadotrophin transcription or storage. In animals with reduced ovarian negative feedback, increases in gonadotrophin secretion would be expected, since a reduction in feedback in the female both directly and indirectly (via the hypothalamus and preoptic area) modulates pituitary gland gonadotrophin transcription, storage and secretion (McNeilly, Crawford et al. 2003).

Both animals in the 5mg/kg and single 20mg/kg TP dose groups showed a significant increase in mean pituitary weight, whilst the 20mg/kg TP dose group showed a reduction in pituitary weight. These findings may relate to those of gonadotrophin gene expression and protein levels, as trend increases in pituitary gonadotrophin proteins and pituitary LH protein were apparent in the 5mg/kg TP dose group and single 20mg/kg TP treated groups respectively. Additionally, both these TP dosage groups showed trend increases in pituitary LHβ mRNA levels. The 20mg/kg TP dose group also showed a trend reduction in αGSU and FSHβ transcription which could potentially explain the reduced pituitary weight observed in this dose group.

The apparent lack of pituitary response to reduced E2 and inhibin B feedback is in line with earlier findings (Chapter 5) and supports the notion that early neonatal TP is able to reprogram the hypothalamic-pituitary axis and alter the pituitary response to hormone positive and negative feedback in one of two ways: Either the female pituitary is masculinised by TP action during early postnatal life, or the pituitary becomes highly sensitive to ovarian feedback hormones, secreting normal levels of gonadotrophins in response to low levels of inhibin and E2 released from the ovary.

Indeed, in male rats prenatal and postnatal androgen surges program the neuroendocrine axis, including the feedback loops which regulate gonadotrophin secretion in response to testicular androgens (Scott, Hutchison et al. 2007; Scott, Hutchison et al. 2008; Welsh, Saunders et al. 2008; Macleod, Sharpe et al. 2010). Since androgen levels in TP treated animals were comparable to those of control animals in 1, 5 and 20mg/kg dosage groups, this may explain why no apparent response was seen in gonadotrophin transcription, storage or secretion from the pituitary. A reduction in plasma LH levels were also observed in the 5mg/kg and 20mg/kg dose groups could potentially be due to a lack of positive androgen feedback, which in the male would induce LH release to facilitate spermatogenesis.

Further investigations into the HPG axis feedback mechanisms operating in the neonatally androgenised female rat are therefore warranted, potentially using *ex-vivo* pituitary and ovary cultures, or cross transplantation of control ovaries into neonatally androgenised animals to observe whether ovarian cyclicity is altered. Such studies would help to elucidate whether it is the ovary or hypothalamic-pituitary axis that is ‘reprogrammed’ in the neonatally androgenised rat model of PCOS.

6.5.2. Effects of TP dose upon severity of metabolic syndrome features

As in previous studies (Chapter 5), no change in adrenal weight was documented in female rats treated with TP. Unlike previous studies however, liver weight was greater only in the 5mg/kg treatment group, which is potentially due to differences between investigations in the age of sacrifice (pnd 60 as opposed to pnd 80) and the number of litters used for each treatment group; litter size was controlled for in the current study in order to minimise the effects of suckling litter size upon the developing metabolism of the pups (Champagne, Francis et al. 2003; Roma, Huntsberry et al. 2007).

Significant weight gain was apparent by pnd 60 only in animals which received two doses of TP during the early window of postnatal life (pnd 1-6). Animals in the single injection 20mg/kg dose group were not significantly heavier than controls. These findings support the notion that the window of TP exposure required for significant weight gain by pnd 60 extends past pnd three. It may be that animals in the single 20mg/kg treatment group were culled too early for an effect upon body weight to be observed. However, it is worth noting that differentiation of adipocytes from preadipocytes probably occurs in the week after birth in the rodent (MacDougald and Lane 1995), thus a single dose of TP on pnd 1 may be insufficient to epigenetically reprogram changes in preadipocyte differentiation and thus whole body weight in the adult animal.

The increases in body weight resulting from early window TP exposure were relatively small, but all TP treatment groups developed a significant increase in mesenteric fat, despite no differences in calorie consumption. This increase in central adiposity occurred alongside an increase in fasting insulin and insulin resistance in all TP treated animals. Although a single dose of TP on pnd 1 of life is insufficient to program significant changes in whole body weight in the adult animal, this period of steroid exposure still elicits changes in body fat distribution and insulin resistance in

the adult animal. Sex differences in body fat distribution and insulin resistance have been documented in many species including humans (Priego, Sanchez et al. 2008; Ribot, Rodriguez et al. 2008). Prenatal and neonatal androgen surges in males and an estrogenic hormonal milieu in females are postulated to be just two reasons for differences in adipocyte size and number between sexes across species (Geer and Shen 2009).

Increased central obesity results from neonatal steroid exposure in other rodent models of PCOS (Beloosesky, Gold et al. 2004; Wang, Sun et al. 2004; Alexanderson, Eriksson et al. 2007). In addition, chronic treatment with androgens is known to lead to adipocyte hyperplasia in female rats (Manneras, Cajander et al. 2007), further supporting the role of high circulating androgens in the pathogenesis of central obesity in animal models and women with PCOS. The raised T levels documented in the single 20mg/kg dose group may therefore be a contributing factor in the development of central obesity and insulin resistance in the absence of significant weight gain in this treatment group.

The development of insulin resistance in these animals may be the result of epigenetic programming of pancreatic islet function. Other rodent, sheep and primate studies into the aetiology of PCOS and the metabolic syndrome have documented similar metabolic abnormalities resulting from fetal/neonatal androgen treatment (Bruns, Baum et al. 2007; Demissie, Lazic et al. 2008; Padmanabhan, Veiga-Lopez et al. 2010). These findings may well be consequences of pancreatic islet dysfunction and the programming of adipocyte hyperplasia (Roland, Nunemaker et al. 2010). Such programmed differences in pancreatic function could also contribute to the changes in body weight and fat deposition documented in neonatally androgenised female rats. Future studies should therefore target the pancreas, for example using histology as well as functional assays of insulin response, in order to further understand how neonatal steroids can affect pancreatic islet development.

6.6. Conclusions

To conclude, relatively small doses of TP of 1mg/kg or greater are required to induce anovulation in the adult animal; increasing the dose of TP does not appear to impact the severity of reproductive dysfunction in the adult female rat at either the pituitary or the ovarian level. There also appears to be no effect of neonatal TP upon adult GC proliferation in follicles of various sizes and at various stages of follicular development. Furthermore a single dose of TP on pnd 1 of life is sufficient to induce anovulation in the adult animal.

Historical investigations have shown that 0.5mg/kg TP is sufficient to induce anovulatory sterility in around 70% of female animals (Gorski and Barraclough 1963). Of these sterile animals, around half could be induced into ovulation through electrical stimulation of the median eminence, not the POA. Their resultant finding was that the degree of neurological remodelling brought about by neonatal TP is dose-dependent (Barraclough and Leathem 1954; Gorski and Barraclough 1963).

By contrast the aim of the current study was to determine if the severity of infertility or metabolic abnormalities which results from neonatal TP exposure are dose dependent. Indeed, a dose of 5mg/kg TP or higher appears required to induce glucose intolerance, whilst a smaller dose of 1mg/kg is sufficient to program insulin resistance and central obesity in the adult animal, with no apparent increases in calorie consumption. Moreover a single dose of 20mg/kg TP on pnd 1 of life is sufficient to induce glucose intolerance, IR, and central obesity potentially augmented by raised levels of plasma T. However, this single injection of TP appears insufficient to induce significant weight gain in the adult animal. These features of metabolic syndrome are likely mediated through the epigenetic programming of preadipocytes (MacDougald and Lane 1995; Ntambi and Young-Cheul 2000) and potentially pancreatic islet function, as has been documented in studies of neonatally androgenised mice and fetally androgenised sheep and primates (Bruns, Baum et al.

2007; Demissie, Lazic et al. 2008; Padmanabhan, Veiga-Lopez et al. 2010; Roland, Nunemaker et al. 2010).

As a PCOS model, the neonatally androgenised rat that receives TP during the early window of postnatal life (pnd one to six) gains weight after weaning, is anovulatory, centrally obese, insulin resistant and potentially glucose intolerant. This further recapitulates the reproductive and metabolic pathophysiological aspects of the syndrome. However, only animals which receive TP on the day after birth (pnd one) develop high circulating levels of T by pnd 60, and this group of animals do not gain weight as they mature. Therefore, potentially two anovulatory models of PCOS have been described in this chapter; one recapitulating the metabolic characteristics of the syndrome and the other recapitulating the high levels of circulating androgens observed in some women with PCOS devoid of the weight gain which occurs after puberty in adolescent PCOS patients.

Chapter 7. Exposure of the female rat to different steroids during early postnatal life

7.1. Introduction

Previous study has identified that early postnatal life in the rat is a critical period of reproductive and endocrine development, during which treatment with aromatisable androgen (TP) between pnd 1-6 leads to a PCOS-like phenotype (Chapters 4-6). As adults, these animals are anovulatory and have ovarian follicles with larger antra. In addition the ovaries from TP treated animals develop a greater stromal compartment in comparison to controls, like those observed in PCO studies (Fulghesu, Ciampelli et al. 2001; Fulghesu, Angioni et al. 2007). Furthermore these animals develop central obesity and gain weight after weaning, with a significant proportion of this weight gain attributable to increases in the mesenteric (central) adipose tissue depot, as often also occurs women with PCOS at adolescence (Rossi, Sukalich et al. 2008). Insulin resistance and glucose intolerance also results from neonatal TP exposure with raised levels of both fasting insulin and glucose (Chapter 6).

These findings are in concordance with other rodent studies into neuroendocrine development, in which neonatal steroid treatment in the rat can lead to reproductive and metabolic dysfunctions in the adult animal. Such effects on reproduction and metabolism have been reported after administration of TP (McDonald and Doughty 1972; Sheridan, Zarrow et al. 1973; Alexanderson, Eriksson et al. 2007), free T (Alklint and Norgren 1971), estradiol valerate (Brawer, Naftolin et al. 1978; Brawer, Munoz et al. 1986; Rosa, Guimaraes et al. 2003), and in some studies high doses of DHT (Iguchi and Takasugi 1981; Mizukami, Yamanouchi et al. 1982). Additionally, rodent investigations into metabolic syndrome development have used synthetic glucocorticoids like DEX, administered during the end of fetal life to program glucose intolerance, insulin resistance and increased adiposity in both male and female adult animals (O'Regan, Kenyon et al.

2004; Seckl 2004; Drake, Livingstone et al. 2005). In the male neonatal rat aromatase expressed in the brain converts testosterone into estrogen, which masculinises the HPG and neuroendocrine axes. Thus, the effects of TP which we see in studies that investigate developmental programming of the mammalian endocrinology may be due to either the actions of androgens, estrogens, or indeed a combination of both.

Early investigations into the developmental origin of sexual behaviour and preference in monkeys used *in utero* testosterone treatment and noted that androgenised primate females did not exhibit regular menstrual cycles (Goy and Phoenix 1972; Pomerantz, Goy et al. 1986; Goy, Bercovitch et al. 1988; Pomerantz, Roy et al. 1988). Researchers then postulated that abnormal androgen exposure during a key window of development could potentially explain the origin of PCOS. However, androgens may also be converted to estrogens by placental aromatase during mammalian fetal development (Means, Mahendroo et al. 1989; Corbin, Khalil et al. 1995). Recent studies in sheep and non-human primates have attempted to address this by comparing the effects of TP to those of a non-aromatisable androgen, DHT (Goy, Bercovitch et al. 1988; Masek, Wood et al. 1999; Steckler, Manikkam et al. 2007; Ortega, Salvetti et al. 2009; Smith, Steckler et al. 2009; Ortega, Rey et al. 2010). However, such research is highly costly and time consuming to perform due to the long gestational length of the animals. Another major caveat of using *in utero* steroid administration to induce a PCOS-like phenotype in an adult mammal is that high doses of steroid must be used in order for the drug to cross the placental barrier.

Given that rodent neuroendocrine development mostly occurs after birth, the rat therefore provides an ideal model to elucidate which aspects of endocrine dysfunction result from developmentally timed exposure to aromatisable androgens. Whether these characteristics are a consequence of androgenic, estrogenic or stress hormone programming, will be the subject of this final investigative chapter.

7.2. Objectives

- To investigate which steroids administered during the early window of postnatal life produce a PCOS-like phenotype in the female rat; EV, TP, DHT, DHEA and DEX.

- To ascertain the effects of these steroids upon reprogramming of the hypothalamic-pituitary axis through measurement of both plasma and pituitary gonadotrophin content in addition to mRNA expression levels of the three gonadotrophin subunits.

- To ascertain the effects of these steroids upon reprogramming of the pituitary feedback through measurement of pituitary ER and GR expression.

- To further explore the effect that each steroid treatment has upon the numbers and proportions of ovarian follicles in the adult ovary at pnd 60 in line with previous investigations (Chapter 4).

- To elucidate the effects of different neonatal steroid treatments upon other endocrine organs such as liver, adrenal and fat depot weights.

- To further investigate the effect of neonatal steroid treatments upon the pancreas through glucose tolerance testing and subsequent analysis of insulin and glucose plasma levels.

7.3. Methods

Two litters of Wistar rats were used for each treatment group and 12 dams underwent timed-mating overnight with stud males. After birth all litters were sacrificed down to an *n*=8 animals at pnd 1 to prevent any differences in suckling and litter size from masking/causing a metabolic phenotype in the adult female animals (Champagne, Francis et al. 2003; Roma, Huntsberry et al. 2007). At weaning (pnd 21) any male litter mates were sacrificed and six females kept in each treatment group. Table 7.1 shows the *n* numbers and designations of each steroid treatment group.

Table 7.1 The number of animals in each experimental control and steroid treatment group: These groups correspond to those outlined in Figure 7.1. Birth litter numbers are divided by sex, animals were sacrificed to an *n=8* in each litter on the day of birth and then sacrificed to an *n=6* at weaning on pnd 21, except for C24 and DHEA22 which had an *n=5*.

Steroid given	**Number of pups**		**Final group *n* number**	
Pnd 1 – 6	Male	Female	Animal / litter designations	Group *n*
Control	5	9	**C20 A – F**	*n=11*
Control	3	5	**C24 A – E**	
Estradiol Valerate	7	11	**EV 15 A – F**	*n=12*
Estradiol Valerate	4	6	**EV 26 A – F**	
Testosterone Proprionate	5	8	**TP 19 A – F**	*n=12*
Testosterone Proprionate	4	6	**TP 25 A – F**	
Dihydrotestosterone	4	6	**DHT 16 A – F**	*n=12*
Dihydrotestosterone	0	8	**DHT23 A – F**	
Dehydroepiandrosterone	7	7	**DHEA 18 A – F**	*n=11*
Dehydroepiandrosterone	8	6	**DHEA 22 A – E**	
Dexamethasone	5	7	**DEX 17 A – F**	*n=12*
Dexamethasone	8	8	**DEX 21 A – F**	

7.3.1. Experimental outline

To elucidate which steroid treatment would produce a PCOS-like phenotype female rats were given a dose of each steroid or control oil during the early window

of postnatal life (with injections on pnd 1 and 4), in accordance with previous studies (Chapters 5 and 6). The steroid treatments are detailed in Table 7.2.

Table 7.2: Summary of steroid hormone injection protocols and doses administered:

Steroid	Dose(s)	How steroid was made up		
	(mg/kg)	Dry steroid (mg)	Ethanol (ml)	Oil (ml)
Testosterone proprionate (TP)	1mg/kg	100	0.5	9.5
Estradiol Valerate (EV)	1mg/kg	5	0.5	9.5
Dihydrotestosterone (DHT)	1mg/kg	5	0.5	9.5
Dehydroepiandrosterone (DHEA)	1mg/kg	5	0.5	9.5
Dexamethasone (DEX)	0.8mg/kg	4	0.5	9.5 (saline)

The treatment window and experimental outline are depicted in Figure 7.1 and the colours used in this figure will correspond to the same steroid treatment groups throughout this chapter.

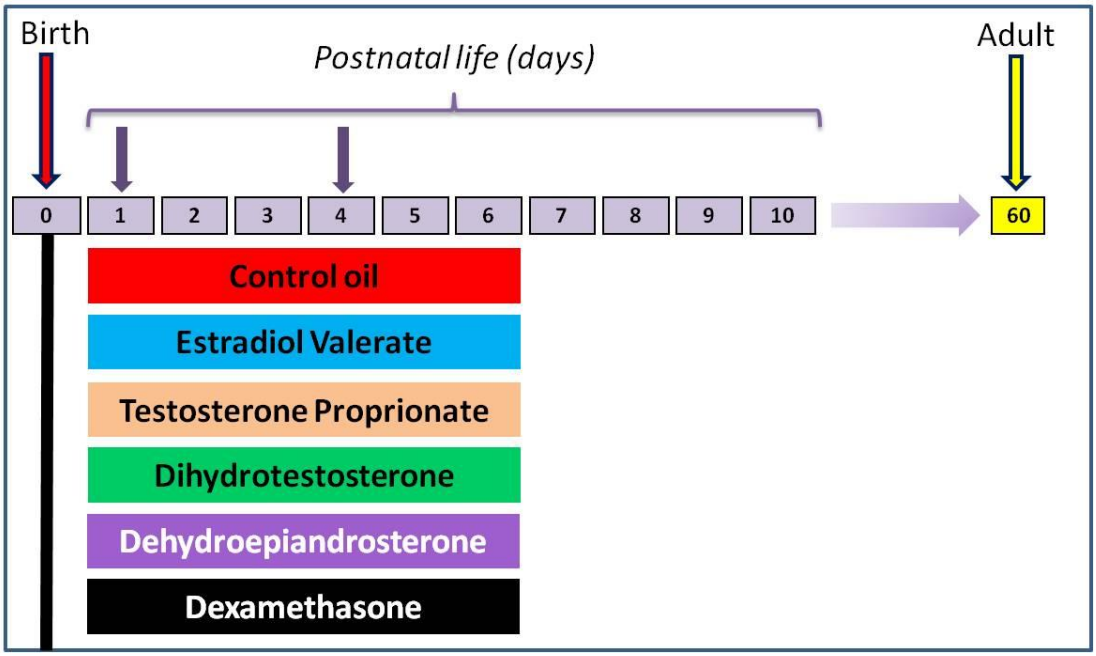

Figure 7.1 Schematic diagram to illustrate the windows of postnatal TP exposure in rats: Downward purple arrows indicate the days of steroid injection during postnatal life. The downward red and yellow arrows indicate the days of birth and sacrifice respectively.

7.3.2. Assessing insulin resistance and glucose tolerance

Insulin resistance and glucose tolerance were assessed after chow consumption measurements during this study. In week eight of life, animals underwent glucose tolerance testing (GTT). Briefly, rats were fasted overnight from 6pm, tail nick blood samples were taken over three time (*t*) points (*t*=0, *t*=30 and *t*=120 minutes) with the *t*=0 sample taken before gavage[‡‡] with a 50% (2g/kg) glucose solution. These blood samples were used for both insulin and glucose assays (Chapter 2, Sections 12 and 13).

7.3.3. Necropsy

The same tissues as in the previous studies (Chapters 5 and 6) were removed and weighed along with the ovary and uterus: Pituitary, liver, adrenal, retroperitoneal adipose, and mesenteric adipose. The hypothalamic area, a portion of subcutaneous adipose and a portion of skeletal quadriceps muscle were also removed but not weighed. One ovary and adrenal was frozen and the second was fixed in Bouins' solution before processing and embedding (Chapter 2, Section 4). Animals were sacrificed on or just after pnd 60 in week eight of life. Blood samples taken at sacrifice by cardiac puncture were spun down and plasma stored at -20ºC for future investigation of plasma gonadotrophin and hormone levels (Chapter 2, Sections 11 and 12).

7.3.4. Ovarian follicle counts

Ovaries from each litter were embedded together and serial sectioned at 5µm intervals. H&E staining was performed on every 10th section for follicle population analysis. Follicle counts were performed as before, with only follicles containing an oocyte nucleus counted and follicles classed based on their GC layering (Chapter 2, Section 6).

---

‡‡ Special thanks to Mr Mark Fisken for performing glucose gavages.

7.4. Results

7.4.1. Effects of exposure to various steroids on vaginal opening, oestrus cyclicity and ovarian morphology in the female rat

Smears were used to assess ovarian cyclicity in animals which developed a vaginal opening. Animals were subsequently grouped into ovulatory and non-ovulatory treatment groups based on assessments of smear cyclicity (Figure 7.2) and ovarian histology (Figure 7.3) after sacrifice.

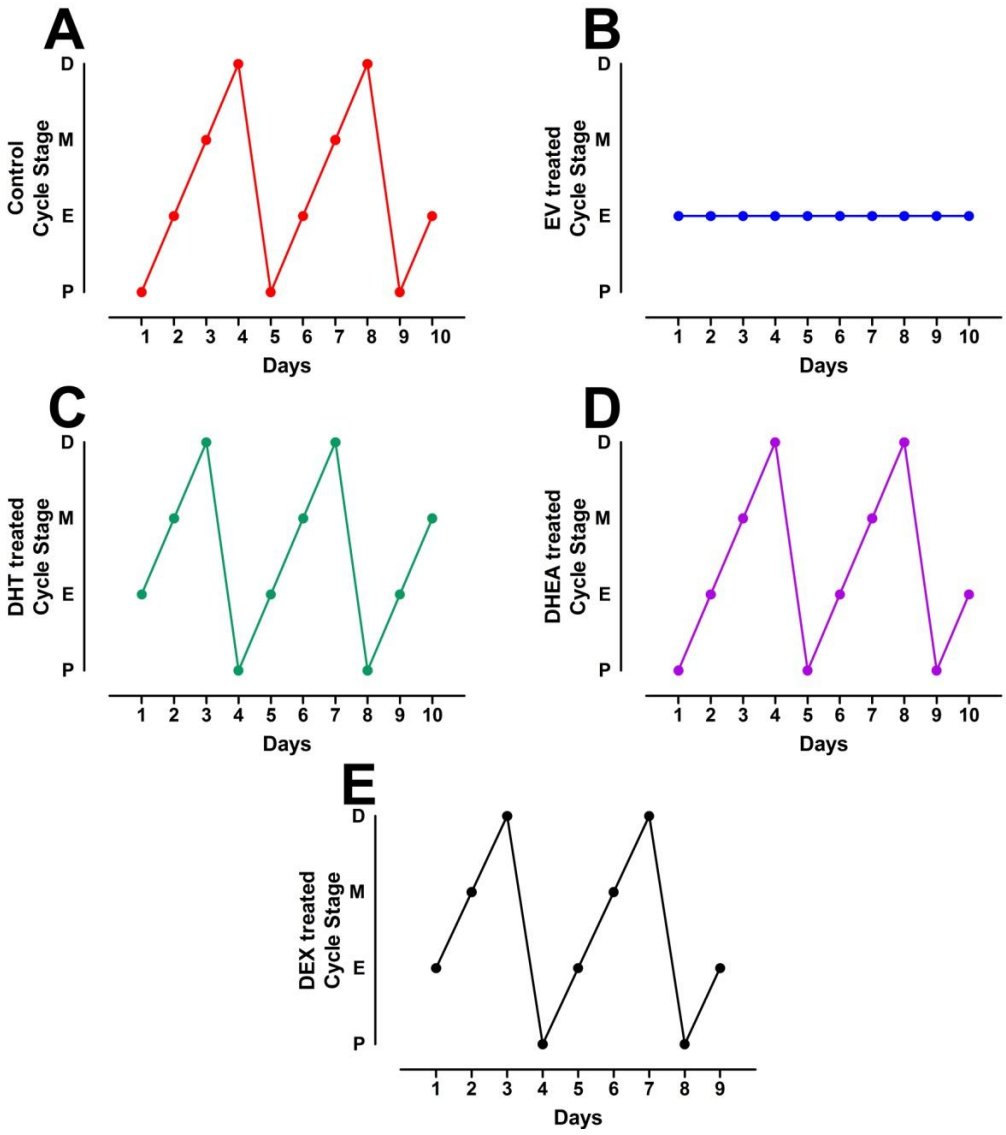

Figure 7.2: Typical estrus cyclicity of animals treated with (A) Control oil (B) EV (C) DHT (D) DHEA and (E) DEX treated animals. Estrus cycles monitored through Proestrus(P), Estrus(E), Metestrus(M) and Diestrus(D). TP treated animals and 5 of 12 DHT treated animals did not develop a vaginal opening.

Vaginal opening was again sensitive to androgen treatment, with all animals in TP treatment group and five of 12 animals in the DHT treatment group failing to develop vaginal openings also. Interestingly, although a vaginal opening did develop in all EV treated animals, in eight animals the opening was small and 'pin-hole' like. Animals treated with EV or TP were anovulatory as evidenced by a lack of CL upon histological examination, unlike ovaries from control, DHT, DHEA and DEX treated animals (Figure 7.3).

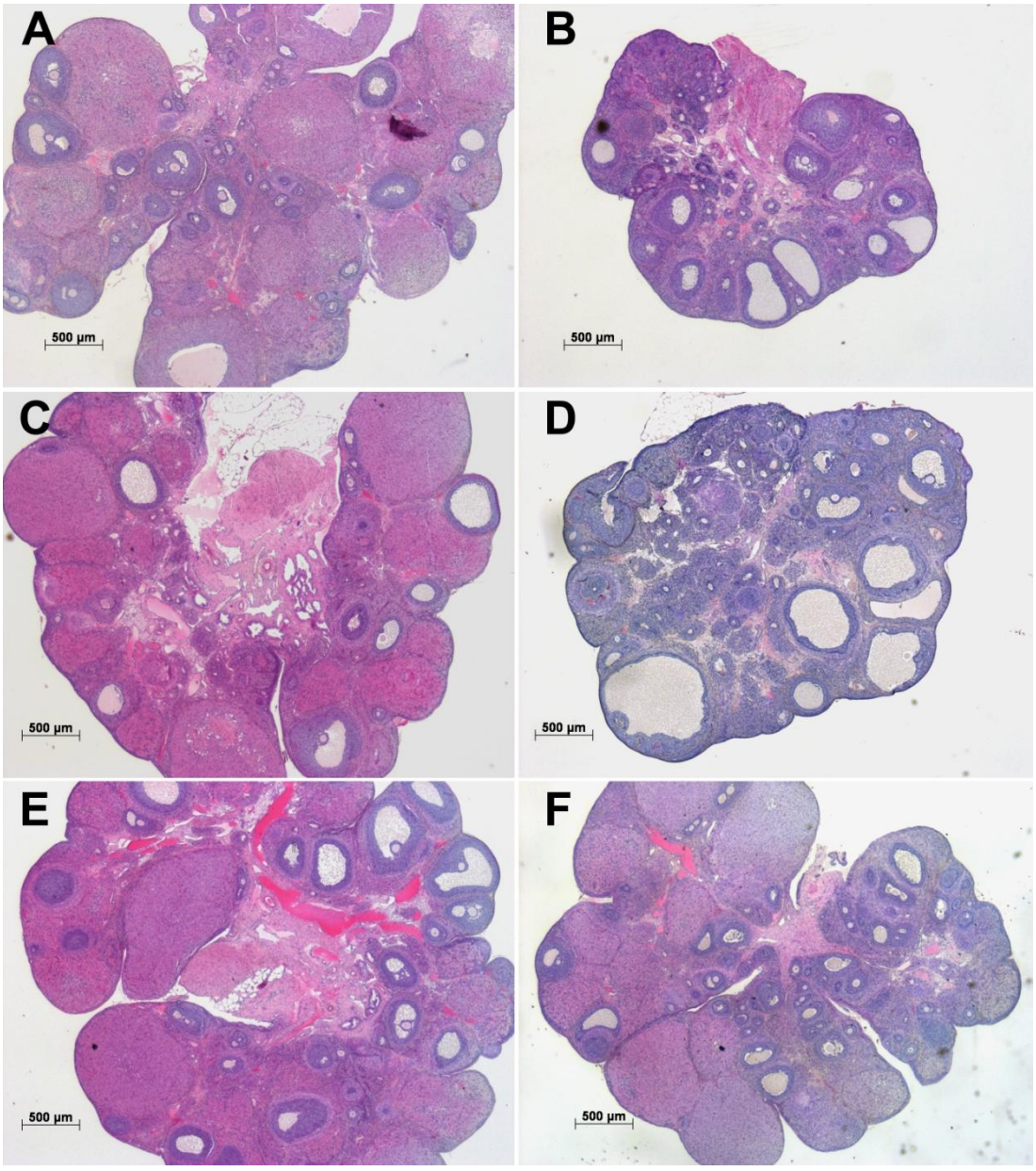

Figure 7.3: Ovarian morphology exemplary of animals treated with neonatal steroids compared to controls, shown for (A) control (B) EV and (C) DHT (D) TP (E) DHEA and (F) DEX treated animals. Images are of H&E stained sections shown at X 2 magnification.

Six ovaries from the control, TP, EV and DHT treatment groups were randomly selected for follicle analysis. Total follicle counts (Figure 7.4) showed that ovaries from animals treated with EV and TP had significantly fewer ovarian follicles (P≤0.001 and P≤0.01 respectively).

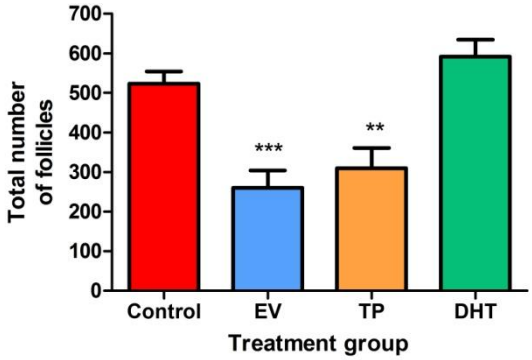

Figure 7.4: Total follicle count of ovaries from animals treated with EV, TP and DHT compared to controls. Values are shown for n=6 animals per treatment group and are expressed as the mean ±SEM. Results were analysed by student's unpaired t-test (**P≤0.01 *** P≤0.001).

To delineate which types of follicles were reduced in ovaries from animals at pnd 60 that received neonatal EV and TP, follicle populations were first assessed based on non growing follicle numbers and proportions i.e. primordial follicles (Figure 7.5). Ovaries from animals in the EV treatment group showed a significant reduction in primordial follicle numbers (P≤0.05). However, proportional analysis of primordial follicles showed that the EV and TP treatment groups had significantly greater proportions of primordial follicles (P≤0.05 and P≤0.001 respectively). Ovaries from animals in the DHT treated group showed no differences in primordial follicle numbers or proportions.

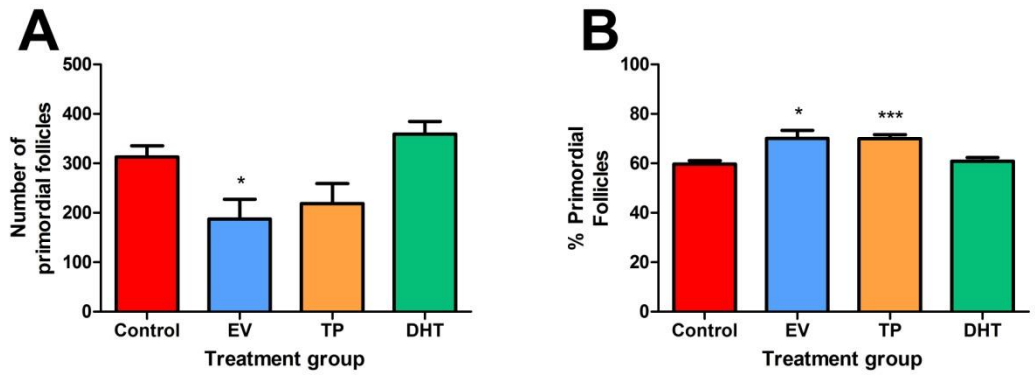

Figure 7.5: Primordial follicle (A) numbers and (B) proportions in ovaries from animals treated with EV, TP and DHT compared to controls. Values are shown for n=6 animals per treatment group and are expressed as the mean ±SEM. Results were analysed by student's unpaired t-test (* P≤0.05; *** P≤0.001).

Next, growing follicle numbers i.e. those between the primary and antral stages of follicular development were also assessed (Figure 7.6). Ovaries from animals in the EV and TP treatment groups both showed a significant reduction in growing follicle numbers (P≤0.001 and P≤0.01 respectively), whereas ovaries from animals in the DHT treated group showed no changes. Proportional analysis of growing follicles in the EV and TP treatment groups also showed them to be significantly reduced (P≤0.05 and P≤0.01 respectively), again with no differences in follicle proportions in ovaries from DHT treated animals.

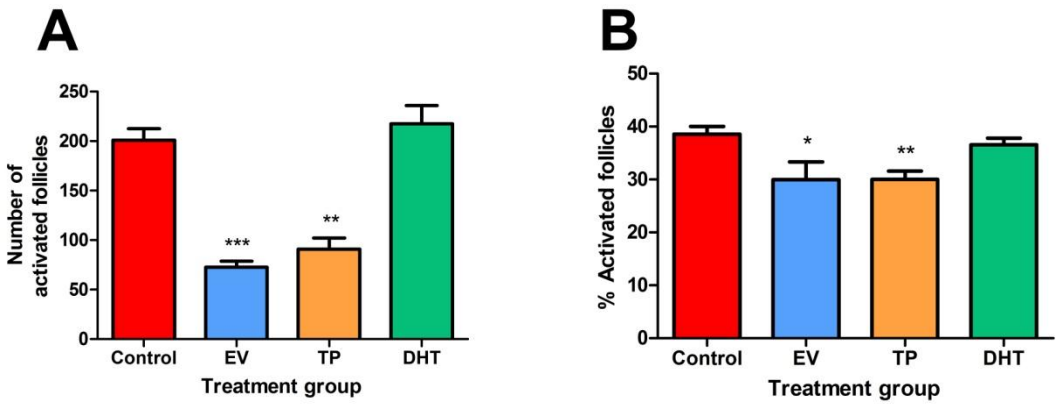

Figure 7.6: Developing follicle (A) numbers and (B) proportions in ovaries from animals treated with EV, TP and DHT compared to controls. Values are shown for n=6 animals per treatment group and are expressed as the mean ±SEM. Results were analysed by two-way ANOVA with Bonferroni post-hoc test (* P≤0.05; ** P≤0.01; *** P≤0.001).

To ascertain which types of growing follicles in ovaries from the EV and TP treatment groups were reduced, further follicle population classifications and proportional analysis was performed (Figure 7.7). Ovaries from animals which received neonatal EV and TP had significantly greater primordial follicle numbers and proportions (P≤0.001), with a significantly lower proportion of growing antral (P≤0.001) follicles. Additionally, ovaries in the EV treated group also had a reduced proportion of growing secondary (P≤0.05) follicles. Ovaries from animals in the DHT treated group once again had no differences in follicle numbers or proportions.

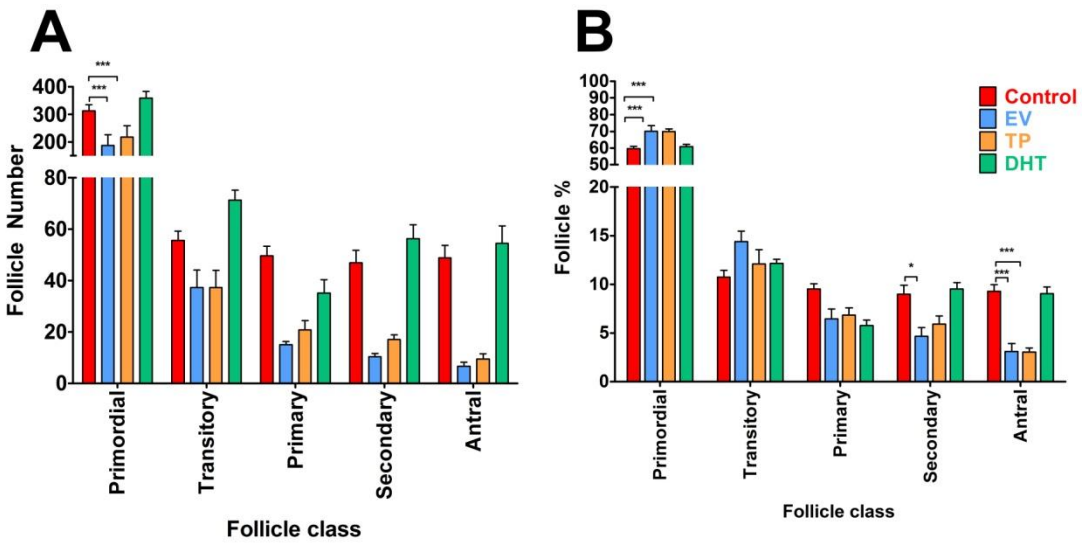

Figure 7.7: Follicle proportion analysis in ovaries from animals treated with EV, TP and DHT compared to controls. Values are shown for n=6 animals per treatment group and are expressed as the mean ±SEM. Results were analysed by two-way ANOVA with Bonferroni post-hoc test (* P≤0.05; *** P≤0.001).

7.4.2. Effects of exposure to various steroids upon the HPG axis

Results presented in this chapter were also analysed in relation to estrus cycle stages between control and ovulatory animals. Such analyses are presented based on estrus cycle stage when significant differences between proestrus and met/diestrus animals occurred.

Uterine and ovarian weights were significantly reduced in animals treated with EV (P≤0.001) and TP (P≤0.05 and P≤0.001 respectively). In addition, the uterine weights of animals treated with DHEA were significantly lighter than those of control animals (P≤0.01), even when accounting for the different estrus cycle stages between treatment groups (data not shown).

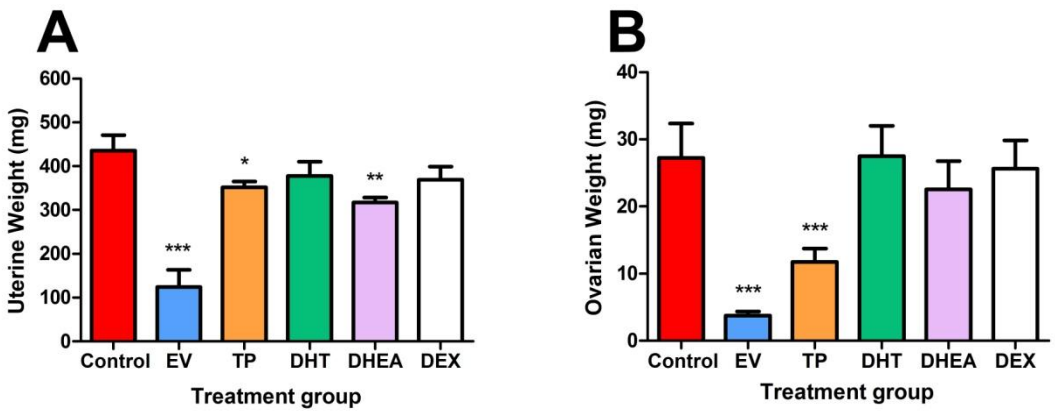

Figure 7.8: (A) Uterine weights and (B) Ovarian weights across treatment groups: Shown for control (n=11), EV (n=12), TP (n=12), DHT (n=12), DHEA (n=11) and DEX (n=12) treated animals. Values are expressed as the mean ±SEM and were analysed by student's unpaired t-test (for uteri against control proestrus (Pro) uterine weights (* P≤0.05; ** P≤0.01; ***P≤0.001).

Animals in the EV, TP and DEX treatment groups did not exhibit significant changes in plasma ovarian androgen levels (Figure 7.9). However animals treated with DHEA showed reduced levels of plasma T ($P \leq 0.05$), and animals treated with DHT showed reduced levels of A4 ($P \leq 0.01$).

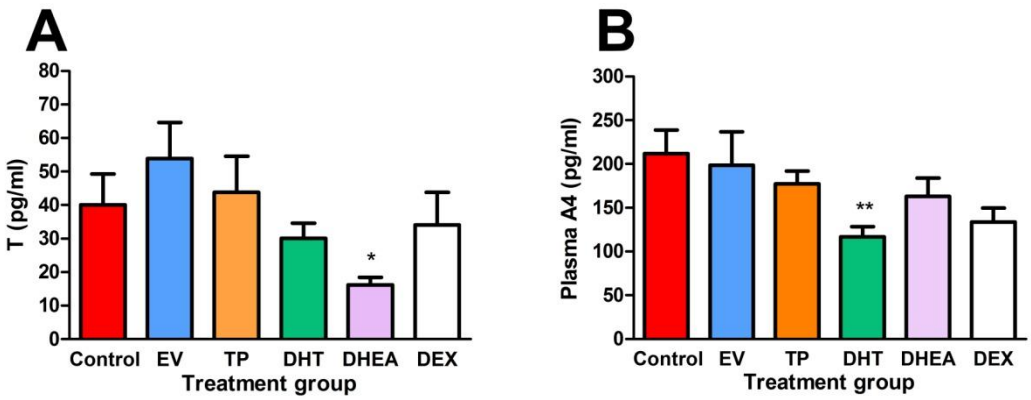

Figure 7.9: (A) Testosterone-T and (B) Androstenedione-A4 steroid hormone levels across treatment groups: Shown for control (n=11), EV (n=12), TP (n=12), DHT (n=12), DHEA (n=11) and DEX (n=12) treated animals. Values are expressed as the mean ±SEM and were analysed by student's unpaired t-test (* P≤0.05; ** P≤0.01).

Analysis of circulating ovarian feedback hormone levels (E2 and inhibin B) showed no significant differences between ovulatory treatment groups when analysed by estrus cycle stage (Figure 7.10). However, in non-ovulatory EV and TP treatment groups, E2 and inhibin B levels were significantly lower when compared to both control proestrus and di/metestrus levels (P≤0.001).

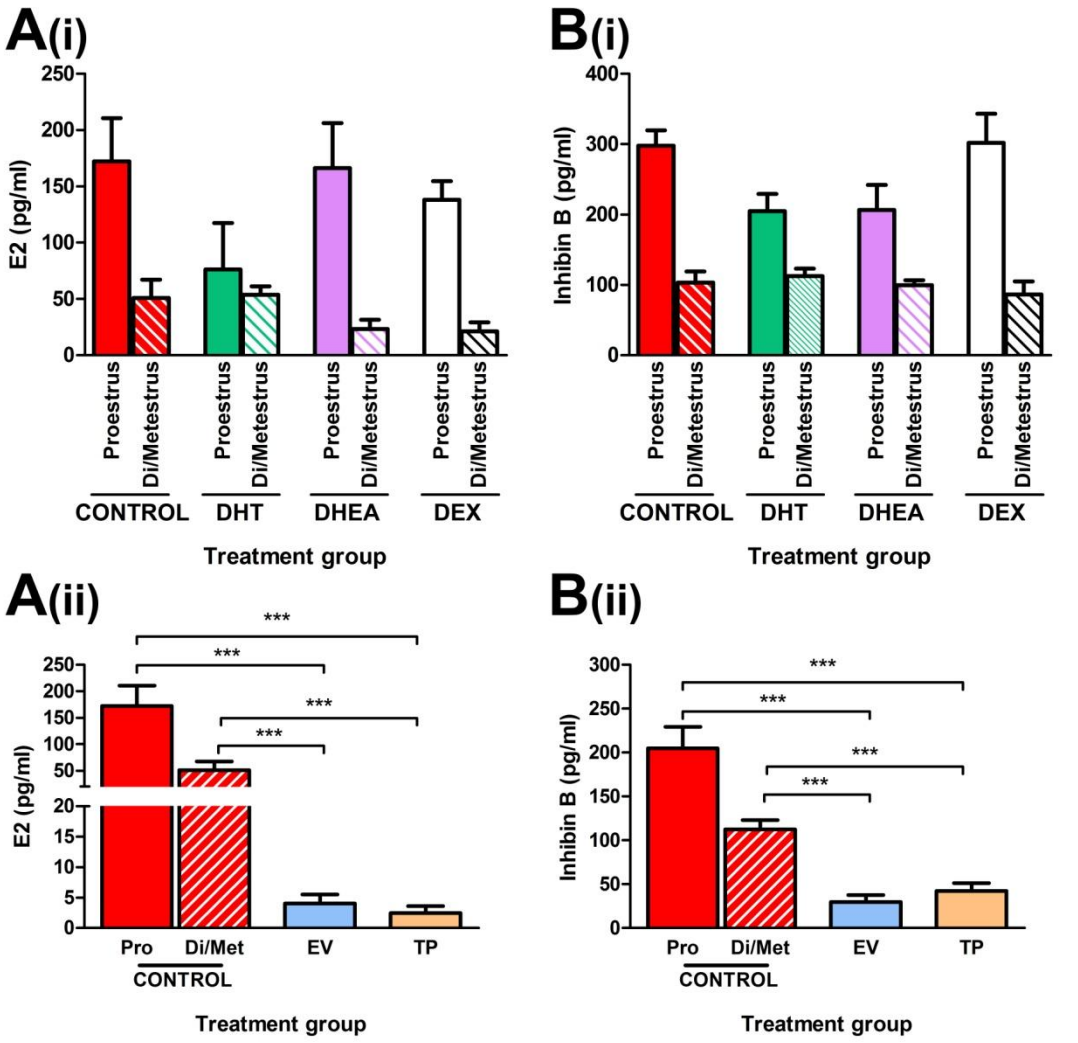

Figure 7.10: (i) Estradiol-E2 and (ii) Inhibin B hormone levels for (A) ovulatory treatment groups and (B) non ovulatory treatment groups: Shown for control (n=11), DHT (n=12), DHEA (n=11), DEX (n=12), EV (n=12) and TP (n=12) treated animals. Values are split based on the time of estrus cycle sacrifice for control and ovulatory treatment groups. Graphs express the mean ±SEM and were analysed by student's unpaired t-test (***P≤0.001).

To investigate whether neonatal androgen or EV treatment affected pituitary gonadotrophin secretion, circulating gonadotrophin levels were measured (Figure 7.11). No differences in FSH levels were observed across treatment groups although LH levels were significantly raised in animals from the DHEA treatment group ($P \leq 0.05$). No further differences were observed when gonadotrophin levels were analysed by estrus cycle stage in any treatment group (data not shown).

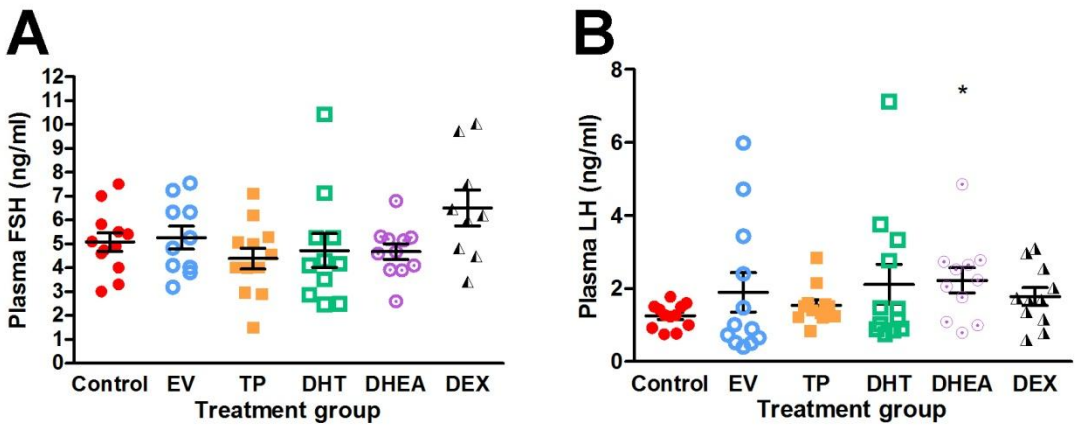

Figure 7.11: (A) Plasma FSH and (B) plasma LH levels across treatment groups: Shown for control (n=11), DHT (n=12), DHEA (n=11), DEX (n=12), EV (n=12) and TP (n=12). Values expressed are actual with the mean ±SEM shown in black. Results were analysed by student's unpaired t-test (* P≤0.05).

To assess the effects of postnatal steroids upon pituitary gonadotrophin storage, homogenised quartered pituitaries underwent gonadotrophin analysis at both the protein (Figure 7.12) and mRNA level (Figure 7.13). No significant differences in pituitary FSH or LH content were found across steroid treatment groups when compared to controls.

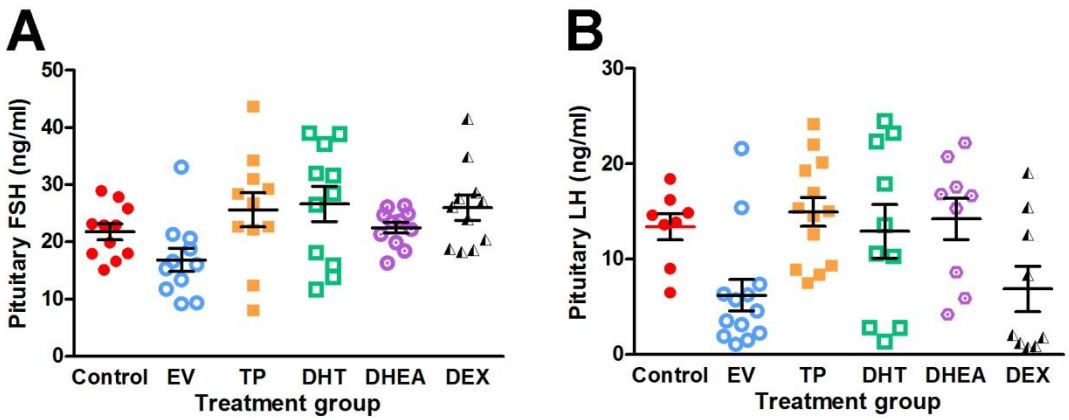

Figure 7.12: (A) Pituitary FSH (B) pituitary LH protein levels across steroid treatment groups: Shown for control (n=11), EV (n=12), TP (n=12), DHT (n=12), DHEA (n=11) and DEX (n=12) treated animals. Values expressed are actual with the mean ±SEM shown in black, and were analysed by student's unpaired t-test.

Pituitary weight was significantly lower in EV treated animals ($P \leq 0.001$) and significantly heavier ($P \leq 0.01$) in TP treated animals (Figure 7.13). No changes in αGSU, LHβ or FSHβ subunit gene expression were observed across steroid treatment groups, except for in EV treated animals, which had significantly raised levels of αGSU and FSHβ expression ($P \leq 0.05$). Pituitary AR and GR expression was also analysed by PCR (Figure 7.14). No changes in AR expression were observed across steroid treatment groups, but pituitary GR expression was greater in animals from the EV ($P \leq 0.01$) and DEX ($P \leq 0.05$) steroid treatment groups.

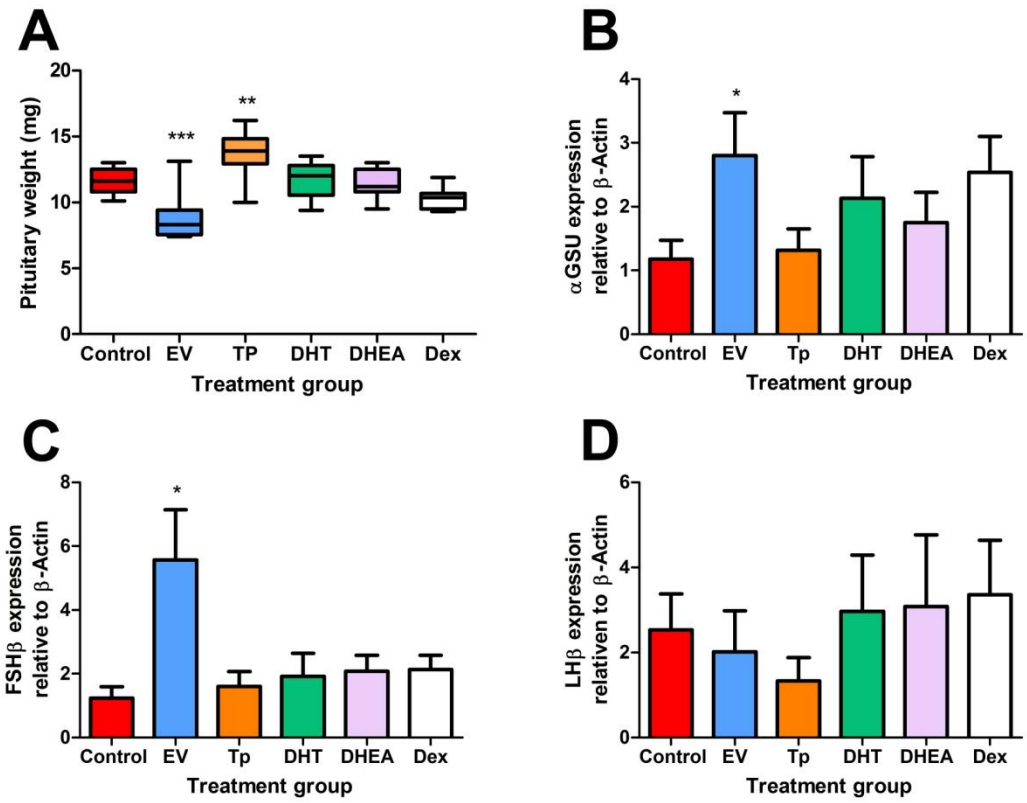

Figure 7.13: (A) Pituitary weight and expression of (B) αGSU (C) FSHβ subunit and (D) LHβ subunit across steroid treatment groups: Shown for control (n=11), EV (n=12), TP (n=12), DHT (n=12), DHEA (n=11) and DEX (n=12) treated animals. Values are expressed as (A) the median and data spread using a box plot and (B-D) the mean ±SEM. Results were analysed by student's unpaired t-test (* P≤0.05; ** P≤0.01; ***P≤0.001).

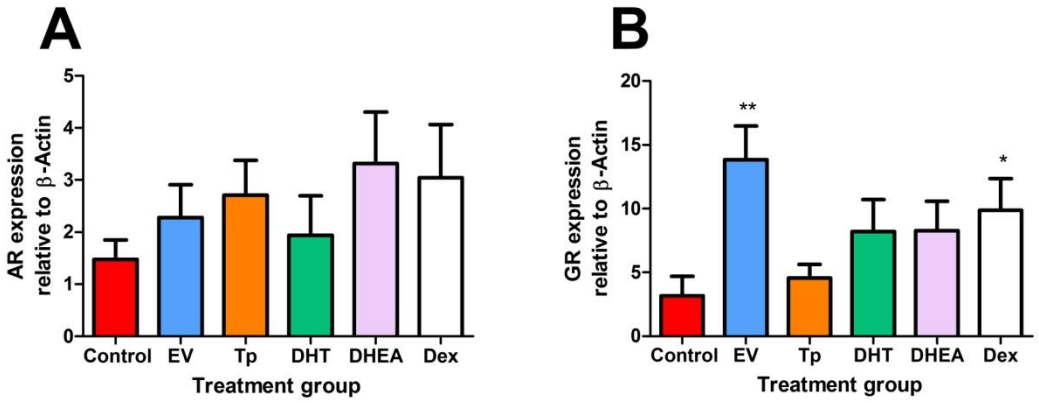

Figure 7.14: Expression of pituitary (A) Androgen receptor-AR and (B) Glucocorticoid receptor-GR, across steroid treatment groups: Shown for control (n=11), EV (n=12), TP (n=12), DHT (n=12), DHEA (n=11) and DEX (n=12) treated animals. Values are expressed as the mean ±SEM and were analysed by student's unpaired t-test (* P≤0.05; ** P≤0.01; *** P≤0.001).

7.4.3. Effects of exposure to various steroids growth, fat and the liver

Animals from the EV, TP and DHT steroid treatment groups were significantly heavier by pnd 65 when compared to control animals (P≤0.001, P≤0.05 and P≤0.01 respectively). These differences in body weight did not occur at weaning (Figure 7.15), as was the case in previous studies (Chapters 5 and 6).

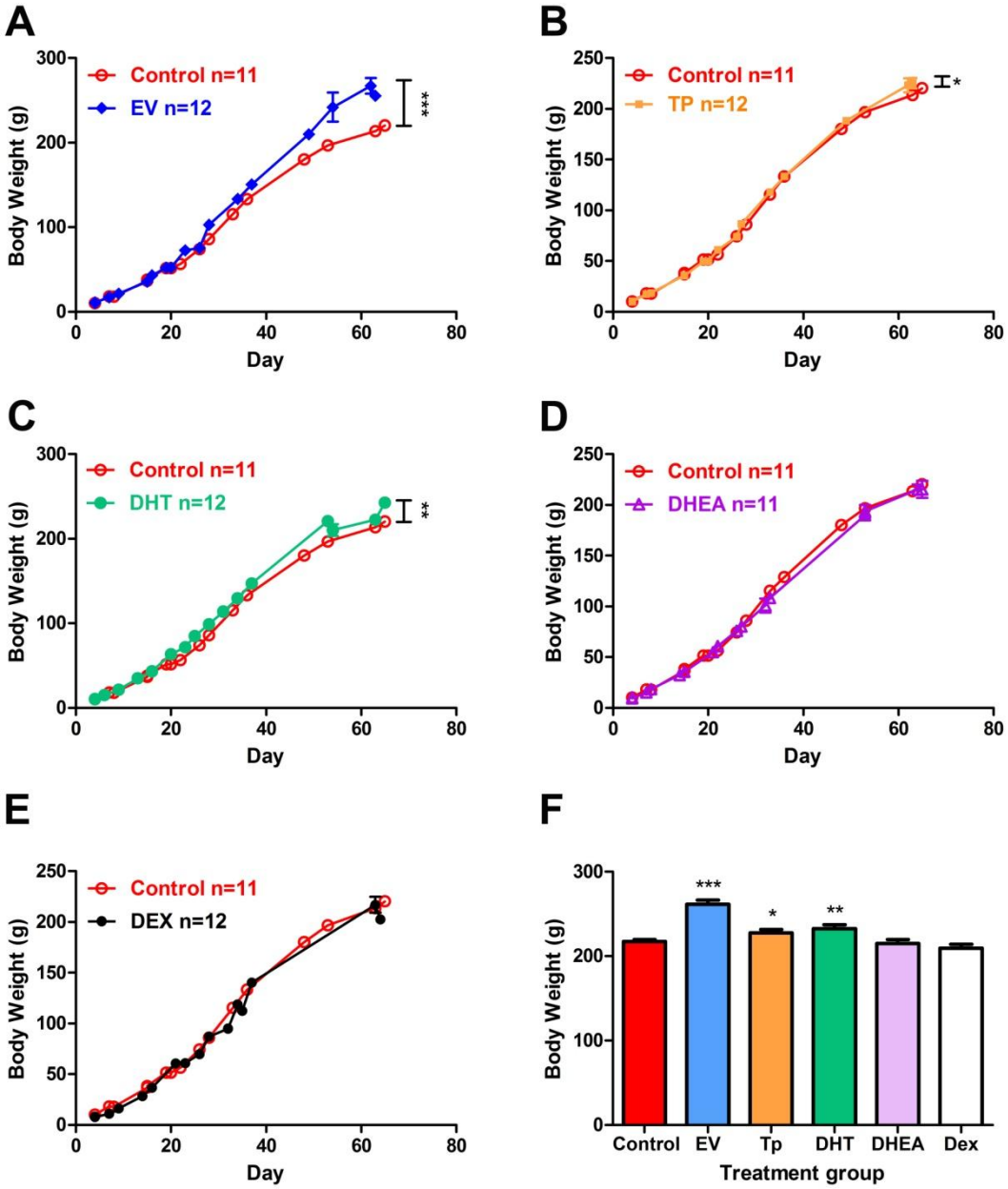

Figure 7.15: Effects of steroid hormones upon pup growth: Control versus (A) TP (B) EV (C) DHT (D) DHEA and (E) DEX treated animals with (F) adult body weight at day 65 with *n* numbers as shown. Values are expressed as the mean ±SEM and were analysed by student's unpaired t-test (* P≤0.05; ** P≤0.01; *** P≤0.001).

To assess for any changes in anabolism, in addition to measuring body weight at the time of sacrifice, animal length was also measured from snout to anus and to tail tip (Figure 7.16). Animals from the EV and DHT steroid treated groups were significantly longer than control animals (P≤0.01), while animals treated with DHEA were significantly shorter when compared to controls (P≤0.05).

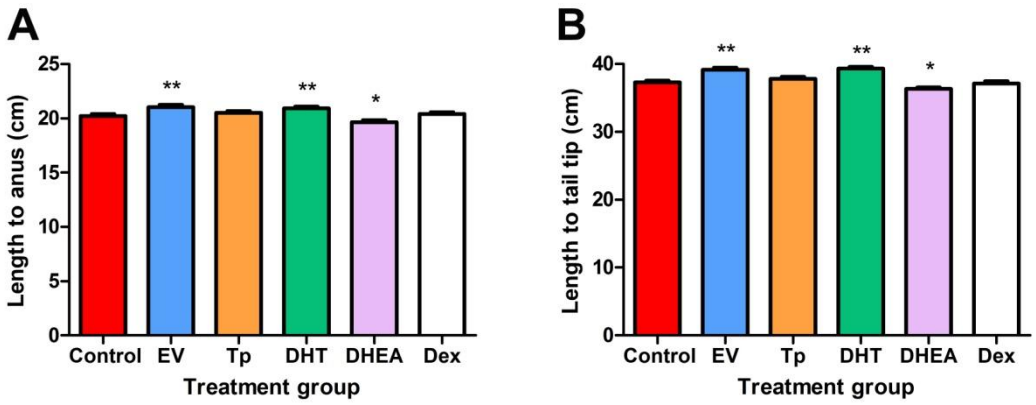

Figure 7.16: Anabolic measurements of body length from (A) snout to anus and (B) snout to tail tip across steroid treatment groups: Shown for control (n=11), EV (n=12), TP (n=12), DHT (n=12), DHEA (n=11) and DEX (n=12) treated animals. Values are expressed as the mean ±SEM and were analysed by student's unpaired t-test (* P≤0.05; **P≤0.01).

At sacrifice, mesenteric and retroperitoneal fat pads were dissected out and weighed to assess for any differences in fat deposition between steroid treated groups (Figure 7.17). Mesenteric fat weight was significantly greater in animals from the EV and TP treatment groups (P≤0.05 and P≤0.01 respectively) and significantly lighter in animals from the DEX treatment group (P≤0.05). However, although this difference was removed by dividing the fat depot weight by body weight in the EV and DEX treated animals, this was not the case in animals from the TP treated group (P≤0.01). DEX treated animals also had a reduced retroperitoneal fat depot weight in comparison to control animals, and this difference was not removed by adjusting for body weight (P≤0.05).

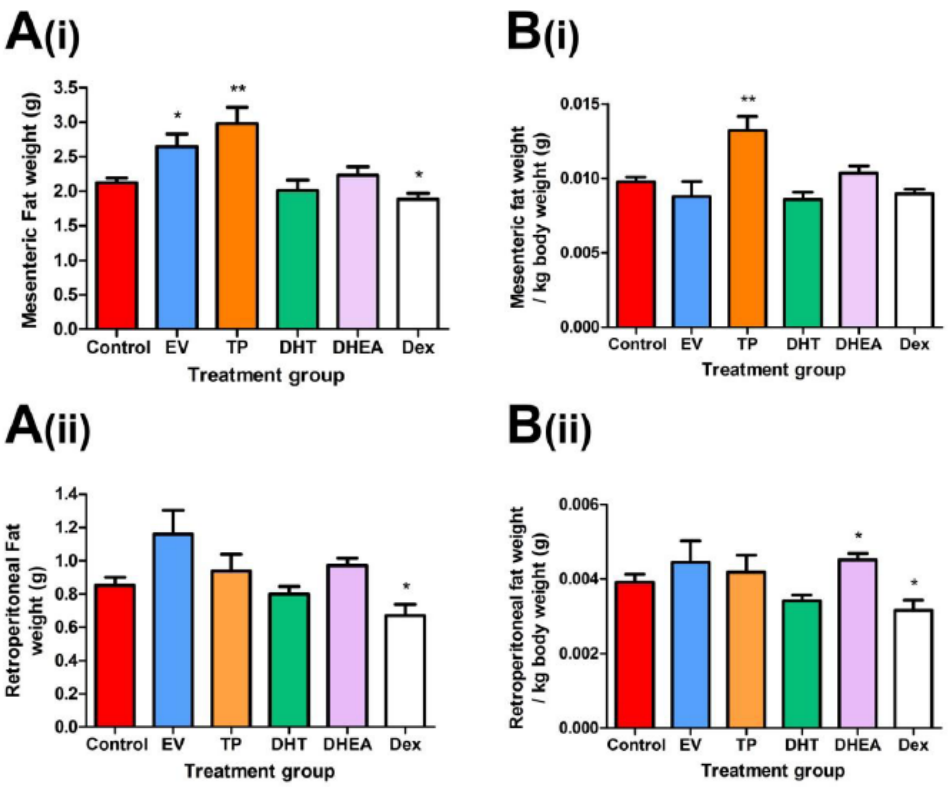

Figure 7.17: (A) Gross weight of (i) mesenteric and (ii) retroperitoneal fat depots (B) shown per g body weight across steroid treatment groups: Shown for control (n=11), EV (n=12), TP (n=12), DHT (n=12), DHEA (n=11) and DEX (n=12) treated animals. Values are expressed as the mean ±SEM and were analysed by student's unpaired t-test (* P≤0.05; **P≤0.01).

Liver weight (Figure 7.18) at sacrifice was significantly greater in EV, TP and DHT treated animals when compared to controls ($P \leq 0.001$, $P \leq 0.05$ and $P \leq 0.05$ respectively). These differences remained when liver weight was divided by animal body weight ($P \leq 0.01$, $P \leq 0.001$ and $P \leq 0.01$ respectively). Neonatal EV and DHT treatment significantly increased animal adrenal weight in these treatment groups ($P \leq 0.001$), whilst TP treatment significantly reduced it ($P \leq 0.01$), when compared to that of control animals (Figure 7.19).

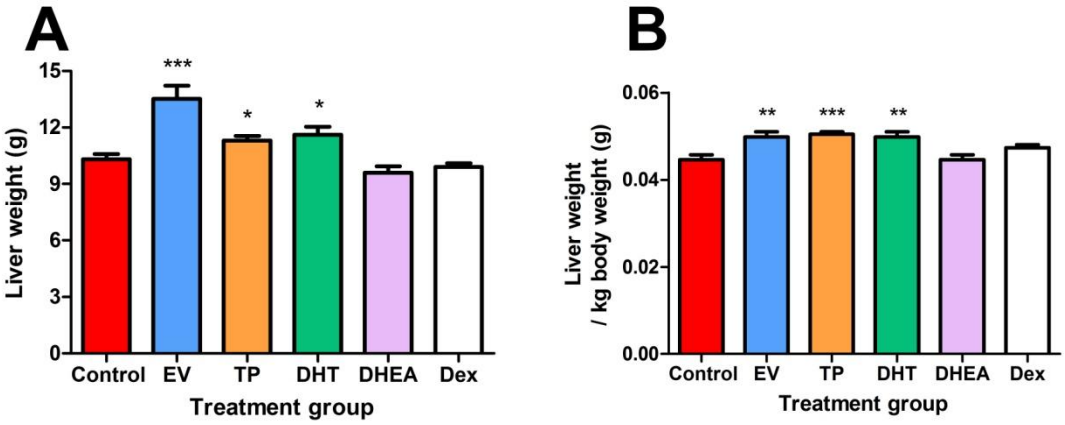

Figure 7.18: (A) Liver weights (B) expressed per g body weight across steroid treatment groups: Shown for control (n=11), EV (n=12), TP (n=12), DHT (n=12), DHEA (n=11) and DEX (n=12) treated animals. Values are expressed as the mean ±SEM and were analysed by student's unpaired t-test (* P≤0.05; ** P≤0.01; *** P≤0.001).

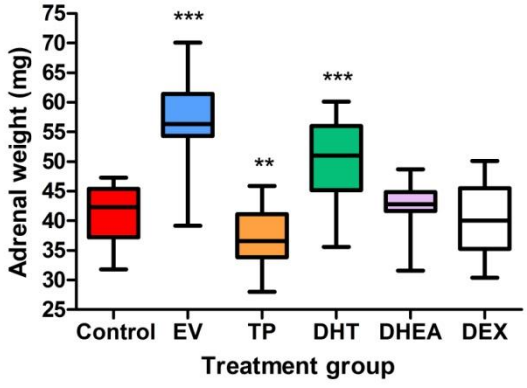

Figure 7.19: Adrenal weight across steroid treatment groups: Shown for control (n=11), EV (n=12), TP (n=12), DHT (n=12), DHEA (n=11) and DEX (n=12) treated animals. Values are expressed as the median and data spread using a box plot and were analysed by student's unpaired t-test (**P≤0.01; *** P≤0.001).

7.4.4. Effects of exposure to various steroids upon insulin and glucose metabolism

Plasma samples taken at *t*=0, 30 and 120 minutes after glucose gavage were used to analyse insulin and glucose levels. The mean insulin response to glucose over two hours is shown for each TP treatment group in Figure 7.20. Analysis of plasma insulin *t*=0 was used to determine the fasting insulin levels, whilst area under the curve analysis of the insulin response to glucose was undertaken to determine if animals were insulin resistant (Figure 7.21).

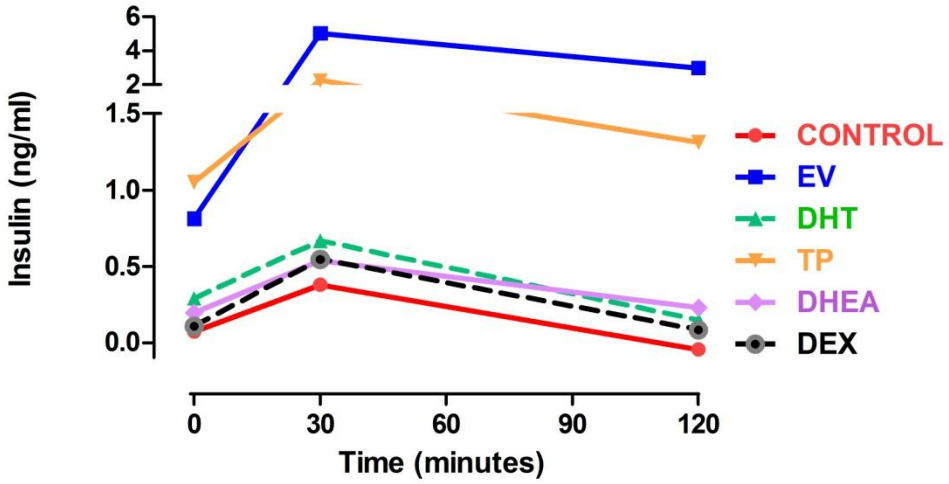

Figure 7.20: Insulin response to glucose gavage: Shown for control (n=11), EV (n=12), TP (n=12), DHT (n=12), DHEA (n=11) and DEX (n=12) treated animals. Values are expressed as the mean ±SEM and were analysed for the area under the curve.

Animals in the EV, DHT and DHEA treatment groups had significantly higher fasting insulin levels than controls ($P \leq 0.001$, $P \leq 0.01$ and $P \leq 0.05$ respectively) and TP treated animals showed a trend for high fasting insulin levels ($P \leq 0.057$). These four treatment groups also showed significantly greater insulin response to glucose than control animals ($P \leq 0.001$). Animals treated with DEX showed fasting insulin levels and an insulin response to glucose comparable to that of control animals.

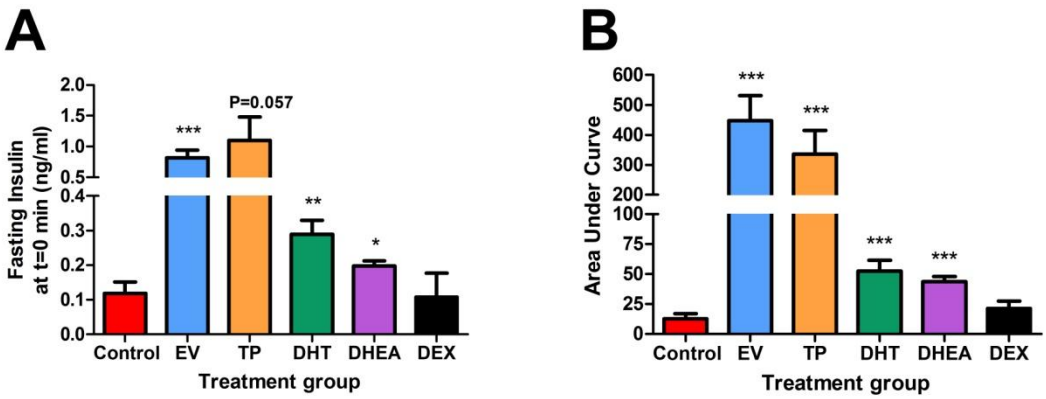

Figure 7.21: (A) Fasting insulin levels and (B) area under the curve analysis of insulin response to glucose: Shown for control (n=11), EV (n=12), TP (n=12), DHT (n=12), DHEA (n=11) and DEX (n=12) treated animals. Values are expressed as the mean ±SEM and were analysed by student's unpaired t-test (* P≤0.05; ** P≤0.01; *** P≤0.001).

The mean blood glucose levels after glucose gavage are shown for each treatment group in Figure 7.22.

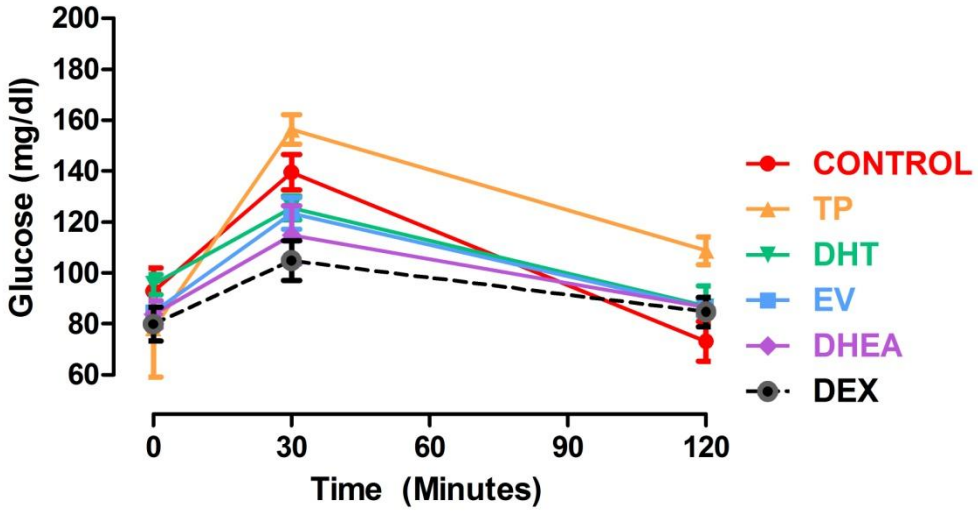

Figure 7.22: Blood glucose levels after to glucose gavage: Shown for control (n=11), EV (n=12), TP (n=12), DHT (n=12), DHEA (n=11) and DEX (n=12) treated animals. Values are expressed as the mean ±SEM and were analysed for the area under the curve.

Analysis of plasma glucose at *t*=0 was used to determine fasting glucose levels, whilst area under the curve analyses of the blood glucose levels after gavage were undertaken to determine if animals were glucose tolerant.

All steroid treatment groups showed no differences in fasting glucose or glucose tolerance when compared to control animal values (Figure 7.23).

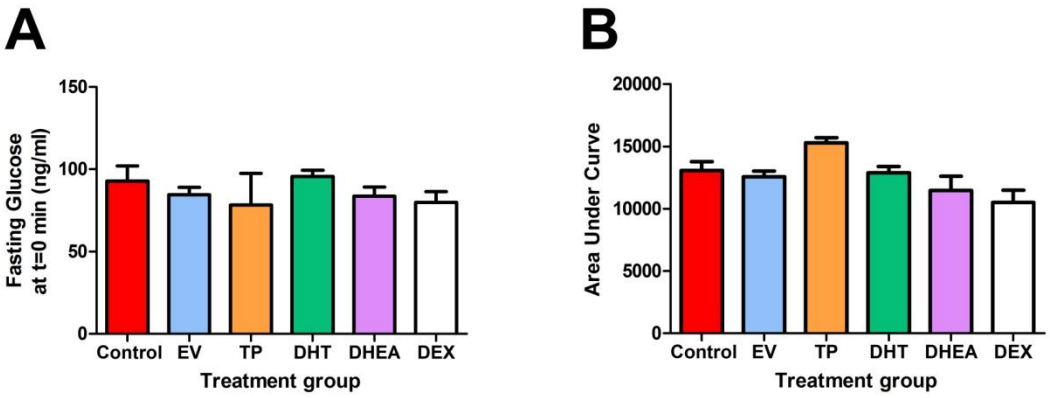

Figure 7.23: (A) Fasting glucose levels and (B) area under the curve analysis of blood glucose after glucose gavage: Shown for control (n=11), EV (n=12), TP (n=12), DHT (n=12), DHEA (n=11) and DEX (n=12) treated animals. Values are expressed as the mean ±SEM and were analysed by student's unpaired t-test.

7.5. Discussion

The experiments described in this chapter have shown that a combination of androgenic and estrogenic action may be responsible for the reproductive and metabolic dysfunction observed in the neonatally androgenised rat model of PCOS previously described (Chapters 4-6).

7.5.1. Effects of postnatal steroid exposure upon the ovary and ovarian hormones

Both early postnatal EV and TP treatment led to a loss of ovarian cyclicity in adult animals by pnd 65, leading to reduced ovarian weight in these treatment groups. The reduction in uterine weight observed in the DHEA treatment group, although potentially accounted for by differences in estrus cycle stage, may also point towards the developmental programming of the uterus by an abnormal steroid milieu during early postnatal life in the rodent. Studies into the effects of postnatal androgens upon the uterus have shown that neonatal TP, in addition to neonatal clomifene treatment in rats, leads to a reduced uterine response to exogenous E2 in the adult animal, with a thinner myometrial membrane sand reduced number of glandular cells (White, Moore et al. 1981; Mena, Arriaza et al. 1992). Although the low uterine weights found in TP and EV treated animals can potentially be attributed to the reduced levels of E2 and inhibin B, further investigation into the effects of neonatal steroid treatment upon the development of rat uterine morphology and function are required.

At the hormonal level, circulating E2 and inhibin B levels were significantly reduced even when compared to those of control metestrus animals. These results are in line with those found in previous investigations (Chapters 5 and 6) and other studies in neonatally androgenised rodents (Barraclough 1961; Barraclough and Haller 1970). In the current study, non-ovulatory treatment groups (TP and EV) showed no differences in circulating ovarian androgens levels (T or A4). Normal androgen levels were observed in another model of PCOS where rats received EV or

DHT within three hours of birth. However, in this same study animals treated with TP had reduced plasma levels of T (Alexanderson, Eriksson et al. 2007). Additionally, a separate investigation reported that early window TP led to an increase in circulating T levels in female offspring (vom Saal and Bronson 1980). Thus, whether neonatally androgenised or estrogenised rodents develop hyperandrogenaemia remains a moot point due to the variability of findings from other published rodent PCOS models.

Animals treated with DHT and DHEA had reduced levels of plasma A4 and T respectively. These differences could be attributed to the androgenic programming of the rodent adrenal or liver since these organs are responsible for endocrine androgen production and steroid hormone catabolism respectively. Moreover differences in SHBG or other hormone binding proteins may exist. The regulation by steroid hormones upon hormone binding proteins have been shown across several species including humans; corticosteroid binding globulin is reduced in the offspring of sows stimulated with ACTH during late gestation, and SHBG is elevated in women who use oral contraceptives and remains elevated after discontinuation of long term use (Kanitz, Otten et al. 2006; Panzer, Wise et al. 2006). SHBG binds around 66% of free T in humans and decreases in association with several factors, including reduced circulating estrogens (also found in this study), hyperandrogenaemia, high glucocorticoids, growth hormone and prolactin, in addition to insulin and obesity – many of which are also features of PCOS (Botwood, Hamilton-Fairley et al. 1995). Additional investigations into intra- and extra-ovarian androgen levels in relation to the amount of free or bound sex-hormone binding globulin could therefore be pursued. This would help to elucidate whether any changes in bound or local ovarian hormone concentrations exist and provide further evaluation of the neonatally androgenised rat as a PCOS model.

Postnatal EV and TP exposure produced similar results with regard to ovarian follicle populations in the adult rat; reduced follicle numbers with greater primordial follicle proportions, reduced activated follicle numbers and reduced activated follicle

proportions at the secondary and antral level. DHT treatment did not have any effect upon ovarian follicle numbers or proportions. Similar changes have been reported in another study where rats were exposed to TP on pnd 1 of life (Ulloa-Aguirre, Damian-Matsumura et al. 1990). A loss of follicles was also reported in the TP exposed ovine mode of PCOS and greater proportions of primordial follicles were observed in the infant females of the non-human primate PCOS model (Smith, Steckler et al. 2009; Abbott 2010). Taken together these investigations indicate that neonatal estrogen, acting via either/both ERα and ERβ, may be responsible for the differences in follicle populations in the EV and TP treatment groups. Aromatase activity in the female rat pituitary and ovary during neonatal life may additionally be responsible for converting TP into estrogens (Picon, Pelloux et al. 1985; Carson and Smith 1986; Carretero, Vazquez et al. 2003; Johnson 2007). This notion is further supported by investigations into mouse germ cell nest breakdown and oocyte apoptosis, where loss of the maternal estrogenic milieu after birth in rodents leads to germ cell nest breakdown (Chen, Breen et al. 2009).

7.5.2. Effects of postnatal steroid exposure upon the hypothalamic-pituitary axis

The apparent lack of pituitary response to reduced E2 and inhibin B feedback in the TP treatment group is in line with earlier findings (Chapters 5 and 6) and may be due to a reprogramming of the hypothalamic-pituitary response to ovarian hormonal feedback. Since no changes in ovarian feedback hormones or pituitary gonadotrophin secretion were observed in DHT treated animals, but were observed in both EV and TP treatment groups, programming of the neonatal hypothalamic-pituitary axis by TP probably occurs via estrogenic hormonal action. It is possible that the pituitaries in EV and TP treated animals are more sensitive to ovarian feedback hormones and secrete normal levels of gonadotrophins in response to low levels of inhibin B and E2. Alternatively, the female pituitary may be masculinised by TP action in the same way that early postnatal T released from the immature testis acts to program to neuroendocrine axis in male rats (Carretero, Vazquez et al. 2003; Johnson 2007).

No differences in circulating or stored pituitary gonadotrophin levels were observed across steroid treatment groups, with the exception of DHEA treated which had raised levels of circulating LH. While this may be due to early morning sacrifice at precisely the LH surge in some animals of the DHEA treatment group, it could also be due to androgenic programming of the hypothalamic-pituitary axis. Indeed, an increased sensitivity of LH secretion in response to GnRH challenge has been reported in the fetally androgenised sheep PCOS model and high circulating levels of LH are one feature of PCOS (Manikkam, Thompson et al. 2008). Furthermore, the estrogenic effects of DHEA treatment must be considered in tandem with those found in the EV treatment group, since DHEA is a precursor steroid in estrogen biosynthesis (Chapter 1, Section 7).

Pituitary weight was reduced in EV treated animals. Data on pituitary weight has not been reported in other rodent studies of PCOS. It may be that the differences in pituitary weight observed in this study are the result of a trend reduction in stored LH and FSH protein. This data is supported by other investigations into the effects of specific ER modulators (for example raloxifene), administered neonatally to female rats, which show a reduction in pituitary gonadotrophin content, reduced LH release and alterations in the LH response to exogenous GnRH (Sanchez-Criado, Guelmes et al. 2002). TP treatment led to an increase in pituitary weight, as was reported in Chapters 5 and 6 and may again relate to levels of gonadotrophin protein storage and gene expression. At this point it is worth noting that the effects of neonatal steroids upon the hypothalamic-pituitary axis are not exclusive to GnRH and the gonadotrophs. Indeed other investigations have noted a disruptive effect of neonatal sex steroid administration upon lactotrophs, somatotrophs and the HPA axis (Gonzazalez-Parra, Argente et al. 2000; Bellido, Martin de las Mulas et al. 2003; Seale, Wood et al. 2005*a*; Seale, Wood et al. 2005*b*). Whilst these endocrine features were not examined here, future investigations into the effect of neonatal steroids upon trophic cell proportions, GnRH and GHRH would be useful in determining

which other aspects of the hypothalamic-pituitary axis are disrupted and/or masculinised by various steroid hormones.

One novel finding in relation to animals treated with EV is the presence of increased gene expression for αGSU, FSHβ and GR. The androgenic actions of TP (as well as DHT and DHEA) may act to reprogram pituitary gonadotrophin gene expression, protein storage and secretion – where EV treatment alone is insufficient to reprogram certain genes at the transcriptional level. One study has examined the effects of neonatal leptin treatment upon the HPAA and showed that adult hippocampal and hypothalamic GR content increased after neonatal leptin administration (Proulx, Clavel et al. 2001).

Moreover, animals in the DEX steroid treatment group also showed an increased level of pituitary GR expression. This result corroborates other findings which have shown programming of GR expression in the paraventricular nucleus through glucocorticoid action (Kapoor and Matthews 2008). In addition, DEX treatment has been shown to affect development of the HPAA (Seckl 2004). Thus investigations into the effects of early window postnatal DEX and other steroid hormones upon the HPAA are warranted, specifically to elucidate the effects of these hormones upon the development of the mammalian stress response by measuring plasma corticosteroid levels.

7.5.3. Effects of postnatal steroid exposure upon features of metabolism

Animals treated with EV, TP and DHT had all gained significant weight by pnd 65. These treatment groups also showed a significant increase in central mesenteric fat depot weight. In the EV and DHT treatment groups, this difference was removed adjusting for body weight. Further anabolic changes were noted in the EV, DHT and DHEA treatment groups, all of which had greater body lengths when compared to those of controls. In contrast, TP treated animals, despite showing a

greater body weight and mesenteric adipose depot at pnd 65, were no longer than controls. Similar increases in body weight have been reported in other rodent studies which use neonatal TP, DHT or EV steroid hormone treatment (Barraclough 1961; vom Saal and Bronson 1980; Alexanderson, Eriksson et al. 2007). In addition, sheep and non-human primate models of PCOS have demonstrated that fetal TP exposure leads to insulin resistance and visceral (central) fat accumulation (Bruns, Baum et al. 2007; Nada, Thompson et al. 2010; Padmanabhan, Veiga-Lopez et al. 2010; Veiga-Lopez, Lee et al. 2010).

The adrenal weights of TP treated animals were reduced (and yet increased in EV and DHT treatment groups). It may be that adrenal weight and anabolism (measured by body length) are related. Such differences in adrenal weight are thus a further indication that the effects of neonatal sex steroids upon the HPAA and growth hormone require further elucidation. One recent study into the effects of antimicrobial parabens upon endocrine organ development have shown that neonatal exposure to these estrogenic compounds increases adult adrenal weight, and has negative effects upon uterine and ovarian development similar to those observed in the current study (Vo, Yoo et al. 2010). The increased adrenal weights in the EV and DHT treatment groups, in addition to the greater body length observed in the DV, DHT and DHEA treatment groups may therefore be due to the actions of these steroids via ERβ, since non-aromatisable androgens can be converted to 3β-diols by the neonatal liver. Furthermore, the changes in adrenal weight could relate to changes in prolactin secretion. Previous investigations have shown adrenal weight to increase in response to exogenous prolactin in rats (Schlein, Zarrow et al. 1974; Vasquez and Kitay 1978). Future investigation into plasma and pituitary prolactin levels and receptor expression content in addition to adrenalectomy studies of the neonatally estrogenised rat might therefore prove useful.

Raised fasting insulin levels and insulin resistance were present in animals treated with EV and TP, and in animals treated with DHT and DHEA to a lesser extent. This insulin resistance may therefore be a consequence of both the androgenic

and estrogenic actions of aromatisable androgens. However, the aforementioned ERβ effects of non-aromatisable androgens through their conversion to 3β-diols would still need to be excluded.

Insulin resistance may also result through the epigenetic programming of pancreatic islet function. Other rodent, sheep and primate studies into the aetiology of PCOS and the metabolic syndrome have documented similar metabolic abnormalities resulting from fetal/neonatal androgen treatment (Bruns, Baum et al. 2007; Demissie, Lazic et al. 2008; Padmanabhan, Veiga-Lopez et al.). Such programmed differences in pancreatic function could contribute to the changes in body weight and fat deposition documented in the EV, TP and DHT treatment groups. Future studies might therefore use AR specific antagonists (flutamide) or SERMs (raloxifene, tamoxifen, ICI-182780) in order to further elucidate which metabolic changes result through the actions of which specific steroids/receptors.

Neonatal animals showed a decrease in neonatal body weight after DEX treatment (data not shown). This is in line with previous studies which have shown corticosteroids to negatively affect animal growth during development (Cleasby, Kelly et al. 2003). Body weight was comparable to that of control animals by pnd 65, although DEX treated animals showed a reduction in retroperitoneal and mesenteric adipose tissue weight, the latter of which became comparable to controls by dividing by body weight. In addition, DEX treated animals showed no changes in insulin resistance or glucose tolerance when compared to controls.

The majority of rodent studies investigating the effects of DEX upon HPAA and metabolic development have used DEX administration during late fetal life in order to model the effects of maternal stress upon development and examine the epigenetics involved. By six months of age, animals treated with DEX during late gestation are significantly obese, insulin resistant and glucose intolerant (Levitt,

Lindsay et al. 1996; Nyirenda, Lindsay et al. 1998; Cleasby, Kelly et al. 2003; O'Regan, Kenyon et al. 2004; Drake, Walker et al. 2005; Mairesse, Lesage et al. 2007), whilst similar findings have been reported in sheep (Fletcher, Ma et al. 2004; De Blasio, Dodic et al. 2007). There are several caveats to the current investigations which may in part account for these differences; the animals used in other studies of maternal stress and metabolic epigenetics are often male, sacrificed at a later age, and are treated with DEX during late foetal development. It may be that were the animals in the current study sacrificed several months later, effects of postnatal DEX upon metabolism might be observed, although this is purely speculative.

7.6. Conclusions

To conclude, the anovulation, changes in ovarian follicle populations, reduced ovarian hormonal feedback, weight gain and insulin resistance which are observed to result in the adult rat after neonatal exposure to TP, are most likely the result of the estrogenic actions of TP after aromatisation in the newborn rat. However, a role for androgens in the programming of the abnormal development of the hypothalamic-pituitary and metabolic axes cannot be completely excluded. Furthermore, neonatal DEX exposure does not appear to effect female fertility, but may yet have effects upon adult rat metabolism.

Chapter 8. General Discussion

The studies described in this thesis used rodent models to examine the role of androgens in the pathogenesis of female infertility. An unsuccessful attempt to generate a granulosa cell specific androgen receptor knockout mouse model was first described, thus an alternative avenue of examining the role of androgens in the ovary was pursued (Chapter 3). Subsequent studies investigated the developmental programming of female rat infertility and various aspects of metabolism by steroid hormones, in particular aromatisable androgens (Chapters 4-7). The core objective of these later studies was to use the rat as a model for exploring the role of androgens in the aetiology of female infertility, with particular reference to PCOS. In addition, these investigations sought to evaluate the use of the neonatally androgenised rat as a model for this reproductive endocrinopathy.

Weight gain was consistently apparent in animals which received neonatal TP (Chapters 5-7). If comparisons are to be made across these different studies and conclusions drawn, changes in control animal weights must be compared between studies (Figure 8.1). Despite differences in the number of control animals and litter sizes, the growth trajectories of control animals were similar across the studies shown.

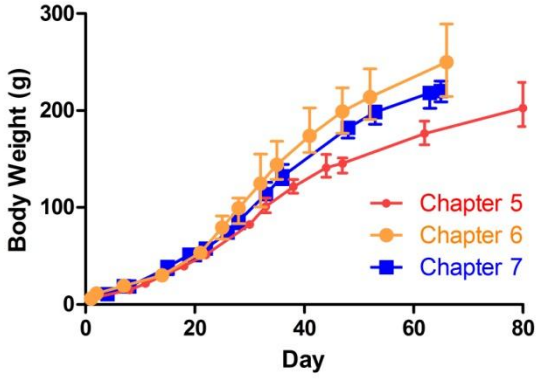

Figure 8.1: Growth trajectories of control group animals in Chapter 5 (*n*=5), Chapter 6 (*n*=15) and Chapter 7 (*n*=11): Litter sizes were kept to an *n* of 8 until weaning (pnd 21) for all three studies. Note, control groups in Chapters 6 and 7 were divided across two litters each. Values are expressed as the mean± SEM and were analysed by one way ANOVA.

The main androgen administered to animals during neonatal life was testosterone conjugated with proprionate (Chapters 4-7). In addition, estradiol conjugated to valerate and non-conjugated forms of DHT, DHEA and DEX were used in Chapter 7. The conjugation of steroid hormones to acidic molecules such as proprionate and valerate reduces peripheral steroid metabolism within the body, hence increasing steroid bioavailability (Chard 1990). This reduces the need to inject animals daily at extremely high doses, maintaining the steroid dose within an effective range. Such conjugation molecules are widely used as food additives, in medical drugs, and may also be produced *in vivo* through fatty acid metabolism (Rang, Dale et al. 2003). As yet, there is no evidence to suggest that they may negatively impact mammalian development. Early studies into rodent programming by neonatal androgens compared conjugated with non-conjugated steroids and found relatively few differences, save that conjugated androgens were more effective in altering development (Alklint and Norgren 1971; McDonald and Doughty 1974). In light of these studies, the results presented in Chapter 7 retain their validity and the doses of steroid chosen throughout this thesis were in line with those of the published literature and studies in male animals (Welsh, Saunders et al. 2008).

Rodents possess differences in estrus cycle length, hormonal feedback and uterine morphology when compared to their ovine, bovine and primate counterparts. In addition they are a poly-ovulatory species and lack a menstrual cycle (Johnson 2007). Nevertheless, rodent models of reproductive dysfunction still provide an excellent and well-established animal model to elucidate the features and mechanisms of mammalian reproductive and metabolic dysfunction.

8.1. The neonatally androgenised rat as a model for PCOS

Approximately 22% of women have PCO, but only around 5-10% of women develop PCOS, thus studies into the aetiology of this complex endocrinopathy are vital in order to understand the pathogenesis of infertility associated with this disorder. Studies into the origin of PCOS have long focused upon the role of abnormal androgen exposure during a key window of developmental life to produce a PCOS-like phenotype in the adult animal (Abbott, Dumesic et al. 1998; Beloosesky, Gold et al. 2004; Manneras, Cajander et al. 2007; Padmanabhan, Veiga-Lopez et al. 2010). The investigations described in this thesis have shown that TP administration during the first 15 days of rat life leads to a valid PCOS-like phenotype in the female that is overweight, anovulatory, has 'cystic' follicles, and an increased ovarian stromal compartment (Chapter 4).

This thesis has described more than one rat model of PCOS; for instance if a single dose of TP is given on the day after birth (Chapter 6), raised levels of T are found in the adult animal, which to some extent recapitulates the abnormal androgen status of many women with PCOS (Rotterdam Consensus 2004). Similarly administration of TP between either pnd 1-6 or 7-15 both result in an anovulatory, overweight phenotype (Chapter 5). These findings are corroborated by other studies in rodents (Dissen, Lara et al. 2000; Alexanderson, Eriksson et al. 2007), in addition to studies in sheep (Steckler, Wang et al. 2005; Veiga-Lopez, Astapova et al. 2009; Nada, Thompson et al. 2010; Padmanabhan, Veiga-Lopez et al. 2010) and non-human primates (Abbott, Dumesic et al. 1998; Abbott, Tarantal et al. 2009; Padmanabhan, Veiga-Lopez et al. 2010). However, the neonatally androgenised rat PCOS model fails to recapitulate circulating gonadotrophin abnormalities associated with the disorder; raised LH and an increased LH:FSH ratio. LH secretion has been shown to be altered in some PCOS models but not others (Manikkam, Thompson et al. 2008; Veiga-Lopez, Ye et al. 2008). Interpretation of the neonatally androgenised rat as a PCOS model should therefore take into consideration the findings of other animal models. Other rodent, sheep and non-human primate PCOS models using developmentally timed steroid hormone treatment have shown similar results, detailed comparatively in Table 8.1.

Table 8.1 : Features of PCOS recapitulated by Chapters 4-7 and other recent animal models referenced in this thesis.

Human PCOS	This study	Other Rodent Studies	Sheep Studies	Primate Studies
Reproductive features				
Irregular menses / anovulation / PCO	Chapters 5 & 7; smear testing Chapters 4-7; anovulation	(Dissen, Lara et al. 2000; Alexanderson, Eriksson et al. 2007; Manneras, Cajander et al. 2007)	(Steckler, Wang et al. 2005; Smith, Steckler et al. 2009)	(Abbott, Dumesic et al. 1998; Dumesic, Damario et al. 2001)
↑ **stromal / thecal area**	Chapter 4; increased stromal compartment	-	(Ortega, Rey et al. 2010)	(Vendola, Zhou et al. 1998)
Hormonal features				
↑ **ovarian androgens**	Chapter 6; high T in single TP dose group	(vom Saal and Bronson 1980; Dissen, Lara et al. 2000; Wu, Li et al. 2010)	-	(Vendola, Zhou et al. 1998)
↑ **LH**	-	(Wu, Li et al. 2010)	(Manikkam, Thompson et al. 2008)	(Dumesic, Abbott et al. 1997; Dumesic, Damario et al. 2001)
↓ **hormonal feedback / ovarian response to exogenous stimulation**	Chapters 5-7; reduced E2 and Inhibin B feedback	-	(Sarma, Manikkam et al. 2005; Steckler, Manikkam et al. 2007; Veiga-Lopez, Ye et al. 2008; Veiga-Lopez, Astapova et al. 2009)	(Steiner, Clifton et al. 1976; Abbott, Tarantal et al. 2009)
Metabolic features				
Insulin resistance / glucose intolerance	Chapters 6-7; ↑ fasting insulin & glucose; Chapter 6; ↓ glucose clearance	(Alexanderson, Eriksson et al. 2007; Manneras, Jonsdottir et al. 2008; Wu, Li et al. 2010)	(Nada, Thompson et al. 2010; Padmanabhan, Sarma et al. 2010)	(Dumesic, Nielsen et al. 1999; Bruns, Baum et al. 2004; Abbott, Tarantal et al. 2009)
↑ **abdominal fat**	Chapters 5-7; increase in mesenteric (central) adipose weight	(vom Saal and Bronson 1980; Alexanderson, Eriksson et al. 2007; Manneras, Cajander et al. 2007)	(Steckler, Herkimer et al. 2009)	(Bruns, Baum et al. 2007)
↑ **lipids / features of NAFLD**	Chapter 5	(Manneras, Cajander et al. 2007)	-	-

↑=increased; ↓=decreased; PCO=polycystic ovary; T=testosterone; LH=luteinising hormone; E2=estradiol; NAFLD=non-alcoholic fatty liver disease

In terms of recapitulating PCOS, chronic treatment of adult rats with DHT has shown that females will gain weight and stop ovulating as a result of this disturbed hormonal milieu (Manneras, Cajander et al. 2007). Whilst such investigations are useful in determining the potential effectiveness of novel PCOS treatments, for example electroacupuncture (Manneras, Jonsdottir et al. 2008), they provide little insight into the aetiology of the disorder and have not been thoroughly examined at the ovarian level for abnormalities or changes in ovarian follicle composition which may result from such treatment.

As a model of PCOS the neonatally androgenised rat provides a valid *in vivo* system for the study of reproductive dysfunction in the female animal. However, the findings shown using this model should be considered in context with other culture and *in vivo* model systems taken into account. The data presented in this thesis does not categorically prove that PCOS results through an abnormal hormonal milieu during a critical window of development and further investigation is required. Early studies into TP exposure during neonatal development showed that cross transplantation of an anovulatory ovary from a neonatally androgenised animal into a control animal allows the ovary to resume ovulation (Barraclough and Leathem 1954; Barraclough 1961; Smith and Peng 1966; Barraclough and Haller 1970). However, in these studies no detailed morphometric analysis of the ovary was performed and animals were only hemi-ovariectomized. Therefore the effects of estrogen through the transplantation of a control ovary cannot be excluded, as this estrogen may act to stimulate ovulation, as was observed in hemi-ovariectomized animals in a similar study (Simard, Brawer et al. 1987). Further investigations should therefore involve complete ovariectomy and cross-transplantation, alongside full investigation into the follicle populations and stromal compartment of the transplanted ovaries; control to neonatally androgenised animals and vice versa, with the inclusion of sham operated animals.

The endocrine response of the neonatally androgenised rat to exogenous estrogen, hCG or even PMSG also have yet to be investigated and such studies would provide valuable insight into HPG axis function. The late window of postnatal life (TP exposure between pnd 7-15; Chapter 5) could also be used in order to investigate estrus cycle function in these animals through vaginal smears. Future investigations into the timing of anovulation and the ovarian ageing (loss of oocytes) which occurs in postnatally androgenised animals might also be undertaken. Particularly since in the current studies, neonatally androgenised animals had fewer total and activated follicles at pnd 65 (Chapter 7), but not at pnd 90 (Chapter 4) when compared with controls.

8.2. Developmental programming of multiple endocrine systems: a role for epigenetics

This thesis has shown that steroid administration during the first 25 days of rat life (Chapters 4, 5 and 7) may reprogram the function of multiple endocrine systems. Ovarian follicle populations are altered (Chapters 4 and 7), and the weight of many endocrine organs increased/decreased in the adult animal (Chapters 4-7); the uterus, pituitary gland, adrenal gland, liver, as well as growth, body length and mesenteric and retroperitoneal adipose tissue depots. Such changes implicate that neonatal TP (and by inference other steroid hormones) can impact not just the reproductive axis but also the metabolic and stress response axes during this key window of development in rats.

In this thesis ovarian follicle populations were altered by neonatal TP/EV treatment with no apparent change in GC apoptosis (Chapters 4, 6 and 7). The molecular mechanism(s) through which neonatal estrogens/aromatisable androgens affect rodent germ cell nest breakdown require further investigation. One way to document whether rat germ cell nest breakdown is affected by neonatal steroid administration would be to assess the changes in germ cell populations on a daily

basis during the course of early postnatal life following TP/EV injections. Furthermore, terminal deoxynucleotidyl transferase dUTP nick end labelling (TUNEL) staining might also be a useful way of assessing the effects of neonatal steroids upon follicle/germ cell death which has so far only been indirectly measured (Chapter 6) through GC proliferation (Gavrieli, Sherman et al. 1992).

Uterine weight was also consistently reduced in animals which received neonatal steroid hormones. As discussed in Chapter 7, this may be due to low levels of plasma estradiol or differences in estrus cycle stage. The uterus may also be another target organ for developmental programming by neonatally administered steroids (White, Moore et al. 1981; Mena, Arriaza et al. 1992). Further investigations into the how the endometrium, myometrium and glandular cells of the uterus are affected by the hormonal milieu during development might prove necessary. This is particularly relevant, since clomiphene citrate, an ER SERM is used to induce ovulation in women with PCOS. Although 70% of women treated with clomiphene citrate do ovulate, only 40% go on to maintain a successful pregnancy. The causes of this discrepancy are unknown but it may in part be due to a non-receptive uterine environment (Amin, Abd el-Aal et al. 2003).

The impact of neonatal hormones upon the HPA axis is well documented and a dichotomy of adrenal function exists between the sexes, since adrenal cortisol output may be affected by the circulating hormonal milieu (Barraclough and Gorski 1961; Seale, Wood et al. 2005). As discussed in Chapters 5-7, investigations into the rodent stress response is warranted since the HPAA is altered by fetal DEX administration in other studies (Seckl 2004; Drake, Livingstone et al. 2005; Drake, Walker et al. 2005). Hypothalamic and pituitary mRNA, protein and plasma CRH, corticosterone and ACTH also require further investigation, as does characterisation of the changes in zona reticularis function which result from neonatal TP treatment, to corroborate the findings of other studies (da Silva, Lopes-Costa et al. 2007; da Silva, Lopes-Costa et al. 2009).

Of the tissues investigated in this thesis, Figure 8.2A details those that undergo maturation during early postnatal development in the rat while Figure 8.2B shows the windows of TP treatment which have affected these tissues. Such stark effects upon reproduction and metabolism may therefore indicate that environmental estrogens, androgens and other steroidal compounds may be partly responsible for epigenetic programming of endocrine functions in humans and animals (discussed in Chapter 1, Section 7).

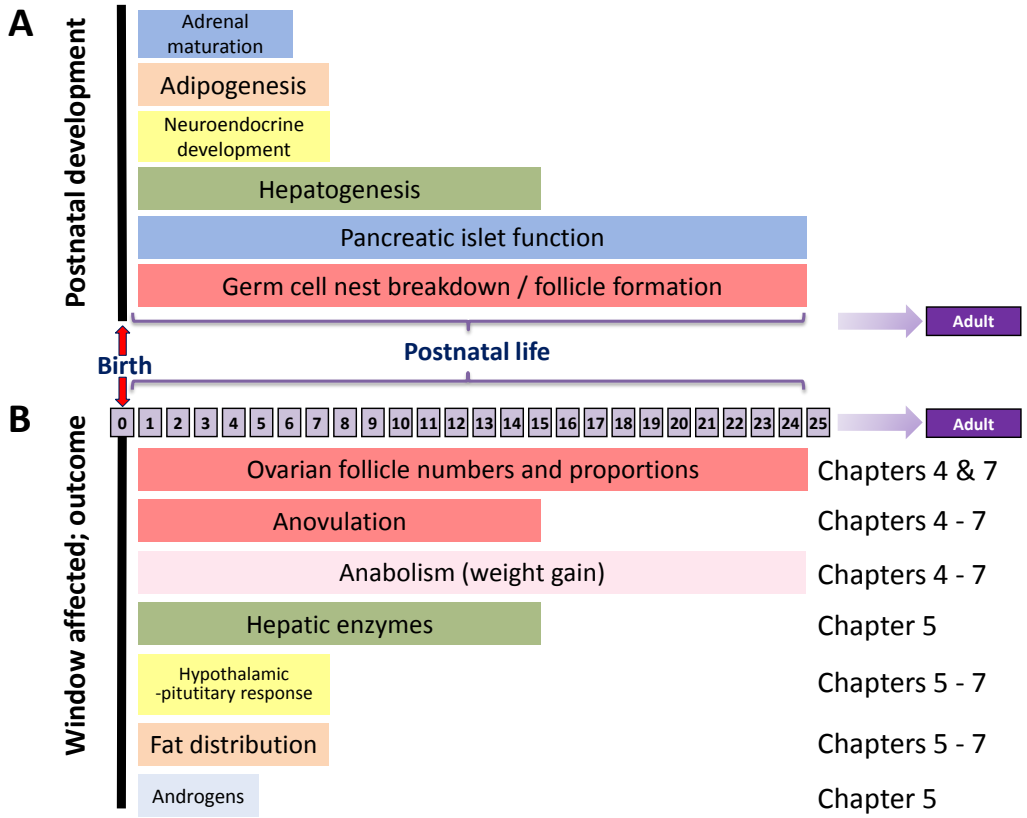

Figure 8.2: Mirror diagram: Top panel (A) shows the tissue processes which undergo maturation/formation during early postnatal life in the rat. Formation of these tissues may be modulated by neonatal TP treatment. Bottom panel (B) shows the ways in which TP treatment has been shown to alter tissue function, and the Chapter(s) in which these changes were reported.

Central (mesenteric) weight gain and IR were documented across several studies (Chapters 5-7). Recently a connection between pituitary insulin receptor and ovarian

function using a pituitary insulin receptor knockout mouse (PitIrKO), where wild type obese animals were infertile, but obese PitIrKO animals had normal reproductive function (Brothers, Wu et al. 2010). These investigations, together with those described in this thesis, point towards a role for peripheral tissue IR in the development of female infertility and should be investigated further. Gene expression analysis of the insulin receptor, IGFs and IGFBPs should ideally be addressed in future investigations at the level of the pituitary, liver, and muscle, in addition to the various adipose tissue depots. This is particularly relevant since even non-obese women with PCOS display a degree of insulin resistance (Shumak 2009). The epigenetic regulation of metabolism, specifically the IGF family of genes may provide a clue as to how obesity and PCOS are interlinked (Chao and D'Amore 2008; Fu, Yu et al. 2009; Guilloteau, Zabielski et al. 2009).

Due to the heterogeneous nature of PCOS, many studies have focused upon the individual gene variants or developing environments which might cause this disorder (Franks, Gharani et al. 1998; Abbott, Barnett et al. 2005; Fratantonio, Vicari et al. 2005; Franks, McCarthy et al. 2006). In recent years, the idea that epigenetic changes are responsible for the development of PCOS has received a lot of attention (Abbott, Dumesic et al. 2002; Norman 2002; Abbott, Zhou et al. 2008; Padmanabhan, Veiga-Lopez et al. 2010). However, few studies into the global/single gene methylation, phosphorylation or acetylation states of PCOS women when compared to normal subjects have been completed (Chapter 1, Section 9; Hickey, Chandy et al. 2002; Hickey, Legro et al. 2006). One small study of 40 women found no differences between age and BMI matched subjects in terms of global methylation status (Xu, Azziz et al.). Recently, bisulphite sequencing of key genes in a mouse model PCOS showed that DHEA treatment of pnd 25 mice led to hypomethylation of the LHr (Zhu, Zhu et al.), although this study so far represents the only PCOS model to undergo epigenome analysis at the individual gene level. Epigenetic changes of genes involved in follicle development might also help explain the alterations to follicle proportions which resulted from TP treatment (Chapters 4 and 7). In a recent study, treatment of mice with diethylstilbestrol, a known estrogenic compound, led to

hypermethylation of NOBOX gene A10; a gene known to be expressed in primordial follicles (Chapter 1, Section 3 Huntriss, Hinkins et al. 2006)

Studies into the epigenetic programming of obesity and the metabolic syndrome have demonstrated for many years the link between *in utero* environment, birth weight and the development of adult disease (Law, Barker et al. 1992; Barker 1995; McCowan, Harding et al. 2000; Barker 2001). Investigations into the developmental programming of mammalian physiology by steroid hormones have noted that various genes involved in the development of endocrine systems and metabolism, particularly that of the IGF gene family, may be epigenetically regulated (Chao and D'Amore 2008; Fu, Yu et al. 2009; Guilloteau, Zabielski et al. 2009). One hypothesis which may explain the heritable nature of PCOS and the metabolic syndrome is that of transgenerational epigenetics. In this hypothesis, improper exposure to endocrine disruptors such as steroidal compounds/poor nutritional diet alters the epigenome of the developing fetus (generation one), and also affects the germ cells within this fetus (generation two) (Skinner, Manikkam et al. ; Anway, Cupp et al. 2005; Anway and Skinner 2006; Nilsson, Anway et al. 2008; Skinner 2008). Although useful as a hypothesis for the aetiology of a disorder such as PCOS, epigenetics poses a relatively novel area of research and the links between epigenetic modifications and disease prevalence remain unclear.

There are other tissues not investigated in this thesis which may also be modulated by the developing hormonal milieu. For example, the thymus is one endocrine organ which is regulated by sex hormones in addition to possessing the enzymatic capacity for androgen metabolism, even in fetal life (Borlak, Schulte et al. 2004). The thymus is known to undergo its final stages of maturation during postnatal life (up to pnd 10) in rodents, known as the ‘immune adaptive period’ (West 2002). Thymectomy during early life results in ovarian dysgenesis like that observed in fetal plus postnatal TP treated animals (Chapter 4; Scalzo and Michael 1988). Recent investigations in mice have shown that neonatal estradiol treatment (pnd 4-7) not only leads to anovulation, but also defective thymocyte function

(Deshpande, Chapman et al. 1997; Chapman, Min et al. 2009). Thymectomy of estradiol treated animals (pnd 3) before estradiol treatment was able to prevent anovulation in most animals (Chapman, Min et al. 2009). Corticosterone treatment during this time period has also been shown to alter thymus function (Chapman, Min et al. 2002). However, associations between PCOS diagnosis and defective thymus function have yet to be clinically reported. Further investigations into the effects of neonatal steroid treatments upon the thymus and innate immune system should therefore be pursued. It is worth noting that steroid hormone action upon other organs during neonatal development are likely to exist, since thymectomy alone results in complete ovarian dysgenesis, but can be rescued by neonatal estradiol treatment (Chapman, Griffin et al. 1995).

In addition to the role of the innate immune system in endocrine development, other PCOS models have documented changes of the sympathetic and nervous systems, which were not investigated in this thesis (Stener-Victorin, Lundeberg et al. 2000; Stener-Victorin and Lindholm 2004; Manni, Holmang et al. 2005; Stener-Victorin, Ploj et al. 2005). If the peripheral nervous system is reprogrammed either directly or indirectly by steroid hormones, it may be that increased sympathetic tone to the ovary is partly responsible for the changes in follicle proportions and increased stromal compartment measured in the current model (Chapters 4 and 7; Lara, Ferruz et al. 1993). Increased vascularisation within the ovarian cortex has also been documented in PCOS women (Loverro, Vicino et al. 2001; Ferrara, Frantz et al. 2003). This could affect follicular blood supply and impact upon follicle development and maturation leading to atresia (Jarvela, Sladkevicius et al. 2004). Future investigations might therefore include the measurement of follicle osmolality, ovarian neurotransmitters (such as adrenaline or noradrenaline), and histological assessment of angiogenesis in the ovary of the neonatally androgenised rat.

8.3. Final conclusions

Investigations into the aetiology of PCOS, in addition to those described in this thesis, have provided valuable insight into the developmental programming of endocrine function in mammalian physiology. This thesis has demonstrated not only that neonatal estrogen or aromatisable androgen treatment of the neonatal rat leads to a PCOS like phenotype, but also that even if PCOS does not result from inappropriate steroid exposure during a critical window of endocrine development, the action of steroids during this window still have a detrimental effect upon adult mammalian fertility and metabolism. Further research into the characterisation, development and inheritance of PCOS and the associated metabolic syndrome in women is therefore required in order to properly match the scientific model with the clinical situation.

Taken collectively, the results described in this thesis demonstrate that the PCOS-like phenotype observed in the neonatally androgenised female rat is likely to be due to the estrogenic actions of testosterone, potentially through epigenetic actions, the precise mechanisms of which remain unclear. The programming of the metabolic components described may additionally be due to the actions of androgens, which is to be expected since many nuclear receptors share common binding motifs. Furthermore, these studies demonstrate a novel estrogenic effect of neonatal steroids upon primordial follicle populations and show that the neonatally androgenised rat is a rational PCOS model in a poly-ovulatory species.

Chapter 9. References

(2004). "Revised 2003 consensus on diagnostic criteria and long-term health risks related to polycystic ovary syndrome." *Fertil Steril* **81**(1): 19-25.

Abbott, D. H. (2010). *Prenatally Androgenised Female Rhesus Monkeys: A model for Polycystic Ovarian Syndrome*. Society for Reproduction and Fertility, Nottingham.

Abbott, D. H., D. K. Barnett, et al. (2005). "Androgen excess fetal programming of female reproduction: a developmental aetiology for polycystic ovary syndrome?" *Hum Reprod Update* **11**(4): 357-374.

Abbott, D. H., D. A. Dumesic, et al. (1998). "Insights into the Development of Polycystic Ovary Syndrome (PCOS) from Studies of Prenatally Androgenized Female Rhesus Monkeys." *Trends Endocrinol Metab* **9**(2): 62-67.

Abbott, D. H., D. A. Dumesic, et al. (2002). "Developmental origin of polycystic ovary syndrome - a hypothesis." *J Endocrinol* **174**(1): 1-5.

Abbott, D. H., A. F. Tarantal, et al. (2009). "Fetal, infant, adolescent and adult phenotypes of polycystic ovary syndrome in prenatally androgenized female rhesus monkeys." *Am J Primatol* **71**(9): 776-784.

Abbott, D. H., R. Zhou, et al. (2008). "Fetal programming of adrenal androgen excess: lessons from a nonhuman primate model of polycystic ovary syndrome." *Endocr Dev* **13**: 145-158.

Adams, J. M., A. E. Taylor, et al. (1994). "The midcycle gonadotropin surge in normal women occurs in the face of an unchanging gonadotropin-releasing hormone pulse frequency." *J Clin Endocrinol Metab* **79**(3): 858-864.

Ahima, R. S. (2008). "Revisiting leptin's role in obesity and weight loss." *J Clin Invest* **118**(7): 2380-2383.

Ahima, R. S. and D. A. Antwi (2008). "Brain regulation of appetite and satiety." *Endocrinol Metab Clin North Am* **37**(4): 811-823.

Ahima, R. S., D. Prabakaran, et al. (1998). "Postnatal leptin surge and regulation of circadian rhythm of leptin by feeding. Implications for energy homeostasis and neuroendocrine function." *J Clin Invest* **101**(5): 1020-1027.

Ahmed, E. I., J. L. Zehr, et al. (2008). "Pubertal hormones modulate the addition of new cells to sexually dimorphic brain regions." *Nat Neurosci* **11**(9): 995-997.

Ailhaud, G., P. Grimaldi, et al. (1992). "Cellular and molecular aspects of adipose tissue development." *Annu Rev Nutr* **12**: 207-233.

Alexanderson, C., E. Eriksson, et al. (2007). "Postnatal testosterone exposure results in insulin resistance, enlarged mesenteric adipocytes, and an atherogenic lipid profile in adult female rats: comparisons with estradiol and dihydrotestosterone." *Endocrinology* **148**(11): 5369-5376.

Alklint, T. and A. Norgren (1971). "Effects of neonatally injected non-esterified testosterone on reproductive functions in female rats." *Acta Endocrinol (Copenh)* **66**(4): 720-726.

Amar, A. P. and M. H. Weiss (2003). "Pituitary anatomy and physiology." *Neurosurg Clin N Am* **14**(1): 11-23, v.

Amin, A. F., D. E. Abd el-Aal, et al. (2003). "Evaluation of the impact of laparoscopic ovarian drilling on Doppler indices of ovarian stromal blood flow, serum vascular endothelial growth factor, and insulin-like growth factor-1 in women with polycystic ovary syndrome." *Fertil Steril* **79**(4): 938-941.

Anderiesz, C. and A. O. Trounson (1995). "The effect of testosterone on the maturation and developmental capacity of murine oocytes in vitro." *Hum Reprod* **10**(9): 2377-2381.

Anderson, E. and G. Y. Lee (1997). "The polycystic ovarian (PCO) condition: apoptosis and epithelialization of the ovarian antral follicles are aspects of cystogenesis in the dehydroepiandrosterone (DHEA)-treated rat model." *Tissue Cell* **29**(2): 171-189.

Anderson, E., G. Y. Lee, et al. (1997). "Polycystic ovarian condition in the dehydroepiandrosterone-treated rat model: hyperandrogenism and the resumption of meiosis are major initial events associated with cystogenesis of antral follicles." *Anat Rec* **249**(1): 44-53.

Andersson, K. B. and B. S. Skalhegg (1998). "[Genetic modification of the mouse]." *Tidsskr Nor Laegeforen* **118**(25): 3952-3957.

Andreu-Vieyra, C., R. Chen, et al. (2008). "Conditional deletion of the retinoblastoma (Rb) gene in ovarian granulosa cells leads to premature ovarian failure." *Mol Endocrinol* **22**(9): 2141-2161.

Antenos, M., J. Zhu, et al. (2008). "An activin/furin regulatory loop modulates the processing and secretion of inhibin alpha- and betaB-subunit dimers in pituitary gonadotrope cells." *J Biol Chem* **283**(48): 33059-33068.

Anway, M. D., A. S. Cupp, et al. (2005). "Epigenetic transgenerational actions of endocrine disruptors and male fertility." *Science* **308**(5727): 1466-1469.

Anway, M. D. and M. K. Skinner (2006). "Epigenetic transgenerational actions of endocrine disruptors." *Endocrinology* **147**(6 Suppl): S43-49.

Armitage, J. A., P. D. Taylor, et al. (2005). "Experimental models of developmental programming: consequences of exposure to an energy rich diet during development." *J Physiol* **565**(Pt 1): 3-8.

Arroyo, A., G. A. Laughlin, et al. (1997). "Inappropriate gonadotropin secretion in polycystic ovary syndrome: influence of adiposity." *J Clin Endocrinol Metab* **82**(11): 3728-3733.

Baba, Y., H. Matsuo, et al. (1971). "Structure of the porcine LH- and FSH-releasing hormone. II. Confirmation of the proposed structure by conventional sequential analyses." *Biochem Biophys Res Commun* **44**(2): 459-463.

Baillargeon, J. P. and A. C. Carpentier (2007). "Brothers of women with polycystic ovary syndrome are characterised by impaired glucose tolerance, reduced insulin sensitivity and related metabolic defects." *Diabetologia* **50**(12): 2424-2432.

Baird, D. T., T. G. Baker, et al. (1975). "Relationship between the secretion of the corpus luteum and the length of the follicular phase of the ovarian cycle." *J Reprod Fertil* **45**(3): 611-619.

Baird, D. T., A. Brown, et al. (2003). "Effect of long-term treatment with low-dose mifepristone on the endometrium." *Hum Reprod* **18**(1): 61-68.

Baird, D. T. and I. S. Fraser (1974). "Blood production and ovarian secretion rates of estradiol-17 beta and estrone in women throughout the menstrual cycle." *J Clin Endocrinol Metab* **38**(6): 1009-1017.

Baird, D. T. and I. S. Fraser (1975). "Concentration of oestrone and oestradiol in follicular fluid and ovarian venous blood of women." *Clin Endocrinol (Oxf)* **4**(3): 259-266.

Baldwin, D. M. and C. H. Sawyer (1974). "Effects of dexamethasone on LH release and ovulation in the cyclic rat." *Endocrinology* **94**(5): 1397-1403.

Balen, A. H., J. S. Laven, et al. (2003). "Ultrasound assessment of the polycystic ovary: international consensus definitions." *Hum Reprod Update* **9**(6): 505-514.

Baravalle, C., N. R. Salvetti, et al. (2007). "The role of ACTH in the pathogenesis of polycystic ovarian syndrome in rats: hormonal profiles and ovarian morphology." *Physiol Res* **56**(1): 67-78.

Barker, D. J. (1995). "Fetal origins of coronary heart disease." *Bmj* **311**(6998): 171-174.

Barker, D. J. (1997). "Fetal nutrition and cardiovascular disease in later life." *Br Med Bull* **53**(1): 96-108.

Barker, D. J. (1997). "Maternal nutrition, fetal nutrition, and disease in later life." *Nutrition* **13**(9): 807-813.

Barker, D. J. (2001). "The malnourished baby and infant." *Br Med Bull* **60**: 69-88.

Barley, J., M. Ginsburg, et al. (1975). "An androgen receptor in rat brain and pituitary." *Brain Res* **100**(2): 383-393.

Barnes, R. B. (1997). "Diagnosis and therapy of hyperandrogenism." *Baillieres Clin Obstet Gynaecol* **11**(2): 369-396.

Barr, G. D. and C. A. Barraclough (1978). "Temporal changes in medial basal hypothalamic LH-RH correlated with plasma LH during the rat estrous cycle and following electrochemical stimulation of the medial preoptic area in pentobarbital-treated proestrous rats." *Brain Res* **148**(2): 413-423.

Barraclough, C. A. (1955). "Influence of age on the response of preweaning female mice to testosterone propionate." *Am J Anat* **97**(3): 493-521.

Barraclough, C. A. (1961). "Production of anovulatory, sterile rats by single injections of testosterone propionate." *Endocrinology* **68**: 62-67.

Barraclough, C. A. and R. A. Gorski (1961). "Evidence that the hypothalamus is responsible for androgen-induced sterility in the female rat." *Endocrinology* **68**: 68-79.

Barraclough, C. A. and R. A. Gorski (1962). "Studies on mating behavior in the androgen-sterilized female rat in relation to the hypothalamic regulation of sexual behaviour." *J Endocrinol* **25**: 175-182.

Barraclough, C. A. and E. W. Haller (1970). "Positive and negative feedback effects of estrogen on pituitary LH synthesis and release in normal and androgen-sterilized rats." *Endocrinology* **86**(3): 542-551.

Barraclough, C. A. and J. H. Leathem (1954). "Infertility induced in mice by a single injection of testosterone propionate." *Proc Soc Exp Biol Med* **85**(4): 673-674.

Beale, E. G., D. E. Clouthier, et al. (1992). "Cell-specific expression of cytosolic phosphoenolpyruvate carboxykinase in transgenic mice." *Faseb J* **6**(15): 3330-3337.

Bellido, C., J. Martin de las Mulas, et al. (2003). "Tamoxifen induces gonadotropin-releasing hormone self-priming through an estrogen-dependent progesterone receptor expression in the gonadotrope of the rat." *Neuroendocrinology* **77**(6): 425-435.

Belmont, J. W. (1996). "Genetic control of X inactivation and processes leading to X-inactivation skewing." *Am J Hum Genet* **58**(6): 1101-1108.

Beloosesky, R., R. Gold, et al. (2004). "Induction of polycystic ovary by testosterone in immature female rats: Modulation of apoptosis and attenuation of glucose/insulin ratio." *Int J Mol Med* **14**(2): 207-215.

Berta, P., J. R. Hawkins, et al. (1990). "Genetic evidence equating SRY and the testis-determining factor." *Nature* **348**(6300): 448-450.

Besser, G. M. (1974). "Hypothalamus as an endocrine organ--I." *Br Med J* **3**(5930): 560-564.

Besser, G. M. (1974). "Hypothalamus as an endocrine organ. II." *Br Med J* **3**(5931): 613-615.

Besser, G. M. and C. H. Mortimer (1974). "Hypothalamic regulatory hormones: a review." *J Clin Pathol* **27**(3): 173-184.

Bilezikjian, L. M., A. L. Blount, et al. (2006). "Pituitary actions of ligands of the TGF-beta family: activins and inhibins." *Reproduction* **132**(2): 207-215.

Borlak, J., I. Schulte, et al. (2004). "Androgen metabolism in thymus of fetal and adult rats." *Drug Metab Dispos* **32**(6): 675-679.

Borsani, G., R. Tonlorenzi, et al. (1991). "Characterization of a murine gene expressed from the inactive X chromosome." *Nature* **351**(6324): 325-329.

Botwood, N., D. Hamilton-Fairley, et al. (1995). "Sex hormone-binding globulin and female reproductive function." *J Steroid Biochem Mol Biol* **53**(1-6): 529-531.

Boyer, A., M. Paquet, et al. (2009). "Dysregulation of WNT/CTNNB1 and PI3K/AKT signaling in testicular stromal cells causes granulosa cell tumor of the testis." *Carcinogenesis* **30**(5): 869-878.

Brawer, J. R., M. Munoz, et al. (1986). "Development of the polycystic ovarian condition (PCO) in the estradiol valerate-treated rat." *Biol Reprod* **35**(3): 647-655.

Brawer, J. R., F. Naftolin, et al. (1978). "Effects of a single injection of estradiol valerate on the hypothalamic arcuate nucleus and on reproductive function in the female rat." *Endocrinology* **103**(2): 501-512.

Bridges, C. B. (1916). "Non-Disjunction as Proof of the Chromosome Theory of Heredity (Concluded)." *Genetics* **1**(2): 107-163.

Britt, K. L., A. E. Drummond, et al. (2001). "The ovarian phenotype of the aromatase knockout (ArKO) mouse." *J Steroid Biochem Mol Biol* **79**(1-5): 181-185.

Brothers, K. J., S. Wu, et al. (2010). "Rescue of obesity-induced infertility in female mice due to a pituitary-specific knockout of the insulin receptor." *Cell Metab* **12**(3): 295-305.

Brown, P. and A. S. McNeilly (1999). "Transcriptional regulation of pituitary gonadotrophin subunit genes." *Rev Reprod* **4**(2): 117-124.

Bruns, C. M., S. T. Baum, et al. (2007). "Prenatal androgen excess negatively impacts body fat distribution in a nonhuman primate model of polycystic ovary syndrome." *Int J Obes (Lond)* **31**(10): 1579-1585.

Bruns, C. M., S. T. Baum, et al. (2004). "Insulin resistance and impaired insulin secretion in prenatally androgenized male rhesus monkeys." *J Clin Endocrinol Metab* **89**(12): 6218-6223.

Bucher, J. R. (2009). "Bisphenol A: where to now?" *Environ Health Perspect* **117**(3): A96-97.

Buckle, R. M., D. Rubinstein, et al. (1961). "Factors influencing the release of free fatty acids from rat adipose tissue." *Endocrinology* **69**: 1009-1015.

Buckle, V. J., Y. Boyd, et al. (1987). "Localisation of Y chromosome sequences in normal and 'XX' males." *J Med Genet* **24**(4): 197-203.

Buhl, E. S., S. Neschen, et al. (2007). "Increased hypothalamic-pituitary-adrenal axis activity and hepatic insulin resistance in low-birth-weight rats." *Am J Physiol Endocrinol Metab* **293**(5): E1451-1458.

Bukovsky, A., M. R. Caudle, et al. (2004). "Origin of germ cells and formation of new primary follicles in adult human ovaries." *Reprod Biol Endocrinol* **2**: 20.

Bukovsky, A., M. R. Caudle, et al. (2005). "Oogenesis in adult mammals, including humans: a review." *Endocrine* **26**(3): 301-316.

Canning, J., Y. Takai, et al. (2003). "Evidence for genetic modifiers of ovarian follicular endowment and development from studies of five inbred mouse strains." *Endocrinology* **144**(1): 9-12.

Cantrell, M. A., B. C. Carstens, et al. (2009). "X chromosome inactivation and Xist evolution in a rodent lacking LINE-1 activity." *PLoS One* **4**(7): e6252.

Carabatsos, M. J., J. Elvin, et al. (1998). "Characterization of oocyte and follicle development in growth differentiation factor-9-deficient mice." *Dev Biol* **204**(2): 373-384.

Carretero, J., G. Vazquez, et al. (2003). "Postnatal differentiation of the immunohistochemical expression of aromatase P450 in the rat pituitary gland." *Histol Histopathol* **18**(2): 419-423.

Carson, R. and J. Smith (1986). "Development and steroidogenic activity of preantral follicles in the neonatal rat ovary." *J Endocrinol* **110**(1): 87-92.

Case, A. M. (2003). "Infertility evaluation and management. Strategies for family physicians." *Can Fam Physician* **49**: 1465-1472.

Caserta, F., T. Tchkonia, et al. (2001). "Fat depot origin affects fatty acid handling in cultured rat and human preadipocytes." *Am J Physiol Endocrinol Metab* **280**(2): E238-247.

Castrillon, D. H., L. Miao, et al. (2003). "Suppression of ovarian follicle activation in mice by the transcription factor Foxo3a." *Science* **301**(5630): 215-218.

Centenera, M. M., J. M. Harris, et al. (2008). "The contribution of different androgen receptor domains to receptor dimerization and signaling." *Mol Endocrinol* **22**(11): 2373-2382.

Chakrabarty, S., B. T. Miller, et al. (2006). "Ovarian dysfunction in peripubertal hyperinsulinemia." *J Soc Gynecol Investig* **13**(2): 122-129.

Champagne, F. A., D. D. Francis, et al. (2003). "Variations in maternal care in the rat as a mediating influence for the effects of environment on development." *Physiol Behav* **79**(3): 359-371.

Chang, C., Y. T. Chen, et al. (2004). "Infertility with defective spermatogenesis and hypotestosteronemia in male mice lacking the androgen receptor in Sertoli cells." *Proc Natl Acad Sci U S A* **101**(18): 6876-6881.

Chao, W. and P. A. D'Amore (2008). "IGF2: epigenetic regulation and role in development and disease." *Cytokine Growth Factor Rev* **19**(2): 111-120.

Chapman, J. C., W. J. Griffin, et al. (1995). "The ovarian dysgenesis normally induced by neonatal thymectomy is prevented by the prior administration of estrogen." *Am J Reprod Immunol* **34**(3): 195-199.

Chapman, J. C., S. Min, et al. (2002). "The administration of cortisone to female B6A mice during their immune adaptive period causes anovulation and the formation of ovarian cysts." *Am J Reprod Immunol* **48**(3): 184-189.

Chapman, J. C., S. H. Min, et al. (2009). "The estrogen-injected female mouse: new insight into the etiology of PCOS." *Reprod Biol Endocrinol* **7**: 47.

Chard, T., Ed. (1990). *Laboratory techniques in biochemistry and molecular biology*, ELSEVIER.

Chassot, A. A., E. P. Gregoire, et al. (2008). "Genetics of ovarian differentiation: Rspo1, a major player." *Sex Dev* **2**(4-5): 219-227.

Chassot, A. A., F. Ranc, et al. (2008). "Activation of beta-catenin signaling by Rspo1 controls differentiation of the mammalian ovary." *Hum Mol Genet* **17**(9): 1264-1277.

Chaumeil, J., P. D. Waters, et al. (2011). "Evolution from XIST-Independent to XIST-Controlled X-Chromosome Inactivation: Epigenetic Modifications in Distantly Related Mammals." *PLoS One* **6**(4): e19040.

Chen, Y., K. Breen, et al. (2009). "Estrogen can signal through multiple pathways to regulate oocyte cyst breakdown and primordial follicle assembly in the neonatal mouse ovary." *J Endocrinol* **202**(3): 407-417.

Chen, Y., W. N. Jefferson, et al. (2007). "Estradiol, progesterone, and genistein inhibit oocyte nest breakdown and primordial follicle assembly in the neonatal mouse ovary in vitro and in vivo." *Endocrinology* **148**(8): 3580-3590.

Childs, G. V. (1985). "Shifts in gonadotropin storage in cultured gonadotropes following GnRH stimulation, in vitro." *Peptides* **6**(1): 103-107.

Childs, G. V., C. Hyde, et al. (1983). "Heterogeneous luteinizing hormone and follicle-stimulating hormone storage patterns in subtypes of gonadotropes separated by centrifugal elutriation." *Endocrinology* **113**(6): 2120-2128.

Chin, D., C. Shackleton, et al. (2000). "Increased 5alpha-reductase and normal 11beta-hydroxysteroid dehydrogenase metabolism of C19 and C21 steroids in a young population with polycystic ovarian syndrome." *J Pediatr Endocrinol Metab* **13**(3): 253-259.

Chomczynski, P. and N. Sacchi (2006). "The single-step method of RNA isolation by acid guanidinium thiocyanate-phenol-chloroform extraction: twenty-something years on." *Nat Protoc* **1**(2): 581-585.

Ciampelli, M., A. M. Fulghesu, et al. (1997). "Heterogeneity in beta cell activity, hepatic insulin clearance and peripheral insulin sensitivity in women with polycystic ovary syndrome." *Hum Reprod* **12**(9): 1897-1901.

Claessens, F., S. Denayer, et al. (2008). "Diverse roles of androgen receptor (AR) domains in AR-mediated signaling." *Nucl Recept Signal* **6**: e008.

Clarke, B. L. and S. Khosla (2009). "New selective estrogen and androgen receptor modulators." *Curr Opin Rheumatol* **21**(4): 374-379.

Clarke, H. G., S. A. Hope, et al. (2006). "Formation of ovarian follicular fluid may be due to the osmotic potential of large glycosaminoglycans and proteoglycans." *Reproduction* **132**(1): 119-131.

Clarke, I. J. and J. T. Cummins (1982). "The temporal relationship between gonadotropin releasing hormone (GnRH) and luteinizing hormone (LH) secretion in ovariectomized ewes." *Endocrinology* **111**(5): 1737-1739.

Clarke, I. J. and J. T. Cummins (1985). "GnRH pulse frequency determines LH pulse amplitude by altering the amount of releasable LH in the pituitary glands of ewes." *J Reprod Fertil* **73**(2): 425-431.

Clarke, I. J. and J. T. Cummins (1987). "The significance of small pulses of gonadotrophin-releasing hormone." *J Endocrinol* **113**(3): 413-418.

Clarke, I. J., J. T. Cummins, et al. (1987). "Pituitary receptors for gonadotropin-releasing hormone in relation to changes in pituitary and plasma luteinizing hormone in ovariectomized-hypothalamo pituitary disconnected ewes. I. Effect of changing frequency of gonadotropin-releasing hormone pulses." *Biol Reprod* **37**(4): 749-754.

Clarke, I. J., J. T. Cummins, et al. (1989). "The oestrogen-induced surge of LH requires a 'signal' pattern of gonadotrophin-releasing hormone input to the pituitary gland in the ewe." *J Endocrinol* **122**(1): 127-134.

Clarke, I. J., R. J. Scaramuzzi, et al. (1976). "Effects of testosterone implants in pregnant ewes on their female offspring." *J Embryol Exp Morphol* **36**(1): 87-99.

Clarke, I. J., G. B. Thomas, et al. (1987). "GnRH secretion throughout the ovine estrous cycle." *Neuroendocrinology* **46**(1): 82-88.

Cleasby, M. E., P. A. Kelly, et al. (2003). "Programming of rat muscle and fat metabolism by in utero overexposure to glucocorticoids." *Endocrinology* **144**(3): 999-1007.

Corbin, C. J., M. W. Khalil, et al. (1995). "Functional ovarian and placental isoforms of porcine aromatase." *Mol Cell Endocrinol* **113**(1): 29-37.

Cottrell, E. C. and J. R. Seckl (2009). "Prenatal stress, glucocorticoids and the programming of adult disease." *Front Behav Neurosci* **3**: 19.

Courel, M., A. Soler-Jover, et al. (2010). "Pro-hormone secretogranin II regulates dense core secretory granule biogenesis in catecholaminergic cells." *J Biol Chem* **285**(13): 10030-10043.

Crandall, D. L., E. M. Quinet, et al. (2006). "Modulation of adipose tissue development by pharmacological inhibition of PAI-1." *Arterioscler Thromb Vasc Biol* **26**(10): 2209-2215.

Crawford, J. L., R. J. Currie, et al. (2000). "Replenishment of LH stores of gonadotrophs in relation to gene expression, synthesis and secretion of LH after the preovulatory phase of the sheep oestrous cycle." *J Endocrinol* **167**(3): 453-463.

Crawford, J. L. and A. S. McNeilly (2002). "Co-localisation of gonadotrophins and granins in gonadotrophs at different stages of the oestrous cycle in sheep." *J Endocrinol* **174**(2): 179-194.

Crawford, J. L., J. R. McNeilly, et al. (2004). "No evidence for pituitary priming to gonadotropin-releasing hormone in relation to luteinizing hormone (LH) secretion prior to the preovulatory LH surge in ewes." *Biol Reprod* **71**(1): 224-235.

Crawford, J. L., J. R. McNeilly, et al. (2002). "Promotion of intragranular co-aggregation with LH by enhancement of secretogranin II storage resulted in increased intracellular granule storage in gonadotrophs of GnRH-deprived male mice." *Reproduction* **124**(2): 267-277.

Critchley, H. O., R. W. Kelly, et al. (2006). "Regulation of human endometrial function: mechanisms relevant to uterine bleeding." *Reprod Biol Endocrinol* **4 Suppl 1**: S5.

Da Silva-Buttkus, P., G. S. Jayasooriya, et al. (2008). "Effect of cell shape and packing density on granulosa cell proliferation and formation of multiple layers during early follicle development in the ovary." *J Cell Sci* **121**(Pt 23): 3890-3900.

Da Silva-Buttkus, P., G. Marcelli, et al. (2009). "Inferring biological mechanisms from spatial analysis: prediction of a local inhibitor in the ovary." *Proc Natl Acad Sci U S A* **106**(2): 456-461.

da Silva, B. B., P. V. Lopes-Costa, et al. (2009). "Evaluation of Ki-67 antigen expression in the zona reticularis of the adrenal cortex of female rats in persistent estrus." *Hum Reprod* **24**(3): 705-709.

da Silva, B. B., P. V. Lopes-Costa, et al. (2007). "Morphological and morphometric analysis of the adrenal cortex of androgenized female rats." *Gynecol Obstet Invest* **64**(1): 44-48.

Daniel, S. A. and D. T. Armstrong (1980). "Enhancement of follicle-stimulating hormone-induced aromatase activity by androgens in cultured rat granulosa cells." *Endocrinology* **107**(4): 1027-1033.

Das, M., O. Djahanbakhch, et al. (2008). "Granulosa cell survival and proliferation are altered in polycystic ovary syndrome." *J Clin Endocrinol Metab* **93**(3): 881-887.

Davey, R. A. and H. E. MacLean (2006). "Current and future approaches using genetically modified mice in endocrine research." *Am J Physiol Endocrinol Metab* **291**(3): E429-438.

De Blasio, M. J., M. Dodic, et al. (2007). "Maternal exposure to dexamethasone or cortisol in early pregnancy differentially alters insulin secretion and glucose homeostasis in adult male sheep offspring." *Am J Physiol Endocrinol Metab* **293**(1): E75-82.

De Gendt, K., J. V. Swinnen, et al. (2004). "A Sertoli cell-selective knockout of the androgen receptor causes spermatogenic arrest in meiosis." *Proc Natl Acad Sci U S A* **101**(5): 1327-1332.

de Greef, W. J. and P. van der Schoot (1987). "Effects of dexamethasone on ovarian activity in rats." *Acta Endocrinol (Copenh)* **116**(3): 350-356.

Deepak, S., K. Kottapalli, et al. (2007). "Real-Time PCR: Revolutionizing Detection and Expression Analysis of Genes." *Curr Genomics* **8**(4): 234-251.

Demeestere, I., C. Gervy, et al. (2004). "Effect of insulin-like growth factor-I during preantral follicular culture on steroidogenesis, in vitro oocyte maturation, and embryo development in mice." *Biol Reprod* **70**(6): 1664-1669.

Demissie, M., M. Lazic, et al. (2008). "Transient Prenatal Androgen Exposure Produces Metabolic Syndrome in Adult Female Rats." *Am J Physiol Endocrinol Metab*.

Dennis, A. P., R. U. Haq, et al. (2001). "Importance of the regulation of nuclear receptor degradation." *Front Biosci* **6**: D954-959.

Deshpande, R. R., J. C. Chapman, et al. (1997). "The anovulation in female mice resulting from postnatal injections of estrogen is correlated with altered levels of CD8+ lymphocytes." *Am J Reprod Immunol* **38**(2): 114-120.

Dewailly, D., S. Catteau-Jonard, et al. (2007). "The excess in 2-5 mm follicles seen at ovarian ultrasonography is tightly associated to the follicular arrest of the polycystic ovary syndrome." *Hum Reprod* **22**(6): 1562-1566.

Diaz, F. J., K. Sugiura, et al. (2008). "Regulation of Pcsk6 expression during the preantral to antral follicle transition in mice: opposing roles of FSH and oocytes." *Biol Reprod* **78**(1): 176-183.

Diaz, F. J., K. Wigglesworth, et al. (2007). "Oocytes determine cumulus cell lineage in mouse ovarian follicles." *J Cell Sci* **120**(Pt 8): 1330-1340.

Dissen, G. A., H. E. Lara, et al. (2000). "Intraovarian excess of nerve growth factor increases androgen secretion and disrupts estrous cyclicity in the rat." *Endocrinology* **141**(3): 1073-1082.

Dohler, K. D., A. Coquelin, et al. (1986). "Pre- and postnatal influence of an estrogen antagonist and an androgen antagonist on differentiation of the sexually dimorphic nucleus of the preoptic area in male and female rats." *Neuroendocrinology* **42**(5): 443-448.

Dohler, K. D., S. S. Srivastava, et al. (1984). "Differentiation of the sexually dimorphic nucleus in the preoptic area of the rat brain is inhibited by postnatal treatment with an estrogen antagonist." *Neuroendocrinology* **38**(4): 297-301.

Dong, J., D. F. Albertini, et al. (1996). "Growth differentiation factor-9 is required during early ovarian folliculogenesis." *Nature* **383**(6600): 531-535.

Drake, A. J., D. E. Livingstone, et al. (2005). "Reduced adipose glucocorticoid reactivation and increased hepatic glucocorticoid clearance as an early adaptation to high-fat feeding in Wistar rats." *Endocrinology* **146**(2): 913-919.

Drake, A. J., B. R. Walker, et al. (2005). "Intergenerational consequences of fetal programming by in utero exposure to glucocorticoids in rats." *Am J Physiol Regul Integr Comp Physiol* **288**(1): R34-38.

Drummond, A. E. (2006). "The role of steroids in follicular growth." *Reprod Biol Endocrinol* **4**: 16.

Dumesic, D. A., D. H. Abbott, et al. (1997). "Prenatal exposure of female rhesus monkeys to testosterone propionate increases serum luteinizing hormone levels in adulthood." *Fertil Steril* **67**(1): 155-163.

Dumesic, D. A., D. H. Abbott, et al. (2007). "Polycystic ovary syndrome and its developmental origins." *Rev Endocr Metab Disord* **8**(2): 127-141.

Dumesic, D. A., M. A. Damario, et al. (2001). "Ovarian morphology and serum hormone markers as predictors of ovarian follicle recruitment by gonadotropins for in vitro fertilization." *J Clin Endocrinol Metab* **86**(6): 2538-2543.

Dumesic, D. A., M. F. Nielsen, et al. (1999). "Insulin action during variable hyperglycemic-hyperinsulinemic infusions in hyperandrogenic anovulatory patients and healthy women." *Fertil Steril* **72**(3): 458-466.

Dumesic, D. A., R. D. Schramm, et al. (2005). "Early origins of polycystic ovary syndrome." *Reprod Fertil Dev* **17**(3): 349-360.

Ebling, F. J. (2005). "The neuroendocrine timing of puberty." *Reproduction* **129**(6): 675-683.

Economou, F., X. Xyrafis, et al. (2009). "In overweight/obese but not in normal-weight women, polycystic ovary syndrome is associated with elevated liver enzymes compared to controls." *Hormones (Athens)* **8**(3): 199-206.

Edson, M. A., A. K. Nagaraja, et al. (2009). "The mammalian ovary from genesis to revelation." *Endocr Rev* **30**(6): 624-712.

El-Hefnawy, T. and A. J. Zeleznik (2001). "Synergism between FSH and activin in the regulation of proliferating cell nuclear antigen (PCNA) and cyclin D2 expression in rat granulosa cells." *Endocrinology* **142**(10): 4357-4362.

Elvin, J. A., A. T. Clark, et al. (1999). "Paracrine actions of growth differentiation factor-9 in the mammalian ovary." *Mol Endocrinol* **13**(6): 1035-1048.

Elvin, J. A., C. Yan, et al. (1999). "Molecular characterization of the follicle defects in the growth differentiation factor 9-deficient ovary." *Mol Endocrinol* **13**(6): 1018-1034.

Eppig, J. J. (2001). "Oocyte control of ovarian follicular development and function in mammals." *Reproduction* **122**(6): 829-838.

ESHRE (2008). "Consensus on infertility treatment related to polycystic ovary syndrome." *Hum Reprod* **23**(3): 462-477.

Evuarherhe, O., J. D. Leggett, et al. (2009). "Organizational role for pubertal androgens on adult hypothalamic-pituitary-adrenal sensitivity to testosterone in the male rat." *J Physiol* **587**(Pt 12): 2977-2985.

Faiman, C., F. I. Reyes, et al. (1988). "Effects of long-term testosterone exposure on ovarian function and morphology in the rhesus monkey." *Anat Rec* **222**(3): 245-251.

Fan, H. Y., Z. Liu, et al. (2009). "Cell type-specific targeted mutations of Kras and Pten document proliferation arrest in granulosa cells versus oncogenic insult to ovarian surface epithelial cells." *Cancer Res* **69**(16): 6463-6472.

Farquhar, C. M., M. Birdsall, et al. (1994). "The prevalence of polycystic ovaries on ultrasound scanning in a population of randomly selected women." *Aust N Z J Obstet Gynaecol* **34**(1): 67-72.

Fassnacht, M., N. Schlenz, et al. (2003). "Beyond adrenal and ovarian androgen generation: Increased peripheral 5 alpha-reductase activity in women with polycystic ovary syndrome." *J Clin Endocrinol Metab* **88**(6): 2760-2766.

Ferrara, N., G. Frantz, et al. (2003). "Differential expression of the angiogenic factor genes vascular endothelial growth factor (VEGF) and endocrine gland-derived VEGF in normal and polycystic human ovaries." *Am J Pathol* **162**(6): 1881-1893.

Flaws, J. A., A. N. Hirshfield, et al. (2001). "Effect of bcl-2 on the primordial follicle endowment in the mouse ovary." *Biol Reprod* **64**(4): 1153-1159.

Fletcher, A. J., X. H. Ma, et al. (2004). "Antenatal glucocorticoids reset the level of baseline and hypoxemia-induced pituitary-adrenal activity in the sheep fetus during late gestation." *Am J Physiol Endocrinol Metab* **286**(2): E311-319.

Fonseca-Alaniz, M. H., J. Takada, et al. (2007). "Adipose tissue as an endocrine organ: from theory to practice." *J Pediatr (Rio J)* **83**(5 Suppl): S192-203.

Forabosco, A., C. Sforza, et al. (1991). "Morphometric study of the human neonatal ovary." *Anat Rec* **231**(2): 201-208.

Ford, C. E., K. W. Jones, et al. (1959). "A sex-chromosome anomaly in a case of gonadal dysgenesis (Turner's syndrome)." *Lancet* **1**(7075): 711-713.

Fortin, J., P. Lamba, et al. (2009). "Conservation of mechanisms mediating gonadotrophin-releasing hormone 1 stimulation of human luteinizing hormone beta subunit transcription." *Mol Hum Reprod* **15**(2): 77-87.

Fowden, A. L. and A. J. Forhead (2004). "Endocrine mechanisms of intrauterine programming." *Reproduction* **127**(5): 515-526.

Fowden, A. L. and A. J. Forhead (2009). "Hormones as epigenetic signals in developmental programming." *Exp Physiol* **94**(6): 607-625.

Fowden, A. L., A. J. Forhead, et al. (2008). "The placenta and intrauterine programming." *J Neuroendocrinol* **20**(4): 439-450.

Fowden, A. L., D. A. Giussani, et al. (2005). "Endocrine and metabolic programming during intrauterine development." *Early Hum Dev* **81**(9): 723-734.

Franks, R. (2010). *Polycystic Ovary Syndrome - SRF Distinguished Scientist 2010*. Society for Reproduction and Fertility, Nottingham.

Franks, S., N. Gharani, et al. (1998). "Genetics of polycystic ovary syndrome." *Mol Cell Endocrinol* **145**(1-2): 123-128.

Franks, S., M. I. McCarthy, et al. (2006). "Development of polycystic ovary syndrome: involvement of genetic and environmental factors." *Int J Androl* **29**(1): 278-285; discussion 286-290.

Franks, S., J. Stark, et al. (2008). "Follicle dynamics and anovulation in polycystic ovary syndrome." *Hum Reprod Update* **14**(4): 367-378.

Fratantonio, E., E. Vicari, et al. (2005). "Genetics of polycystic ovarian syndrome." *Reprod Biomed Online* **10**(6): 713-720.

Fu, Q., X. Yu, et al. (2009). "Epigenetics: intrauterine growth retardation (IUGR) modifies the histone code along the rat hepatic IGF-1 gene." *Faseb J* **23**(8): 2438-2449.

Fulghesu, A. M., S. Angioni, et al. (2007). "Ultrasound in polycystic ovary syndrome--the measuring of ovarian stroma and relationship with circulating androgens: results of a multicentric study." *Hum Reprod* **22**(9): 2501-2508.

Fulghesu, A. M., M. Ciampelli, et al. (2001). "A new ultrasound criterion for the diagnosis of polycystic ovary syndrome: the ovarian stroma/total area ratio." *Fertil Steril* **76**(2): 326-331.

Gallardo, N., E. Bonzon-Kulichenko, et al. (2007). "Tissue-specific effects of central leptin on the expression of genes involved in lipid metabolism in liver and white adipose tissue." *Endocrinology* **148**(12): 5604-5610.

Gavrieli, Y., Y. Sherman, et al. (1992). "Identification of programmed cell death in situ via specific labeling of nuclear DNA fragmentation." *J Cell Biol* **119**(3): 493-501.

Gaytan, F., C. Bellido, et al. (1998). "Both prolactin and progesterone in proestrus are necessary for the induction of apoptosis in the regressing corpus luteum of the rat." *Biol Reprod* **59**(5): 1200-1206.

Gaytan, F., C. Morales, et al. (1998). "Ovarian follicle macrophages: is follicular atresia in the immature rat a macrophage-mediated event?" *Biol Reprod* **58**(1): 52-59.

Gaytan, F., C. Morales, et al. (1998). "Macrophages, cell proliferation, and cell death in the human menstrual corpus luteum." *Biol Reprod* **59**(2): 417-425.

Geer, E. B. and W. Shen (2009). "Gender differences in insulin resistance, body composition, and energy balance." *Gend Med* **6 Suppl 1**: 60-75.

Gluckman, P. D., W. Cutfield, et al. (2005). "The fetal, neonatal, and infant environments-the long-term consequences for disease risk." *Early Hum Dev* **81**(1): 51-59.

Gluckman, P. D. and M. A. Hanson (2004). "The developmental origins of the metabolic syndrome." *Trends Endocrinol Metab* **15**(4): 183-187.

Gonzazalez-Parra, S., J. Argente, et al. (2000). "Effect of neonatal and adult testosterone treatment on the cellular composition of the adult female rat anterior pituitary." *J Endocrinol* **164**(3): 265-276.

Gorski, R. A. and C. A. Barraclough (1962). "Adenohypophyseal LH content in normal androgen-sterilized and progesteroneprimed sterile female rats." *Acta Endocrinol (Copenh)* **39**: 13-21.

Gorski, R. A. and C. A. Barraclough (1962). "Studies on hypothalamic regulation of FSH secretion in the androgen-sterilized female rat." *Proc Soc Exp Biol Med* **110**: 298-300.

Gorski, R. A. and C. A. Barraclough (1963). "Effects of Low Dosages of Androgen on the Differentiation of Hypothalamic Regulatory Control of Ovulation in the Rat." *Endocrinology* **73**: 210-216.

Gosmain, Y., N. Dif, et al. (2005). "Regulation of SREBP-1 expression and transcriptional action on HKII and FAS genes during fasting and refeeding in rat tissues." *J Lipid Res* **46**(4): 697-705.

Goy, R. W., F. B. Bercovitch, et al. (1988). "Behavioral masculinization is independent of genital masculinization in prenatally androgenized female rhesus macaques." *Horm Behav* **22**(4): 552-571.

Goy, R. W. and C. H. Phoenix (1972). "The effects of testosterone propionate administered before birth on the development of behavior in genetic female rhesus monkeys." *UCLA Forum Med Sci* **15**: 193-201.

Green, S. H., A. M. Mandl, et al. (1951). "The proportion of ovarian follicles in different stages of development in rats and monkeys." *J Anat* **85**(4): 325-329.

Greenfeld, C. R., M. E. Pepling, et al. (2007). "BAX regulates follicular endowment in mice." *Reproduction* **133**(5): 865-876.

Gregoire, F. M., C. M. Smas, et al. (1998). "Understanding adipocyte differentiation." *Physiol Rev* **78**(3): 783-809.

Grossmann, R., F. J. Diez-Guerra, et al. (1987). "Neonatal testosterone modifies LH secretion in the adult female rat by altering the opioid-noradrenergic interaction in the medial preoptic area." *Brain Res* **415**(2): 205-210.

Group, E. C. W. (2006). "Nutrition and reproduction in women." *Hum Reprod Update* **12**(3): 193-207.

Guastella, E., R. A. Longo, et al. (2010). "Clinical and endocrine characteristics of the main polycystic ovary syndrome phenotypes." *Fertil Steril*.

Guilloteau, P., R. Zabielski, et al. (2009). "Adverse effects of nutritional programming during prenatal and early postnatal life, some aspects of regulation and potential prevention and treatments." *J Physiol Pharmacol* **60 Suppl 3**: 17-35.

Gustafsson, J. A. and A. Stenberg (1974). "Irreversible androgenic programming at birth of microsomal and soluble rat liver enzymes active on androstene-3,17-dione and 5alpha-androstane-3alpha,17beta-diol." *J Biol Chem* **249**(3): 711-718.

Gustafsson, J. A. and A. Stenberg (1974). "Neonatal programming of androgen responsiveness of liver of adult rats." *J Biol Chem* **249**(3): 719-723.

Hagen, C., K. P. McNatty, et al. (1976). "Immunoreactive alpha- and beta-subunits of luteinizing hormone in human peripheral blood and follicular fluid throughout the menstrual cycle, and their effect on the secretion rate of progesterone by human granulosa cells in tissue culture." *J Endocrinol* **69**(1): 33-46.

Haisenleder, D. J., A. C. Dalkin, et al. (1991). "A pulsatile gonadotropin-releasing hormone stimulus is required to increase transcription of the gonadotropin subunit genes: evidence for differential regulation of transcription by pulse frequency in vivo." *Endocrinology* **128**(1): 509-517.

Haisenleder, D. J., G. A. Ortolano, et al. (1993). "Regulation of gonadotropin subunit messenger ribonucleic acid expression by gonadotropin-releasing hormone pulse amplitude in vitro." *Endocrinology* **132**(3): 1292-1296.

Haisenleder, D. J., M. Yasin, et al. (1997). "Gonadotropin subunit and gonadotropin-releasing hormone receptor gene expression are regulated by alterations in the frequency of calcium pulsatile signals." *Endocrinology* **138**(12): 5227-5230.

Han, Y. K., Y. G. Kim, et al. (2010). "Hyperosmotic stress induces autophagy and apoptosis in recombinant Chinese hamster ovary cell culture." *Biotechnol Bioeng* **105**(6): 1187-1192.

Handa, R. J. and J. A. Resko (1989). "Alpha-adrenergic regulation of androgen receptor concentration in the preoptic area of the rat." *Brain Res* **483**(2): 312-320.

Harlow, C. R., S. G. Hillier, et al. (1986). "Androgen modulation of follicle-stimulating hormone-induced granulosa cell steroidogenesis in the primate ovary." *Endocrinology* **119**(3): 1403-1405.

Harlow, C. R., H. J. Shaw, et al. (1988). "Factors influencing follicle-stimulating hormone-responsive steroidogenesis in marmoset granulosa cells: effects of androgens and the stage of follicular maturity." *Endocrinology* **122**(6): 2780-2787.

Heard, E., J. Chaumeil, et al. (2004). "Mammalian X-chromosome inactivation: an epigenetics paradigm." *Cold Spring Harb Symp Quant Biol* **69**: 89-102.

Hickey, T., A. Chandy, et al. (2002). "The androgen receptor CAG repeat polymorphism and X-chromosome inactivation in Australian Caucasian women with infertility related to polycystic ovary syndrome." *J Clin Endocrinol Metab* **87**(1): 161-165.

Hickey, T. E., R. S. Legro, et al. (2006). "Epigenetic modification of the X chromosome influences susceptibility to polycystic ovary syndrome." *J Clin Endocrinol Metab* **91**(7): 2789-2791.

Hickey, T. E., D. L. Marrocco, et al. (2005). "Androgens augment the mitogenic effects of oocyte-secreted factors and growth differentiation factor 9 on porcine granulosa cells." *Biol Reprod* **73**(4): 825-832.

Hillier, S. G. and F. A. De Zwart (1981). "Evidence that granulosa cell aromatase induction/activation by follicle-stimulating hormone is an androgen receptor-regulated process in-vitro." *Endocrinology* **109**(4): 1303-1305.

Hillier, S. G., R. A. Knazek, et al. (1977). "Androgenic stimulation of progesterone production by granulosa cells from preantral ovarian follicles: further in vitro studies using replicate cell cultures." *Endocrinology* **100**(6): 1539-1549.

Hillier, S. G. and M. Tetsuka (1997). "Role of androgens in follicle maturation and atresia." *Baillieres Clin Obstet Gynaecol* **11**(2): 249-260.

Hillier, S. G., E. L. Yong, et al. (1991). "Effect of recombinant inhibin on androgen synthesis in cultured human thecal cells." *Mol Cell Endocrinol* **75**(2): R1-6.

Hillier, S. G., A. J. Zeleznik, et al. (1980). "Hormonal regulation of preovulatory follicle maturation in the rat." *J Reprod Fertil* **60**(1): 219-229.

Hirshfield, A. N. and A. R. Midgley, Jr. (1978). "Morphometric analysis of follicular development in the rat." *Biol Reprod* **19**(3): 597-605.

Hoepfner, B. A. and I. L. Ward (1988). "Prenatal and neonatal androgen exposure interact to affect sexual differentiation in female rats." *Behav Neurosci* **102**(1): 61-65.

Holte, J. (1998). "Polycystic ovary syndrome and insulin resistance: thrifty genes struggling with over-feeding and sedentary life style?" *J Endocrinol Invest* **21**(9): 589-601.

Honnma, H., T. Endo, et al. (2006). "Altered expression of Fas/Fas ligand/caspase 8 and membrane type 1-matrix metalloproteinase in atretic follicles within dehydroepiandrosterone-induced polycystic ovaries in rats." *Apoptosis* **11**(9): 1525-1533.

Hu, Y. C., P. H. Wang, et al. (2004). "Subfertility and defective folliculogenesis in female mice lacking androgen receptor." *Proc Natl Acad Sci U S A* **101**(31): 11209-11214.

Hughesdon, P. E. (1982). "Morphology and morphogenesis of the Stein-Leventhal ovary and of so-called "hyperthecosis"." *Obstet Gynecol Surv* **37**(2): 59-77.

Huhtaniemi, I. and A. Bartke (2001). "Perspective: male reproduction." *Endocrinology* **142**(6): 2178-2183.

Huntriss, J., M. Hinkins, et al. (2006). "cDNA cloning and expression of the human NOBOX gene in oocytes and ovarian follicles." *Mol Hum Reprod* **12**(5): 283-289.

Hwang, S. O. and G. M. Lee (2008). "Nutrient deprivation induces autophagy as well as apoptosis in Chinese hamster ovary cell culture." *Biotechnol Bioeng* **99**(3): 678-685.

Iguchi, T. and N. Takasugi (1981). "Occurrence of permanent anovulation in mouse ovaries and permanent changes in the vaginal and uterine epithelia following neonatal treatment with large doses of 5 alpha-dihydrotestosterone." *Endocrinol Jpn* **28**(2): 207-213.

Ikenasio-Thorpe, B. A., B. H. Breier, et al. (2007). "Prenatal influences on susceptibility to diet-induced obesity are mediated by altered neuroendocrine gene expression." *J Endocrinol* **193**(1): 31-37.

Illera, J. C., G. Silvan, et al. (2005). "The effect of dexamethasone on disruption of ovarian steroid levels and receptors in female rats." *J Physiol Biochem* **61**(3): 429-438.

Irion, S., H. Luche, et al. (2007). "Identification and targeting of the ROSA26 locus in human embryonic stem cells." *Nat Biotechnol* **25**(12): 1477-1482.

Irving-Rodgers, H. F., M. Krupa, et al. (2003). "Cholesterol side-chain cleavage cytochrome P450 and 3beta-hydroxysteroid dehydrogenase expression and the concentrations of steroid hormones in the follicular fluids of different phenotypes of healthy and atretic bovine ovarian follicles." *Biol Reprod* **69**(6): 2022-2028.

Jaaskelainen, J., S. Korhonen, et al. (2005). "Androgen receptor gene CAG length polymorphism in women with polycystic ovary syndrome." *Fertil Steril* **83**(6): 1724-1728.

Jabbour, H. N., R. W. Kelly, et al. (2006). "Endocrine regulation of menstruation." *Endocr Rev* **27**(1): 17-46.

Jacobs, P. A. and J. A. Strong (1959). "A case of human intersexuality having a possible XXY sex-determining mechanism." *Nature* **183**(4657): 302-303.

Jakimiuk, A. J., S. R. Weitsman, et al. (1999). "5alpha-reductase activity in women with polycystic ovary syndrome." *J Clin Endocrinol Metab* **84**(7): 2414-2418.

Jarvela, I. Y., P. Sladkevicius, et al. (2004). "Comparison of follicular vascularization in normal versus polycystic ovaries during in vitro fertilization as measured using 3-dimensional power Doppler ultrasonography." *Fertil Steril* **82**(5): 1358-1363.

Jefferson, W., R. Newbold, et al. (2006). "Neonatal genistein treatment alters ovarian differentiation in the mouse: inhibition of oocyte nest breakdown and increased oocyte survival." *Biol Reprod* **74**(1): 161-168.

Jia, X. C., B. Kessel, et al. (1985). "Androgen inhibition of follicle-stimulating hormone-stimulated luteinizing hormone receptor formation in cultured rat granulosa cells." *Endocrinology* **117**(1): 13-22.

Johnson, M. H. (2007). *Essential Reproduction*, Blackwell Publishing.

Jonard, S. and D. Dewailly (2004). "The follicular excess in polycystic ovaries, due to intra-ovarian hyperandrogenism, may be the main culprit for the follicular arrest." *Hum Reprod Update* **10**(2): 107-117.

Kaaijk, E. M., H. Sasano, et al. (2000). "Distribution of steroidogenic enzymes involved in androgen synthesis in polycystic ovaries: an immunohistochemical study." *Mol Hum Reprod* **6**(5): 443-447.

Kalantaridou, S. N. and L. M. Nelson (2000). "Premature ovarian failure is not premature menopause." *Ann N Y Acad Sci* **900**: 393-402.

Kalantry, S. (2011). "Recent advances in X-chromosome inactivation." *J Cell Physiol* **226**(7): 1714-1718.

Kanitz, E., W. Otten, et al. (2006). "Changes in endocrine and neurochemical profiles in neonatal pigs prenatally exposed to increased maternal cortisol." *J Endocrinol* **191**(1): 207-220.

Kapoor, A. and S. G. Matthews (2008). "Prenatal stress modifies behavior and hypothalamic-pituitary-adrenal function in female guinea pig offspring: effects of timing of prenatal stress and stage of reproductive cycle." *Endocrinology* **149**(12): 6406-6415.

Kelberman, D., K. Rizzoti, et al. (2009). "Genetic regulation of pituitary gland development in human and mouse." *Endocr Rev* **30**(7): 790-829.

Kelly, R. W. and H. O. Critchley (1997). "Immunomodulation by human seminal plasma: a benefit for spermatozoon and pathogen?" *Hum Reprod* **12**(10): 2200-2207.

Kezele, P. and M. K. Skinner (2003). "Regulation of ovarian primordial follicle assembly and development by estrogen and progesterone: endocrine model of follicle assembly." *Endocrinology* **144**(8): 3329-3337.

Knight, P. G. and C. Glister (2003). "Local roles of TGF-beta superfamily members in the control of ovarian follicle development." *Anim Reprod Sci* **78**(3-4): 165-183.

Knobil, E. (1974). "On the control of gonadotropin secretion in the rhesus monkey." *Recent Prog Horm Res* **30**(0): 1-46.

Kopelman, P. G. (1994). "Hormones and obesity." *Baillieres Clin Endocrinol Metab* **8**(3): 549-575.

Kopinke, L. C. M. a. D. (2008). Pancreatic stem cells. *StemBook: Harvard Stem Cell Institute*. L. G. H. S. C. Institute).

Krechowec, S. O., M. Vickers, et al. (2006). "Prenatal influences on leptin sensitivity and susceptibility to diet-induced obesity." *J Endocrinol* **189**(2): 355-363.

Lacombe, A., H. Lee, et al. (2006). "Disruption of POF1B binding to nonmuscle actin filaments is associated with premature ovarian failure." *Am J Hum Genet* **79**(1): 113-119.

Lagaly, D. V., P. Y. Aad, et al. (2008). "Role of adiponectin in regulating ovarian theca and granulosa cell function." *Mol Cell Endocrinol* **284**(1-2): 38-45.

Lara, H. E., J. L. Ferruz, et al. (1993). "Activation of ovarian sympathetic nerves in polycystic ovary syndrome." *Endocrinology* **133**(6): 2690-2695.

Larsen, B., A. J. Markovetz, et al. (1977). "Relationship of vaginal cytology to alterations of the vaginal microflora of rats during the estrous cycle." *Appl Environ Microbiol* **33**(3): 556-562.

Lau, Y. F. and Y. Li (2009). "The human and mouse sex-determining SRY genes repress the Rspol/beta-catenin signaling." *J Genet Genomics* **36**(4): 193-202.

Law, C. M., D. J. Barker, et al. (1992). "Early growth and abdominal fatness in adult life." *J Epidemiol Community Health* **46**(3): 184-186.

Lecureuil, C., I. Fontaine, et al. (2002). "Sertoli and granulosa cell-specific Cre recombinase activity in transgenic mice." *Genesis* **33**(3): 114-118.

Lee, J. H., M. E. Miele, et al. (1996). "KiSS-1, a novel human malignant melanoma metastasis-suppressor gene." *J Natl Cancer Inst* **88**(23): 1731-1737.

Lee, Y. S. (2009). "The role of genes in the current obesity epidemic." *Ann Acad Med Singapore* **38**(1): 45-43.

Lei, L., S. Jin, et al. (2010). "The regulatory role of Dicer in folliculogenesis in mice." *Mol Cell Endocrinol* **315**(1-2): 63-73.

Lephart, E. D., S. B. Call, et al. (2001). "Neuroendocrine regulation of sexually dimorphic brain structure and associated sexual behavior in male rats is genetically controlled." *Biol Reprod* **64**(2): 571-578.

Levitt, N. S., R. S. Lindsay, et al. (1996). "Dexamethasone in the last week of pregnancy attenuates hippocampal glucocorticoid receptor gene expression and elevates blood pressure in the adult offspring in the rat." *Neuroendocrinology* **64**(6): 412-418.

Lillycrop, K. A., J. L. Slater-Jefferies, et al. (2007). "Induction of altered epigenetic regulation of the hepatic glucocorticoid receptor in the offspring of rats fed a protein-restricted diet during pregnancy suggests that reduced DNA methyltransferase-1 expression is involved in impaired DNA methylation and changes in histone modifications." *Br J Nutr* **97**(6): 1064-1073.

Lin, L. and J. C. Achermann (2004). "The adrenal." *Horm Res* **62 Suppl 3**: 22-29.

Lin, Y., X. Li, et al. "The Role of the Medial and Central Amygdala in Stress-Induced Suppression of Pulsatile LH Secretion in Female Rats." *Endocrinology*.

Liu, K. H., Y. L. Chan, et al. (2006). "Mesenteric fat thickness is an independent determinant of metabolic syndrome and identifies subjects with increased carotid intima-media thickness." *Diabetes Care* **29**(2): 379-384.

Liu, L., S. Rajareddy, et al. (2007). "Infertility caused by retardation of follicular development in mice with oocyte-specific expression of Foxo3a." *Development* **134**(1): 199-209.

Lourenco, D., R. Brauner, et al. (2009). "Mutations in NR5A1 associated with ovarian insufficiency." *N Engl J Med* **360**(12): 1200-1210.

Loverro, G., M. Vicino, et al. (2001). "Polycystic ovary syndrome: relationship between insulin sensitivity, sex hormone levels and ovarian stromal blood flow." *Gynecol Endocrinol* **15**(2): 142-149.

Luo, W. and M. C. Wiltbank (2006). "Distinct regulation by steroids of messenger RNAs for FSHR and CYP19A1 in bovine granulosa cells." *Biol Reprod* **75**(2): 217-225.

MacDougald, O. A. and M. D. Lane (1995). "Transcriptional regulation of gene expression during adipocyte differentiation." *Annu Rev Biochem* **64**: 345-373.

Maciel, G. A., E. C. Baracat, et al. (2004). "Stockpiling of transitional and classic primary follicles in ovaries of women with polycystic ovary syndrome." *J Clin Endocrinol Metab* **89**(11): 5321-5327.

Macleod, D. J., R. M. Sharpe, et al. (2010). "Androgen action in the masculinization programming window and development of male reproductive organs." *Int J Androl* **33**(2): 279-287.

Maeda, K., S. Adachi, et al. (2007). "Metastin/kisspeptin and control of estrous cycle in rats." *Rev Endocr Metab Disord* **8**(1): 21-29.

Maeda, K., H. Tsukamura, et al. (1995). "The LHRH pulse generator: a mediobasal hypothalamic location." *Neurosci Biobehav Rev* **19**(3): 427-437.

Magoffin, D. A. (2005). "Ovarian theca cell." *Int J Biochem Cell Biol* **37**(7): 1344-1349.

Mahesh, V. B., T. M. Mills, et al. (1987). "Animal models for study of polycystic ovaries and ovarian atresia." *Adv Exp Med Biol* **219**: 237-257.

Mairesse, J., J. Lesage, et al. (2007). "Maternal stress alters endocrine function of the feto-placental unit in rats." *Am J Physiol Endocrinol Metab* **292**(6): E1526-1533.

Manikkam, M., R. C. Thompson, et al. (2008). "Developmental programming: impact of prenatal testosterone excess on pre- and postnatal gonadotropin regulation in sheep." *Biol Reprod* **78**(4): 648-660.

Manneras, L., S. Cajander, et al. (2007). "A new rat model exhibiting both ovarian and metabolic characteristics of polycystic ovary syndrome." *Endocrinology* **148**(8): 3781-3791.

Manneras, L., I. H. Jonsdottir, et al. (2008). "Low Frequency Electro-Acupuncture and Physical Exercise Improve Metabolic Disturbances and Modulate Gene Expression in Adipose Tissue in Rats with Dihydrotestosterone-Induced Polycystic Ovary Syndrome." *Endocrinology*.

Manni, L., A. Holmang, et al. (2005). "Ovarian expression of alpha (1)- and beta (2)-adrenoceptors and p75 neurotrophin receptors in rats with steroid-induced polycystic ovaries." *Auton Neurosci* **118**(1-2): 79-87.

Marshall, J. C., A. C. Dalkin, et al. (1993). "GnRH pulses--the regulators of human reproduction." *Trans Am Clin Climatol Assoc* **104**: 31-46.

Marshall, J. C. and M. L. Griffin (1993). "The role of changing pulse frequency in the regulation of ovulation." *Hum Reprod* **8 Suppl 2**: 57-61.

Marteil, G., L. Richard-Parpaillon, et al. (2009). "Role of oocyte quality in meiotic maturation and embryonic development." *Reprod Biol* **9**(3): 203-224.

Martinerie, L., C. Bouvattier, et al. (2009). "[SF-1, a key player in adrenal and gonadal differentiation: implications in gonadal dysgenesis and primary ovarian insufficiency]." *Ann Endocrinol (Paris)* **70 Suppl 1**: S26-32.

Masek, K. S., R. I. Wood, et al. (1999). "Prenatal dihydrotestosterone differentially masculinizes tonic and surge modes of luteinizing hormone secretion in sheep." *Endocrinology* **140**(8): 3459-3466.

Matsuda-Minehata, F., N. Inoue, et al. (2006). "The regulation of ovarian granulosa cell death by pro- and anti-apoptotic molecules." *J Reprod Dev* **52**(6): 695-705.

Matsumoto, T., K. Takeyama, et al. (2003). "Androgen receptor functions from reverse genetic models." *J Steroid Biochem Mol Biol* **85**(2-5): 95-99.

Matzuk, M. M. (2000). "Revelations of ovarian follicle biology from gene knockout mice." *Mol Cell Endocrinol* **163**(1-2): 61-66.

Matzuk, M. M., K. H. Burns, et al. (2002). "Intercellular communication in the mammalian ovary: oocytes carry the conversation." *Science* **296**(5576): 2178-2180.

McConnell, N. A., R. S. Yunus, et al. (2002). "Water permeability of an ovarian antral follicle is predominantly transcellular and mediated by aquaporins." *Endocrinology* **143**(8): 2905-2912.

McCowan, L. M., J. E. Harding, et al. (2000). "A pilot randomized controlled trial of two regimens of fetal surveillance for small-for-gestational-age fetuses with normal results of umbilical artery doppler velocimetry." *Am J Obstet Gynecol* **182**(1 Pt 1): 81-86.

McDonald, P. G. and C. Doughty (1972). "Comparison of the effect of neonatal administration of testosterone and dihydrotestosterone in the female rat." *J Reprod Fertil* **30**(1): 55-62.

McDonald, P. G. and C. Doughty (1974). "Effect of neonatal administration of different androgens in the female rat: correlation between aromatization and the induction of sterilization." *J Endocrinol* **61**(1): 95-103.

McMillen, I. C. and J. S. Robinson (2005). "Developmental origins of the metabolic syndrome: prediction, plasticity, and programming." *Physiol Rev* **85**(2): 571-633.

McNatty, K. P., Quirke, L.D., Fidler, A., Smith, P., Heath, D.A. & Tisdall, D. (2000). Ovarian Development: Fetus to Puberty. *Hormones and Women's Heath*. H. A. P. Ed. L.A. Salamonsen, The Netherlands.**:** pp9-22.

McNeilly, A. S., J. L. Crawford, et al. (2003). "The differential secretion of FSH and LH: regulation through genes, feedback and packaging." *Reprod Suppl* **61**: 463-476.

McTernan, C. L., P. G. McTernan, et al. (2002). "Resistin, central obesity, and type 2 diabetes." *Lancet* **359**(9300): 46-47.

Meachem, S. J., E. Nieschlag, et al. (2001). "Inhibin B in male reproduction: pathophysiology and clinical relevance." *Eur J Endocrinol* **145**(5): 561-571.

Means, G. D., M. S. Mahendroo, et al. (1989). "Structural analysis of the gene encoding human aromatase cytochrome P-450, the enzyme responsible for estrogen biosynthesis." *J Biol Chem* **264**(32): 19385-19391.

Mena, M. A., C. A. Arriaza, et al. (1992). "Early postnatal androgenization imprints selective changes in the action of estrogens in the rat uterus." *Biol Reprod* **46**(6): 1080-1085.

Midgley, A. R., Jr. and R. B. Jaffe (1968). "Regulation of human gonadotropins. IV. Correlation of serum concentrations of follicle stimulating and luteinizing hormones during the menstrual cycle." *J Clin Endocrinol Metab* **28**(12): 1699-1703.

Midgley, A. R., Jr. and R. B. Jaffe (1971). "Regulation of human gonadotropins. X. Episodic fluctuation of LH during the menstrual cycle." *J Clin Endocrinol Metab* **33**(6): 962-969.

Misugi, T., K. Ozaki, et al. (2006). "Insulin-lowering agents inhibit synthesis of testosterone in ovaries of DHEA-induced PCOS rats." *Gynecol Obstet Invest* **61**(4): 208-215.

Miyamoto, J., T. Matsumoto, et al. (2007). "The pituitary function of androgen receptor constitutes a glucocorticoid production circuit." *Mol Cell Biol* **27**(13): 4807-4814.

Mizukami, S., K. Yamanouchi, et al. (1982). "Failure of ovulation after neonatal administration of 5 alpha-dihydrotestosterone to female rats." *Endokrinologie* **79**(1): 1-6.

Mohlig, M., A. Jurgens, et al. (2006). "The androgen receptor CAG repeat modifies the impact of testosterone on insulin resistance in women with polycystic ovary syndrome." *Eur J Endocrinol* **155**(1): 127-130.

Moran, L. and R. J. Norman (2004). "Understanding and managing disturbances in insulin metabolism and body weight in women with polycystic ovary syndrome." *Best Pract Res Clin Obstet Gynaecol* **18**(5): 719-736.

Moran, L. J., G. Brinkworth, et al. (2006). "Effects of lifestyle modification in polycystic ovarian syndrome." *Reprod Biomed Online* **12**(5): 569-578.

Morey, C. and P. Avner (2010). "Genetics and epigenetics of the X chromosome." *Ann N Y Acad Sci* **1214**: E18-33.

Morita, Y., G. I. Perez, et al. (1999). "Targeted expression of Bcl-2 in mouse oocytes inhibits ovarian follicle atresia and prevents spontaneous and chemotherapy-induced oocyte apoptosis in vitro." *Mol Endocrinol* **13**(6): 841-850.

Morris, J. A., C. L. Jordan, et al. (2004). "Sexual differentiation of the vertebrate nervous system." *Nat Neurosci* **7**(10): 1034-1039.

Morton, N. M., L. Ramage, et al. (2004). "Down-regulation of adipose 11beta-hydroxysteroid dehydrogenase type 1 by high-fat feeding in mice: a potential adaptive mechanism counteracting metabolic disease." *Endocrinology* **145**(6): 2707-2712.

Muir, A. I., L. Chamberlain, et al. (2001). "AXOR12, a novel human G protein-coupled receptor, activated by the peptide KiSS-1." *J Biol Chem* **276**(31): 28969-28975.

Murakami, K., T. Ohhira, et al. (2009). "Identification of the chromatin regions coated by non-coding Xist RNA." *Cytogenet Genome Res* **125**(1): 19-25.

Murray, A. A., A. K. Swales, et al. (2008). "Follicular growth and oocyte competence in the in vitro cultured mouse follicle: effects of gonadotrophins and steroids." *Mol Hum Reprod* **14**(2): 75-83.

Myers, M., K. L. Britt, et al. (2004). "Methods for quantifying follicular numbers within the mouse ovary." *Reproduction* **127**(5): 569-580.

Myers, M., E. Gay, et al. (2007). "In vitro evidence suggests activin-A may promote tissue remodeling associated with human luteolysis." *Endocrinology* **148**(8): 3730-3739.

Myers, M., S. van den Driesche, et al. (2008). "Activin A reduces luteinisation of human luteinised granulosa cells and has opposing effects to human chorionic gonadotropin in vitro." *J Endocrinol* **199**(2): 201-212.

Nada, S. E., R. C. Thompson, et al. (2010). "Developmental programming: differential effects of prenatal testosterone excess on insulin target tissues." *Endocrinology* **151**(11): 5165-5173.

Nahum, R., K. J. Thong, et al. (1995). "Metabolic regulation of androgen production by human thecal cells in vitro." *Hum Reprod* **10**(1): 75-81.

Naor, Z. (2009). "Signaling by G-protein-coupled receptor (GPCR): studies on the GnRH receptor." *Front Neuroendocrinol* **30**(1): 10-29.

Nelson, L. M. (2009). "Clinical practice. Primary ovarian insufficiency." *N Engl J Med* **360**(6): 606-614.

Nelson, V. L., R. S. Legro, et al. (1999). "Augmented androgen production is a stable steroidogenic phenotype of propagated theca cells from polycystic ovaries." *Mol Endocrinol* **13**(6): 946-957.

Nicol, L., S. C. Bishop, et al. (2009). "Homozygosity for a single base-pair mutation in the oocyte-specific GDF9 gene results in sterility in Thoka sheep." *Reproduction* **138**(6): 921-933.

Nicol, L., J. R. McNeilly, et al. (2002). "Influence of steroids and GnRH on biosynthesis and secretion of secretogranin II and chromogranin A in relation to LH release in LbetaT2 gonadotroph cells." *J Endocrinol* **174**(3): 473-483.

Nilsson, E. E., M. D. Anway, et al. (2008). "Transgenerational epigenetic effects of the endocrine disruptor vinclozolin on pregnancies and female adult onset disease." *Reproduction* **135**(5): 713-721.

Norman, R. J. (2002). "Hyperandrogenaemia and the ovary." *Mol Cell Endocrinol* **191**(1): 113-119.

Norman, R. J., M. J. Davies, et al. (2002). "The role of lifestyle modification in polycystic ovary syndrome." *Trends Endocrinol Metab* **13**(6): 251-257.

Norman, R. J., G. Homan, et al. (2006). "Lifestyle choices, diet, and insulin sensitizers in polycystic ovary syndrome." *Endocrine* **30**(1): 35-43.

Norman, R. J., M. Noakes, et al. (2004). "Improving reproductive performance in overweight/obese women with effective weight management." *Hum Reprod Update* **10**(3): 267-280.

Notini, A. J., R. A. Davey, et al. (2005). "Genomic actions of the androgen receptor are required for normal male sexual differentiation in a mouse model." *J Mol Endocrinol* **35**(3): 547-555.

Ntambi, J. M. and K. Young-Cheul (2000). "Adipocyte differentiation and gene expression." *J Nutr* **130**(12): 3122S-3126S.

Nyirenda, M. J., R. S. Lindsay, et al. (1998). "Glucocorticoid exposure in late gestation permanently programs rat hepatic phosphoenolpyruvate carboxykinase and glucocorticoid receptor expression and causes glucose intolerance in adult offspring." *J Clin Invest* **101**(10): 2174-2181.

Nyirenda, M. J. and J. R. Seckl (1998). "Intrauterine events and the programming of adulthood disease: the role of fetal glucocorticoid exposure (Review)." *Int J Mol Med* **2**(5): 607-614.

O'Regan, D., C. J. Kenyon, et al. (2004). "Glucocorticoid exposure in late gestation in the rat permanently programs gender-specific differences in adult cardiovascular and metabolic physiology." *Am J Physiol Endocrinol Metab* **287**(5): E863-870.

Orisaka, M., K. Tajima, et al. (2009). "Oocyte-granulosa-theca cell interactions during preantral follicular development." *J Ovarian Res* **2**(1): 9.

Ortega, H. H., F. Rey, et al. (2010). "Developmental programming: effect of prenatal steroid excess on intraovarian components of insulin signaling pathway and related proteins in sheep." *Biol Reprod* **82**(6): 1065-1075.

Ortega, H. H., N. R. Salvetti, et al. (2009). "Developmental programming: prenatal androgen excess disrupts ovarian steroid receptor balance." *Reproduction* **137**(5): 865-877.

Ota, H., A. Wakizaka, et al. (1986). "Enhanced ovarian gonadotropin receptors in the testosterone-induced polycystic ovary in rats." *Tohoku J Exp Med* **148**(3): 313-325.

Ozcimen, E. E., A. Uckuyu, et al. (2009). "The effect of metformin treatment on ovarian stromal blood flow in women with polycystic ovary syndrome." *Arch Gynecol Obstet* **280**(2): 263-269.

Padmanabhan, V. and A. S. McNeilly (2001). "Is there an FSH-releasing factor?" *Reproduction* **121**(1): 21-30.

Padmanabhan, V., H. N. Sarma, et al. (2010). "Developmental reprogramming of reproductive and metabolic dysfunction in sheep: native steroids vs. environmental steroid receptor modulators." *Int J Androl* **33**(2): 394-404.

Padmanabhan, V. and T. P. Sharma (2001). "Neuroendocrine vs. paracrine control of follicle-stimulating hormone." *Arch Med Res* **32**(6): 533-543.

Padmanabhan, V., A. Veiga-Lopez, et al. (2010). "Developmental programming: impact of prenatal testosterone excess and postnatal weight gain on insulin sensitivity index and transfer of traits to offspring of overweight females." *Endocrinology* **151**(2): 595-605.

Pagano, C., G. Soardo, et al. (2005). "Plasma adiponectin is decreased in nonalcoholic fatty liver disease." *Eur J Endocrinol* **152**(1): 113-118.

Painter, R. C., S. R. de Rooij, et al. (2007). "Maternal nutrition during gestation and carotid arterial compliance in the adult offspring: the Dutch famine birth cohort." *J Hypertens* **25**(3): 533-540.

Pak, R. C., K. W. Tsim, et al. (1985). "The role of neonatal and pubertal gonadal hormones in regulating the sex dependence of the hepatic microsomal testosterone 5-reductase activity in the rat." *J Endocrinol* **106**(1): 71-79.

Pakarainen, T., F. P. Zhang, et al. (2005). "Knockout of luteinizing hormone receptor abolishes the effects of follicle-stimulating hormone on preovulatory maturation and ovulation of mouse graafian follicles." *Mol Endocrinol* **19**(10): 2591-2602.

Panadero, M., E. Herrera, et al. (2000). "Peroxisome proliferator-activated receptor-alpha expression in rat liver during postnatal development." *Biochimie* **82**(8): 723-726.

Panadero, M., H. Vidal, et al. (2001). "Nutritionally induced changes in the peroxisome proliferator-activated receptor-alpha gene expression in liver of suckling rats are dependent on insulinaemia." *Arch Biochem Biophys* **394**(2): 182-188.

Panning, B. (2008). "X-chromosome inactivation: the molecular basis of silencing." *J Biol* **7**(8): 30.

Panzer, C., S. Wise, et al. (2006). "Impact of oral contraceptives on sex hormone-binding globulin and androgen levels: a retrospective study in women with sexual dysfunction." *J Sex Med* **3**(1): 104-113.

Papadimitriou, A. and K. N. Priftis (2009). "Regulation of the hypothalamic-pituitary-adrenal axis." *Neuroimmunomodulation* **16**(5): 265-271.

Parsanezhad, M. E., M. H. Bagheri, et al. (2003). "Ovarian stromal blood flow changes after laparoscopic ovarian cauterization in women with polycystic ovary syndrome." *Hum Reprod* **18**(7): 1432-1437.

Pasquali, R. and A. Gambineri (2004). "Role of changes in dietary habits in polycystic ovary syndrome." *Reprod Biomed Online* **8**(4): 431-439.

Patel, M. S., M. Srinivasan, et al. (2009). "Metabolic programming: Role of nutrition in the immediate postnatal life." *J Inherit Metab Dis* **32**(2): 218-228.

Payne, A. H. and D. B. Hales (2004). "Overview of steroidogenic enzymes in the pathway from cholesterol to active steroid hormones." *Endocr Rev* **25**(6): 947-970.

Pepling, M. E. (2006). "From primordial germ cell to primordial follicle: mammalian female germ cell development." *Genesis* **44**(12): 622-632.

Pepling, M. E. and A. C. Spradling (2001). "Mouse ovarian germ cell cysts undergo programmed breakdown to form primordial follicles." *Dev Biol* **234**(2): 339-351.

Picon, R., M. C. Pelloux, et al. (1985). "Conversion of androgen to estrogen by the rat fetal and neonatal female gonad: effects of dcAMP and FSH." *J Steroid Biochem* **23**(6A): 995-1000.

Plagemann, A., I. Heidrich, et al. (1992). "Lifelong enhanced diabetes susceptibility and obesity after temporary intrahypothalamic hyperinsulinism during brain organization." *Exp Clin Endocrinol* **99**(2): 91-95.

Pomerantz, S. M., R. W. Goy, et al. (1986). "Expression of male-typical behavior in adult female pseudohermaphroditic rhesus: comparisons with normal males and neonatally gonadectomized males and females." *Horm Behav* **20**(4): 483-500.

Pomerantz, S. M., M. M. Roy, et al. (1988). "Social and hormonal influences on behavior of adult male, female, and pseudohermaphroditic rhesus monkeys." *Horm Behav* **22**(2): 219-230.

Priego, T., J. Sanchez, et al. (2008). "Sex-differential expression of metabolism-related genes in response to a high-fat diet." *Obesity (Silver Spring)* **16**(4): 819-826.

Proulx, K., S. Clavel, et al. (2001). "High neonatal leptin exposure enhances brain GR expression and feedback efficacy on the adrenocortical axis of developing rats." *Endocrinology* **142**(11): 4607-4616.

Puurunen, J., T. Piltonen, et al. (2009). "Adrenal androgen production capacity remains high up to menopause in women with polycystic ovary syndrome." *J Clin Endocrinol Metab* **94**(6): 1973-1978.

Qi, L. and Y. A. Cho (2008). "Gene-environment interaction and obesity." *Nutr Rev* **66**(12): 684-694.

Qin, Y., Y. Choi, et al. (2007). "NOBOX homeobox mutation causes premature ovarian failure." *Am J Hum Genet* **81**(3): 576-581.

Quinn, P. G. and D. Yeagley (2005). "Insulin regulation of PEPCK gene expression: a model for rapid and reversible modulation." *Curr Drug Targets Immune Endocr Metabol Disord* **5**(4): 423-437.

Quirk, S. M., R. G. Cowan, et al. (2004). "Ovarian follicular growth and atresia: the relationship between cell proliferation and survival." *J Anim Sci* **82 E-Suppl**: E40-52.

Qureshi, A. I., S. S. Nussey, et al. (2008). "Testosterone selectively increases primary follicles in ovarian cortex grafted onto embryonic chick membranes: relevance to polycystic ovaries." *Reproduction* **136**(2): 187-194.

Rang, H. P., M. M. Dale, et al. (2003). *Pharmacology*, Elsevier Science.

Ratchford, A. M., C. R. Esguerra, et al. (2008). "Decreased oocyte-granulosa cell gap junction communication and connexin expression in a type 1 diabetic mouse model." *Mol Endocrinol* **22**(12): 2643-2654.

Recabarren, S. E., R. Smith, et al. (2008). "Metabolic profile in sons of women with polycystic ovary syndrome." *J Clin Endocrinol Metab* **93**(5): 1820-1826.

Reddy, P., L. Liu, et al. (2008). "Oocyte-specific deletion of Pten causes premature activation of the primordial follicle pool." *Science* **319**(5863): 611-613.

Reddy, P., L. Shen, et al. (2005). "Activation of Akt (PKB) and suppression of FKHRL1 in mouse and rat oocytes by stem cell factor during follicular activation and development." *Dev Biol* **281**(2): 160-170.

Ren, Y., R. G. Cowan, et al. (2009). "Dominant activation of the hedgehog signaling pathway in the ovary alters theca development and prevents ovulation." *Mol Endocrinol* **23**(5): 711-723.

Rey, R., C. Lukas-Croisier, et al. (2003). "AMH/MIS: what we know already about the gene, the protein and its regulation." *Mol Cell Endocrinol* **211**(1-2): 21-31.

Ribeiro, R. C., P. J. Kushner, et al. (1995). "The nuclear hormone receptor gene superfamily." *Annu Rev Med* **46**: 443-453.

Ribot, J., A. M. Rodriguez, et al. (2008). "Adiponectin and resistin response in the onset of obesity in male and female rats." *Obesity (Silver Spring)* **16**(4): 723-730.

Ristic, N., N. Nestorovic, et al. (2008). "Maternal dexamethasone treatment reduces ovarian follicle number in neonatal rat offspring." *J Microsc* **232**(3): 549-557.

Rizzoti, K. and R. Lovell-Badge (2005). "Early development of the pituitary gland: induction and shaping of Rathke's pouch." *Rev Endocr Metab Disord* **6**(3): 161-172.

Rockwell, L. C. and R. D. Koos (2009). "Dexamethasone enhances fertility and preovulatory serum prolactin levels in eCG/hCG primed immature rats." *J Reprod Dev* **55**(3): 247-251.

Rodgers, R. J., H. F. Irving-Rodgers, et al. (2003). "Extracellular matrix of the developing ovarian follicle." *Reproduction* **126**(4): 415-424.

Rodriguez-Acebes, S., N. Palacios, et al. (2010). "Gene expression profiling of subcutaneous adipose tissue in morbid obesity using a focused microarray: Distinct expression of cell-cycle- and differentiation-related genes." *BMC Med Genomics* **3**(1): 61.

Roelfsema, F., P. Kok, et al. (2010). "Cortisol production rate is similarly elevated in obese women with or without the polycystic ovary syndrome." *J Clin Endocrinol Metab* **95**(7): 3318-3324.

Roland, A. V., C. S. Nunemaker, et al. (2010). "Prenatal androgen exposure programs metabolic dysfunction in female mice." *J Endocrinol* **207**(2): 213-223.

Roma, P. G., M. E. Huntsberry, et al. (2007). "Separation stress, litter size, and the rewarding effects of low-dose morphine in the dams of maternally separated rats." *Prog Neuropsychopharmacol Biol Psychiatry* **31**(2): 429-433.

Rosa, E. S. A., M. A. Guimaraes, et al. (2003). "Prepubertal administration of estradiol valerate disrupts cyclicity and leads to cystic ovarian morphology during adult life in the rat: role of sympathetic innervation." *Endocrinology* **144**(10): 4289-4297.

Roseboom, T. J., J. H. van der Meulen, et al. (2001). "Adult survival after prenatal exposure to the Dutch famine 1944--45." *Paediatr Perinat Epidemiol* **15**(3): 220-225.

Roseboom, T. J., J. H. van der Meulen, et al. (2001). "Maternal nutrition during gestation and blood pressure in later life." *J Hypertens* **19**(1): 29-34.

Rossi, B., S. Sukalich, et al. (2008). "Prevalence of metabolic syndrome and related characteristics in obese adolescents with and without polycystic ovary syndrome." *J Clin Endocrinol Metab* **93**(12): 4780-4786.

S.S. Nussey, S. A. W. (2001). *Endocrinology: An Integrated Approach*, Oxford: BIOS Scientific Publishers.

Sam, S., Y. A. Sung, et al. (2008). "Evidence for pancreatic beta-cell dysfunction in brothers of women with polycystic ovary syndrome." *Metabolism* **57**(1): 84-89.

Sanchez-Criado, J. E., P. Guelmes, et al. (2002). "Tamoxifen but not other selective estrogen receptor modulators antagonizes estrogen actions on luteinizing hormone secretion while inducing gonadotropin-releasing hormone self-priming in the rat." *Neuroendocrinology* **76**(4): 203-213.

Sanchez-Criado, J. E., A. Ruiz, et al. (1996). "Follicular and luteal progesterone synergize to maintain 5-day cyclicity in rats." *Rev Esp Fisiol* **52**(4): 223-229.

Sarma, H. N., M. Manikkam, et al. (2005). "Fetal programming: excess prenatal testosterone reduces postnatal luteinizing hormone, but not follicle-stimulating hormone responsiveness, to estradiol negative feedback in the female." *Endocrinology* **146**(10): 4281-4291.

Sathyapalan, T. and S. L. Atkin (2010). "Mediators of inflammation in polycystic ovary syndrome in relation to adiposity." *Mediators Inflamm* **2010**: 758656.

Scalzo, C. M. and S. D. Michael (1988). "Source of high testosterone levels associated with autoimmune ovarian dysgenesis in neonatally thymectomized B6A mice." *Biol Reprod* **38**(5): 1115-1121.

Schally, A. V., A. Arimura, et al. (1971). "Gonadotropin-releasing hormone: one polypeptide regulates secretion of luteinizing and follicle-stimulating hormones." *Science* **173**(4001): 1036-1038.

Schlein, P. A., M. X. Zarrow, et al. (1974). "The role of prolactin in the depressed or 'buffered' adrenocorticosteroid response of the rat." *J Endocrinol* **62**(1): 93-99.

Schulz, K. M., H. A. Molenda-Figueira, et al. (2009). "Back to the future: The organizational-activational hypothesis adapted to puberty and adolescence." *Horm Behav* **55**(5): 597-604.

Schwimmer, J. B., O. Khorram, et al. (2005). "Abnormal aminotransferase activity in women with polycystic ovary syndrome." *Fertil Steril* **83**(2): 494-497.

Scott, H. M., G. R. Hutchison, et al. (2008). "Relationship between androgen action in the "male programming window," fetal sertoli cell number, and adult testis size in the rat." *Endocrinology* **149**(10): 5280-5287.

Scott, H. M., G. R. Hutchison, et al. (2007). "Role of androgens in fetal testis development and dysgenesis." *Endocrinology* **148**(5): 2027-2036.

Seale, J. V., S. A. Wood, et al. (2005). "Postnatal masculinization alters the HPA axis phenotype in the adult female rat." *J Physiol* **563**(Pt 1): 265-274.

Seale, J. V., S. A. Wood, et al. (2005). "Organizational role for testosterone and estrogen on adult hypothalamic-pituitary-adrenal axis activity in the male rat." *Endocrinology* **146**(4): 1973-1982.

Seckl, J. R. (2001). "Glucocorticoid programming of the fetus; adult phenotypes and molecular mechanisms." *Mol Cell Endocrinol* **185**(1-2): 61-71.

Seckl, J. R. (2004). "Prenatal glucocorticoids and long-term programming." *Eur J Endocrinol* **151 Suppl 3**: U49-62.

Seckl, J. R., M. Cleasby, et al. (2000). "Glucocorticoids, 11beta-hydroxysteroid dehydrogenase, and fetal programming." *Kidney Int* **57**(4): 1412-1417.

Seckl, J. R., R. C. Dow, et al. (1993). "The 11 beta-hydroxysteroid dehydrogenase inhibitor glycyrrhetinic acid affects corticosteroid feedback regulation of hypothalamic corticotrophin-releasing peptides in rats." *J Endocrinol* **136**(3): 471-477.

Sekido, R., I. Bar, et al. (2004). "SOX9 is up-regulated by the transient expression of SRY specifically in Sertoli cell precursors." *Dev Biol* **274**(2): 271-279.

Sen, A. and S. R. Hammes (2010). "Granulosa cell-specific androgen receptors are critical regulators of ovarian development and function." *Mol Endocrinol* **24**(7): 1393-1403.

Senner, C. E. and N. Brockdorff (2009). "Xist gene regulation at the onset of X inactivation." *Curr Opin Genet Dev* **19**(2): 122-126.

Seow, K. M., Y. L. Tsai, et al. (2009). "Omental adipose tissue overexpression of fatty acid transporter CD36 and decreased expression of hormone-sensitive lipase in insulin-resistant women with polycystic ovary syndrome." *Hum Reprod* **24**(8): 1982-1988.

Setji, T. L. and A. J. Brown (2007). "Comprehensive clinical management of polycystic ovary syndrome." *Minerva Med* **98**(3): 175-189.

Setji, T. L., N. D. Holland, et al. (2006). "Nonalcoholic steatohepatitis and nonalcoholic Fatty liver disease in young women with polycystic ovary syndrome." *J Clin Endocrinol Metab* **91**(5): 1741-1747.

Sharpe, R. M. "Bisphenol A exposure and sexual dysfunction in men: editorial commentary on the article 'Occupational exposure to bisphenol-A (BPA) and the risk of self-reported male sexual dysfunction' Li et al., 2009." *Hum Reprod* **25**(2): 292-294.

Sharpe, R. M., A. Rivas, et al. (2003). "Effect of neonatal treatment of rats with potent or weak (environmental) oestrogens, or with a GnRH antagonist, on Leydig cell development and function through puberty into adulthood." *Int J Androl* **26**(1): 26-36.

Sheridan, P. J., M. X. Zarrow, et al. (1973). "Androgenization of the neonatal female rat with very low doses of androgen." *J Endocrinol* **57**(1): 33-45.

Short, R. V. (1964). "Ovarian Steroid Snnthesis and Secretion in Vivo." *Recent Prog Horm Res* **20**: 303-340.

Shumak, S. L. (2009). "Even lean women with PCOS are insulin resistant." *Bmj* **338**: b954.

Simanainen, U., C. M. Allan, et al. (2007). "Disruption of prostate epithelial androgen receptor impedes prostate lobe-specific growth and function." *Endocrinology* **148**(5): 2264-2272.

Simard, M., J. R. Brawer, et al. (1987). "An intractable, ovary-independent impairment in hypothalamo-pituitary function in the estradiol-valerate-induced polycystic ovarian condition in the rat." *Biol Reprod* **36**(5): 1229-1237.

Simpson, J. L. (2008). "Genetic and phenotypic heterogeneity in ovarian failure: overview of selected candidate genes." *Ann N Y Acad Sci* **1135**: 146-154.

Sinclair, A. H., P. Berta, et al. (1990). "A gene from the human sex-determining region encodes a protein with homology to a conserved DNA-binding motif." *Nature* **346**(6281): 240-244.

Sisk, C. L., H. N. Richardson, et al. (2001). "In vivo gonadotropin-releasing hormone secretion in female rats during peripubertal development and on proestrus." *Endocrinology* **142**(7): 2929-2936.

Skinner, M. K. (2008). "What is an epigenetic transgenerational phenotype? F3 or F2." *Reprod Toxicol* **25**(1): 2-6.

Skinner, M. K., M. Manikkam, et al. "Epigenetic transgenerational actions of environmental factors in disease etiology." *Trends Endocrinol Metab* **21**(4): 214-222.

Slob, A. K., R. den Hamer, et al. (1983). "Prenatal testosterone propionate and postnatal ovarian activity in the rat." *Acta Endocrinol (Copenh)* **103**(3): 420-427.

Smith, J. T., D. K. Clifton, et al. (2006). "Regulation of the neuroendocrine reproductive axis by kisspeptin-GPR54 signaling." *Reproduction* **131**(4): 623-630.

Smith, M. F., E. W. McIntush, et al. (1994). "Mechanisms associated with corpus luteum development." *J Anim Sci* **72**(7): 1857-1872.

Smith, M. S., M. E. Freeman, et al. (1975). "The control of progesterone secretion during the estrous cycle and early pseudopregnancy in the rat: prolactin, gonadotropin and steroid levels associated with rescue of the corpus luteum of pseudopregnancy." *Endocrinology* **96**(1): 219-226.

Smith, P., T. L. Steckler, et al. (2009). "Developmental programming: differential effects of prenatal testosterone and dihydrotestosterone on follicular recruitment, depletion of follicular reserve, and ovarian morphology in sheep." *Biol Reprod* **80**(4): 726-736.

Smith, W. N. (1970). "Transplacental influence of androgen upon ovulatory mechanisms in the rat." *J Endocrinol* **48**(3): 477-478.

Smith, W. N. and M. T. Peng (1966). "Influence of testosterone upon sexual maturation in the rat." *J Physiol* **185**(3): 655-666.

Soder, O. (2007). "Sexual dimorphism of gonadal development." *Best Pract Res Clin Endocrinol Metab* **21**(3): 381-391.

Sonderegger, S., J. Pollheimer, et al. "Wnt signalling in implantation, decidualisation and placental differentiation--review." *Placenta* **31**(10): 839-847.

Speroff, L. and R. L. Vande Wiele (1971). "Regulation of the human menstrual cycle." *Am J Obstet Gynecol* **109**(2): 234-247.

Spicer, L. J., J. L. Voge, et al. (2004). "Insulin-like growth factor-II stimulates steroidogenesis in cultured bovine thecal cells." *Mol Cell Endocrinol* **227**(1-2): 1-7.

Spradling, A. C., M. de Cuevas, et al. (1997). "The Drosophila germarium: stem cells, germ line cysts, and oocytes." *Cold Spring Harb Symp Quant Biol* **62**: 25-34.

Srinivas, S., T. Watanabe, et al. (2001). "Cre reporter strains produced by targeted insertion of EYFP and ECFP into the ROSA26 locus." *BMC Dev Biol* **1**: 4.

Srinivasan, M., C. Dodds, et al. (2008). "Maternal obesity and fetal programming: effects of a high-carbohydrate nutritional modification in the immediate postnatal life of female rats." *Am J Physiol Endocrinol Metab* **295**(4): E895-903.

Srinivasan, M., P. Mitrani, et al. (2008). "A high-carbohydrate diet in the immediate postnatal life of rats induces adaptations predisposing to adult-onset obesity." *J Endocrinol* **197**(3): 565-574.

Steckler, T., M. Manikkam, et al. (2007). "Developmental programming: follicular persistence in prenatal testosterone-treated sheep is not programmed by androgenic actions of testosterone." *Endocrinology* **148**(7): 3532-3540.

Steckler, T., J. Wang, et al. (2005). "Fetal programming: prenatal testosterone treatment causes intrauterine growth retardation, reduces ovarian reserve and increases ovarian follicular recruitment." *Endocrinology* **146**(7): 3185-3193.

Steckler, T. L., C. Herkimer, et al. (2009). "Developmental programming: excess weight gain amplifies the effects of prenatal testosterone excess on reproductive cyclicity--implication for polycystic ovary syndrome." *Endocrinology* **150**(3): 1456-1465.

Steiner, R. A., D. K. Clifton, et al. (1976). "Sexual differentiation and feedback control of luteinizing hormone secretion in the rhesus monkey." *Biol Reprod* **15**(2): 206-212.

Stener-Victorin, E. and C. Lindholm (2004). "Immunity and beta-endorphin concentrations in hypothalamus and plasma in rats with steroid-induced polycystic ovaries: effect of low-frequency electroacupuncture." *Biol Reprod* **70**(2): 329-333.

Stener-Victorin, E., T. Lundeberg, et al. (2000). "Effects of electro-acupuncture on nerve growth factor and ovarian morphology in rats with experimentally induced polycystic ovaries." *Biol Reprod* **63**(5): 1497-1503.

Stener-Victorin, E., K. Ploj, et al. (2005). "Rats with steroid-induced polycystic ovaries develop hypertension and increased sympathetic nervous system activity." *Reprod Biol Endocrinol* **3**: 44.

Stevens, J. (1995). "Obesity, fat patterning and cardiovascular risk." *Adv Exp Med Biol* **369**: 21-27.

Stimson, R. H., G. E. Lobley, et al. (2010). "Effects of proportions of dietary macronutrients on glucocorticoid metabolism in diet-induced obesity in rats." *PLoS ONE* **5**(1): e8779.

Stocco, C. (2008). "Aromatase expression in the ovary: hormonal and molecular regulation." *Steroids* **73**(5): 473-487.

Stocco, C., C. Telleria, et al. (2007). "The molecular control of corpus luteum formation, function, and regression." *Endocr Rev* **28**(1): 117-149.

Stouffs, K., H. Tournaye, et al. (2009). "Male infertility and the involvement of the X chromosome." *Hum Reprod Update* **15**(6): 623-637.

Stouffs, K., D. Vandermaelen, et al. (2009). "[Genetics and male infertility]." *Verh K Acad Geneeskd Belg* **71**(3): 115-139.

Stubbs, S. A., J. Stark, et al. (2007). "Abnormal preantral folliculogenesis in polycystic ovaries is associated with increased granulosa cell division." *J Clin Endocrinol Metab* **92**(11): 4418-4426.

Su, Y. Q., K. Sugiura, et al. (2008). "Oocyte regulation of metabolic cooperativity between mouse cumulus cells and oocytes: BMP15 and GDF9 control cholesterol biosynthesis in cumulus cells." *Development* **135**(1): 111-121.

Sugiura, K., Y. Q. Su, et al. (2010). "Estrogen promotes the development of mouse cumulus cells in coordination with oocyte-derived GDF9 and BMP15." *Mol Endocrinol* **24**(12): 2303-2314.

Svendsen, P. F., L. Nilas, et al. (2008). "Obesity, body composition and metabolic disturbances in polycystic ovary syndrome." *Hum Reprod*.

Taylor, A. E., B. McCourt, et al. (1997). "Determinants of abnormal gonadotropin secretion in clinically defined women with polycystic ovary syndrome." *J Clin Endocrinol Metab* **82**(7): 2248-2256.

Templeton, A. (2000). "Infertility and the establishment of pregnancy--overview." *Br Med Bull* **56**(3): 577-587.

Tetsuka, M., P. F. Whitelaw, et al. (1995). "Developmental regulation of androgen receptor in rat ovary." *J Endocrinol* **145**(3): 535-543.

Thomas, P. and D. W. Waring (1997). "Modulation of stimulus-secretion coupling in single rat gonadotrophs." *J Physiol* **504 (Pt 3)**: 705-719.

Thomas, S. G. and I. J. Clarke (1997). "The positive feedback action of estrogen mobilizes LH-containing, but not FSH-containing secretory granules in ovine gonadotropes." *Endocrinology* **138**(3): 1347-1350.

Tohei, A., H. Sakamoto, et al. (2001). "Dexamethasone increases inhibin and estradiol secretion mediated by endogenous FSH in equine chorionic gonadotropin (eCG)-primed immature female rats." *Life Sci* **69**(3): 281-288.

Tohei, A., S. Sakamoto, et al. (2000). "Dexamethasone or triamcinolone increases follicular development in immature female rats." *Jpn J Pharmacol* **84**(3): 281-286.

Tomlinson, J. W., J. Finney, et al. (2008). "Impaired glucose tolerance and insulin resistance are associated with increased adipose 11beta-hydroxysteroid dehydrogenase type 1 expression and elevated hepatic 5alpha-reductase activity." *Diabetes* **57**(10): 2652-2660.

Toulis, K. A., D. G. Goulis, et al. (2009). "Adiponectin levels in women with polycystic ovary syndrome: a systematic review and a meta-analysis." *Hum Reprod Update* **15**(3): 297-307.

Trombly, D. J., T. K. Woodruff, et al. (2009). "Roles for transforming growth factor beta superfamily proteins in early folliculogenesis." *Semin Reprod Med* **27**(1): 14-23.

Trombly, D. J., T. K. Woodruff, et al. (2009). "Suppression of Notch signaling in the neonatal mouse ovary decreases primordial follicle formation." *Endocrinology* **150**(2): 1014-1024.

Tsai, C. L., R. K. Rowntree, et al. (2008). "Higher order chromatin structure at the X-inactivation center via looping DNA." *Dev Biol* **319**(2): 416-425.

Tsilchorozidou, T., J. W. Honour, et al. (2003). "Altered cortisol metabolism in polycystic ovary syndrome: insulin enhances 5alpha-reduction but not the elevated adrenal steroid production rates." *J Clin Endocrinol Metab* **88**(12): 5907-5913.

Ulloa-Aguirre, A., P. Damian-Matsumura, et al. (1990). "Effects of neonatal androgenization on the chromatofocusing pattern of anterior pituitary FSH in the female rat." *J Endocrinol* **126**(2): 323-332.

Vainio, S., M. Heikkila, et al. (1999). "Female development in mammals is regulated by Wnt-4 signalling." *Nature* **397**(6718): 405-409.

Vasquez, S. B. and J. I. Kitay (1978). "Effects of prolactin on pituitary-adrenal function in intact and ovariectomized rats." *Acta Endocrinol (Copenh)* **88**(4): 744-753.

Veiga-Lopez, A., O. I. Astapova, et al. (2009). "Developmental programming: contribution of prenatal androgen and estrogen to estradiol feedback systems and periovulatory hormonal dynamics in sheep." *Biol Reprod* **80**(4): 718-725.

Veiga-Lopez, A., J. S. Lee, et al. (2010). "Developmental programming: insulin sensitizer treatment improves reproductive function in prenatal testosterone-treated female sheep." *Endocrinology* **151**(8): 4007-4017.

Veiga-Lopez, A., W. Ye, et al. (2008). "Developmental programming: deficits in reproductive hormone dynamics and ovulatory outcomes in prenatal, testosterone-treated sheep." *Biol Reprod* **78**(4): 636-647.

Vendola, K. A., J. Zhou, et al. (1998). "Androgens stimulate early stages of follicular growth in the primate ovary." *J Clin Invest* **101**(12): 2622-2629.

Venken, K., K. De Gendt, et al. (2006). "Relative impact of androgen and estrogen receptor activation in the effects of androgens on trabecular and cortical bone in growing male mice: a study in the androgen receptor knockout mouse model." *J Bone Miner Res* **21**(4): 576-585.

Visser, J. A., A. L. Durlinger, et al. (2007). "Increased oocyte degeneration and follicular atresia during the estrous cycle in anti-Mullerian hormone null mice." *Endocrinology* **148**(5): 2301-2308.

Vo, T. T., Y. M. Yoo, et al. (2010). "Potential estrogenic effect(s) of parabens at the prepubertal stage of a postnatal female rat model." *Reprod Toxicol* **29**(3): 306-316.

vom Saal, F. S. and F. H. Bronson (1978). "In utero proximity of female mouse fetuses to males: effect on reproductive performance during later life." *Biol Reprod* **19**(4): 842-853.

vom Saal, F. S. and F. H. Bronson (1980). "Sexual characteristics of adult female mice are correlated with their blood testosterone levels during prenatal development." *Science* **208**(4444): 597-599.

W.H.O. (2006). "What are the health consequences of being overweight?". Retrieved 14th August, 2010, from www.who.int.

Wang, Y., J. Fortin, et al. (2008). "Activator protein-1 and smad proteins synergistically regulate human follicle-stimulating hormone beta-promoter activity." *Endocrinology* **149**(11): 5577-5591.

Wang, Y., Y. Sun, et al. (2004). "Expression of resistin mRNA in adipose tissue of rat model with polycystic ovarian syndrome and its implication." *J Huazhong Univ Sci Technolog Med Sci* **24**(6): 621-624.

Ward, O. B., A. M. Wexler, et al. (1996). "Critical periods of sensitivity of sexually dimorphic spinal nuclei to prenatal testosterone exposure in female rats." *Horm Behav* **30**(4): 407-415.

Webb, R., P. C. Garnsworthy, et al. (2004). "Control of follicular growth: local interactions and nutritional influences." *J Anim Sci* **82 E-Suppl**: E63-74.

Webber, L. J., S. Stubbs, et al. (2003). "Formation and early development of follicles in the polycystic ovary." *Lancet* **362**(9389): 1017-1021.

Welsh, M., D. J. MacLeod, et al. "Critical androgen-sensitive periods of rat penis and clitoris development." *Int J Androl* **33**(1): e144-152.

Welsh, M., D. J. MacLeod, et al. (2010). "Critical androgen-sensitive periods of rat penis and clitoris development." *Int J Androl* **33**(1): e144-152.

Welsh, M., P. T. Saunders, et al. (2008). "Identification in rats of a programming window for reproductive tract masculinization, disruption of which leads to hypospadias and cryptorchidism." *J Clin Invest* **118**(4): 1479-1490.

Welt, C. K., A. E. Taylor, et al. (2005). "Follicular arrest in polycystic ovary syndrome is associated with deficient inhibin A and B biosynthesis." *J Clin Endocrinol Metab* **90**(10): 5582-5587.

West, L. J. (2002). "Defining critical windows in the development of the human immune system." *Hum Exp Toxicol* **21**(9-10): 499-505.

White, J. O., P. A. Moore, et al. (1981). "The relationship of the oestrogen and progestin receptors in the abnormal uterus of the adult anovulatory rat. Effects of neonatal treatment with testosterone propionate or clomiphene citrate." *Biochem J* **196**(2): 557-565.

Whittle, J. R., M. J. Powell, et al. (2007). "Sirtuins, nuclear hormone receptor acetylation and transcriptional regulation." *Trends Endocrinol Metab* **18**(9): 356-364.

Wild, R. A., E. Carmina, et al. (2010). "Assessment of cardiovascular risk and prevention of cardiovascular disease in women with the polycystic ovary syndrome: a consensus statement by the Androgen Excess and Polycystic Ovary Syndrome (AE-PCOS) Society." *J Clin Endocrinol Metab* **95**(5): 2038-2049.

Wolf CJ, H. A., Ostby JS, LeBlanc GA, Gray LE Jr (2002). "ffects of prenatal testosterone propionate on the sexual development of male and female rats: a dose-response study." *Toxicol Sci* **65**(1): 71-86.

Wolf, C. J., G. A. LeBlanc, et al. (2004). "Interactive effects of vinclozolin and testosterone propionate on pregnancy and sexual differentiation of the male and female SD rat." *Toxicol Sci* **78**(1): 135-143.

Wong, H. Y., J. A. Burghoorn, et al. (2004). "Phosphorylation of androgen receptor isoforms." *Biochem J* **383**(Pt 2): 267-276.

Wood, R. I. and D. L. Foster (1998). "Sexual differentiation of reproductive neuroendocrine function in sheep." *Rev Reprod* **3**(2): 130-140.

Workshop, R. (2004). "Revised 2003 consensus on diagnostic criteria and long-term health risks related to polycystic ovary syndrome (PCOS)." *Hum Reprod* **19**(1): 41-47.

Wu, X. Y., Z. L. Li, et al. (2010). "Endocrine traits of polycystic ovary syndrome in prenatally androgenized female Sprague-Dawley rats." *Endocr J* **57**(3): 201-209.

Xu, N., R. Azziz, et al. "Epigenetics in polycystic ovary syndrome: a pilot study of global DNA methylation." *Fertil Steril* **94**(2): 781-783 e781.

Xu, Q., H. Y. Lin, et al. (2007). "Infertility with defective spermatogenesis and steroidogenesis in male mice lacking androgen receptor in Leydig cells." *Endocrine* **32**(1): 96-106.

Yao, H. H., M. M. Matzuk, et al. (2004). "Follistatin operates downstream of Wnt4 in mammalian ovary organogenesis." *Dev Dyn* **230**(2): 210-215.

Yeh, S., M. Y. Tsai, et al. (2002). "Generation and characterization of androgen receptor knockout (ARKO) mice: an in vivo model for the study of androgen functions in selective tissues." *Proc Natl Acad Sci U S A* **99**(21): 13498-13503.

Yong, E. L., D. T. Baird, et al. (1992). "Hormonal regulation of the growth and steroidogenic function of human granulosa cells." *J Clin Endocrinol Metab* **74**(4): 842-849.

Young, J. M. and A. S. McNeilly (2010). "Theca: the forgotten cell of the ovarian follicle." *Reproduction* **140**(4): 489-504.

Yu, Y. S., H. S. Sui, et al. (2004). "Apoptosis in granulosa cells during follicular atresia: relationship with steroids and insulin-like growth factors." *Cell Res* **14**(4): 341-346.

Zhang, C., S. Yeh, et al. (2006). "Oligozoospermia with normal fertility in male mice lacking the androgen receptor in testis peritubular myoid cells." *Proc Natl Acad Sci U S A* **103**(47): 17718-17723.

Zhang, Z. W., Z. M. Yang, et al. (2010). "Transgelin induces apoptosis of human prostate LNCaP cells through its interaction with p53." *Asian J Androl* **12**(2): 186-195.

Zheng, K., F. Yang, et al. (2010). "Regulation of male fertility by X-linked genes." *J Androl* **31**(1): 79-85.

Zhou, R., I. M. Bird, et al. (2005). "Adrenal hyperandrogenism is induced by fetal androgen excess in a rhesus monkey model of polycystic ovary syndrome." *J Clin Endocrinol Metab* **90**(12): 6630-6637.

Zhu, J. Q., L. Zhu, et al. "Demethylation of LHR in dehydroepiandrosterone-induced mouse model of polycystic ovary syndrome." *Mol Hum Reprod* **16**(4): 260-266.

Zorn, A. M. (2008). Liver development. *StemBook: Harvard Stem Cell Institute*. L. G. H. S. C. Institute).